



HAL
open science

Temporal and spatial control of fungal filamentous growth in *Candida albicans*

Patricia Maria de Oliveira E Silva

► **To cite this version:**

Patricia Maria de Oliveira E Silva. Temporal and spatial control of fungal filamentous growth in *Candida albicans*. Cellular Biology. COMUE Université Côte d'Azur (2015 - 2019), 2018. English. NNT : 2018AZUR4030 . tel-02615585

HAL Id: tel-02615585

<https://theses.hal.science/tel-02615585>

Submitted on 23 May 2020

HAL is a multi-disciplinary open access archive for the deposit and dissemination of scientific research documents, whether they are published or not. The documents may come from teaching and research institutions in France or abroad, or from public or private research centers.

L'archive ouverte pluridisciplinaire **HAL**, est destinée au dépôt et à la diffusion de documents scientifiques de niveau recherche, publiés ou non, émanant des établissements d'enseignement et de recherche français ou étrangers, des laboratoires publics ou privés.

THÈSE DE DOCTORAT

**Contrôle spatio-temporel de la croissance
filamenteuse chez *Candida albicans***

**Temporal and spatial control of fungal
filamentous growth in *Candida albicans***

Patrícia Maria de Oliveira e Silva

Institut de Biologie Valrose

**Présentée en vue de l'obtention
du grade de docteur en Sciences
de l'Université Côte d'Azur**

Spécialité: Interactions Moléculaires et
Cellulaires

Dirigée par: Robert Arkowitz

Soutenue le: 22 Mai 2018

Devant le jury, composé de:

Dr Robert Arkowitz, CNRS DR, iBV, Université Côte d'Azur

Dr Martine Bassilana, CNRS DR, iBV, Université Côte d'Azur

Pr Neil Gow, University of Aberdeen UK

Pr Sophie Martin, University of Lausanne CH

Pr Joachim Morschhäuser, Universität Würzburg DE

Dr Agnese Seminara, CNRS HDR, Université Côte d'Azur



**Contrôle spatio-temporel de la croissance
filamenteuse chez *Candida albicans***

**Temporal and spatial control of fungal
filamentous growth in *Candida albicans***

Jury:

Président du Jury: Dr Martine Bassilana, CNRS DR, iBV, Université Côte d'Azur

Directeur de Thèse: Dr Robert Arkowitz, CNRS DR, iBV, Université Côte d'Azur

Rapporteuse: Pr Sophie Martin, University of Lausanne CH

Rapporteur: Pr Neil Gow, University of Aberdeen UK

Examinatrice: Dr Agnese Seminara, CNRS HDR, Université Côte d'Azur

Examineur: Pr Joachim Morschhäuser, Universität Würzburg DE

*You know it's true
All the things you do, come back to you*

*Sing with me
Sing for the year
Sing for the laughter
And sing for the tear
Sing with me, if it's just for today
Maybe tomorrow the good Lord will take you away*

*Dream On
Dream On
Dream On
Dream until the dream comes true*

– Steven Tyler
Aerosmith, 1972

Printed by

CPNU UNS – Centre de Production Numérique Universitaire Impressions Nice,
France

© 2018 CNRS

Final version submitted to UCA the 30th July 2018

Contents

Abstract.....	vii
Résumé.....	ix
Acknowledgements.....	xi
List of Abbreviations.....	xiii
Introduction.....	1
I – Polarized growth and morphogenesis.....	1
II – <i>Candida albicans</i> , an opportunistic pathogen.....	7
III – The small Rho-GTPase Cdc42 in fungi.....	16
IV – Cell reorganization during polarized growth in filamentous fungi.....	24
V – Protein recruitment systems.....	31
VI – Objective of this work.....	39
Results.....	41
A dynamic polarity axis is established in the absence of directional growth.....	45
Additional Results.....	77
Discussion.....	81
<i>i)</i> How is the initial polarized growth site disrupted?.....	82
<i>ii)</i> How is new growth initiated?.....	83
<i>iii)</i> What influences the location of new growth?.....	84
<i>iv)</i> What is the relationship between the Spitzenkörper and the new cluster of secretory vesicles?.....	85
<i>v)</i> What is the Spitzenkörper?.....	85
<i>vi)</i> How does the new cluster of secretory vesicles form, move, and settle?.....	87
Conclusions and Future Perspectives.....	87
Materials & Methods.....	89
I – Molecular biology.....	89
II – Plasmids.....	91
III – Strains.....	94
IV – Growth conditions.....	95
V – Yeast transformation.....	95
VI – Actin cytoskeleton staining and actin cables quantification.....	96
VII – Microscopy.....	97
Annex.....	107
References.....	117

Abstract

Temporal and spatial control of fungal filamentous growth in *Candida albicans*

Candida albicans is a fungal human pathogen that can cause life-threatening infections in immunocompromised patients, in part, due to its ability to switch between an oval budding form and a filamentous hyphal form. The small-Rho GTPase Cdc42 is crucial for filamentous growth and, in its active form, localizes as a tight cluster at the tips of growing hyphae. I have used a light-activated membrane recruitment system comprised of the *Arabidopsis thaliana* Cry2PHR-CibN domains to control the recruitment of constitutively active Cdc42 to the plasma membrane. I have determined how photorecruitment of constitutively active Cdc42 perturbs filamentous growth and where, when and how new filamentous growth is subsequently initiated. My results demonstrate that, upon photorecruitment of constitutively active Cdc42, filament extension is abrogated and a new growth site can be established in the cell. Location of a new filamentous growth site correlated with the length of the initial filament. I have investigated the molecular mechanisms that underlie the disassembly of an initial growth site and the specific location of the new filamentous growth site. In growing hyphae a cluster of vesicles, referred to as a Spitzenkörper, is localized at the tip of the filament. Upon photorecruitment of constitutively active Cdc42, a new cluster of vesicles, with a similar composition to that of the initial Spitzenkörper, appears in the mother cell. I have followed the dynamics of the Spitzenkörper, active Cdc42, sites of endocytosis, secretory vesicles and actin cables subsequent to disruption of the initial growth site in the filament. Taken together, my results suggest that there is competition for growth between the Spitzenkörper and the cluster of vesicles that forms immediately after the photorecruitment of constitutively active Cdc42 and that a dynamic polarity axis can be established in the absence of directional growth.

I have presented this work at 2 international meetings and received an Elsevier Outstanding Young Investigator Award for an elevator talk. This work will be submitted shortly to a peer reviewed journal (Silva P.M., Puerner C., Seminara A., Bassilana M. & Arkowitz R.A., A dynamic polarity axis is established in the absence of directional growth). In addition, I am co-inventor of a patent (N. Minc, V. Davì, H. Tanimoto, P. Silva & R. Arkowitz) entitled « PROCÉDE DE MESURE EN TEMPS REEL DE L'ÉPAISSEUR DE LA PAROI ET SES APPLICATIONS » n° PCT/EP2017/070729.

Key Words

Candida albicans, Cdc42, Rho GTPase, cell polarity, morphogenesis, membrane traffic.

Résumé

Contrôle spatio-temporel de la croissance filamenteuse chez *Candida albicans*

Candida albicans est un pathogène fongique opportuniste de l'Homme, qui peut causer des infections superficielles mais aussi systémiques chez les patients immunodéprimés. Sa virulence est associée à sa capacité de changer d'une forme bourgeonnante à une forme hyphale. La petite GTPase de type Rho, Cdc42, est critique pour la croissance filamenteuse et, sous forme activée, sa localisation est restreinte à l'extrémité des hyphes. J'ai utilisé un système photoactivable, constitué des domaines d'*Arabidopsis thaliana* Cry2PHR-CibN, pour contrôler le recrutement de Cdc42 constitutivement actif à la membrane plasmique. J'ai déterminé comment le photo-recrutement de Cdc42 constitutivement actif perturbe la croissance filamenteuse et où, quand et comment une nouvelle croissance filamenteuse est ré-initiée. Mes résultats démontrent que, lors du photo-recrutement de Cdc42 constitutivement actif, l'extension du filament cesse puis un nouveau site de croissance s'établit dans la cellule. La localisation de ce nouveau site de croissance est corrélée à la longueur du filament. J'ai étudié les mécanismes moléculaires qui sous-tendent le désassemblage du site de croissance initial et l'emplacement spécifique du nouveau site de croissance filamenteuse. Dans les hyphes en croissance, un « cluster » de vésicules, appelé Spitzenkörper, est localisé à l'extrémité du filament. Lors du photo-recrutement de Cdc42 constitutivement actif, un nouveau « cluster » de vésicules, de composition similaire à celui du Spitzenkörper initial, apparaît dans la cellule mère. J'ai suivi la dynamique du Spitzenkörper et la localisation de Cdc42 sous forme activée, des sites d'endocytose, des vésicules de sécrétion et des câbles d'actine suite à la perturbation du site de croissance initial dans le filament. Dans l'ensemble, mes résultats indiquent qu'il existe une compétition pour la croissance entre le Spitzenkörper et le « cluster » de vésicules qui se forme immédiatement après le photo-recrutement de Cdc42 constitutivement actif et qu'un axe de polarité dynamique peut être établi en l'absence de croissance directionnelle.

Mots Clés:

Candida albicans, Cdc42, Rho GTPase, polarité cellulaire, morphogenèse, trafic membranaire.

Acknowledgements

My father once told me a story, many many years ago, from his university years when he was presented with the opportunity to choose the teacher he wanted for some disciplines, among a couple or three. Every student would rush to choose the teachers who had the reputation of being soft and gentle on their students. My dad didn't rush to choose, he wanted the teachers who were demanding, who challenged their students and who made them think! Back then, when I listened to this, I didn't understand what he meant, but the story stuck with me...

I will never forget the day that I knew I had been accepted in Rob and Martine's lab – I rushed to Google “Nice France”... woooooow! I couldn't believe I was going to live in this amazing place and with such a good scholarship! Tomorrow will be exactly 4 years that I arrived in this sunny blue corner of France and today my dad's story makes every sense to me. I am very grateful for having been a student in Robert (Rob) Arkowitz and Martine Bassilana's lab. I want to thank both of you for welcoming me in your lab, teaching me, guiding me, discussing the project with me, believing in me even when I couldn't. It has been a pleasure to be your student and I wish great success to the Arkowitz lab!

During this amazing journey I have met incredible people from all corners of the world, whom I will always remember with a smile: Rocio Garcia Rodas, Rohan and Archana Wakade, Hayet Labbaoui, Stephanie (Stephy) Bogliolo, Miguel Basante, Danièle Stalder, Martina Iapichino, Charles (Charlie) and Maddy Puerner, Alon Weiner, Darren Thomson, Marjorie Heim, Jeshlee Cyril, Anup Shegaonkar, Madhu Hedge, Taras Ostapchuk, Yumiko Sugita, Alex Bisbal, and of course the coolest housemate/cat owner Nadiaaaaa Formicola (and Tatini, whom I love, even if she doesn't love me back)! You are my family from Nice and you have filled my stay here with smiles and laughter, you are the reason why I love this city. People, everything is about people, everything in this life that's worth a damn.

Thank you for always being there for me - and for laughing at my silly jokes!

Charlitos and Miguelito, who will take this great desk? By the window, great sun light, you can aaaaalmost see the Mediterranean AAAAAAND there is a stand for the

Acknowledgements

computer, built by a *great* engineer (pffffhhh me, of course...)! Don't drive Stephy crazy, please, guys!! =)

I couldn't forget of course the Fungibrain family, Valeria Davì, Paola Bardetti, Hugo Amoedo Machi, Cassandre Kinnaer, Luigi (Gigi, the future of Science) di Vietro, Pavlos Geranios, Stefania Vitale, Patricia Ortiz, Mariana Almeida, Tânia Fernandes, Saskia du Pré, Klara Junker and Antonio Serrano! What a great pleasure it was to share this experience with you, starting from the moment we met in Copenhagen (and Salamanca)! Every year, I couldn't wait for the chance to see you again in a different city (Paris, Aubergine or Berlin), eating all the burgers, steaks and fries that one person can have XD love you all! I want to thank as well to all the PIs who made this project possible, Nick Read, Antonio Di Pietro, Alex Brand, Nicolas Minc, Gerhard Braus, André Fleißner, Jürgen Wendland, Jason Oliver, José Pérez-Martín, Philippe Perret, and specially Sophie Martin and Neil Gow for accepting the invitation to be a part of my defense jury. And of course last but not least, Colette Inkson, the best Marie Curie Program Manager!

I would like to extend my acknowledgements to the other members of my defense jury, Agnese Seminara and Joachim Morschhäuser.

To all the PRISM team, Magali Mondin, Sébastien Schaub, Maéva Gesson and Simon Lachambre, thank you for your patience, for your tremendous help with image acquisition and analysis. Thank you, Corinne Fiorucci and Brigitte Grlj for technical support in the lab. I am grateful to the Marie Curie ITN Fungibrain and Fondation pour la Recherche Médicale (FRM) for funding.

E claro que não poderia deixar de agradecer à minha família, que apesar de estar longe, está sempre no meu coração. À minha mãe Maria Filomena Oliveira, ao meu pai Rogério Silva, à minha mana Verónica Silva, ao meu mano João Silva e avózinha Emília Franco! Obrigada pelas vossas palavras de encorajamento e por acreditarem em mim! E por fim quero agradecer ao meu companheiro Pedro Fonseca, por me dar todo o apoio sempre, por ter estado presente ao longo desta etapa tão importante para mim. Dás-me imensa força, txi bom! Amo-vos todos muito!

Patrícia Silva

Nice, 16th April 2018

List of Abbreviations

The following table describes the significance of the most relevant abbreviations and acronyms used throughout the thesis. The page where each one is defined/used for the first time is also given.

Abbreviation	Meaning	Page
Abp1	Actin Binding Protein 1	26
CAAX	Carboxyl-terminal tetrapeptide motif (C = cysteine, A = aliphatic amino acid, X = terminal residue)	17
cAMP-PKA	Cyclic AMP protein kinase A	14
Cdc42	Cell division control protein 42	5
Cdc42[G12V,C188S]	Mutated Cdc42, constitutively active (G12V) and cytoplasmic (C188S)	21/38
Cdc42•GTP	Active, GTP-bound Cdc42	6
Cdc42•GDP	Inactive, GDP-bound Cdc42	6
Cib1	Cryptochrome-interactive basic helix-loop-helix 1	35
CibN	Truncated version of Cib1 – aminoacids 1-170	35
CRIB	Cdc42/Rac1-interactive binding domain	17
Cry2	Chryptochrome 2	35
Cry2PHR	Chryptochrome 2 photolyase homology region	35
DH/PH	Dbl homology and Pleckstrin homology domain	16
F-actin	Filamentous actin	24
FCS	Fetal calf serum	68
GAP	GTPase-activating protein	2
GDI	Guanine nucleotide exchange inhibitors	18
GDP/GTP	Guanosine diphosphate/triphosphate	2
GEF	Guanine nucleotide-exchange factor	2
GFP	Green fluorescent protein	22
GTPase	GTP binding/hydrolyzing protein	2

List of Abbreviations

MAPK	Mitogen-activated protein kinase	14
mCh	mCherry, red fluorescent protein	43
Mlc1	Myo2-regulatory light chain 1	29
PAK	p21-activated kinase	6
Sec4	Secretion protein 4	27
SNARE	Soluble NSF(N-ethylmaleimide-sensitive factor) Attachment Protein Receptor	3

Introduction

I – Polarized growth and morphogenesis

a) Cell Polarity

polarity (noun) ► Biology

the tendency of living organisms or parts to develop with distinct anterior and posterior (or uppermost and lowermost) ends, or to grow or orientate in a particular direction.

The Oxford English Dictionary

During development, a cell differentiates into a specific cell type as it receives signals and the asymmetric localization of internal components coordinates its behaviour as a single cell or as part of a tissue. As a result of differentiation, the cell develops distinct ends, which can be distinguished according to shape, physical and mechanical properties, molecular gradients and structure. This asymmetric organization of cellular components and properties, which is termed cell polarity, is crucial for normal tissue function and its misregulation can result in developmental disorders and cancers (Wodarz and Näthke, 2007; Lee and Vasioukhin, 2008). Neurons and fungal hyphae are examples of highly polarized and specialized cells. Polarization enables long-range communication by neurons, as axons carry the chemical and electrical signals that allow us to feel a hot surface and carry the same type of signals to our muscles, to react to the elevated temperature (Pogorzala *et al.*, 2013). *Escherichia coli* grows as a rod-shaped cell before it divides (Bramkamp and van Baarle, 2009) – this type of cell shape is also present in Archaea species (Ettema *et al.*, 2011). Pollen tubes grow inside the carpel to deliver the male gametes to the ovules (Feijó, 2010); fungi form hyphal filaments that invade and infect the host tissues (*e.g.*, *Candida* and *Aspergillus* species) (Mayer *et al.*, 2013; Croft *et al.*, 2016). The

ability to polarize transiently or in a stable fashion is an important structural and functional specialization for a range of species. From a reductionist point of view, there is a signal that triggers an internal response to be integrated in a signal transduction pathway, leading to the redistribution of cellular contents - polarization.

The coordination of a range of conserved and specialized molecular mechanisms such as *i*) sensing mechanisms, *ii*) signalling pathways, *iii*) membrane trafficking mechanisms, *iv*) cytoskeletal distribution/dynamics and *v*) organelle positioning, ensures proper polarization. There are two observations supporting this idea: first, all eukaryotic cells share common cellular machineries for protein trafficking and compartmentalization (Palade, 1975; Gurkan *et al.*, 2007); second, cells adopt different shapes and functions in response to specific physiological conditions, *e.g.*, *Saccharomyces cerevisiae* and *Schizosaccharomyces pombe* grow as budding and fission yeasts, respectively, but during the mating process they grow towards a pheromone gradient produced by partner cells (chemotropism) (Arkowitz, 2013; Merlini *et al.*, 2013); cancerous epithelial cells lose polarity (through epithelial-mesenchymal transition – EMT), arrest multicellular interactions, migrate and undergo structural and functional reorganization to integrate into a new tissue (Halaoui and McCaffrey, 2015).

Cell polarization is achieved through spatially restricted cytoskeleton remodelling. The remodelling is induced by signalling of several Rho GTPases, which are highly conserved cellular switches that are, in turn, activated by cortical multi-protein complexes such as the PAR, SCRIBBLE and CRUMBS complexes in animals (Campanale *et al.*, 2017). A key multiprotein complex involved in regulating the actin cytoskeleton and secretory machinery required for polarized growth in fungi, is the polarisome (Köhli *et al.*, 2008; Jones and Sudbery, 2010; Lichius *et al.*, 2012). Rho GTPases cycle between an active GTP-bound state and an inactive GDP-bound state with guanine nucleotide-exchange factors (GEFs) facilitating their activation and GTPase-activating proteins (GAPs) promoting inactivation. Many Rho GTPase effectors, which typically bind to the active form of Rho GTPases, bring downstream signalling pathways into proximity and regulate, as well as remodel, the cytoskeleton. A loss of activity of specific Rho GTPases leads to an impairment of the cytoskeletal organization and hence the polarization process (Mellman and Nelson, 2008). The model yeasts *S. cerevisiae* and *S. pombe* have been very useful in the

study of the molecular mechanisms responsible for cell polarity and of the role of Rho GTPases as modulators of polarized growth (reviewed in Perez & Rincón, 2010).

Cell polarity can be divided into polarity establishment, which can be referred to as symmetry breaking, and polarity maintenance. Symmetry breaking, *i.e.*, establishment of polarity in a round symmetric yeast cell, is driven by a reorganization of the cytoskeleton, which forms a network that allows the transmission of forces inside the cell and vesicular transport (reviewed in Mullins, 2010). The actin cytoskeleton is essential for cell shape change and motility and organelles organization and dynamics (reviewed in Rottner *et al.*, 2017). In yeasts, the actin cytoskeleton marks the location of exocytosis and endocytosis. In contrast, the microtubule cytoskeleton is not used as a major vesicular transport route but is crucial for nuclear migration and division in *S. cerevisiae* and *S. pombe* (reviewed in Martin and Arkowitz, 2014).

In addition to the cytoskeleton, other cellular components that contribute to cell polarity are the plasma membrane (Hammond and Hong, 2017) and endomembranes – endoplasmic reticulum, Golgi and endosomes (Baschieri and Farhan, 2015; Navarro and Miller, 2016). Transport between different membrane compartments is sequential and is mediated by sorting vesicles that are selected or excluded *via* recognition of cargo proteins. Sorting proteins as they travel through the endomembrane system is a mechanism to generate different protein distribution in polarized cells. This protein sorting mechanism must be coupled with the cytoskeleton, for delivery of the vesicles, and protein complexes – Rab-GTPases, vesicle-tethering complexes and SNAREs (Soluble NSF(N-ethylmaleimide-sensitive factor) Attachment Protein REceptor) (Rothman, 1994; Grosshans *et al.*, 2006; Papadopoulos, 2017) – that ensure the docking and fusion to different membrane domains.

b) Polarized Growth in Fungi

The fungal kingdom is extremely diverse and is estimated to have 3.5-5.1 million species (O'Brien *et al.*, 2005), with species that play important roles in health, ecology and industry. Of all the estimated species of fungi, only a few hundred are human pathogens, such as *Aspergillus fumigatus*, *Cryptococcus neoformans*, *Histoplasma capsulatum* and *Candida albicans* (Köhler *et al.*, 2015; Kim, 2016). The Ascomycota phyla are the most extensively studied at

the molecular level and include the yeasts *S. cerevisiae*, *S. pombe* and *C. albicans*. The latter is a diploid polymorphic fungus that is a well-known causative agent of opportunistic infections, which can be deadly depending on the context of infection. In this study, I have examined the initiation and maintenance of polarity in the human fungal pathogen *C. albicans*, specifically during filamentous growth. This introduction focuses mainly on the known aspects of polarized growth in *C. albicans*, with an introduction of the yeast models *S. cerevisiae* and *S. pombe*. Other fungal species are mentioned where relevant.

The budding yeast *S. cerevisiae* can be easily maintained in the laboratory as a haploid or diploid (Morin *et al.*, 2009). After cell division, each daughter cell is round and grows by budding, placing a new bud next to the previous division site or at the opposite pole. Division occurs between the mother cell and daughter bud. Initially, the bud grows apically, extending in length. Then a transition to isotropic growth occurs and with growth throughout the bud, so it expands spherically (Fig. 1a).

The fission yeast *S. pombe* grows as haploid but it can diploidize by conjugation and initiate meiosis when starved for nutrients, especially nitrogen (Yamashita *et al.*, 2017). These rod shaped cells maintain a constant diameter, growing in length by tip extension and dividing by medial fission. Fission yeast cells exhibit several polarity transitions during a mitotic cycle: - a daughter cell initially grows at the “old” pole, which existed before cell division (Fig. 1b); then, in the G2 cell cycle phase, the second “new” pole initiates growth in a process called NETO (New End Take-Off); at the end of G2, the cell stops growing and enters mitosis, redirecting the growth machinery to building the septum in the centre of the cell in the transverse plane.

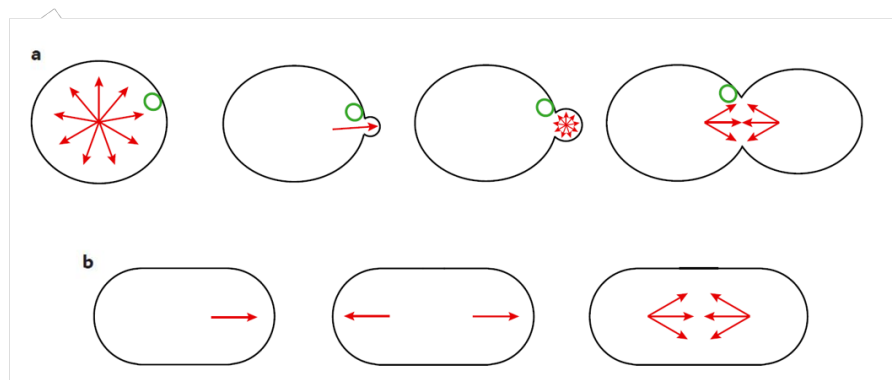


Figure 1. Location of growth sites during mitotic cell division. Red arrows indicate the local addition of new plasma membrane material (proteins, lipids, and cell wall biosynthetic enzymes), which alternates between single and multiple sites in both yeasts. Green indicates bud landmark (Martin and Arkowitz, 2014).

Small GTPases, particularly the conserved small Rho GTPase Cdc42, play an important role at many levels in polarized growth in virtually all eukaryotes (Etienne-Manneville, 2004; Park and Bi, 2007; Bi and Park, 2012). Cdc42 was first discovered in yeast (Adams *et al.*, 1990) and since then it has been shown to be required for cell polarization in many eukaryotic organisms (Etienne-Manneville, 2004). *S. cerevisiae cdc42* mutants continue to grow but are unable to bud at the restrictive temperature (Adams *et al.*, 1990; Johnson and Pringle, 1990) and depletion of Cdc42 produce large, round unbudded cells (Gladfelter *et al.*, 2001). In contrast, Cdc42 depletion in *S. pombe* cells results in small and round cells that do not appear to grow substantially (Miller and Johnson, 1994). Cdc42 will be introduced in more detail in the section III of the Introduction – The Small Rho-GTPase Cdc42 in fungi.

S. cerevisiae cells exhibit a unique axis of polarization, with polarized growth occurring only at one location in a cell at any given moment (Wu *et al.*, 2013). Haploid cells form new single bud in an axial pattern, adjacent to the previous division site, whereas diploid cells form the new bud in a bipolar pattern, at the opposite pole from the previous division site (Chant and Pringle, 1995). A unique axis of polarization is determined by the activation and clustering of Cdc42 in response to internal cues that dictate where the new bud will emerge (Pringle *et al.*, 1995; Johnson *et al.*, 2011), but these internal signals can also be overridden in response to external cues that trigger the formation of mating projections (Herskowitz, 1988; Chang and Peter, 2003; Arkowitz, 2009; Turrà *et al.*, 2015). The location of the active GTP-bound Cdc42 cluster is determined by upstream cortical markers formed by the bud site selection machinery or the site of ligand bound mating pheromone receptors (Bender and Pringle, 1989; Chant and Herskowitz, 1991; Kang *et al.*, 2010). The bud site selection machinery is controlled by the Ras-family GTPase Rsr1/Bud1 (Wu *et al.*, 2013).

In wild-type yeast cells, landmark transmembrane proteins are deposited at specific places during bud formation and then inherited by daughter cells. These proteins include Axl2/Bud10 (forming a ring on both sides of the site of cleavage), Bud8 and Bud9 (localized at the distal and proximal poles of new born cells, respectively), Rax1 and Rax2 (localized as a ring around bud scars) (Chant and Pringle, 1995; Chen *et al.*, 2000, 2004; Harkins *et al.*, 2001; Kang *et al.*, 2004; Gao *et al.*, 2007). These landmark proteins interact

with Bud5, which is a GEF that activates Rsr1/Bud1 locally (Park *et al.*, 1999, 2002; Kang *et al.*, 2001; Marston *et al.*, 2001). Rsr1/Bud1-GTP interacts with Cdc24 recruiting it to the incipient bud site, promoting the activation of Cdc42 and the formation of a cluster of Cdc42•GTP, leading to a new site of polarized growth influenced by the location of landmark proteins (Shimada *et al.*, 2004). Cells lacking Rsr1/Bud1 form a bud at a random location (Bender and Pringle, 1989; Chant and Herskowitz, 1991). The same strain has been reported to have the ability to sustain more than one cluster of Cdc42•GTP at the same time, but then the clusters compete with each other and a single winner emerges (Howell *et al.*, 2012).

Bem1 is a scaffold protein that forms a complex with Cdc24 (the sole Cdc42 GEF) (Sloat *et al.*, 1981; Zheng *et al.*, 1994; Ziman and Johnson, 2004; Irazoqui *et al.*, 2003), Cdc42•GTP and a Cdc42 effector (PAK, p21-activated kinase). When this complex forms, Cdc24 enables the activation of neighbouring molecules of Cdc42•GDP, creating a positive feedback loop that promotes the growth of a cortical cluster of Cdc42•GTP (Goryachev and Pokhilko, 2008; Kozubowski *et al.*, 2008; Howell *et al.*, 2009; Johnson *et al.*, 2011).

The formation of a polarized hypha is a defining feature of filamentous fungi, allowing them to efficiently colonize and exploit new substrates. Filamentous fungi extend over long distances and invade multiple substrates (including soil and host tissues) by hyphal growth (Sheppard and Filler, 2014; Yang *et al.*, 2014; Zeilinger *et al.*, 2016). Fungal hyphae can extend at rates at least two-fold greater than yeast buds or mating projections (Trinci, 1974) by exocytosis at the apex (Bartnicki-Garcia and Lippman, 1969; Wessels, 1988; Pantazopoulou *et al.*, 2014; Guo *et al.*, 2015; Sánchez-León *et al.*, 2015; Takeshita, 2016). Exocytosis is balanced with endocytic uptake of soluble and membrane-bound material to be recycled within the cell (Peñalva, 2010). Another role for the coupling of these two processes could be to enable the spontaneous generation of local asymmetries that potentiate a polarity axis (Steinberg *et al.*, 2017).

Hyphal tip growth, similar to bud growth, is initiated by establishment of a growth site and the subsequent maintenance of the growth axis, while growth supplies are delivered to the apex by motors, along the cytoskeleton (Steinberg, 2007; Schultzhaus and Shaw, 2015). But unlike budding growth, the identity of landmark/marker systems

involved in the establishment of filamentous growth in fungi remains unknown to date, and it is still unclear if such a system is indeed required. *S. pombe* displays two polarized growth modes: an intrinsic vegetative growth, determined by an internal positioning mechanism, and an extrinsic shmooing growth, activated by external pheromone (Merlini *et al.*, 2013, 2017).

Hyphal growth is distinguished by the presence of a structure localized at the tip of growing hyphae, the Spitzenkörper – from German Spitze (“point”) + Körper (“body”), which name derives from light microscopy observations by Brunswick, in 1924 (Brunswick, 1924; Girbardt, 1969; Harris *et al.*, 2005; Virag and Harris, 2006). This accumulation of vesicular components was confirmed in 1969 in fixed cells by ultrastructural studies using electron microscopy (Girbardt, 1969; Grove and Bracker, 1970). Since then, it is still unknown whether this vesicle accumulation has functional importance or rather represents the transient gathering of individual vesicles before they fuse with the plasma membrane. Until this question is resolved, the term Spitzenkörper should be retained (Girbardt, 1969). Despite the Spitzenkörper being considered a defining feature of hyphae, a Spitzenkörper-like structure has been observed in mating projections of *C. albicans* and *S. cerevisiae* and in the constitutive pseudohyphal phenotype of *S. cerevisiae* mutants containing various septin assembly defects (Chapa-y-Lazo *et al.*, 2011; Kim and Rose, 2015).

II – *Candida albicans*, an opportunistic pathogen

a) Species and Genome

Species from the *Candida* genus are typically harmless eukaryotic commensal yeasts, which colonize environmental, human and other mammalian sources. The currently understood position of the genus *Candida* within the fungal kingdom is shown in Fig. 2. These fungi belong to the *Ascomycota* phylum, which has 3 sub-phyla, one of which is the sub-phylum Saccharomycotina. The Saccharomycotina sub-phylum contains the class Saccharomycetes and the order Saccharomycetales (Suh *et al.*, 2006). This order comprises approximately 16 families, two of which diverged approximately 170 million years ago (Wolfe and Shields, 1997; Massey *et al.*, 2003). One of these families, the Saccharomycetales incertae sedis family, contains a subgroup known as the CTG clade, the members of which unusually

translate the CTG codon as serine instead of leucine. The transfer RNA Ser-tRNA_{CAG} first appeared approximately 270 million years ago but the mechanism(s) of this codon reassignment is still unclear (Massey *et al.*, 2003; Miranda *et al.*, 2009; Gomes *et al.*, 2012). This clade contains the majority of the medically relevant *Candida* species. Another clade within the order Saccharomycetales consists predominantly of the *Saccharomyces*, which are species for which the genomes have undergone complete duplication (Wolfe and Shields, 1997; Diezmann *et al.*, 2004; Fitzpatrick *et al.*, 2006), referred to as the whole genome duplication (WGD) clade.

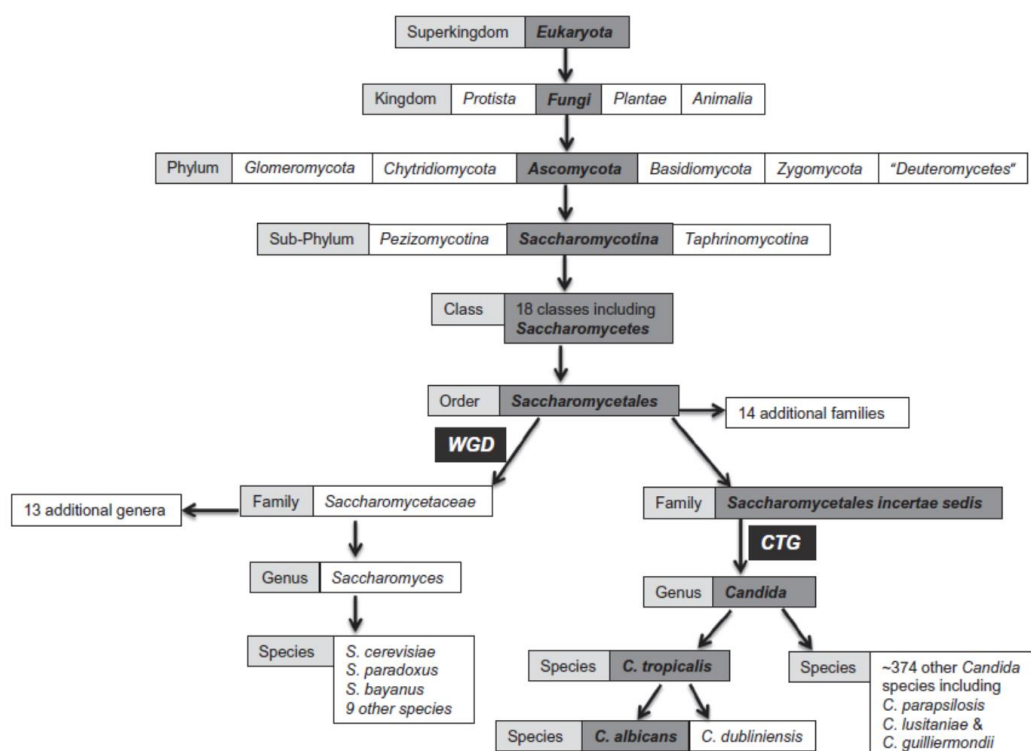


Figure 2. Summary of the current understanding of the ancestry and phylogeny of *Candida albicans*. The evolutionary pathway of *C. albicans* is indicated in bold italicised typeface on a darker grey background. Taxonomic classifications are indicated in plain typeface on a lighter grey background. The genus *Candida* is currently classified with the Saccharomycetales incertae sedis until its family classification is more accurately resolved. The divergence of *C. albicans* and *C. dubliniensis* from its *C. tropicalis* ancestor, thought to have occurred approximately 20 million years ago is illustrated, as is the separation of the whole genome duplication (WGD) and CTG lineages (McManus and Coleman, 2014).

These eukaryotes are part of the commensal microbiota, reside on mucosal surfaces of the gastrointestinal and genitourinary tracts (Kumamoto, 2011) of healthy individuals and cause infection when the host immune defenses become compromised. Only a relatively small number of *Candida* species are of clinical importance for humans, such as *Candida albicans*, *Candida glabrata*, *Candida tropicalis*, *Candida parapsilosis* and *Candida dubliniensis*. *C. albicans* is the most prevalent and the most pathogenic of the *Candida* species

and is responsible for the majority of oral and systemic candidiasis cases and nosocomial candidaemias (Moran *et al.*, 2004; Pfaller *et al.*, 2010; Thompson *et al.*, 2010; Zomorodian *et al.*, 2011). Nosocomial infections are associated with elevated costs and candidaemia – presence in the blood of fungi of the genus *Candida* – is the most common clinical manifestation of invasive candidiasis. Although species prevalence has been shifting in the past decades, *C. albicans* still remains the predominant agent of infection of its genus, accounting for 50% of all cases (Quindós, 2014).

The *C. albicans* genome consists of eight pairs of chromosomal homologs comprising 16 Mb in total (Chibana *et al.*, 2000). The species is predominantly diploid, but can exhibit a high degree of genome plasticity and frequent losses of heterozygosity, as well as massive chromosomal rearrangements, resulting in aneuploidy in azole-resistant strains (Selmecki *et al.*, 2006, 2009, 2010). *C. albicans* does not undergo meiosis, however it can go through a parasexual cycle with the formation of tetraploid progeny following the mating of diploid parents and subsequently diploidy is then restored by chromosome loss (Bennett and Johnson, 2003; Bennett, 2015; Hickman *et al.*, 2015). The parasexual cycle occurs rarely in nature and is thought to occur only under stress conditions (Berman and Hadany, 2012).

b) Morphogenic States

C. albicans is widely referred to as a dimorphic fungi, due to its proliferation in either a budding yeast form or a hyphal form (Fig. 3a). In the former state, growth occurs similar to *S. cerevisiae* budding growth, each daughter cell is round and grows by budding, placing a new bud next to the previous division site or at the opposite pole. The budding form is associated with commensalism (Fig. 3b). During hyphal growth, a germ tube emerges in the mother cell in response to external cues and polarized growth is sustained to grow long hyphae - tube-like filaments with completely parallel sides and no constrictions at the site of septation (Sudbery, 2011) - that are important for tissue invasion (Fig. 3c). This study examines the transition between isotropic and polarized types of growth, focusing predominantly on the hyphal growth.

In spite of the term dimorphic being widely used to describe *C. albicans*, yeast and hyphae are not the only morphological states of *C. albicans*: *i*) pseudohyphae – a form of filamentous growth that involves cell elongation without the formation of true hyphae and

of a Spitzenkörper, with constrictions separating the cells. This form of growth is stimulated by environmental conditions, such as phosphate or alkane rich medium, and by the mutation of genes involved in the cell cycle regulation (Fig. 3a) (Sorkhoh *et al.*, 1990; Hornby *et al.*, 2004; Bensen *et al.*, 2005; Li *et al.*, 2006; Mukaremera *et al.*, 2017; Noble *et al.*, 2017). The pseudohyphal form often coexists with the yeast and hyphal forms during infection (Fig. 3d) (Sudbery *et al.*, 2004; Noble *et al.*, 2017); *ii*) the chlamydoconidia – the ability to form chlamydoconidia has been extensively used to distinguish between *Candida* species in the clinic. These large cells with thick walls, high lipid and carbohydrate content, develop in environments low in oxygen, light, temperature and nutrients, which are thought to be somehow related to the commensal/opportunistic lifestyle of these species (Fig. 3e) (Fabry *et al.*, 2003; Palige *et al.*, 2013; Böttcher *et al.*, 2016); *iii*) the opaque cells. The white-opaque switch is a phenotypic switch, intimately coupled to the sexual mating process in *C. albicans*, exclusive to strains that are homozygous for the MTL locus that controls cell type (Fig. 3f-g) (Morschhäuser, 2010; Zhang *et al.*, 2015; Li *et al.*, 2016).

In both *C. albicans* budding and hyphal growth, cells exhibit polarized growth, yet polarity is more extreme in the hyphal state, as the switch from polarized to isotropic growth, characteristic of budding growth, is replaced by the maintained apical growth of the hypha. The differences between the distinct morphological forms of *C. albicans* include the extent of polarized growth, nuclear migration, position of septation and ability to separate after cytokinesis (Sudbery *et al.*, 2004). In the yeast form, budding occurs either next to the bud scar from the previous cell cycle (axial pattern) or at the opposite end of the cell from where the previous bud formed (bipolar pattern) in a temperature-dependent manner (Chaffin, 1984). A septin ring appears before bud emergence, marking where a bud will emerge (Warenda and Konopka, 2002). Septins are highly conserved structural components that have important roles in *C. albicans* polarization, cell division and virulence (Warenda and Konopka, 2002; Warenda *et al.*, 2003; Blankenship *et al.*, 2014). This septin ring will be the plane across which mitosis will occur between mother and daughter cells (Sudbery *et al.*, 2004). After mitosis is complete, the septin ring separates in two rings and a primary septum, composed of chitin (made by chitin synthase 1, *CHS1*, or *CHS3*) forms between them (Lenardon *et al.*, 2010). An actomyosin ring then forms, contracts and cells separate (González-Novo *et al.*, 2009).

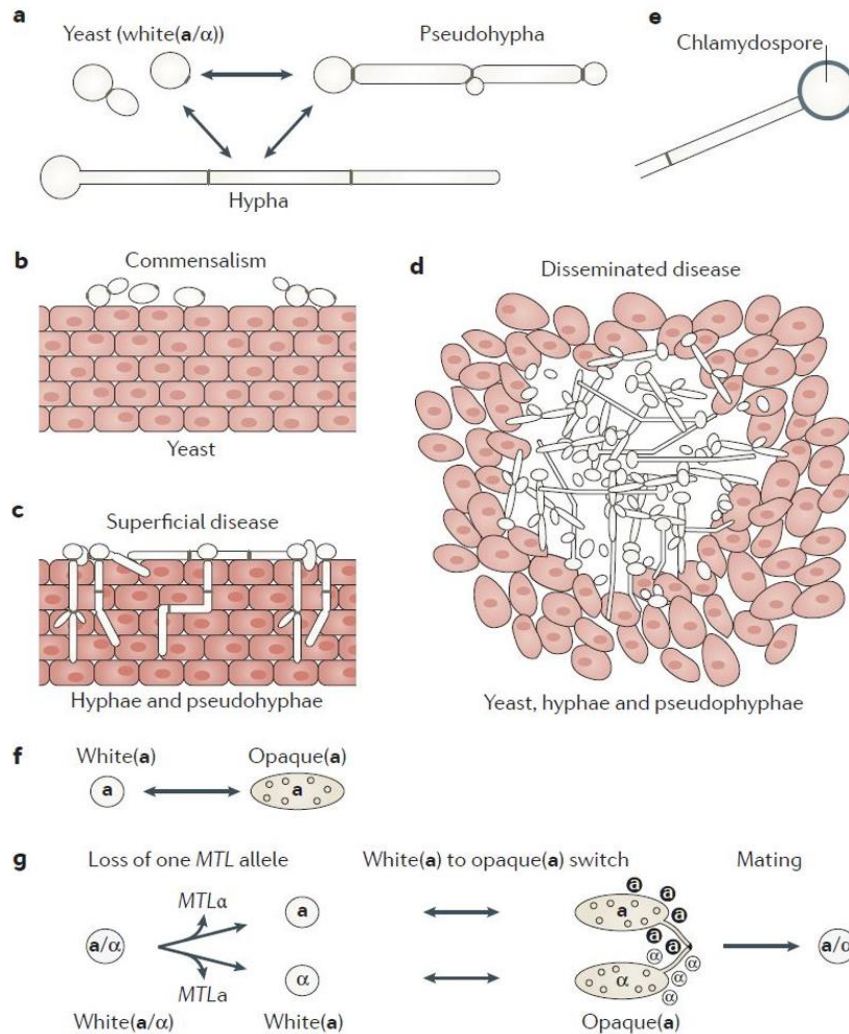


Figure 3. *Candida albicans* cell type transitions. **a** | *C. albicans* switches reversibly between yeast (also known as white(a/α)), hyphal and pseudohyphal cell types under different environmental conditions. **b,c** | In mucocutaneous infection models, such as oropharyngeal candidiasis, yeasts are associated with commensalism (part **b**), whereas the filamentous forms (hyphae and pseudohyphae) are associated with tissue invasion and damage (part **c**). **d** | Yeasts, hyphae and pseudohyphae all seem to have roles in disseminated disease — for example, in abscesses within internal organs of the host. **e** | Chlamydospores are produced by terminal (suspensor) cells of mycelia (multicellular hyphae or pseudohyphae) under adverse growth conditions. **f** | Mating-type-like (MTL) loci $MTLa$ (a) or $MTL\alpha$ (α) cells can undergo an epigenetic switch between white(a or α) and opaque(a or α) phenotypes. White (a or α) cells have the same appearance as typical budding yeasts, whereas opaque (a or α) cells are elongated and have ‘pimple’ structures on their cell surface. **g** | Mating in *C. albicans* requires three events: loss of one allele of the MTL locus ($MTL\alpha$ or $MTLa$) to generate white (a) or white (α) strains; an epigenetic switch from white (a or α) to opaque (a or α); and pheromone sensing by opaque (a or α) cells of the opposite mating type, which triggers sexual filament production and mating (figure from Noble *et al.*, 2017).

The incipient point of evagination of germ tubes is marked by a septin patch, which then forms a band at the base of the germ tube and a cap at the tip (Warenda and Konopka, 2002). As the germ tube elongates, the septin cap at the tip generates a ring in the germ tube that remains fixed in position as the tip continues to elongate. The nucleus then migrates out of the mother cell and mitosis occurs within the germ tube. After

mitosis, one daughter nucleus migrates back to the mother cell and the other nucleus migrates to the apical side of the septin ring (Sudbery, 2001; Finley and Berman, 2005). The septum of hyphal cells forms similarly to the septum of yeast or pseudohyphae, with a contraction of the actomyosin ring, yet cytokinesis does not result in a constriction, so the characteristic long tube-like structure is maintained (Sudbery, 2011).

c) Virulence

During both superficial and systemic infections, *C. albicans* relies on a wide arsenal of virulence factors and fitness attributes. Morphological transition between yeast and hyphal forms, expression of adhesins and invasins on the cell surface, and thigmotropism, capacity to form biofilms, phenotypic switching and secretion of hydrolytic enzymes are considered virulence factors (reviewed in Mayer *et al.*, 2013). In addition, the ability to adapt rapidly to environmental changes contributes to this fungus increased fitness (Nicholls *et al.*, 2011). During hyphal formation, a subset of genes is expressed. These genes encode virulence factors that are not directly involved in hyphal formation but provide an adaptative advantage as *C. albicans* invades the host tissues and causes infection (Mayer *et al.*, 2013). The most highly expressed genes encode the extensively studied adhesin agglutinin-like sequence protein 3 (*ALS3*), the GPI-anchored hyphal wall protein 1 (*HWP1*), secreted aspartyl protease (*SAP*) family proteins, such as *SAP4*, *SAP5* and *SAP6*, and Extent of Cell Elongation protein 1 (*ECE1*), a fragment of which is now referred to as candidalysin – a fungal peptide toxin (Fan *et al.*, 2013; Hoyer *et al.*, 2014; Orsi *et al.*, 2014; Modrezewka and Kurnatowski, 2015; Moyes *et al.*, 2016; Richardson *et al.*, 2018). These proteins become of primary importance in the interaction of *C. albicans* with host cell surface receptors. Specifically, targeting virulence factors has been proposed as an alternate antifungal strategy (Gauwerky *et al.*, 2009), hence, the understanding the pathogenicity mechanisms used by *C. albicans* during infection is of utmost importance.

C. albicans ability to switch from yeast to hypha has drawn interest because of its relevance to pathogenicity; it is believed that each form of growth provides critical functions important for the pathogenic lifecycle (Sudbery *et al.*, 2004; Jacobsen *et al.*, 2012). Hyphae and pseudohyphae are postulated to promote tissue penetration during the early stages of infection, whereas the yeast form is thought to be more suited for dissemination

in the bloodstream (Saville *et al.*, 2003; Jacobsen *et al.*, 2012; Noble *et al.*, 2017). However, it is important to note that most dimorphic fungi that infect humans exhibit growth by budding in infected tissues and exist as filamentous mycelial fungi in the external environment, such as *H. capsulatum* or *Sporothrix schenckii* (Lorenz *et al.*, 2004; Gauthier, 2015). This fact suggests that filamentous growth is not mandatorily coupled with tissue invasion. However, *C. albicans* mutants that are unable to form or sustain hyphal growth *in vitro*, are attenuated in virulence (Lo *et al.*, 1997; Iranzo *et al.*, 2003; Kavanaugh *et al.*, 2014; Labbaoui *et al.*, 2017). This observation supports the view that the ability to form hyphae is an important virulence attribute for this fungus.

d) Polarized Filamentous Growth

As mentioned previously, the ability to switch from yeast to hyphal growth is a striking characteristic of *C. albicans*, which is clinically relevant (Mayer *et al.*, 2013). *C. albicans* is well adapted to growth in its human host and forms hyphae under a varied range of environmental conditions. For example, hyphae form in response to the presence of serum (Taschdjian *et al.*, 1960), neutral pH (Buffo *et al.*, 1984), 5% CO₂ (Mardon *et al.*, 1969), N-acetyl-glucosamine (GlcNAc) (Simonneti *et al.*, 1974), and generally requires a temperature of 37 °C. The combination of serum and 37 °C provides a powerful signal for germ tube formation from yeast-form cells. The ability to form hyphae can be assessed in liquid or in solid media. Liquid media conditions are used to test the ability to initiate hyphal growth and the solid media conditions are used to test whether the organism can maintain invasive hyphal growth in a complex and changing environment as the colony develops in the agar.

The interaction with the microflora, which *C. albicans* encounters in its environment, acts as a regulator for the morphological switch. Communication with other cells, not only other *C. albicans* cells but also bacteria, relies on quorum sensing (Shareck and Belhumeur, 2011). For example, farnesol, a sesquiterpene that is secreted by *C. albicans* inhibits hyphal formation (Hornby *et al.*, 2001; Lu *et al.*, 2014). In contrast, the aromatic alcohol tyrosol promotes hyphal formation in biofilms (Chen *et al.*, 2004). *C. albicans* can also form mixed infections with bacterial species, such as *Pseudomonas aeruginosa*, as both species are often recovered from lung infections of cystic fibrosis patients or infections in burned patients (De Sordi and Muhlschlegel, 2009). The bacteria attach specifically to the hyphae, leading

to the death of the fungal cell. As a response, *C. albicans* senses the presence of bacteria, *via* 3-oxo-C(12)-homoserine lactone (HSL) - a component of the *P. aeruginosa* quorum sensing mechanism – and hyphal growth is repressed in favour of budding growth (Hogan and Kolter, 2002; Hogan *et al.*, 2004; Hogan, 2006; De Sordi and Muhlschlegel, 2009).

The expression of hyphal-specific genes is negatively controlled by the general transcriptional co-repressor Tup1, which forms a complex together with Nrg1 or Rfg1 (Braun and Johnson, 1997; Braun *et al.*, 2001; Murad *et al.*, 2001; Kadosh and Johnson, 2005). Positive regulation of hyphal-specific genes is carried out by a variety of transcription factors, including Efg1 (Stoldt *et al.*, 1997), Cph1 (Liu *et al.*, 1994; Leberer *et al.*, 1996), Cph2 (Lane, Zhou, *et al.*, 2001), Tec1 (Lane, Birse, *et al.*, 2001), Flo8 (Simonneti *et al.*, 1974), Czf1 (Cao *et al.*, 2006), Rim101 (Fig. 4; Davis *et al.*, 2000; El Barkani *et al.*, 2000). Efg1 is thought to be the major regulator of hyphal formation under most conditions (Braun and Johnson, 2000; Sohn *et al.*, 2003; Nobile *et al.*, 2012; Jakubovics, 2017). Efg1 and Cph1 are activated *via* different upstream signalling pathways (Biswas and Morschhäuser, 2005). The former is activated through the cyclic AMP protein kinase A (cAMP-PKA) pathway (Tebarth *et al.*, 2003), whereas the latter depends on the mitogen-activated protein kinase (MAPK) signalling pathway (Liu *et al.*, 1994; Malathi *et al.*, 1994). The guanine nucleotide binding protein Ras1 is involved in both pathways: it activates Cyr1 in the cAMP-PKA pathway and Cdc42 in the MAPK pathway (Feng *et al.*, 1999; Leberer *et al.*, 2001). These signalling pathways are the most studied in *C. albicans* hyphal growth. They share several upstream components and respond to multiple host environmental conditions including serum, body temperature (37 °C), nitrogen starvation, high CO₂ levels, GlcNAc, certain amino acids and quorum sensing molecules (Sudbery, 2011). Other pathways have been described to regulate *C. albicans* hyphal growth. These include the high osmolarity glycerol (Hog), the protein kinase C (Pkc) 1 cell wall integrity, the regulation of Ace2 and morphogenesis (RAM), the Rac1 activation and the Rim101 pathways (Alonso-Monge *et al.*, 1999; Brown *et al.*, 1999; Davis *et al.*, 2000; Kullas *et al.*, 2004; Li *et al.*, 2004; Kumamoto, 2005; Bassilana and Arkowitz, 2006; Song *et al.*, 2008; Hope *et al.*, 2008; Shapiro *et al.*, 2011; Saputo *et al.*, 2012; Calderón-Noreña *et al.*, 2015).

C. albicans has a single adenylyl cyclase encoded by *CYR1*. This gene has the role of integrating a range of environmental signals into the cAMP-PKA pathway and is essential

for hyphal formation (Rocha *et al.*, 2001; Zou *et al.*, 2010). Serum-mediated hyphal induction stimulates Cyr1 through the interaction with Ras1 with a RAS-associated domain in Cyr1 (Fang and Wang, 2006; Piispanen *et al.*, 2011, 2013). Elevated temperature is required for all hypha-inducing conditions (except growth in embedded matrix). Temperature is sensed by the heat shock protein 90 (Hsp90) (Shapiro *et al.*, 2009). Inhibition of Hsp90 using geldanamycin leads to hyphal growth, and mutant strains with a reduction in Hsp90 levels form hyphae in a media with serum at 30 °C instead of 37 °C (Shapiro *et al.*, 2009). Hsp90 has been shown to activate hyphal growth *via* the cAMP-PKA pathway, although an *efg1* mutant still forms hyphae when Hsp90 is inhibited, which suggests an alternative downstream target for Hsp90 (Shapiro *et al.*, 2009). This pathway is also activated by the transmembrane ammonium permease Mep2, under nitrogen starvation conditions (Biswas and Morschhäuser, 2005). The previously mentioned quorum sensing molecules farnesol and HSL both inhibit *C. albicans* Cyr1 activity, inhibiting the cAMP-PKA signalling cascade and hyphal growth (Lindsay *et al.*, 2012).

Ras1 activates the Cdc42 Rho GTPase *via* its GEF Cdc24 (Piispanen *et al.*, 2011). Cdc42 then activates the MAPK signalling pathway, and the terminal MAPK of this cascade, Cek1, is important to activate Cph1 (Csank *et al.*, 1998) - the downstream transcription factor for this cascade and an homolog of *S. cerevisiae* Ste12 (involved in mating pheromone response) (Liu *et al.*, 1994). Cph1, in turn, controls the level of activation of some hyphal-specific target genes (Leng *et al.*, 2001; Brown *et al.*, 2007; Shapiro *et al.*, 2011). During serum-induced hyphal growth, both Cdc42 and Cdc24 localized to the hyphal tip (Hazan and Liu, 2002; Bassilana *et al.*, 2005).

Hypha formation requires both sustained apical growth and inhibition of cell separation. Strains with reduced expression levels of Cdc42 and its GEF Cdc24 are viable but unable to switch to polarized hyphal growth in response to serum (Bassilana *et al.*, 2005). While Cdc42 and Cdc24 both localize at the tip of growing hyphae (Hazan and Liu, 2002; Bassilana *et al.*, 2005), one of the two Cdc42 GAPs, Rga2, no longer localizes at the hyphal tip upon CDK/Hgc1 phosphorylation (Court and Sudbery, 2007; Zheng *et al.*, 2007). During budding growth in *S. cerevisiae*, a number of proteins associate with the septin ring and cell separation is ensured by enzymes coded by genes from the RAM pathway (Roncero and Sanchez, 2010). In *C. albicans*, deletion of genes of the RAM pathway results in cell septation defects (Kelly *et al.*, 2004; Song *et al.*, 2008; Saputo *et al.*, 2012)

III – The small Rho-GTPase Cdc42 in fungi

a) Rho GTPases

The Ras superfamily of GTPases is particularly interesting, as its members are master regulators of many varied aspects of cell behaviour, such as regulation of gene expression, cell proliferation, differentiation, cell polarity, cell movement, cell-cell interactions, endocytosis and exocytosis, vesicle formation and fusion with the acceptor compartment, vesicle transport and nucleocytoplasmic transport of RNA and proteins (Wennerberg *et al.*, 2005). This superfamily of monomeric GTPases, with over 60 representatives in mammals, is divided in 5 major families: Ras, Rho, Rab, Arf and Ran (Wennerberg *et al.*, 2005). The first reports of the cellular functions of Rho GTPases date from 1990, when they were identified in yeast and human cells (Bender and Pringle, 1989; Adams *et al.*, 1990; Johnson and Pringle, 1990; Munemitsu *et al.*, 1990; Shinjo *et al.*, 1990). Here, I focus specifically on Rho GTPases, emphasizing the role of the master regulator of polarized growth, Cdc42, in fungi. Other Rho GTPases play a role in hyphal growth, Rho3 is required for actin polarization, Rho1 is required for invasive filamentous growth and Rac1 and its GEF, Dck1, are required for matrix embedded filamentous growth (Basilana and Arkowitz, 2006; Hope *et al.*, 2008; Corvest *et al.*, 2013).

Rho GTPases are highly conserved molecular switches in eukaryotes involved in the regulation of morphogenesis (Etienne-Manneville and Hall, 2002; Etienne-Manneville, 2004; Arkowitz and Basilana, 2015; Hervé and Bourmeyster, 2015). There are 2 distinct RhoGEF families, the DH/PH (Dbl homology and Pleckstrin homology)-domain-containing proteins (Rossman *et al.*, 2005) and DOCK (Dedicator of cytokinesis) homology domain (Meller, 2005). These proteins can hydrolyze GTP and hence cycle between two conformational states: a GTP-bound active state and a GDP-bound inactive state (Fig. 4). In the active GTP-bound state, they interact with effector proteins and, in contrast, in the inactive GDP-bound state, they typically do not interact with their targets, thereby interrupting signaling (Vetter and Wittinghofer, 2001; Etienne-Manneville and Hall, 2002; DerMardirossian and Bokoch, 2005).

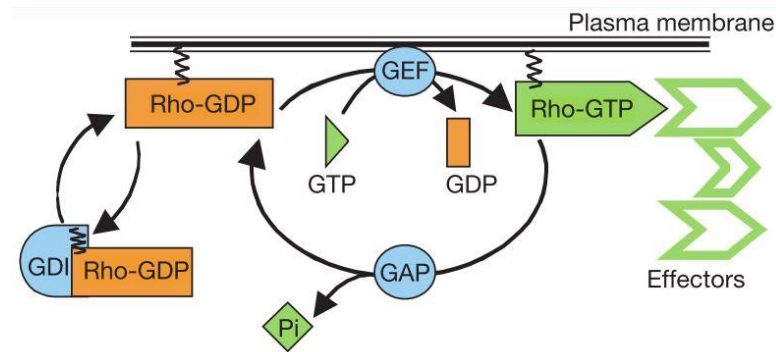


Figure 4. The Rho GTPase cycle. Rho GTPases cycle between an active (GTP-bound) and an inactive (GDP-bound) conformation. In the active state, they interact with one of over 60 target proteins (effectors) in mammalian cells. The cycle is highly regulated by three classes of proteins: the guanine nucleotide exchange factors (GEFs) catalyze nucleotide exchange and thereby mediate activation; the GTPase-activating proteins (GAPs) stimulate GTP hydrolysis, leading to inactivation; and the guanine nucleotide exchange inhibitors (GDIs) extract the inactive GTPase from membranes. All Rho GTPases are prenylated at their C terminus, a process required for their function (Etienne-Manneville and Hall, 2002).

Rho GTPases share a common G-domain fold, which consists of 5 α -helices and 6-strand β -sheet (Vetter and Wittinghofer, 2001). The formation of the active GTP-bound state occurs with a conformational change in the N-terminal regions, known as switch I and switch II (Fig. 5). These two regions not only constitute the nucleotide binding pocket but also engage with their regulators (GEFs, GAPs and GDIs) and downstream effectors (for example kinases) (Ihara *et al.*, 1998; Burrige and Wennerberg, 2004; Miyazaki *et al.*, 2006; Parri and Chiarugi, 2010). Rho GTPase GEFs contain the catalytically active Dbl homology (DH domain) followed by an adjacent pleckstrin homology (PH) domain (Erickson and Cerione, 2004). These two domains interact with switch I and switch II regions inducing a conformational rearrangement that promotes nucleotide ejection and is the defining mechanism of activation and inactivation of the GTPases, termed the loaded-spring mechanism (Vetter and Wittinghofer, 2001). GTP can be hydrolysed from the Rho GTPase by an intrinsic reaction that can be stimulated through the interaction of the GTPase with GAPs; GAPs have a conserved catalytic domain, which is sufficient for GTPase binding and for the stimulation of the GTP-hydrolysis reaction (Vetter and Wittinghofer, 2001). Effectors containing a Cdc42/Rac1-interactive binding (CRIB) domain bind to Cdc42/Rac1 at the switch I domain (Abdul-Manan *et al.*, 1999; Morreale *et al.*, 2000). At the C-terminus of Rho GTPases is the CAAX box, where post-translational isoprenylation on the cysteine residue facilitates the specific binding to the plasma membrane, which is essential for their biological activity (Olofsson, 1999; McTaggart, 2006; Park and Bi, 2007).

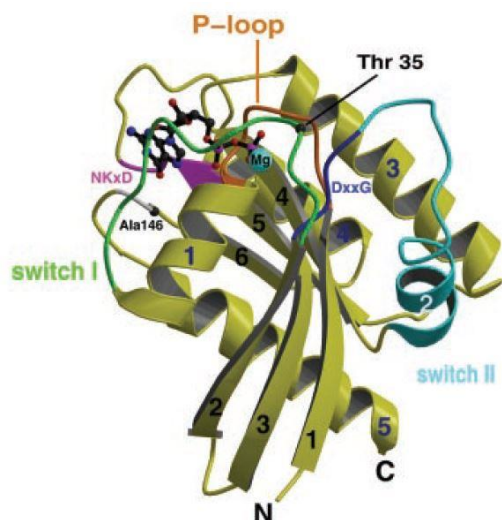


Figure 5. Structure of guanine nucleotide binding proteins. Ribbon plot of the minimal G domain, with the conserved sequence elements and the switch regions in different colors as indicated. The nucleotide and Mg²⁺ ion are shown in ball-and-stick representation (Vetter and Wittinghofer, 2001).

GEFs interact with Rho proteins and alter the nucleotide-binding site, facilitating the release of the nucleotide and, since the cytoplasmic concentration of GTP is higher than that of GDP, it is more likely that Rho proteins will bind with GTP (Bos *et al.*, 2007). In addition, GAPs promote the hydrolysis of GTP from Rho proteins (Bos *et al.*, 2007). There are more Rho GEFs and GAPs than Rho proteins - one Rho protein can be regulated by more than one GEF and GAP, and these regulators can interact with more than one Rho protein (García *et al.*, 2006). For example, *S. pombe* Cdc42 has two GEFs, Scd1 and Gef1, which regulate apical growth and cytokinesis, respectively (Coll *et al.*, 2003; Hirota *et al.*, 2003). It is thought that this promiscuity accounts for a process-specific regulation of a Rho protein. Rho GEFs and GAPs also have the ability to bind other proteins and membranes due to their multidomain configuration. In turn, these proteins change the activation state of Rho proteins and can also act as scaffold proteins, aiding Rho protein localization and coupling upstream signals with downstream effectors (Toenjes *et al.*, 1999; Bose *et al.*, 2001; Ito *et al.*, 2001; Gimona *et al.*, 2002; Bos *et al.*, 2007; Lemmon, 2008; Yohe *et al.*, 2008). Other regulators of Rho proteins are GDIs, which control the access of Rho GTPases to GEFs and GAPs. GDIs interact only with the GDP-bound state and sequester the GTPase from the membrane into the cytoplasm (DerMardirossian and Bokoch, 2005).

b) Cdc42-Cdc24 Module in fungi

In the fungal kingdom, polarized growth depends on a number of different small GTPases of the Ras family. Bud site selection in the budding yeast *S. cerevisiae* is one of the best studied cell polarization systems. Wild-type yeast cells use landmark-directed cues and a GTPase cascade that transduces these signals, which is initiated with Rsr1/Bud1, to choose the polarization axis in a process called symmetry breaking (Singh *et al.*, 2017). However, cells can also polarize in the absence of spatial information, *i.e.*, in an *rsr1/bud1* deletion mutant (Wedlich-Söldner and Li, 2003). In *S. cerevisiae*, the activation at the bud landmark of the essential Rho GTPase Cdc42 requires the GEF Cdc24, which binds the GTP bound form of Rsr1/Bud1 (Park and Bi, 2007; Kang *et al.*, 2010). *C. albicans* mutants that lack Rsr1/Bud1 or Bud2 form wider hyphae than wild type cells and are unable to maintain hyphal growth in one direction (Hausauer *et al.*, 2005). Rsr1/Bud1 *C. albicans* mutants have also been demonstrated to be less virulent, this can be attributed to the reduced germination, shorter hyphae and defects in thigmotropism and galvanotropism (hyphal turning in response to changes in substrate topography and imposed electrical fields, respectively) and penetration into semisolid substrates (Yaar *et al.*, 1997; Brand *et al.*, 2008).

The current model of symmetry breaking suggests that Cdc42•GTP accumulates stochastically and induces a positive feedback loop mediated by Cdc42•GTP, the Cdc24 scaffold protein Bem1 and the PAK kinase Cla4, (Howell *et al.*, 2012; Rapali *et al.*, 2017). This protein complex is required for polarity establishment and *in vivo* and computational model analysis of symmetry breaking are consistent with positive feedback *via* local Cdc42 activation (Chenevert *et al.*, 1992; Holly and Blumer, 1999; Bose *et al.*, 2001; Butty *et al.*, 2002; Ozbudak *et al.*, 2005; Goryachev and Pokhilko, 2008). When this complex forms, Cdc24 GEF activity is increased, enhancing the activation of neighbouring molecules of Cdc42•GDP. A positive feedback loop is initiated and promotes the formation of a cortical cluster of activated Cdc42 at the polarization site (Gulli *et al.*, 2000; Bose *et al.*, 2001; Goryachev and Pokhilko, 2008; Kozubowski *et al.*, 2008; Howell *et al.*, 2009; Johnson *et al.*, 2011; Woods *et al.*, 2015). On the other hand, Bem1 triggers a negative feedback loop as it brings Cdc24 and Cla4 together, resulting in subsequent Cdc24 phosphorylation by Cla4, leading to the disruption of its GEF activity, and release from the Bem1 scaffold complex (Howell *et al.*, 2012; Rapali *et al.*, 2017). An actin-dependent process has also been

implicated in a second positive feedback loop for symmetry breaking, *via* local delivery of Cdc42 (GDP or GTP bound). Actin nucleation depends upon the formation of a Cdc42•GTP cluster at the cortex and, in turn, the accumulation and stabilization of the Rho GTPase relies on actin-dependent vesicle transport and endocytosis (Wedlich-Söldner *et al.*, 2003; Marco *et al.*, 2007; Slaughter *et al.*, 2009, 2013). These two models are not mutually exclusive, however findings from different laboratories lead to contradictory conclusions regarding their relative importance.

Cdc42 is a central regulator of the polarisome, a complex of the proteins localized at sites of growth that is required for actin polarization and polarized growth. This complex was initially identified in budding yeast and is composed of the proteins Spa2, Pea2 and Bud6 (Sheu *et al.*, 1998). The polarisome has been observed in several filamentous fungi, such as *Neurospora crassa*, *Aspergillus nidulans*, *Ashbya gossypii* and *C. albicans*, where it localizes to a crescent at the tip of growing hyphae (Crampin *et al.*, 2005; Köhli *et al.*, 2008; Jones and Sudbery, 2010; Lichius *et al.*, 2012).

Bud initiation and growth are tightly coordinated with the cell cycle. In the budding yeast model, cell polarization occurs only once per cell cycle, being dependent on signals that are triggered by the cyclin-dependent kinase 1 (CDK1) Cdc28 and its cyclin partners (Enserink and Kolodner, 2010). Cdc28 activity has been suggested to be required for proper localization of the GEF of Cdc42, Cdc24, to the presumptive bud site (Gulli *et al.*, 2000; Moffat and Andrews, 2004). Although Cdc28 phosphorylates Cdc24 *in vitro* (McCusker *et al.* 2007), Cdc24 function *in vivo* is not affected by mutation of predicted phosphorylation sites (Gulli *et al.*, 2000; Wai *et al.*, 2009; Rapali *et al.*, 2017). The PAK-like kinase Cla4 is thought to phosphorylate Cdc24 (Gulli *et al.*, 2000), and Cla4 has been implicated in a Cdc28-Clb-dependent pathway that promotes the switch from polar to isotropic bud (Tjandra *et al.*, 1998).

During the G1/S transition of the cell cycle of *S. cerevisiae*, Cdc42•GTP localizes to the polarization site which becomes the bud tip. When bud growth switches from apical to isotropic, Cdc42 redistributes from a tip cortical location to the septin ring in late anaphase (Lew and Reed, 1993). The uniqueness of a site of growth at any given time in *S. cerevisiae* is controlled by the Cdc28/G1 CDK-cyclin complex regulation of Cdc42, so when Cdc42 is

no longer under the control of the cyclin complex, *e.g.*, upon overexpression of a constitutively active mutant (Cdc42[G12V] or Cdc42[Q61L]), and in the absence of all G1 cyclins, polarization occurs at multiple sites (Gulli *et al.*, 2000; Wedlich-Söldner and Li, 2003). Mathematical modelling and studies on artificially rewired cells suggest that there is a fast competition between polarization clusters, which is ultimately responsible for restricting polarization to a single site (Goryachev and Pokhilko, 2008; Howell *et al.*, 2009). Increased expression of a constitutively active form of Cdc42 at the plasma membrane led to an increased number of cells initiating polarization at two or more sites (Wedlich-Söldner *et al.*, 2003). Mutations (dominant negative, Cdc42[T17N], and constitutively active, Cdc42[G12V] and [Q61L]) in the Cdc42 putative GTP binding and hydrolysis domains negatively impact cell proliferation (Ziman *et al.*, 1991; Vanni *et al.*, 2005). FRAP experiments of the inactive Cdc42[D57Y] mutant and the constitutively active Cdc42[Q61L] mutant revealed a much slower recovery of fluorescence compared to wild-type Cdc42 (Wedlich-Söldner *et al.*, 2004). Taken together, these results suggest that the ability of Cdc42 to cycle between the active and inactive states plays an important role in the exchange of Cdc42 between the polarization site and the cytosol, hence proper function (Ziman *et al.*, 1991; Wedlich-Söldner *et al.*, 2004; Vanni *et al.*, 2005).

Cdc42 is essential for polarized growth in the fission yeast *S. pombe*, and the spatial control of its activation determines cell width (Kelly and Nurse, 2011). Active Cdc42 localizes at the cells tips, where it cycles between the active and inactive states, and unlike what has been observed in *S. cerevisiae*, the expression of constitutively active Cdc42 promotes a non-polarized phenotype, resulting in round cells (Miller and Johnson, 1994; Bendezú *et al.*, 2015). *S. pombe* has two known Cdc42 GEFs, Scd1 and Gef1, which are essential and localize to the cell tip and division site (Coll *et al.*, 2003; Rincon *et al.*, 2007), where active Cdc42 is observed (Miller and Johnson, 1994; Tatebe *et al.*, 2008). Cells lacking Scd1 are also round and have endocytosis defects (Murray and Johnson, 2001), while deletion of Gef1 results in slightly thinner cells with defects in bipolar growth and cytokinesis (Coll *et al.*, 2003). The formin For3 is activated by Cdc42 and is responsible for the formation of the actin cables that stabilize the axis of polarity by directing secretion towards the tips (Bendezú and Martin, 2011; Estravís *et al.*, 2011; Kelly and Nurse, 2011; Bonazzi *et al.*, 2015). Both GAPs, Rga4 and Rga6, localize to non-growing tips and lateral areas of the plasma membrane, spatially restricting active Cdc42 at the cell tips to maintain

cell width (Kelly and Nurse, 2011; Revilla-Guarinos *et al.*, 2016; Singh *et al.*, 2017). All these proteins promote the formation of a polarity axis by restricted activation of Cdc42. Homologues of Cdc42 and its GEF, Cdc24, are essential in other fungi, such as *C. albicans* (Ushinsky *et al.*, 2002; Bassilana *et al.*, 2003), *A. gossypii* (Wendland and Philippsen, 2001) and *Penicillium marneffei* (Boyce *et al.*, 2003). In *N. crassa*, mutants with deletion of either Cdc42 or Rac are viable, yet deletion of both genes is lethal (Araujo-Palomares *et al.*, 2011).

In *C. albicans*, reduced expression of Cdc42, using the *MET3* regulatable promoter, is sufficient for viability but not for sustained hyphal growth, indicating that a higher level of Cdc42 is required for polarized hyphal growth as opposed to budding growth (Bassilana *et al.*, 2003). In addition, *C. albicans* Cdc42 and Cdc24 are also required for the expression of hypha specific genes (VandenBerg *et al.*, 2004; Bassilana *et al.*, 2005). Similar to budding and fission yeast, *C. albicans* Cdc42 localizes to the plasma membrane (Hazan and Liu, 2002) and in the active GTP-bound state it forms a cluster at the site of the incipient germ tube (Corvest *et al.*, 2013). The dynamics of the formation of this cluster suggests that it is due to site-specific GEF activity (Corvest *et al.*, 2013), rather than of diffusion in the plane of the membrane, as diffusion of a modified prenylated GFP has been demonstrated to be too slow (Vernay *et al.*, 2012). In addition to increased GEF activity, decreased GAP activity is involved in the sustained localized active Cdc42 at the hyphal tip (Court and Sudbery, 2007; Zheng *et al.*, 2007). During *C. albicans* hyphal growth, active GTP-bound Cdc42 and its GEF Cdc24 localize at the tip of growing hyphae (Hazan and Liu, 2002; Bassilana *et al.*, 2005). An increase in the amount of the activated form of Cdc42 by deleting its GAPs, *RGA2* and *BEM3*, leads to the formation of hyphae under conditions that would normally only induce pseudohyphal formation (Court and Sudbery, 2007).

Tight regulation of the proteins that control the GTPase cycling has been predicted to be required for the maintenance of Cdc42 activity and its fast turnover (Goryachev and Pokhilko, 2006). In *S. cerevisiae*, Cdc42 is recycled to the polarity site *via* the fast cytosolic route, which requires the only known GDI, Rdi1 (Masuda *et al.*, 1994; Tiedje *et al.*, 2008), or *via* the slower membrane-mediated route of endocytosis for eventual recycling through the secretory pathway (Wedlich-Söldner *et al.*, 2004; Goryachev and Pokhilko, 2008; Slaughter *et al.*, 2009). The latter route will be further introduced in the next chapter of the Introduction. In budding yeast, Rdi1 extracts Cdc42 from vacuolar (Eitzen *et al.*, 2001) and

internal membranes as well as from the plasma membrane (Richman *et al.*, 2004; Tiedje *et al.*, 2008). Cells expressing inactive Cdc42[D57Y] or constitutively active Cdc42[Q61L] are defective in complex formation with Rdi1 (Slaughter *et al.*, 2009). In addition, the interaction between Cdc42[Q61L] and Cdc42 effectors is stabilized and hence the constitutively activated mutant is protected from endocytosis (Slaughter *et al.*, 2009). These results suggest that the GTPase cycle regulates both Cdc42 recycling pathways by enabling interaction with Rdi1 and releasing Cdc42 from its effectors, hence promoting endocytosis. In *C. albicans*, an Rdi1 homologue has been identified, and the loss of Rdi1 greatly reduces filamentous growth (Court and Sudbery, 2007). Cathodal emergence of hyphae in a galvanotropic system was also impaired when apical recycling pathways were disrupted in an *rdi1* and *bnr1* mutants, but was completely restored by extracellular Ca(2+) (Brand *et al.*, 2014).

In a study from 2002, it has been shown that ectopic expression of the Cdc42 hyperactive allele G12V and dominant negative D118A allele blocked proliferation of *C. albicans* in yeast growth medium, with the formation of large, round, multinucleated cells (Ushinsky *et al.*, 2002). The hyperactive allele generated multi-budded cells, whereas the dominant negative allele generated unbudded cells. The lethality of ectopic expression of Cdc42[G12V] was suppressed by deletion of *Cst20* but not by deletion of *Cla4*. *Cst20* and *Cla4* are the homologs of *S. cerevisiae* Ste20 and Cla4 CRIB-containing PAK kinases, respectively (Kohler and Fink, 1996; Leberer *et al.*, 1996; Csank *et al.*, 1998). When examined under hypha-inducing conditions, ectopic expression of the Cdc42[G12V] and Cdc42[D118A] produced aberrant filaments. These phenotypes were dependent on the presence of the CAAX box (Ushinsky *et al.*, 2002). Deletion of *CLA4* caused defects in hyphal formation *in vitro*, in both liquid and solid media, and reduced virulence and colonization of the kidneys in a mouse model for systemic candidiasis (Leberer *et al.*, 1997). Small Rho GTPases play critical roles in polarized growth for a range of organisms. Many of these proteins are important in filamentous growth and pathogenicity *via* regulation of cell wall integrity, growth site selection as well as polarity establishment and maintenance. Diverse studies, referred to in this work, are starting to reveal common mechanisms of temporal and spatial growth control.

IV – Cell reorganization during polarized growth in filamentous fungi

a) Actin cytoskeleton

The actin cytoskeleton is crucial for *C. albicans* filamentous growth (Yokoyama *et al.*, 1990; Hazan and Liu, 2002; Jones and Sudbery, 2010; Pointer *et al.*, 2015). When the actin cytoskeleton is disrupted with specific drugs that inhibit the formation of microfilaments of actin (filamentous actin, F-actin), latrunculin A or cytochalasin A, growth is inhibited and filamentation is blocked (Akashi *et al.*, 1994; Hazan and Liu, 2002; Crampin *et al.*, 2005; Jones and Sudbery, 2010). Septins, cytoskeletal proteins which are important for cell division, are also critical for proper morphogenesis in *C. albicans*, as mutants in the septins Cdc10 and Cdc11 are defective for invasive growth and virulence (Warenda and Konopka, 2002; Warenda *et al.*, 2003).

While the actin cytoskeleton is essential for filamentous growth in *C. albicans*, the same is not the case for microtubules, which are involved in nuclear migration and division (Yokoyama *et al.*, 1990; Finley and Berman, 2005; Rida *et al.*, 2006). Treatment of cells with nocodazole, a specific microtubule inhibitor, does not block the ability of cells to form hyphae, while it does inhibit nuclear division and migration (Yokoyama *et al.*, 1990; Rida *et al.*, 2006). Similar to what has been demonstrated for *C. albicans*, studies in *A. nidulans* and *A. gossypii* demonstrated that actin-disrupting drugs cause hyphal tips to arrest extension and swell, suggesting that exocytosis still occurs but is delocalized (Knechtle *et al.*, 2006; Taheri-Talesh *et al.*, 2008). In contrast to *C. albicans*, microtubules are also crucial for polarized hyphal growth in the filamentous fungi *N. crassa* and *A. nidulans*, (Harris *et al.*, 2005; Lichius *et al.*, 2011). In *A. nidulans*, actin has also been shown to mediate endocytosis, contributing to normal polarized growth (Taheri-Talesh *et al.*, 2008; Upadhyay and Shaw, 2008). In addition to being involved in exocytosis and endocytosis, actin has an essential role in cytokinesis and organelle transport in budding and fission yeast and in filamentous fungi (Novick and Botstein, 1985; Ayscough *et al.*, 1997; Suelmann and Fischer, 2000; Virag and Griffiths, 2004; Rida *et al.*, 2006; Lin *et al.*, 2016; Pollard, 2017).

In *S. cerevisiae*, Cdc42 regulates the polarisome, which is required for actin polarization and polarized growth. In *C. albicans*, upon initiation of hyphal growth Cdc42 is

recruited to the site of growth (Hazan and Liu, 2002), where it remains restricted in its active GTP-bound form (Corvest *et al.*, 2013). The localization of Cdc42 in *C. albicans* is disrupted by treatment with the actin-depolymerizing drug latrunculin A in hyphal cells but not in budding cells, which suggests that the actin cytoskeleton is required for maintaining Cdc42 localization during hyphal growth but not during budding growth (Hazan and Liu, 2002).

Actin is a protein polymer that is abundant and highly conserved in all eukaryotes. The smallest unit of actin is the 43 kDa monomeric form, globular actin (G-actin), a single polypeptide chain with two major domains and a deep cleft for ATP binding (reviewed in Dominguez and Holmes, 2011). Microfilaments of actin are composed of a double helix structure and form when two parallel filaments of G-actin assemble, with a 7 nm diameter and the loop of the helix repeating every 37 nm (reviewed in Dominguez and Holmes, 2011). Microfilaments assemble dynamically into an intrinsically polarized structure, which is an essential attribute for their cellular functions. Assembly is regulated by ATP hydrolysis and multiple actin-binding proteins (ABPs). The higher-order structures into which F-actin can rapidly assemble have varied functional roles, providing cells with an energy-efficient means of cellular organization. These higher-order actin structures include rings, patches and cables (reviewed in Dominguez and Holmes, 2011).

Actin rings are essential constituents of the fungal cytokinetic machinery in the form of contractile actomyosin rings (CAR). The CAR consists of actin, myosin II and associated proteins that form a force-generating ring linked to the plasma membrane (Pollard, 2010; Stachowiak *et al.*, 2014). The contraction of the ring is mediated by sliding of myosin II present in the filaments, guiding membrane invagination and cell wall synthesis. The mechanism of contractile rings is present in fungi, animals and protists (Pollard, 2010; Stachowiak *et al.*, 2014).

Actin patches are accumulations of F-actin and other proteins that mediate endocytosis in fungal cells. In *S. cerevisiae*, actin patches are assembled initially at the plasma membrane and as the membrane invaginates, endocytic vesicles are formed. While vesicles are transported away from the plasma membrane, actin and other components coating the vesicles are lost. Uncoated vesicles eventually fuse with endosomal compartments

(Huckaba *et al.*, 2004). In *S. cerevisiae*, actin patch movement along actin cables matches the elongation rate of actin, suggesting that polymerization could be the driving force of random undirected movement of patches at the plasma membrane (Pelham Jr and Chang, 2001; Huckaba *et al.*, 2004), while in *N. crassa* and *A. nidulans* actin patches can undergo a rapid linear saltatory translocation along actin cables, which suggest the involvement of myosin motors in these fungi (Upadhyay and Shaw, 2008; Berepiki *et al.*, 2010). Translocation along a single actin cable is unidirectional but actin patches move in both directions within a hypha of in *N. crassa*, suggesting that cables are nucleated from basal and apical regions (Berepiki *et al.*, 2010). Alternatively, fast patch transport could be due to nonspecific interactions with the network of actin cables and myosin V (Berepiki *et al.*, 2010). In *C. albicans*, phosphorylation of Sla1 regulates the Arp2/3 complex, which in turn regulates actin nucleation and polymerization, contributing to actin patch dynamics (Zeng *et al.*, 2012). The Arp2/3 complex is also involved in clathrin-mediated endocytosis (Epp *et al.*, 2010, 2013). Cells expressing a phosphomimetic version of Sla1 exhibited markedly reduced actin patch dynamics, impaired endocytosis, and defective hyphal development, whereas a nonphosphorylatable Sla1 had the opposite effect (Zeng *et al.*, 2012). *C. albicans* Abp1, a homologue of *S. cerevisiae* Abp1 (Martin *et al.*, 2007) which is involved in endocytosis and is used to visualize actin patches, localizes as a collar behind the apex region, suggesting the absence of endocytosis close to the apex of the tip and an extensive band farther back from the tip (Caballero-Lima *et al.*, 2013; Ghugtyal *et al.*, 2015).

Actin cables are composed of bundles of formin-nucleated F-actin crosslinked with tropomyosin and fimbrin (Evangelista *et al.*, 2002; Pruyne *et al.*, 2002; Moseley and Goode, 2006). In budding and fission yeast and filamentous fungi, actin cables serve as tracks for the transport of secretory vesicles, peroxisomes, Golgi vesicles, mitochondria, vacuoles and mRNA (Suelmann and Fischer, 2000; Motegi *et al.*, 2001; Rossanese *et al.*, 2001; Fehrenbacher *et al.*, 2003; Rida *et al.*, 2006; Upadhyay and Shaw, 2008; Pantazopoulou and Penalva, 2009; Berepiki *et al.*, 2010) Formins are conserved nucleators of actin filaments that include a formin homology 1 (FH1) domain, containing profilin-actin binding sites and a domain responsible for actin nucleation and cable assembly, the DH domain, based on work in budding and fission yeast (Evangelista *et al.*, 1997, 2002; Pruyne *et al.*, 2002; Sagot *et al.*, 2002; Kovar *et al.*, 2003; Moseley, 2003; Zigmond *et al.*, 2003; Chesarone *et al.*, 2010). The actin cable dynamics was first visualized in living cells of *S. cerevisiae*, using an

Abp140-GFP fusion (Yang and Pon, 2002) It was shown that cables assemble in the bud and polarize along the mother-bud axis, *i.e.*, during *de novo* assembly and elongation, there is retrograde flow of newly assembled actin cables into the mother cell, which is in agreement with the models that depict formin-mediated F-actin assembly (Yang and Pon, 2002). Cables and patches are extremely susceptible to inhibitors of actin polymerization, suggesting that these structures have a rapid turnover of filaments (Yang and Pon, 2002; Berepiki *et al.*, 2010).

b) Exocytosis and Endocytosis

The ubiquitous cellular processes of exocytosis and endocytosis underlie the remarkable polarized growth exhibited by filamentous fungi and are pivotal for hyphal growth (Araujo-Bazán *et al.*, 2008; Upadhyay and Shaw, 2008; Taheri-Talesh *et al.*, 2008; Hervás-Aguilar and Peñalva, 2010; Shaw *et al.*, 2011; Epp *et al.*, 2013; Bernardo *et al.*, 2014; Caballero-Lima and Sudbery, 2014; Riquelme *et al.*, 2014; Ghugtyal *et al.*, 2015; Bar-Yosef *et al.*, 2017). In budding yeast, over 60 proteins (Weinberg and Drubin, 2012, 2014; Brach *et al.*, 2014), tethering complexes, lipids and the cytoskeleton are involved in the regulation of secretion and membrane internalization (Finger and Novick, 1998; Feng *et al.*, 1999; Jahn and Südhof, 1999; He and Guo, 2009). Our knowledge on exocytosis and endocytosis is essentially based on studies in *S. cerevisiae*, yet there are some differences in these processes in hyphal cells compared to budding cells. *C. albicans* hyphae have a Spitzenkörper, which is characteristic of filamentous fungi (Howard, 1981; Bartnicki-Garcia *et al.*, 1989; Taheri-Talesh *et al.*, 2008; He and Guo, 2009; Sudbery, 2011; Dijksterhuis and Molenaar, 2013; Riquelme and Sánchez-León, 2014).

Exocytosis is the process by which secretory vesicles release their contents, by fusing with the plasma membrane (Finger and Novick, 1998; Jahn and Südhof, 1999; Li *et al.*, 2007; He and Guo, 2009; Pinar *et al.*, 2013; Guo *et al.*, 2016). For fusion to occur in budding yeast, sequential processes take place: the Rab GTPase Sec4, in its active GTP-bound state, associates with secretory vesicles and interacts with Sec15, a subunit of the exocyst and the myosin-V motor Myo2 (Donovan and Bretscher, 2015); a pair of SNARE proteins is required for proper interaction of the vesicle with the plasma membrane, a v-SNARE on the vesicle side and a t-SNARE on the target membrane side (Ferro-Novick and Jahn, 1994; Burri and Lithgow, 2004); the exocyst, a tethering complex, is involved in

vesicle fusion with the plasma membrane (TerBush *et al.*, 1996; Gurunathan *et al.*, 2000; Gupta and Brent Heath, 2002). Sec4 is a major component of the protein secretion machinery playing a critical role in targeting and fusion of secretory vesicles to the plasma membrane, which is also present and critical in *C. albicans* (Clément *et al.*, 1998; Mao *et al.*, J Bact. 1999) and has been used as a reporter to visualize secretory vesicles in a number of studies, aimed at understanding secretion and filamentous growth (Li *et al.*, 2007; Jones and Sudbery, 2010; Ghugtyal *et al.*, 2015; Labbaoui *et al.*, 2017; Wakade *et al.*, 2017).

Disruption of the exocyst leads to an accumulation of vesicles in the cytoplasm and to severely compromised polarized growth (Guo *et al.*, 1999; Li *et al.*, 2007). Although the role the exocyst plays in fusion is not yet fully understood, it acts as a scaffold for fusion between Rab proteins and v-SNAREs on secretory vesicles, and t-SNAREs on the plasma membrane (TerBush *et al.*, 1996; Guo *et al.*, 1999; He and Guo, 2009). The fungal exocyst is composed of eight proteins, corresponding to *S. cerevisiae* Exo70p, Exo84p, Sec3p, Sec5p, Sec6p, Sec8p, Sec10p and Sec15p (TerBush *et al.*, 1996; Guo *et al.*, 1999; Mei *et al.*, 2018). All these components are essential, except for Sec3p (Haarer *et al.*, 1996), which is also the case for *Aspergillus niger* and *C. albicans* (Li *et al.*, 2007; Kwon *et al.*, 2014). In *C. albicans*, the exocyst forms a stable apical crescent that persists even when the cytoskeleton is disrupted (Jones and Sudbery, 2010). Li *et al.* (Li *et al.*, 2007) have demonstrated that *C. albicans* mutants in Sec3 exhibit hyphal growth defects - under hyphal-induction conditions, cells initially grew normal-looking germ tubes, but later in growth, the tip apex growth suddenly switched to isotropic growth, and tips became swollen. These cells did not divide further, indicating a terminal defect. In these swollen tips, there is an accumulation of secretory vesicles, visualized with Sec4. Besides Sec4, Sec15 and actin patches also lost their localization. Sec3 has been proposed to have an important role in filamentous growth by restricting exocytosis to the tip of hyphae (Li *et al.*, 2007). A mutant for another exocyst component, Sec15, also displays filamentation defects – while most of the cells were able to generate a germ tube during the initial phase of hyphal development, they were not able to maintain the hyphal extension in prolonged growth (Guo *et al.*, 2016). Taken together, these studies on Sec3 and Sec15 demonstrate the importance of the exocyst for filamentous growth.

The membrane required for tip growth in some filamentous fungi is supplied by the Spitzenkörper, which is localized as a cluster in the tips of growing hyphae (Gierz and Bartnicki-Garcia, 2001; Crampin *et al.*, 2005; Riquelme and Sánchez-León, 2014). In *S. cerevisiae*, the class V myosin Myo2 and its regulatory light chain Mlc1, are responsible for the transport of secretory vesicles along actin cables towards the growing bud (Johnston *et al.*, 1991; Schott *et al.*, 1999; Karpova *et al.*, 2000) and Mlc1 has been demonstrated to localize to a Spitzenkörper-like structure in the tips of *C. albicans* hyphae (Crampin *et al.*, 2005). This accumulation suggests that membrane fusion occurs at a lower rate than that of vesicle fusion. When the t-SNARE Sso2 is repressed, germ tube emergence still occurs in *C. albicans*, but the Spitzenkörper disassembles and the rate of hyphal extension decreases after some hours (Bernardo *et al.*, 2014). These cells exhibit accumulated secretory vesicles and abnormal hyphal growth (Bernardo *et al.*, 2014). Following the interruption of hyphal growth, the hyphal tip of the repressed *sso2* mutant strain becomes globular, similar to the *C. albicans sec3* mutant strain, in which polarized growth is lost following initial germ tube evagination (Li *et al.*, 2007). Studies in *N. crassa* and *A. nidulans* have shown that there are two populations of vesicles within the Spitzenkörper, containing different cargos, such as the flippases DnfA (ScDnf1 homolog) and DnfB (ScDrs2 homolog), and being regulated by different molecular switches (Verdín *et al.*, 2009; Pantazopoulou and Peñalva, 2011; Sánchez-León *et al.*, 2015). Distinct populations of vesicles have not been shown so far in *C. albicans*.

The fungal Golgi consists of isolated membranous cisternae that do not form the characteristic stacks observed in mammalian cells (Rida *et al.*, 2006; Klumperman, 2011; Pantazopoulou, 2016). In a general way, the Golgi is an intrinsically transient and heterogeneous entity that is constantly fed by anterograde coat protein complex II (COPII) carriers budding from the endoplasmic reticulum (ER) (Klumperman, 2011; Pantazopoulou *et al.*, 2014). It is thought that the traffic between the ER and the plasma membrane, *via* the Golgi, relies on cisternae maturation rather than vesicles connecting the discrete cisternae. Vesicles originating from the ER progressively change lipid and protein content, becoming gradually enriched in cargo proteins. Cisternae at this stage are named “late” or “TGN” cisternae. This progressive change is thought to be assisted by COPI retrograde vesicle traffic that send back to early cisternae the components that do not belong in late cisternae (Klumperman, 2011; Pantazopoulou, 2016). In *C. albicans*, the Golgi

is critical for the yeast to filamentous growth transition and, in filamentous cells, it redistributes to the tip of hyphae, in a formin-dependent manner (Rida *et al.*, 2006; Ghugtyal *et al.*, 2015). The budding of secretory vesicles from the late Golgi and their targeting to the plasma membrane is perturbed in a strain where Golgi PI(4)P levels are reduced. This strain is unable to form hyphae, most likely due to a build-up in the Golgi (Ghugtyal *et al.*, 2015).

Such Golgi polarization during hyphal growth has been proposed to be regulated by cAMP-PKA signaling via the Rab GAP Gyp1 (Huang *et al.*, 2014). Gyp1, a Golgi-associated protein, critically regulates membrane trafficking from the endoplasmic reticulum to the plasma membrane (Du and Novick, 2001; Pan *et al.*, 2006; Rivera-Molina and Novick, 2009). During hyphal induction, Gyp1 is phosphorylated through the cAMP-PKA pathway, interacting with the actin motor Myo2 and promoting the recruitment of Sec7 to late Golgi compartments (Huang *et al.*, 2014). In *C. albicans*, a small fraction of secretory vesicles and Golgi cisternae exhibit directed movement in budding and filamentous cells and the Golgi is likely to exhibit a combination of Brownian and directed movement perhaps indicative of maturation (Ghugtyal *et al.*, 2015).

An active endocytic pathway has been demonstrated to be required for hyphal morphogenesis in *C. albicans* (Bar-Yosef *et al.*, 2018). It has been suggested that the role of endocytosis in *C. albicans* is to recycle membranes as well as membrane proteins deposited by vesicle exocytosis at the tip of the extending hypha (Shaw *et al.*, 2011). In *S. cerevisiae*, Jose *et al.* (Jose *et al.*, 2013) proposed through a stochastic mathematical model, that Cdc42•GTP auto-amplification drives polarized secretion towards the bud tips and clusters exocytic activity while endocytic corralling ensures a unique focused cluster for robust polarity establishment. In *A. gossypii*, endocytosis and exocytosis are spatially separated: exocytic sites are essentially apical and endocytic sites predominantly sub-apical (Köhli *et al.*, 2008), which is also the case in *C. albicans* (Martin *et al.*, 2007; Ghugtyal *et al.*, 2015). Filamentous fungi possess most of the endocytic proteins present in yeast and in mammals and are able to take up the lipophilic dye FM4-64 (Fischer-Parton *et al.*, 2000; Wedlich-Söldner *et al.*, 2000; Taheri-Talesh *et al.*, 2008; Upadhyay and Shaw, 2008; Schultzhaus *et al.*, 2015). Clathrin-mediated endocytosis is a well-studied process of endocytosis in eukaryotic cells (Brach *et al.*, 2014; Kaksonen and Roux, 2018). While *S. cerevisiae* has proven to be an

excellent model for understanding the molecular details of endocytosis, loss of clathrin-mediated endocytosis is so detrimental that it has been difficult to study alternate pathways functioning in its absence (reviewed in Lu *et al.*, 2016). Although *C. albicans* has a clathrin-mediated endocytosis pathway that functions similarly to that of *S. cerevisiae*, inactivation of this pathway does not compromise growth of yeast-form *C. albicans*. Indeed, endocytosis still occurs, in an actin-dependent manner, in the absence of one key player that drives clathrin-mediated endocytosis, the Arp2/3 complex (Epp *et al.*, 2010).

V – Protein recruitment systems

Morphogenesis is a complex process that involves the concerted action of a variety of molecules at specific locations and at defined times. The physiological function of proteins within cells depends on their localization, with high temporal and spatial resolution. The activity of these proteins results in changes in cell behaviour, which ultimately determines the function and shape of the cell and tissues. Therefore, methods that allow the manipulation of protein activity at the subcellular level, with high spatiotemporal precision, are powerful tools to explore cellular functions. These methods are typically based on genetic manipulations, such as knockdowns, knockouts, overexpression and mutation, but, while extremely powerful, these methods are limited by the possible broad effect on the organism and repercussions on long timescales. Chemical approaches can rapidly switch on or off the function of specific proteins, and usually rely on the dimerization of the FK506-binding protein (FKBP12) and its binding partner FRB in the presence of rapamycin or its analogs (Spencer *et al.*, 1993; Derosé *et al.*, 2013). However, chemically inducible dimerization does not allow the spatial control of the dimer at the subcellular level and effects are difficult to titrate (Komatsu *et al.*, 2010). The identification of light-switchable proteins, such as channelrhodopsins (Nagel *et al.*, 2002, 2003; Boyden *et al.*, 2005), was a landmark discovery for biology and it has defined the beginning of a new research area named “optogenetics”.

Optogenetics is the combination of optics, genetics and bioengineering to either stimulate or inhibit cellular activity *via* light-sensitive proteins (Tischer and Weiner, 2014). Light induced dimerization based on light-sensitive proteins allows for protein perturbation with high spatial precision and on a timescale consistent with the speed and

reversibility of intracellular reactions. This approach has been used in various organisms to address questions related with a multitude of processes, such as cytoskeleton dynamics (Maiuri *et al.*, 2015; Adikes *et al.*, 2018), Rho GTPase activation and morphogenesis (Valon *et al.*, 2015, 2017; Witte *et al.*, 2017; Zimmerman *et al.*, 2017), intracellular vesicle transport (Harterink *et al.*, 2016; Adrian *et al.*, 2017; Wood *et al.*, 2017), organelle transport and positioning (Van Bergeijk *et al.*, 2015), cytokinesis (Kotýnková *et al.*, 2016) and phosphoinositide metabolism (Idevall-Hagren *et al.*, 2012; Ji *et al.*, 2017).

The field of optogenetics has evolved well past rhodopsins, and many other proteins containing light-responsive domains have been incorporated as optogenetic tools. Some of the reversible systems most recently used include the Dronpa protein, phytochrome B (PhyB), light-oxygen-voltage (LOV) domains from phototropins and cryptochrome 2 (Cry2) (Zhang and Cui, 2015; Guglielmi *et al.*, 2016; Liu and Tucker, 2017; Repina *et al.*, 2017; Benedetti *et al.*, 2018). A comparison of these systems is shown in Figure 6 and Table 1.

The Dronpa protein

Dronpa is a monomeric fluorescent protein derived from a tetrameric protein complex, isolated from a coral from the Pectiniidae family (Ando *et al.*, 2004). This system has been used by fusing Dronpa to both carboxyl and amino termini of a protein of interest, so when the system is switched on under violet light (390 nm, 3 seconds) (Ando *et al.*, 2004), the two Dronpa domains will bind to each other, altering the protein's conformation and preventing it from exerting its function (Andresen *et al.*, 2007; Zhou *et al.*, 2012). This system can also be reverted to the monomeric state using a higher wavelength light, 490 nm for 30 seconds, or waiting for 5 minutes in the dark (Zhou *et al.*, 2012) (Fig. 6). The advantage of Dronpa is the possibility to turn the system off using a specific wavelength and that it does not require an external cofactor. A disadvantage of this system is the time it requires for the monomers to dissociate, 20 seconds with 400 nm light (Zhou *et al.*, 2012), which can be toxic to the cells and may not be compatible with studies that require the acquisition of images in multiple focal planes and with a high temporal resolution. Dronpa has been used in mammalian cells to control a viral protease activity, and the activation of Cdc42 to induce the formation of filipodia, by uncaging the Rho-GEF Intersectin-1 at the plasma membrane (Zhou *et al.*, 2012).

The Phytochrome B protein

Phytochrome B (PhyB) is a protein from *Arabidopsis thaliana* that is activated by red light (650 nm) and inactivated by infrared light (750 nm) (Fig. 6). This protein only becomes photosensitive in the presence of phycocyanobilin (PCB) – a chromophore present in photosynthetic organisms. Hence, when used in non-photosynthetic organisms, PCB must be delivered directly or the enzymes that produce it need to be expressed in the cells (Gambetta and Lagarias, 2001; Müller *et al.*, 2013), which is a disadvantage of this system. Additional disadvantages to having to provide PCB externally, is that the size of PhyB can be a challenge for genetic manipulation and the fact that the system is sensitive to expression level (Levskaya *et al.*, 2009). After photoactivation with red light, PCB-bound PhyB changes conformation and binds to a phytochrome interacting factor (PIF) protein. PhyB and PIF can be dissociated within seconds using infrared light or remain bound for hours in the dark (Ni *et al.*, 1999; Levskaya *et al.*, 2009), hence, like Dronpa, the advantage is to be able to switch this system on and off with two different wavelengths. Examples of applications include the control of the activation of Cdc42 and Rac1 to induce the formation of filipodia and lamellipodia in mammalian cells, by recruiting the DH-PH domains of the respective GEFs to the plasma membrane (Levskaya *et al.*, 2009); the induction of genes under the control of promoters with a Gal4 DNA-binding site in yeast (Shimizu-Sato *et al.*, 2002), the study of signal transmission in the Ras/Erk Module in mammalian cells (Toettcher *et al.*, 2013); the activation of protein splicing and control of DNA transcription in yeast (Tyszkiewicz and Muir, 2008; Hughes *et al.*, 2012).

The LOV domains

LOV domains from different organisms have been used as optogenetic tools. These proteins are sensitive to blue-light (<500 nm) and require flavin as a chromophore, which is expressed ubiquitously (Strickland *et al.*, 2012) (Fig. 6). Following photo-excitation with blue light (1.125 seconds), LOV changes its conformation, undocking the C-terminal J α helix from its core (Harper *et al.*, 2003; Yao *et al.*, 2008). In the dark and after less than 2 minutes, the J α helix is caged once again (Wu *et al.*, 2009; Strickland *et al.*, 2012). This domain can be used alone, such as *Avena sativa* LOV2 (Wu *et al.*, 2009), *N. crassa* LOV-containing protein Vivid (Zoltowski *et al.*, 2009; Wang *et al.*, 2012), *Erythrobacter litoralis* LOV-containing protein EL222 (Motta-Mena *et al.*, 2014), or together with the binding

partner PDZ in the TULIPs (tunable, light-controlled interacting protein) system, which binds the uncaged J α helix (Strickland *et al.*, 2012). This system can be used with high spatial precision, even in small cells, such as yeast, with LOV tagged to the plasma membrane and PDZ in the cytoplasm (Strickland *et al.*, 2012). Other systems based in LOV domains are the iLID (improved light inducible dimer) system (Guntas *et al.*, 2015) and the Magnets system (Kawano *et al.*, 2015). The iLID system uses a plant LOV domain in combination with two bacterial peptides, SsrA and its binding partner SspB (Guntas *et al.*, 2015). SsrA is recombined with LOV to its C-terminal α helix, and becomes exposed when LOV is photo-excited, allowing SsrA to bind with SspB (Guntas *et al.*, 2015). SsrA and SspB have a high basal affinity (Guntas *et al.*, 2015), so there is some interaction between them even before photo-activation (Benedetti *et al.*, 2018). The Magnets system uses a VIVID protein from *N. crassa*, which is a LOV domain involved in the circadian clock system (Zoltowski *et al.*, 2007; Kawano *et al.*, 2015; Zhou *et al.*, 2017). This system relies on dimerization between altered VIVID domains to prevent homo-dimerization, giving rise to the pair nMag and pMag (negative Magnet and positive Magnet; Kawano *et al.*, 2015). Magnets is the LOV-based system that offers the most precise spatial recruitment, although this comes at the expense of the total level of dimers formed (Benedetti *et al.*, 2018). Magnets variants have been developed to allow fast switch-off kinetics and slow switch-on kinetics and *vice-versa* (Kawano *et al.*, 2015). While the fast photo-switches provide a powerful tool for spatially and temporally confined optical control of protein activities in the cells, slow photo-switches require only a one-shot irradiation to act as a continuously active optogenetic tool. The slow photo-switches could be used to avoid some unwanted side effects caused by continuous irradiation, such as phototoxicity and unfocused activation owing to sample drift (Kawano *et al.*, 2015). Magnets system is enhanced by using a tandem repeat fusions of each of the pairs (Kawano *et al.*, 2015). This system has recently been further improved into the CAD-Magnet system, to overcome low binding affinity, used in combination with a Ca²⁺/calmodulin-dependent protein kinase II α (CaMKII α) association domain (CAD) to generate an assembly of 12 pMag photo-switches, which exhibit stronger interaction with nMag after photoactivation, when compared with monomeric (Furuya *et al.*, 2017).

When choosing to use an optogenetic system based on LOV domains, one must consider that the “on state” is shorter compared to other systems, requiring continuous

photo-activation. Furthermore, LOV is sensitive to orientation, *i.e.* the C-terminal is where uncaging occurs, and this influences the orientation in which membrane-bound sequences and other proteins are recombined to LOV domains. However, components of LOV based systems are small (easy to manipulate genetically) and there is no requirement for exogenous cofactor, which are advantageous. Applications of LOV-based systems include: a) light-activated cellular signalling, by locally recruiting Cdc24 to the plasma membrane to determine orientation of the mating projection in α F-arrested cells, using TULIPs (Strickland *et al.*, 2012); b) control of cell polarity by recruiting Cdc24 to the plasma membrane of *S. cerevisiae*, to induce budding (Witte *et al.*, 2017), or the Rho GEF DH-PH domains of Intersectin or Tiam to activate Cdc42 or Rac1, respectively, and drive the formation of lamellipodia or filipodia in mammalian cells, using iLID and CAD-Magnets (O'Neill *et al.*, 2016; Furuya *et al.*, 2017; Zimmerman *et al.*, 2017); c) control of gene expression in mammalian cells, mice or zebra fish, taking advantage of the homo-dimerization of bacterial or fungal LOV domains upon photo-activation (Wang *et al.*, 2012; Motta-Mena *et al.*, 2014); d) selective PI3P level reduction on a single endosome, in mammalian cells, by recruiting the PI3P phosphatase MTMR1, using Magnets (Benedetti *et al.*, 2018); e) control of cell motility, by fusion of Rac1 to *A*₁LOV2 C-terminal in mammalian cells, to form a Photoactivatable Rac1 (PA-Rac1). The proximity of *A*₁LOV2 and Rac1 in the dark prevents Rac1 from interacting with downstream effectors, and, after light-activation and uncaging of the α helix, Rac1 can be locally released on one side of the cell to orient grow direction (Wu *et al.*, 2009);

The Cryptochrome 2 protein

Cryptochrome 2 (Cry2), from *A. thaliana*, is sensitive to blue light, requiring FAD as a chromophore (Fig. 6). Upon activation, Cry2 homo-oligomerizes and binds to its binding partner Cib1 (cryptochrome-interactive basic helix-loop-helix 1) within seconds. In the dark, Cry2 reverts to its initial state and dissociates from Cib1 (Más *et al.*, 2000; Kennedy *et al.*, 2010; Bugaj *et al.*, 2013). Both Cry2 and Cib1 can be modified to increase the performance of the light-activated system: plant chryptochromes contain a conserved domain that mediates light responsiveness and binds the photolyase homology region (PHR) to flavin and pterin chromophores. Cry2 PHR domain (1-498 aa) is expressed to a higher level than full-length Cry2 in yeast cells, and is sufficient for interacting with Cib1

upon blue-light activation (488 nm, 100 ms); a truncated version of Cib1 (CibN, aminoacids 1-170, Liu *et al.*, 2008), lacking the conserved basic helix-loop-helix domain that mediates dimerization and DNA binding, is also sufficient for the Cry2PHR interaction (Kennedy *et al.*, 2010). In the dark, after approximately 5 minutes, the two domains dissociate (Kennedy *et al.*, 2010). Recently, the versatility and tunability of this system has been improved, through truncated versions that alter the lifetime of Cry2/Cib1 interaction (Taslimi *et al.*, 2016). The Cry2 truncation Cry2(535) shows tighter light control than Cry2PHR, is shorter than full length Cry2, and may be preferable to regulate cellular activities, whereas a 81 residue fragment of Cib1, Cib81, retains interaction with Cry2 and can be used to control protein localization. Cib81 is expected to be useful with protein targets that cannot tolerate a larger fusion tag, or for packaging the dimerization system into size-restricted viral vectors (Taslimi *et al.*, 2016). The uninduced, in the dark, interaction between Cry2 and Cib1 can be a downside of this system, as well as the Cry2 oligomerization, as CibN recruitment is less effective, when bound to membranes, and spatial recruitment is less precise (Che *et al.*, 2015; Hallett *et al.*, 2016; Benedetti *et al.*, 2018). Recently, a new Cry2 module, called Cry2clust, has been developed to induce rapid and efficient homo-oligomerization of target proteins (Park *et al.*, 2017).

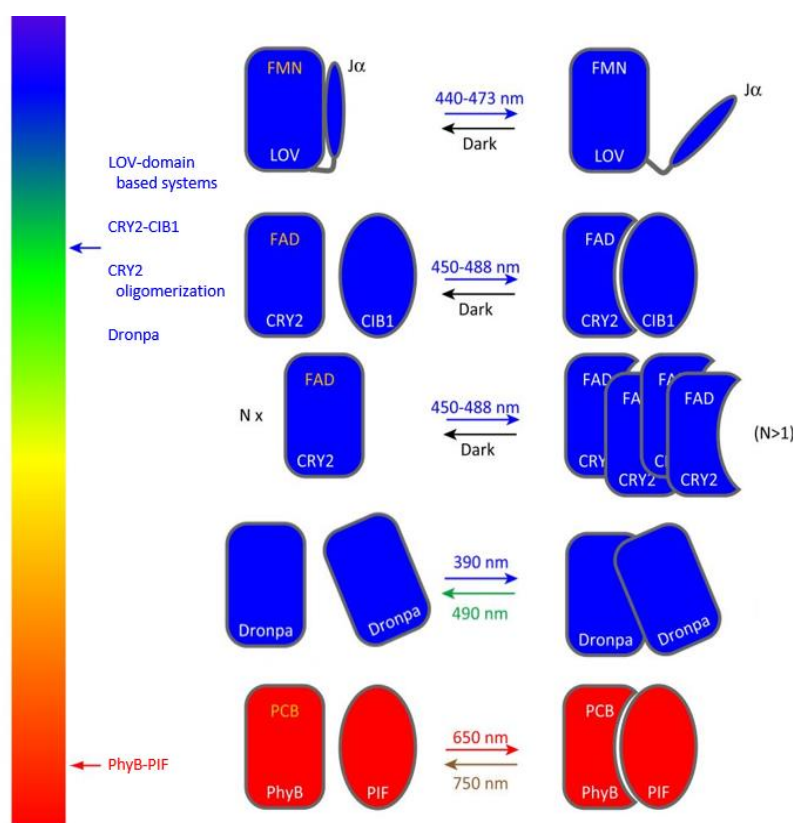


Figure 6. Scheme of light-induced conformational change in various photoactivatable proteins. The left bar illustrates the color of light (wavelength) used to stimulate photoactivation. Various systems are shown on the right: LOV based systems, Cry2–Cib1, Cry2 alone, Dronpa and PhyB–PIF. Proteins containing cofactors [flavin mononucleotide (FMN), FAD, PCB]. Figure adapted from (Zhang and Cui, 2015).

Cry2-based optogenetic systems have been used to study the role of Cdc42, by locally perturbing its activation (Valon *et al.*, 2015); to regulate protein transcription and translocation in mammalian cells (Kennedy *et al.*, 2010; Konermann *et al.*, 2013) and yeast (Hughes *et al.*, 2012); Cre recombinase-mediated DNA recombination in mammalian cells (Kennedy *et al.*, 2010) and the fruit fly *Drosophila melanogaster* (Boulina *et al.*, 2013); to selectively reduce PI3P levels on a single endosome, in mammalian cells, by recruiting MTMR1 (Benedetti *et al.*, 2018); to modulate cell contractility during tissue morphogenesis, in the embryo of *D. melanogaster*, by interfering with PIP₂ level in the plasma membrane (Guglielmi *et al.*, 2015).

Photosensitive protein	Turn-on rate	Turn-off rate ($t_{1/2}$)	Chromophore requirement	Compatible imaging wavelengths (nm)	λ_{on} (nm)	λ_{off} (nm)	Size (amino acids)	References
Dronpa	3 seconds	<ul style="list-style-type: none"> • 20 seconds (illuminated at 390 nm) • 5 minutes (dark reversion) 	None	≥ 600	390	490	257	Ando <i>et al.</i> , 2004 Andresen <i>et al.</i> , 2007 Zhou <i>et al.</i> , 2012
PHYB	1.3 seconds	<ul style="list-style-type: none"> • 4 seconds (illuminated at 750 nm) • 2 hours (dark reversion) 	PCB; exogenous or synthesized <i>in situ</i>	≤ 514	650	750	<ul style="list-style-type: none"> • PHYB: 908 • PIF: 100 	Ni <i>et al.</i> , 1999 Levsikaya <i>et al.</i> , 2009
LOV	<ul style="list-style-type: none"> • AsLOV2: Seconds • TULIPs: Seconds • iLID: 30s to 1min • Magnets: 1.5 seconds 	<ul style="list-style-type: none"> • AsLOV2: 30-50 seconds • TULIPs: 1 minute • iLID: Minutes • Magnets: 6.8 seconds 	Flavin; endogenous	≥ 514	440-473	NA	<ul style="list-style-type: none"> • AsLOV2: 143 • PDZ: 194 • iLID: 148 • SspB: 113 • nMag: 152 • pMag: 150 	Harper <i>et al.</i> , 2003 Yao <i>et al.</i> , 2008 Wu <i>et al.</i> , 2009 Strickland <i>et al.</i> , 2012 Wang <i>et al.</i> , 2012 Guntas <i>et al.</i> , 2015 Kawano <i>et al.</i> , 2015 Zhou <i>et al.</i> , 2017
CRY2	<ul style="list-style-type: none"> • CRY2PHR-CIBN: 90% recruited in 10 seconds • CRY2PHR oligomerization 	<ul style="list-style-type: none"> • CRY2-CIBN: 100% dissociated in 12 minutes • CRY2 oligomerization: 5.5 minutes 	Flavin; endogenous	≥ 561	450-488	NA	<ul style="list-style-type: none"> • CRY2PHR: 498 • CIBN: 170 	Más <i>et al.</i> , 2000 Liu <i>et al.</i> , 2008 Kennedy <i>et al.</i> , 2010 Bugaj <i>et al.</i> , 2013

Table 1. Four photosensitive proteins at the core of current reversible optogenetic systems and their derivatives. Note that some systems represent a collection of proteins from different organisms to control different signaling systems. This is particularly true of the light-oxygen-voltage (LOV) domains. This table summarizes the features of the classes of photosensitive proteins; the features will vary based on the particular protein used. | **Turn-on rate** is the half-time in which the system activates when illuminated with stimulatory light (λ_{on}). | **Turn-off rate** is the half-time in which the system resets in the dark or when illuminated with inhibitory light (λ_{off}). | **Chromophore requirements** are the small molecule, if any, needed to make the protein photosensitive and whether they are produced by the cell or have to be provided. | **Compatible imaging wavelengths** are not stimulatory and can be used to image other fluorophores without notably activating the optogenetic system. | λ_{on} . The wavelength (or wavelengths) of light most effective at activating the system. Wavelengths outside these ranges could still activate the system but may require higher intensities and/or longer exposures. | λ_{off} . The wavelength, if any, actively resetting the system. Wavelengths outside this range could still inhibit the system but may require higher intensities and/or longer exposures. | **Size (amino acids)** of the components for each system.

To approach the questions of my project, I have used an optogenetics system to recruit a dominant active form of Cdc42[G12V,C188S]¹, to the plasma membrane. I have initiated my project, in 2014, by setting up an optogenetics system in the lab. I have tried to use the TULIPs system, the PhyB-PIF system and the Cry2PHR-CibN system. The first system I was successful with was the Cry2 system. Even though improved versions of existing optogenetics systems have been developed since then, more efficient and more precise, the Cry2 system allowed me to recruit Cdc42•GTP to the whole plasma membrane and has been the central technique, along with spinning-disk confocal microscopy, that I have used in my project.

¹ The mutation C188S, replacing the cysteine 188 by a serine, interferes with the post-translational isoprenylation on the cysteine, and disabling Cdc42 from binding to the plasma membrane.

VI – Objective of this work

In symmetrical cells, such as unbudded *S. cerevisiae* cells, Cdc42 in the active GTP-bound state can form a cluster anywhere in the cell from which polarized growth can potentially occur (Richman *et al.*, 2002; Tong *et al.*, 2007; Okada *et al.*, 2017). However, once a growth site is already established, it is not known whether a new growth site can be initiated and what is its relationship to the initial growth site. Similarly to *S. cerevisiae*, during *C. albicans* hyphal filamentous growth, Cdc42•GTP localizes as a tight cluster to the tips of filaments (Vernay *et al.*, 2012). It is believed that this cluster of activated Cdc42 initiates initial asymmetry and subsequent polarized growth in the cell.

I have used an optogenetic system to recruit a constitutive active form of Cdc42, the hub of cell polarity, to the plasma membrane. I have initiated this work examining different optogenetic systems in *C. albicans*, *i.e.* the TULIPs system, the PhyB-PIF system and the Cry2PHR-CibN system, and chose to use the Cry2 system to recruit active Cdc42 to the plasma membrane and follow its cellular repercussions. Following photoactivation, Cy2PHR-linker-GFP γ -Cdc42[G12V,C188S] is recruited to the plasma membrane (Fig. 7) and I have quantitated cell growth, as well as the distribution of polarity markers and membrane compartments, in particular secretory vesicles, actin cytoskeleton and sites of endocytosis. My objective is to understand how cells respond to the perturbation of active Cdc42 and how a new polarity axis can be established.

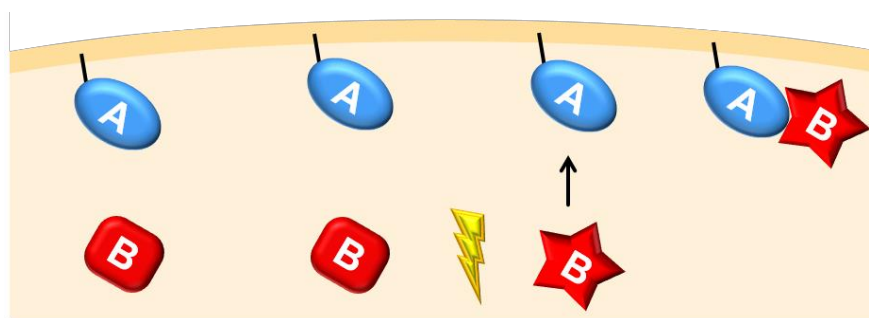


Figure 7. Scheme of the optogenetic system layout used in this work. From left to right, domain A is attached to the plasma membrane and domain B is in the cytoplasm, in the dark state. After photoactivation (yellow mark) of B, the affinity between the domains increases and B is recruited to the plasma membrane. A: CibN; B: Cry2PHR Cdc42[G12V,C188S].

Results

When I initiated this project, I began by using the three main optogenetic systems available, CRY-CIBN, TULIPs and PHY-PIF (Fig. 8). Each system was used in WT and mutant strains and I generated a total of 18 plasmids and 28 strains (Fig. 9). The CRY-CIBN system was the first one that I observed clear plasma membrane recruitment and therefore I continued to further optimize this system. I have tried two orientations, uniform plasma membrane recruitment – the CRY domain expressed in the cytoplasm and the CIBN domain targeted to the plasma membrane, and site-specific recruitment – the CIBN domain expressed in the cytoplasm and the CRY domain targeted to the plasma membrane.

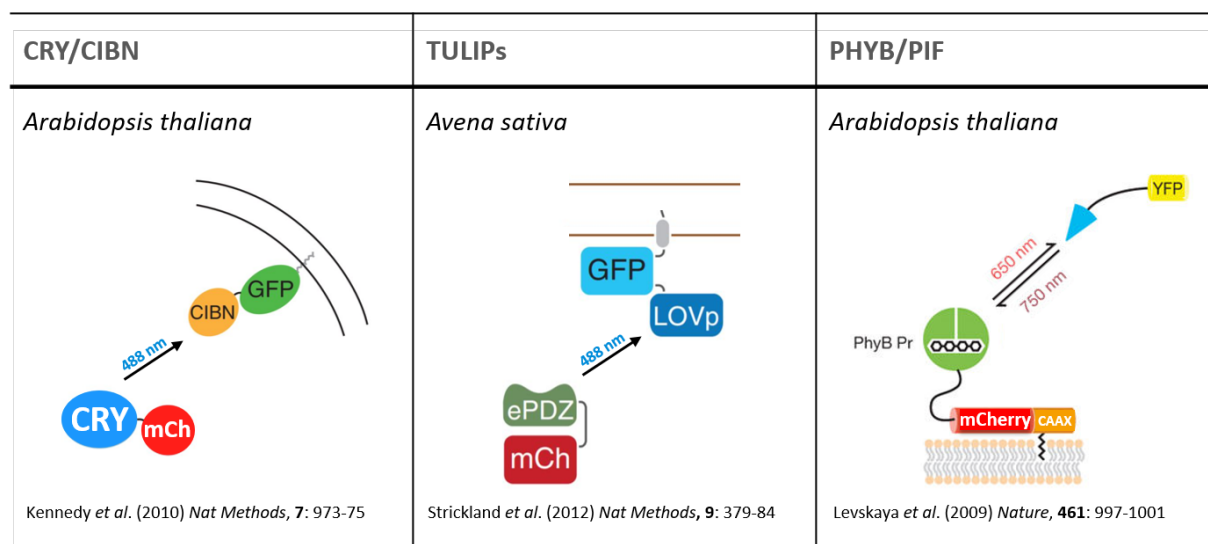


Figure 8. Main optogenetic systems. CRY-CIBN, CRY is the photosensitive domain and is localized in the cytoplasm, after photoactivation it is recruited to the CIBN domain which is attached to the plasma membrane. TULIPs and PHYB-PIF, the photosensitive domain is attached to the plasma membrane, LOV or PHYB respectively, hence these two systems allow site specific recruitment if only a part of the membrane is irradiated with light.

Strains expressing the two domains in the site-specific orientation revealed bright clusters of CRY-linker-GFP-CtRac1 at the plasma membrane, prior to photoactivation, which could be due to the oligomerization of CRY domain. This oligomerization could potentially interfere with the interaction between CRY and CIBN, so this orientation was not further pursued.

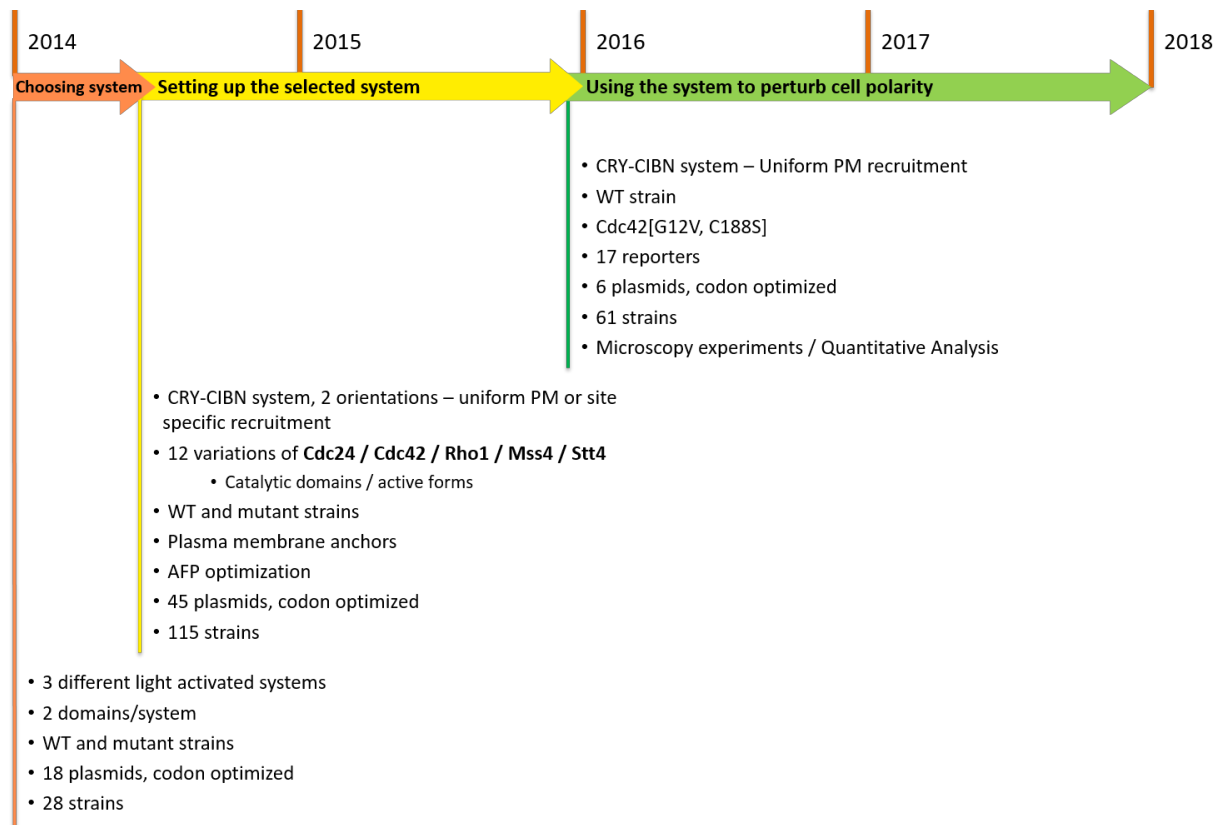


Figure 9. Time frame of PhD project over 4 years.

I have also tried a total of 12 variations using different proteins or domains of Cdc24, Cdc42, Rho1, Mss4 and Stt4 – including full length proteins, catalytic domains and active or inactive forms, in WT or mutant background strains; I have also tried several plasma membrane anchors and optimized autofluorescent proteins, generating a total of 45 plasmids and 115 strains (Fig. 9). Strains expressing the CRY-CIBN system to recruit Cdc24 or Cdc42, in the respective mutants backgrounds (non filamentous), resulted in a recovery of filamentation in the absence of photoactivation. Such recovery is most likely due to the basal interaction between CRY and CIBN that occurs even when the system is not activated with blue light. A strain expressing the CRY-CIBN system set up to recruit the Mss4 PI(4)P-5-kinase was generated, however the CRY-MSS4 fusion was localized to

the plasma membrane in the absence of photoactivation. Furthermore strains expressing the CRY-CIBN system set up to recruit the Stt4 PI-4-kinase strains were generated but no recruitment was observed following photoactivation. As a result, I did not further analyse strains with CRY fused to Cdc24, Mss4 and Stt4. Hence, I focussed on using the CRY-CIBN system to perturb cell polarity, uniformly recruiting active Cdc42 to the plasma membrane in a WT background.

I have examined 17 different reporters and generated 6 plasmids and 61 strains. I have optimized the number of photoactivations, the time between photoactivations, laser power and exposure times, number of Z-sections and temporal resolution for each reporter. Strains with reporters whose fluorescent signals were very low or bleached rapidly were not further used, as signals were not sufficiently strong for the temporal (up to image acquisition every minute) and spatial (number of Z-sections) resolution requirements of the photorecruitment experiments. These include the reporters Cdc10-yemCherry, Sec3-yemCherry, Sec3-yemScarlet, Sec7-yemScarlet, Sec61-yemCherry, Sec61-yemScarlet, Bni1-yemCherry, Bem1-yemCherry, LifeAct-yemScarlet, ActinChromobody-(yemScarlet)₃ and cytoplasmic yemiRFP670.

Table 2 lists the proteins examined for the optogenetic system and orientation of the system domains, plasma membrane anchor, proteins to recruit, background strain and reporters. The proteins used in my project are indicated in bold - the CRY-CIBN system, with the C-terminal part of Rac1 as plasma membrane anchor for the CIBN domain, was used for uniform plasma membrane recruitment of Cdc42[G12V,C188S] in a WT strain. I have generated and analysed data with the reporters Mlc1 for the Spitzenkörper, Abp1 for endocytosis, CRIB for active Cdc42 and Sec4 for secretory vesicles. Plasmids, oligonucleotides, synthesized genes and strains used in this study are listed in Tables 3, 4, 5 and 6, respectively. Additional plasmids and strains generated, but not used for results of the study, are listed in tables 7 and 8 as an annex of the section Materials & Methods.

Optogenetic systems	CRY-CIBN TULIPs (LOVpep-PDZ) PHYB-PIF
Plasma membrane anchor	C-terminal Rac1 – Prenylation t-SNARE Sso2 – 1 TMD G-protein alpha subunit Gpa2 – Myristoylation Protein phosphatase Psr1 – Palmitoylation Glycosidase Phr2 – GPI anchor / 1 TMD Glycoprotein Dfi1 – 2 TMDs Cell surface sensor Wsc1 – 1 TMD
Orientation	Uniform PM recruitment Site specific recruitment
Protein to recruit	Cdc24 (full length, catalytic domain (DHPH, DH)) Cdc42 (WT, Q61L, G12V, C188S) Rho1 (WT, Q67L, C195S), Mss4 and Stt4 variants
Background strain	WT <i>cdc42</i> <i>cdc24</i> <i>mss4</i>
Reporters	CRIB, Abp1, Mlc1, Sec4 , Bem1, Bni1, Cdc10, Sec7, Sec3, Sec2, Sec61, actin chromobody, LifeAct, cytoplasmic mScarlet (volume), Nop1, Nup49

Table 2. Summary of experimental approach.

The following section is comprised of the results of this study, divided into two parts: the first part is a paper to be submitted shortly and the second part shows additional results and controls that further support the data in the paper.

A dynamic polarity axis is established in the absence of directional growth

Patrícia M. Silva^{1,2,3}, Charles Puerner^{1,2,3}, Agnese Seminara^{4,5}, Martine Bassilana^{1,2,3} and Robert A. Arkowitz^{1,2,3*}

¹University of Côte d'Azur; Institute of Biology Valrose (iBV), Centre de Biochimie, Faculté des Sciences, Parc Valrose, Nice, FRANCE.

²UMR CNRS 7277; Institute of Biology Valrose (iBV), Centre de Biochimie, Faculté des Sciences, Parc Valrose, Nice, FRANCE.

³UMR INSERM 1091; Institute of Biology Valrose (iBV), Centre de Biochimie, Faculté des Sciences, Parc Valrose, Nice, FRANCE.

⁴University of Côte d'Azur; Institute Physics of Nice (INPHINI), Faculté des Sciences, Valrose, Nice, FRANCE.

⁵UMR CNRS 7010; Institute Physics of Nice (INPHINI), Faculté des Sciences, Valrose, Nice, FRANCE.

Corresponding author

E-mail: arkowitz@unice.fr

Cell polarity is a fundamental process, which in most cases, is not fixed but rather is dynamic, allowing cells to readjust to their environment, in response to a range of temporal and spatial cues. The key regulator of cell polarity in eukaryotes is the highly conserved, small Rho GTPase Cdc42. The establishment of a polarity axis has been extensively studied in symmetrical cells¹⁻⁴ and such symmetry breaking involves a local higher concentration of active Cdc42 at a defined site, which subsequently becomes stabilized by an amplification process⁴⁻⁹. However, little is known about how a new site of cell polarity is established in an already asymmetric cell. Cell polarization has been extensively studied in the budding yeast

Saccharomyces cerevisiae, in which an internal landmark signal dictates the polarity axis during budding growth^{1,10,11}. The human fungal pathogen *Candida albicans* can switch from budding growth to filamentous hyphal growth in response to external cues, a transition controlled, in particular, by Cdc42¹²⁻¹⁷. Here we have used optogenetic manipulation to probe cell polarity and reset growth in an already asymmetric filamentous *C. albicans* cell. We show that increasing the levels of active Cdc42 on the plasma membrane results in *de novo* secretory vesicle clustering to a discrete site and that this cluster of vesicles is highly dynamic until a new growth site is subsequently established.

Results

Uniform recruitment of constitutively active Cdc42 disrupts polarized growth

In order to investigate cell polarization in an asymmetric cell, we established optogenetic tools to recruit the key regulator of cell polarity Cdc42 to the cortex in *C. albicans* cells based on *Arabidopsis thaliana* cryptochromes¹⁸. Specifically we co-expressed membrane tethered CibN (CibN-GFP-Ct_{Rac1}) with Cry2-mCherry fused to a constitutively active Cdc42 (henceforth mentioned Cdc42[G12V]) mutant lacking its C-terminal membrane targeting prenylation sequence (Figure 1A). A single pulse of 488 nm light was sufficient to recruit Cry2-mCh-Cdc42[G12V]_{cyto} to the plasma membrane. Cells co-expressing this fusion together with the CibN fusion grew normally in the dark and this Cdc42 mutant was quantitatively recruited to the plasma membrane (Figure 1B). Following a pulse of 488 nm light, maximal plasma membrane recruitment was observed after approximately a minute, concomitant with depletion from the cytosol. Within 10 min after maximal plasma membrane recruitment there was a decrease in plasma membrane signal (to the values prior to photo-activation) and a concomitant increase in the cytoplasmic signal. Figure 1C shows that we were able to repetitively recruit this fusion to the plasma membrane. We next examined whether recruitment of this fusion

protein perturbs growth in budding and filamentous cells. Plasma membrane recruitment of constitutively active Cdc42 dramatically perturbed polarized bud growth in comparison to control cells that were not exposed to 488 nm light (Figure 2A). Measurements of the bud and mother cell size indicated that recruitment of constitutively active Cdc42 largely blocks growth (Figure 2B). Bud volume increased by on average only 2.6-fold following 4 photo-activation pulses, compared to an average of 33-fold in the absence of Cdc42 recruitment. Together these results indicate that plasma membrane recruitment of constitutively active Cdc42 blocks polarized growth.

In cells that have begun to filament after induction with serum, constitutively active Cdc42 plasma membrane recruitment upon photo-activation blocked filament extension and subsequently a germ tube emerged elsewhere. We confirmed that there was no correlation between the location of plasma membrane recruited constitutively active Cdc42 and the site of new growth (Figure S1B). Furthermore, it should be noted that new growth occurred more than 20 min after the last photo-activation pulse, when the Cry2 fusion was no longer detectable at the cell cortex (Figure 1C and S1A).

New growth in the mother cell or along the filament

Subsequent to optogenetic recruitment in filamentous cells, growth resumed and hence we examined where growth occurs. Following 3 photo-recruitment pulses, new growth, irrespective of where it occurred, initiated on average 20 min after the last pulse. These results indicate that new growth occurs subsequent to the dissociation of Cry2-mCh-Cdc42[G12V] from the plasma membrane. We observed new filamentous growth emerge either from the mother cell or the filament. In the latter case, growth either occurred along the filament or resumed at the filament tip (Figure 2C). New filament growth, whether in the mother cell or the filament, appeared identical to initial filament growth with an indistinguishable extension rate (Figure 2D). The majority of cells, ~75 % resumed growth at the filament tip. Approximately

20% of the cells initiated growth elsewhere in the mother cell and ~5% initiated growth in the filament. Cells with shorter germ tubes (2-6 μm long) were more likely to initiate new growth in the mother cell, whereas cells with longer filaments (8-12 μm long) were more likely to initiate growth in the filament (Figure 2E). Overall our results suggest that the growth in longer filaments is more refractory to disruption. We next examined the location of growth along the filament as a function of filament length at the time of photo-activation. New growth could occur anywhere along the filament with a preference farther away from the tip with increasing initial filament lengths (Figure 2F). We also examined the angle between the new filament and initial filament when growth occurred in the mother cell. Figure 2G shows that growth occurred predominantly in the distal half of the mother cell (between ± 60 - 180° from the initial filament). Together the location of new growth in the mother cell and the filament suggest *de novo* growth site formation.

Recruitment of Cdc42•GTP disrupts endogenous active Cdc42 localization

The timing of new filamentous growth relative to light-dependent constitutively active Cdc42 plasma membrane recruitment suggested that the new growth occurs subsequently to the dissociation of Cry2-mCh-Cdc42[G12V] from the membrane. To determine whether constitutively active Cdc42 recruitment either directly induces polarized growth or instead resets cell polarity, we followed the distribution of a reporter for active Cdc42 derived from the *S. cerevisiae* Cdc42 effector protein Gic2 (CRIB-mCh). In filamentous cells prior to photo-activation a cluster of active Cdc42 was observed at the filament apex (Figure 3A). Surprisingly, following recruitment of Cry2-GFP-Cdc42[G12V]_{cyto} there was a dramatic reduction of CRIB-mCh at the filament tip. This result suggested that the Cry2 fusion is not able to bind the CRIB-mCh reporter, which we attribute to the large Cry2-GFP moiety fused to the Cdc42 amino-terminus. A cluster of the CRIB-mCh reporter was not detectable until just

prior to new growth, approximately 30 minutes after the last photo-activation pulse (28 ± 6 min; $n = 15$ cells). Quantitation of the ratio of growth site (filament tip) plasma membrane to cytoplasmic CRIB-mCh signal revealed an average ratio greater than 2 immediately following the first photo-activation compared to a ratio of ~ 1 immediately following the second or third photo-activation (Figure 3B).

Endocytic sites disperse subsequent to Cdc42•GTP recruitment

Our results suggest that optogenetic recruitment of constitutively active Cdc42 resets cell polarity and hence we examined whether the sites of endocytosis and exocytosis remained localized following photo-recruitment. In growing hyphal filaments endocytic sites localize as a collar 1-3 μm from the filament tip¹⁹⁻²¹ and secretory vesicles localize to the tip of the filament, in a cluster commonly referred to as a Spitzenkörper^{22,23}. We visualized sites of endocytosis using actin binding protein 1 (Abp1) which localizes to this endocytic collar. Following recruitment of constitutively active Cdc42 to the plasma membrane the cluster of the Abp1-mCh sites became dispersed throughout the cell and ~ 10 min after the last photo-activation pulse an increase in Abp1-mCh signal was observed in the mother cell, which clustered at the incipient germ tube ~ 30 min later (Figure 3C and 3D). These results suggest that site-specific endocytosis is blocked by uniform recruitment of constitutively active Cdc42 to the plasma membrane.

Cdc42•GTP recruitment results in a dramatic increase in the *de novo* secretory vesicle cluster

To visualize secretory vesicles, following recruitment of constitutively active Cdc42, we used the myosin light chain Mlc1 and the Rab GTPase Sec4 which have been shown to associate on secretory vesicles in *S. cerevisiae*²⁴, as well as localize to a cluster of secretory vesicles that localize at the tip of the filament²⁵⁻²⁷. Strikingly, immediately following plasma membrane

recruitment of Cdc42•GTP a second cluster of Mlc1-mCh was observed, typically in the cell body or base of the filament (Figure 3E and S2). The initial cluster of Mlc1-mCh persisted for some time after the appearance of the second Mlc1 cluster and moved down the filament over time, following photoactivation, and eventually appeared to coalesce with the second Mlc1 cluster. Subsequently, the coalesced Mlc1 cluster was highly dynamic within the mother cell before settling down to site of the incipient germ tube (Figure 3F, S2 and S3A). The highly dynamic Mlc1 cluster was always localized to the cell cortex, suggesting it was connected to the plasma membrane. While, in general, one cluster of Mlc1 was observed subsequent to photo-activation, occasionally we observed 2 or more clusters (Figure S3B). In experiments starting with cells that had germ tubes of different lengths, fewer photo-activation pulses were required to disrupt the initial Spitzenkörper in cells with shorter filaments compared to cells with longer filaments (Figure 2G). These results suggest that growth site in shorter filaments is less robust compared to that of longer filaments. In the absence of photo-activation, the cluster of Mlc1 is restricted to the filament tip and moves as the filament extends at a rate of $\sim 0.3 \mu\text{m}/\text{min}$. Following photo-activation there was a dramatic increase in the instantaneous velocity of the Mlc1 cluster with peaks of up to 10-fold higher, *i.e.* $3\text{-}4 \mu\text{m}/\text{min}$ (Figure S4A). The increases in Mlc1 cluster instantaneous velocity occurred progressively over 3-4 minutes, inconsistent with rapid association and dissociation of secretory vesicles. Finally, we examined the shape of the Mlc1 cluster and in the absence of photo-activation it appeared as sphere (projected onto XY plane) with major and minor axes of similar length. However, following photo-activation this cluster elongated along axis of movement, further consistent with its displacement (Figure S4B).

In *C. albicans* hyphae, Mlc1 is observed at the Spitzenkörper, with little to no signal elsewhere in the cell^{25,26}, however the Rab GTPase Sec4 is found both at this apical location, but also individual secretory vesicles can be observed^{20,26-28}. Hence we followed the distribution of secretory vesicles using mScarlet-Sec4 after photo-activation. Figure 4A shows

Sec4 at the tip of an emerging germ tube and within 1 min of photo-recruitment of constitutively active Cdc42 a new cluster of Sec4 was observed in the mother cell. This new cluster was substantially larger than the initial cluster and formed concomitant with an apparent decrease in cytoplasmic fluorescence. The new cluster of Sec4 was highly dynamic and rapid displacement was observed subsequent to each photo-recruitment pulse (Figure S4C). We quantitated the average signal of the Sec4 cluster and the cytoplasm from 8 cells and Figure 4B and 4C show that there is a ~4-fold increase in Sec4 signal following photo-activation, concomitant with a decrease in the cytoplasmic signal. These results suggest that secretory vesicles are rapidly recruited to the new cluster, which then becomes highly dynamic during the photo-activation pulses, continuing for ~ 10 min after the last pulse. Our results suggest that there is a dramatic recruitment of Sec4 upon photo-activation, yet the levels of Mlc1 appear to be unaffected. To directly examine this possibility, we carried out photo-recruitment of constitutively active Cdc42 in a strain expressing together mScarlet-Sec4 and Mlc1-miRFP. Figure 4C shows a time course with Sec4 in green and Mlc1 in magenta in the merged images where a striking shift in the cluster of vesicles from magenta to green upon photo-activation and then back to magenta ~10 min after the last photo-activation pulse (Figure 4C). This shift was confirmed by quantitation of the ratio of Sec4 to Mlc1 (Figure 4D). This increase is essentially due to an approximate 5-fold increase in the amount of Sec4 (Figure S5A) as the Mlc1 signal was relatively constant throughout the time course. We also determined if the recruitment of Sec4 occurred at the two clusters by examining the Sec4:Mlc1 ratio at each. Figure S5B shows that roughly a 2-fold increase in the Sec4:Mlc1 is observed at the initial Spitzenkörper, compared to the 4-fold increase in the Sec4:Mlc1 ratio at the new cluster. These results indicate that photo-recruitment of constitutively active Cdc42 increases the number of secretory vesicles at initial Spitzenkörper as well as forming a cluster *de novo*.

The presence of a cluster of secretory vesicles at the filament apex depends upon the actin cytoskeleton as depolymerization of F-actin has been shown to result in loss of this

cluster²⁵. In wild-type hyphal filaments actin cables are thought to be important for delivery of secretory vesicles to the Spitzenkörper and they can be observed emanating from this structure²⁵ (Figure 4E). To determine whether actin cables were intact following constitutively active Cdc42 photo-recruitment, we imaged cells expressing Mlc1-miRFP and following photo-activation and the appearance of two clusters, cells were fixed and actin was visualized. Figure 4E shows an apparent decrease in the actin cables clustered around the initial Spitzenkörper following photo-activation. However the new cluster of secretory vesicles appears to have actin cables emanating from it that are oriented towards the back of the mother cell, suggesting that movement of this new cluster of vesicles might be actin driven, much like actin-dependent propulsion of endosomes, pinosomes and phagosome²⁹⁻³¹.

Conclusion

Based on these data we propose that photo-recruitment of constitutively active Cdc42 to the plasma membrane resets growth by disrupting a site-specific link to a cluster of secretory vesicles. Increasing the levels of active Cdc42 on the plasma membrane favors the spontaneous clustering of secretory vesicles elsewhere in the cell, which is highly dynamic. Re-establishment of active Cdc42 at a new location anchors the cluster of secretory vesicles allowing subsequent fusion with the plasma membrane. Optogenetic manipulation of cell polarity reveals that such a cluster of secretory vesicles, found in plants, fungi and neurons, does not require directed cell growth to form.

Figure 1

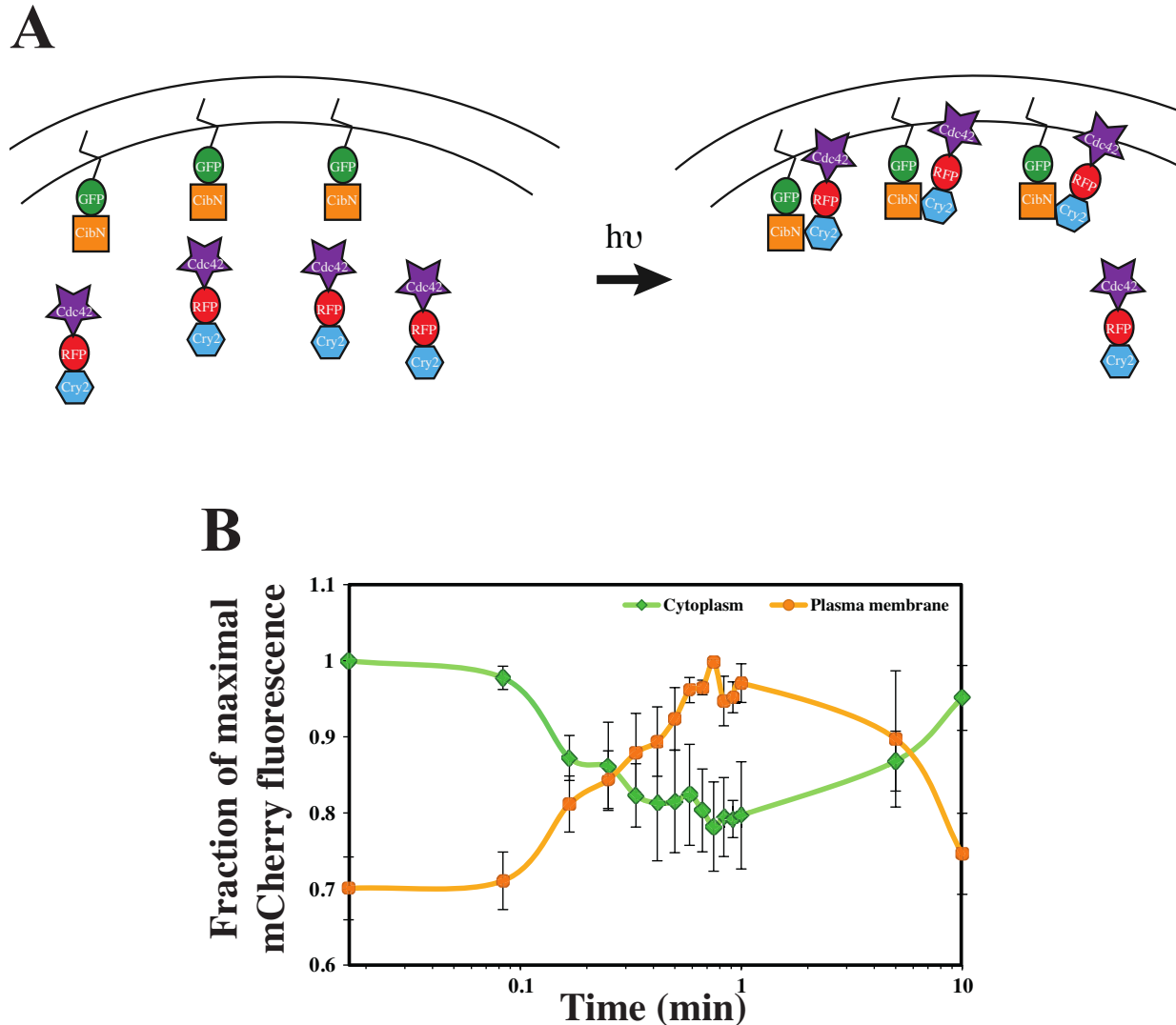


Figure 1. Rapid recruitment of Cdc42•GTP to the plasma membrane. A) Schematic of optogenetic system for recruitment of Cdc42•GTP to the plasma membrane in *C. albicans*. B) Recruitment of Cdc42•GTP to the plasma membrane occurs concomitant with depletion from the cytoplasm. A strain expressing CibN-GFP-CtRac1 and Cry2-mCh-Cdc42[G12V]cyto was incubated on agar pads at 30 °C and exposed to a 300 msec 488 nm pulse (10 % of a 25 mWatt laser) immediately after the initial time point. Plasma membrane and cytoplasmic signals were quantified from 3 cells; the average and standard deviation are shown. C) Cdc42•GTP can be recruited to the plasma membrane multiple times. Strain was incubated on agar pads as in Fig. 1B and similarly exposed to a 488 nm light pulse every 20 min. The normalized ratio for plasma membrane to cytoplasmic mCherry fluorescence was determined from 3 cells with bars indicating standard deviation.

Figure 1

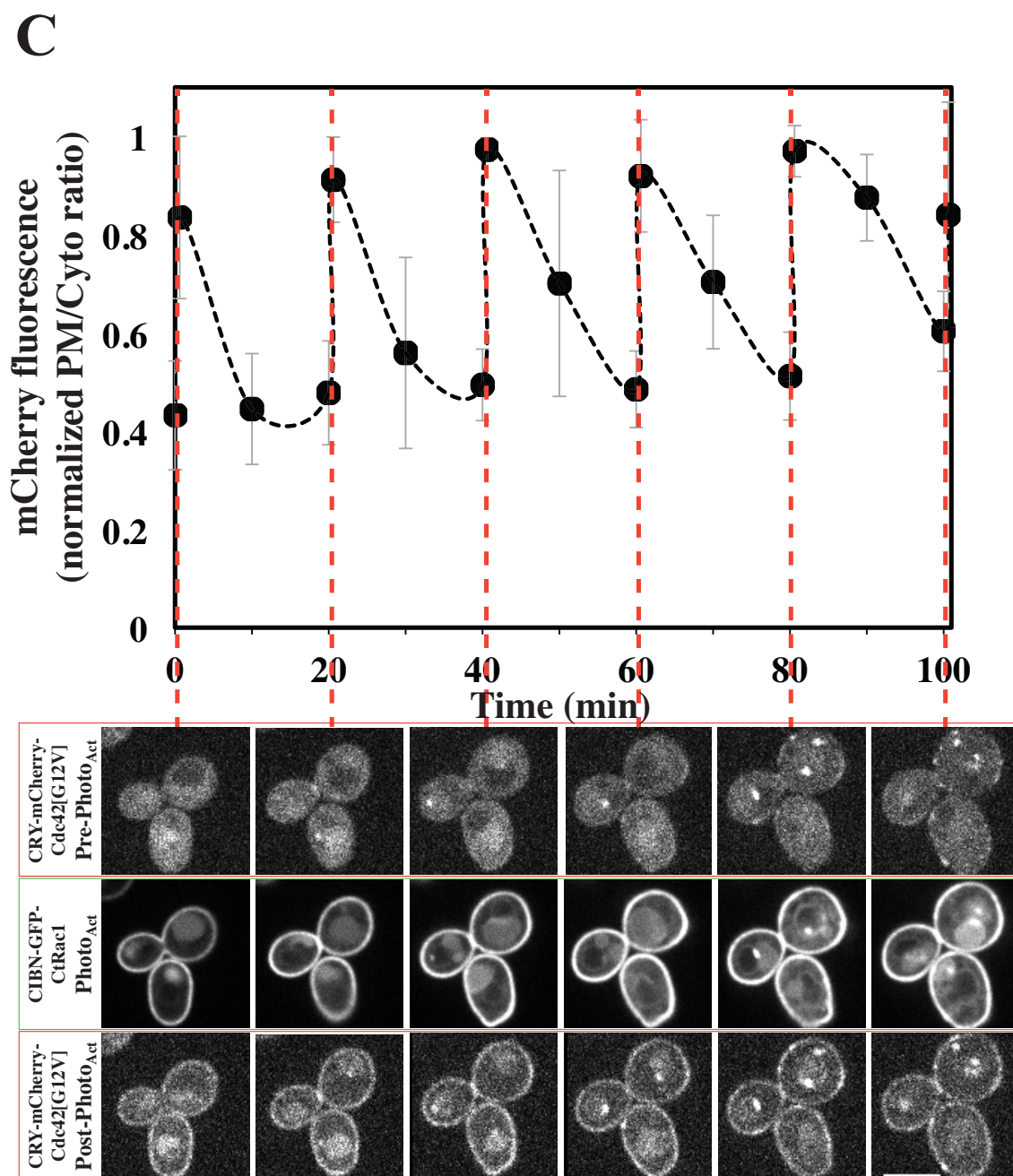


Figure 2

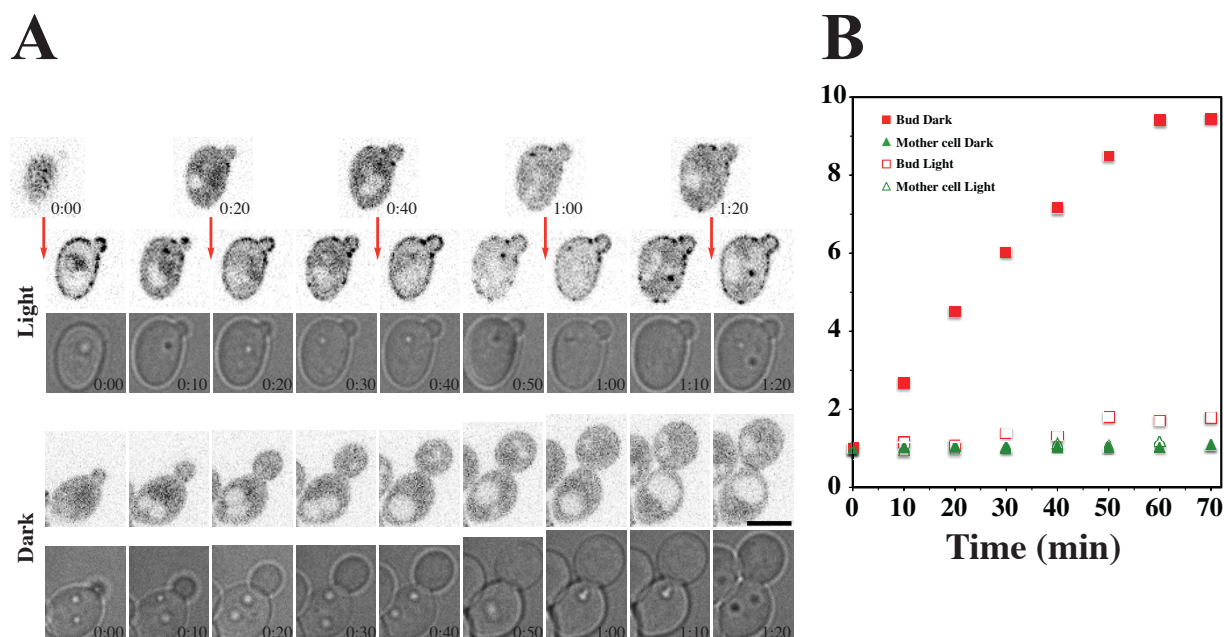
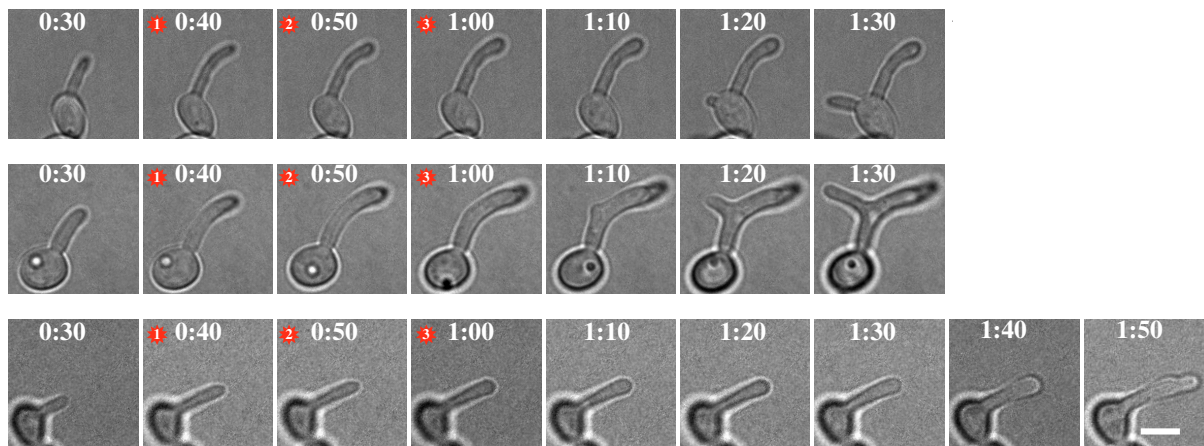


Figure 2. Uniform plasma membrane recruitment of Cdc42•GTP disrupts polarized growth.

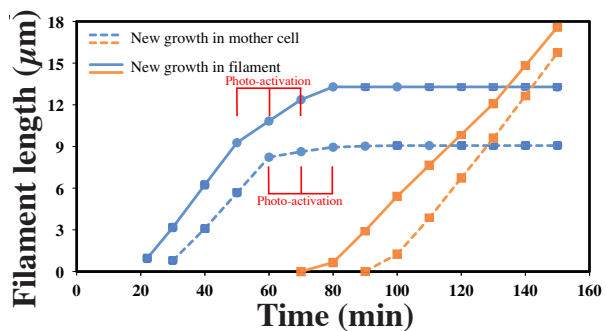
A) Budding growth is blocked following plasma membrane recruitment of Cdc42•GTP. Strain was incubated as in Fig. 1B and either exposed to a 488 nm light as described in Fig. 1C (Light) or not irradiated (Dark). The upper panel for each time course shows the mCherry images and the lower panel the DIC images. B) Quantification of bud and mother cell area following photo-recruitment of Cdc42•GTP. Relative area is the average from 5 cells with photo-activation pulses at 0, 20, 40 and 60 min. C) Following recruitment of Cdc42•GTP in filamentous cell, new growth can occur in the mother cell or along the filament. Strain as in Fig. 1B was incubated on agar pads containing serum at 37 °C and subject to 3 pulses of 488 nm light indicated by red stars. DIC images were acquired every 10 min. D) New growth at same rate as the initial filament. Quantification of filament length over time in which growth emerged from filament (solid lines) or mother cell (dashed lines). Red symbols indicate photo-activation pulses. E) New growth location depends on initial filament length. Percentage of cells in each filament length class in which new growth emerged from mother cell (yellow), filament (green) and resumed from filament tip (blue). Strain as in Fig. 2 subjected to 3 pulses of 488 nm light and followed by time-lapse microscopy. Quantification from 11 experiments with a total of 425 cells followed by time-lapse microscopy and 15-80 cells per length class. F) New growth in filament occurs preferentially toward the back of the filament for cells with longer initial filaments. Strain as in Fig. 2C subjected to 3 pulses of 488 nm light indicated. Location of growth in filament divided by initial filament length as function of initial filament length is shown from 8 experiments with a total of 16 cells followed by time-lapse microscopy. G) New growth in the mother cell occurs medially to initial filament. Strain as in Fig. 2C. Angle of the new germ tube relative to the filament was quantified from 9 experiments with a total of 66 cells followed by time-lapse microscopy.

Figure 2

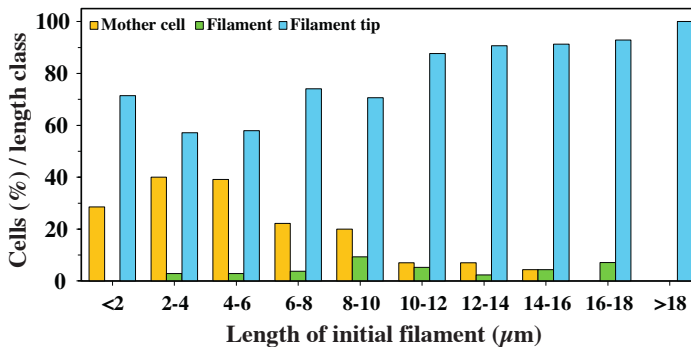
C



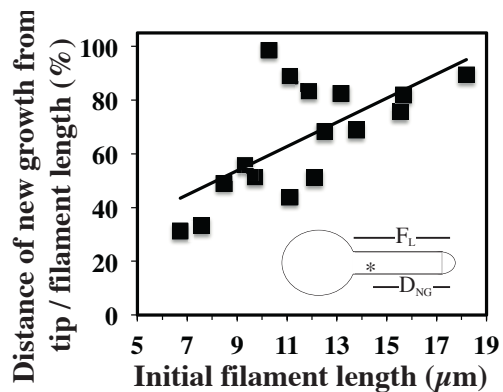
D



E



F



G

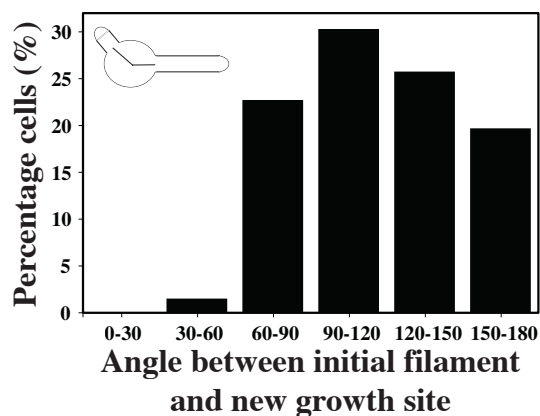


Figure 3. Optogenetic recruitment of Cdc42•GTP disrupts Cdc42 activation and endocytosis sites at filament tip. A) Following photo-activation, active Cdc42 at the filament tip is not detectable. A strain expressing CibN-CtRac1, Cry2-GFP-Cdc42[G12V]cyto and CRIB-mCh was incubated as in Fig. 2C and subjected to 6 pulses of 488 nm light every 5 minutes at indicated times. At each time DIC and mCherry images were acquired and maximum projections are shown from 3 time lapses. B) The level of active Cdc42 at the growth site decreases following photoactivation. The ratio of filament tip plasma membrane signal to cytoplasmic signal was determined at the 1st and either 2nd or 3rd photoactivation (5 min between photoactivations) from 15 time lapses and 5 independent experiments, colors indicate same cell. The difference in the mean values from these two conditions was statistically significant, $p < 0.0001$. C). Endocytosis sites become dispersed upon plasma membrane recruitment of Cdc42•GTP. A Strain expressing CibN-CtRac1, Cry2-GFP-Cdc42[G12V]cyto and Abp1-mCh was incubated as in Figure 3A with red star indicating photo-activation. At each time DIC and mCherry images were acquired and maximum projections are shown from a representative time lapse. D) Abp1 in the mother cell increases following photo-activation. Quantification of Abp1-mCh signal in the mother cell from 7 time lapses and 3 independent experiments followed by time-lapse microscopy. Signal in the mother cell at time of new germ tube emergence was normalized to a value of 1. E) Cluster of secretory vesicles becomes highly dynamic following recruitment of active Cdc42. A strain expressing CibN-CtRac1, Cry2-GFP-Cdc42[G12V]cyto and Mlc1-mCh was incubated as in Figure 3A with red star indicating photo-activation. At each time (every 2.5 min prior to photoactivation and every 1 min thereafter) DIC and mCherry images were acquired and sum projections are shown from a representative time lapse (left panel). Right panel shows location of cluster of Mlc1 in the final cell shape with location in initial extending germ tube (red), existence of two clusters (green), dynamic cluster in mother cell (purple) and cluster in final extending germ tube (blue). F) Mlc1 cluster is highly dynamic following recruitment of active Cdc42. Location of Mlc1 cluster in 5 cells as in E). G) Mlc1 cluster is more easily disrupted in shorter filament than longer filaments. Strain was analyzed as in Fig. 3E and the number of photoactivation pulses necessary to disrupt initial Mlc1 cluster was determined as a function of filament length from 9 experiments with a total of 25 cells followed by time-lapse microscopy. The difference in the mean values between these two conditions was statistically significant, $p < 0.0001$.

Figure 3

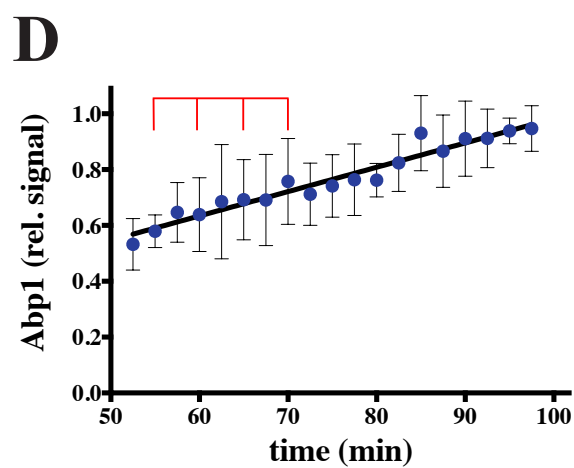
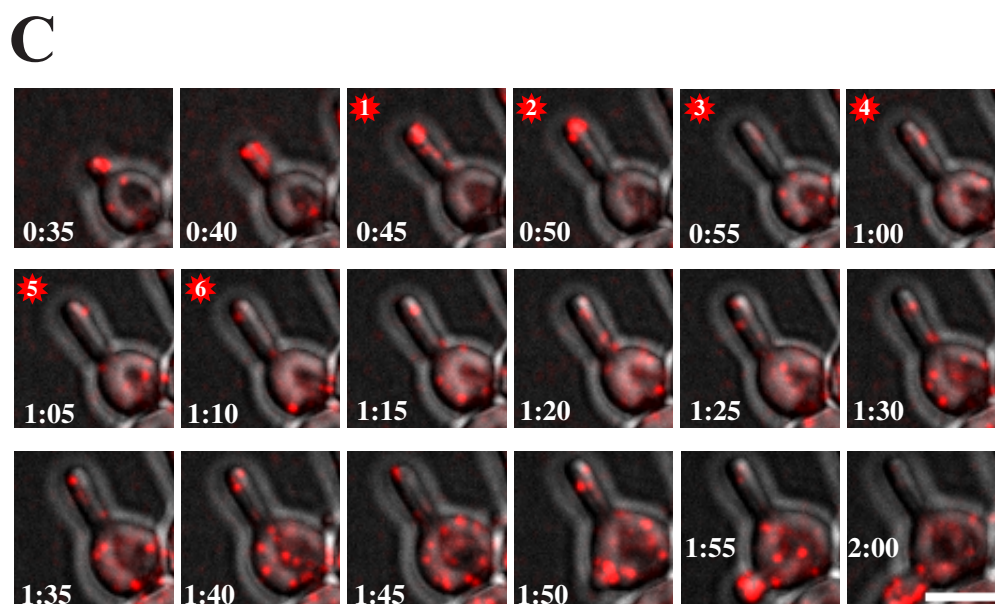
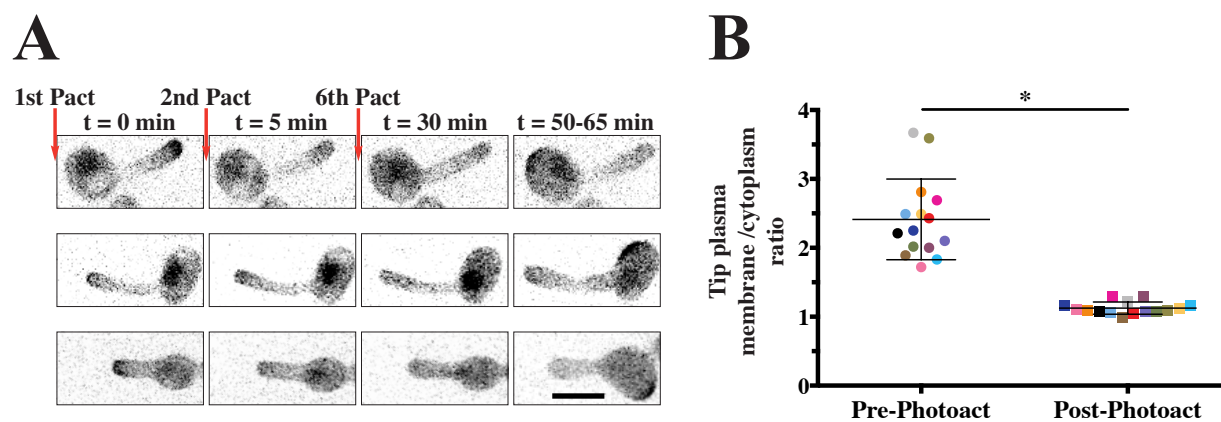
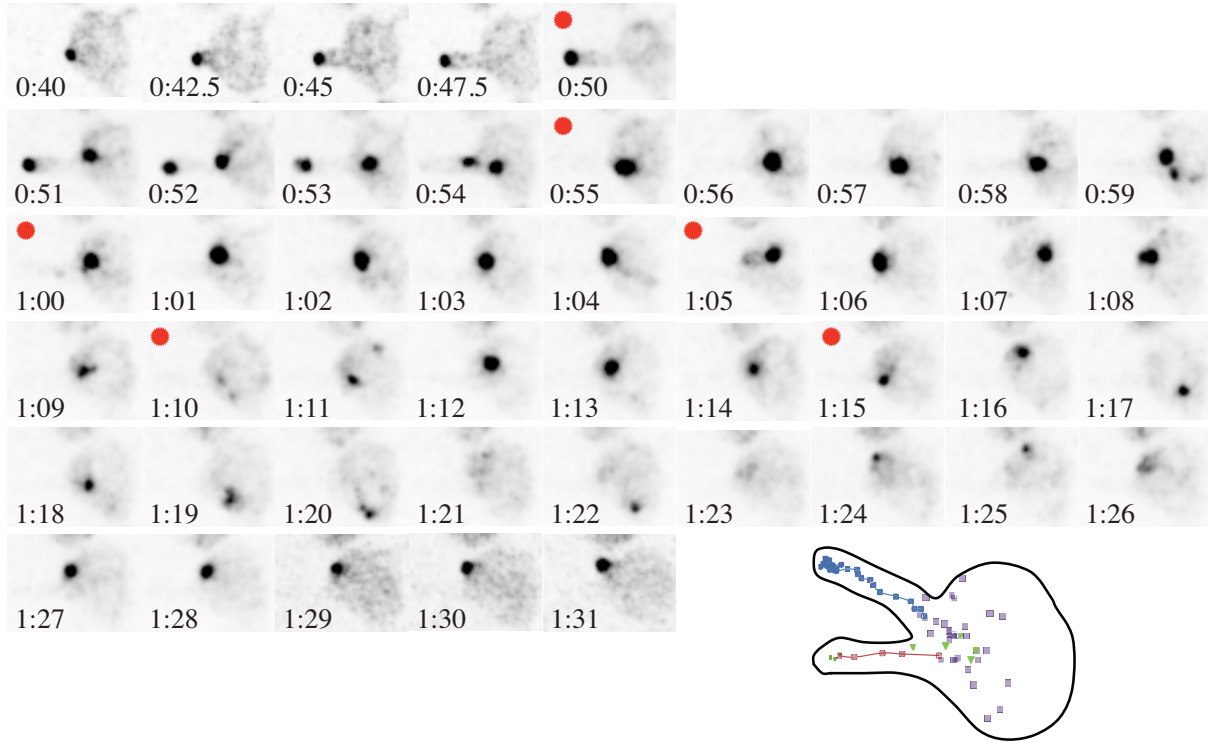
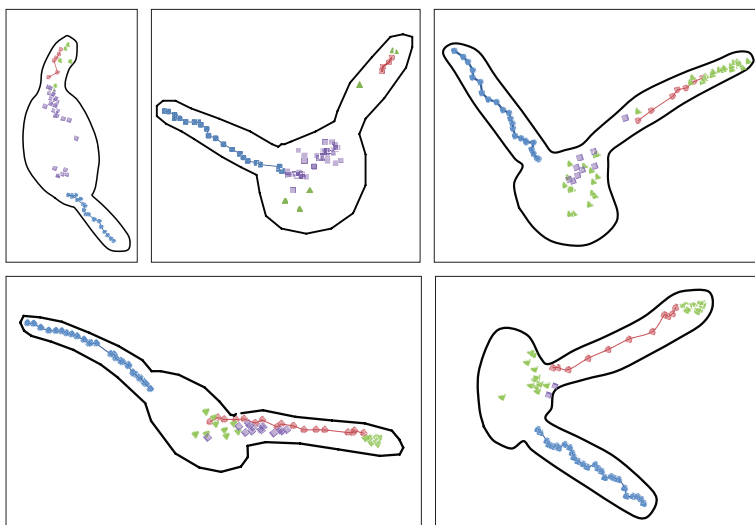


Figure 3

E



F



G

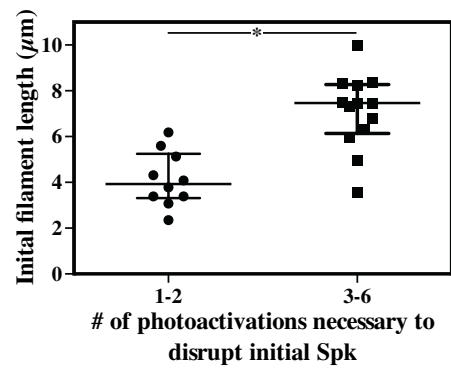
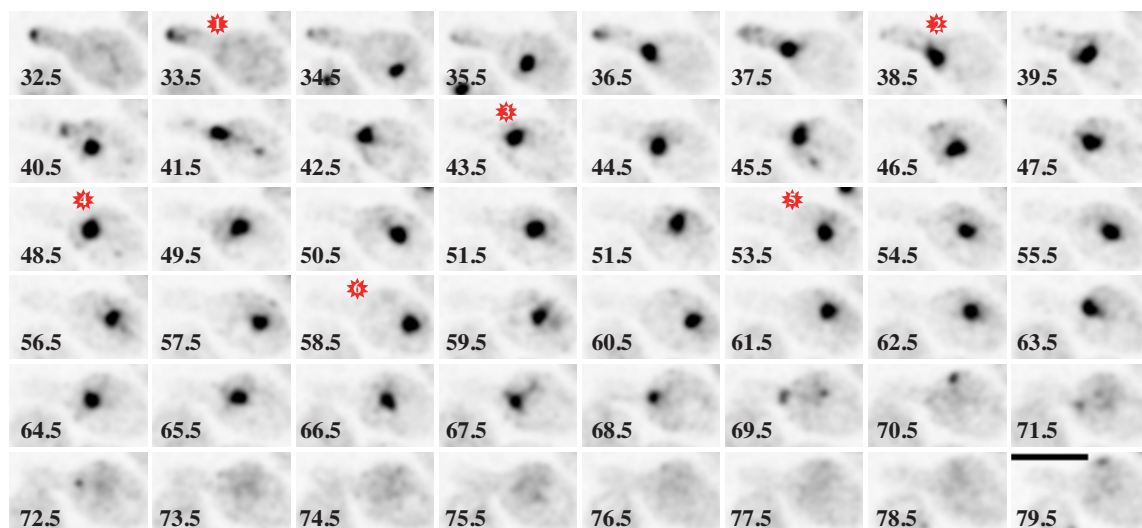


Figure 4. Recruitment of Cdc42•GTP induces a dramatic increase in de novo secretory vesicle clustering. A) Sec4 distribution following photo-recruitment of Cdc42•GTP. A strain expressing CibN-CtRac1, Cry2-GFP-Cdc42[G12V]cyto and mScarlet-Sec4 was incubated as in Fig. 3A with red star indicating photo-activation. At indicated times, DIC and RFP images were acquired and sum projections are shown from a representative time lapse. B) Dramatic increase in Sec4 cluster occurs concomitant with a decrease in cytoplasmic signal. Quantification of RFP signal from 8 cells expressing mScarlet-Sec4 as in Fig. 4A. Intensities were corrected for photobleaching by fitting the total signal from each cell analyzed to an exponential and correcting cytoplasmic and Spitzenkörper signals over time. Cytoplasmic signal is the average from 3 different areas in the cell. The Spitzenkörper signal represents the total of the initial and new cluster, where relevant. The maximum values from each compartment in each experiment were set to 1 and the mean is shown with SEM indicated. C) The increase in Sec4 cluster does not correlate with an increase in Mlc1 cluster. A strain expressing CibN-CtRac1, Cry2-GFP-Cdc42[G12V]cyto, mScarlet-Sec4 and Mlc1-miRFP as in Figure 3A, with red star indicating photo-activation. At indicated times DIC, RFP (magenta) and miRFP (green) images were acquired and sum projections are shown from a representative time lapse. Inset (images at 2.5, 17.5 and 52.5 min) shows an enlargement of secretory vesicle cluster. D) Dramatic increase in the ratio of Sec4 to Mlc1 occurs upon recruitment of Cdc42•GTP. Quantification of RFP and miRFP signals at the cluster of secretory vesicles from 6 cells followed by time-lapse microscopy as in Fig. 4E. Mean ratios and standard deviation are shown. E) Actin cables emanate from newly formed cluster of secretory vesicles. A strain expressing CibN-CtRac1, Cry2-GFP-Cdc42[G12V]cyto, and Mlc1-miRFP incubated on a glass bottom dish containing media and serum at 37 °C subjected to a pulse of 488 nm light (Light) or kept in the dark (Dark). After photoactivation (5 min) cells were fixed and the actin cytoskeleton was stained with Alexa-560 phalloidin. In middle panel cells were imaged every 2.5 min before fixing at 7.5 min. Maximum projections of fixed cells 18-28 0.2 μm z-sections with the Mlc1 (magenta) and the F-actin (green) shown.

Figure 4

A



B

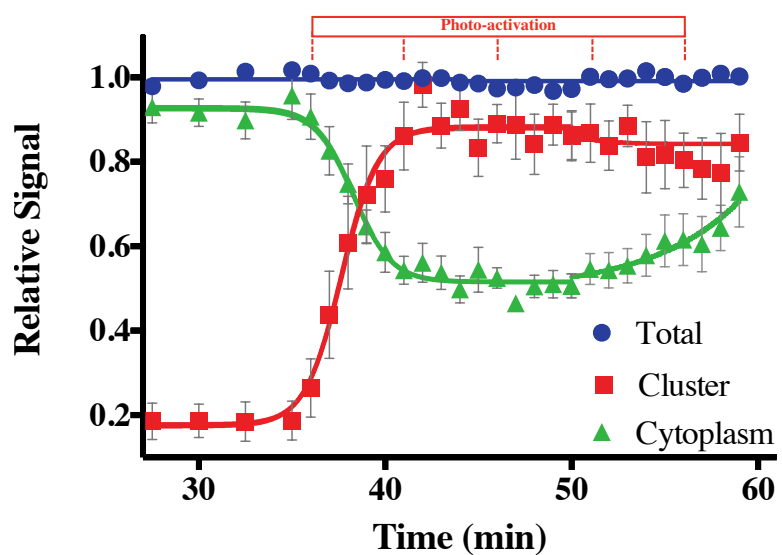
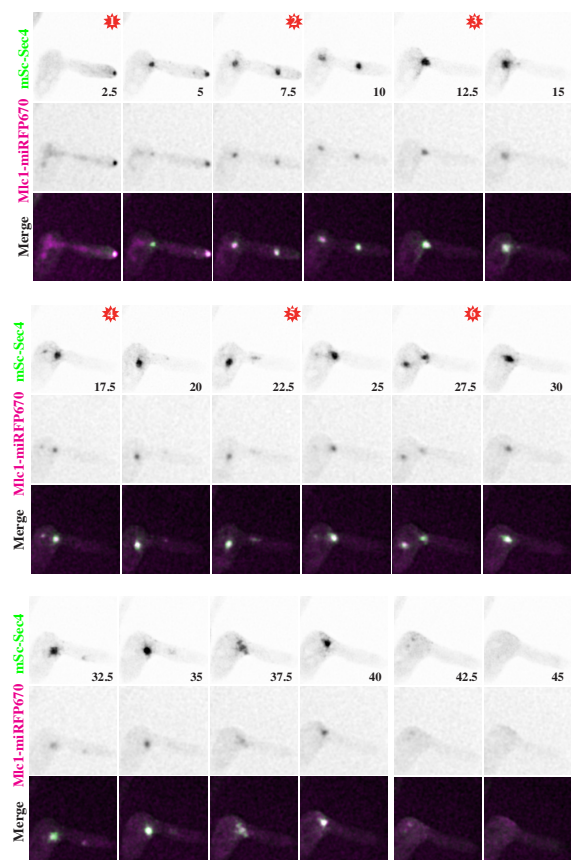
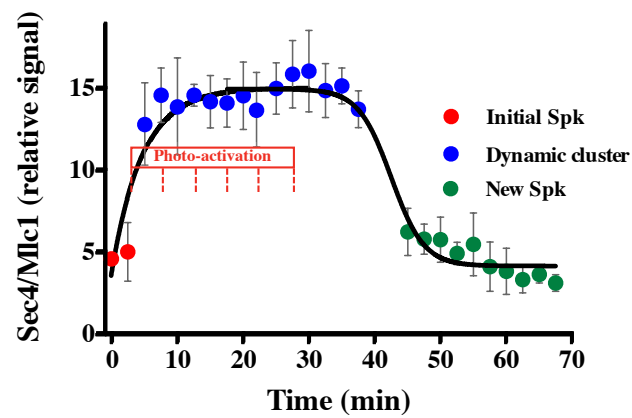


Figure 4

C



D



E

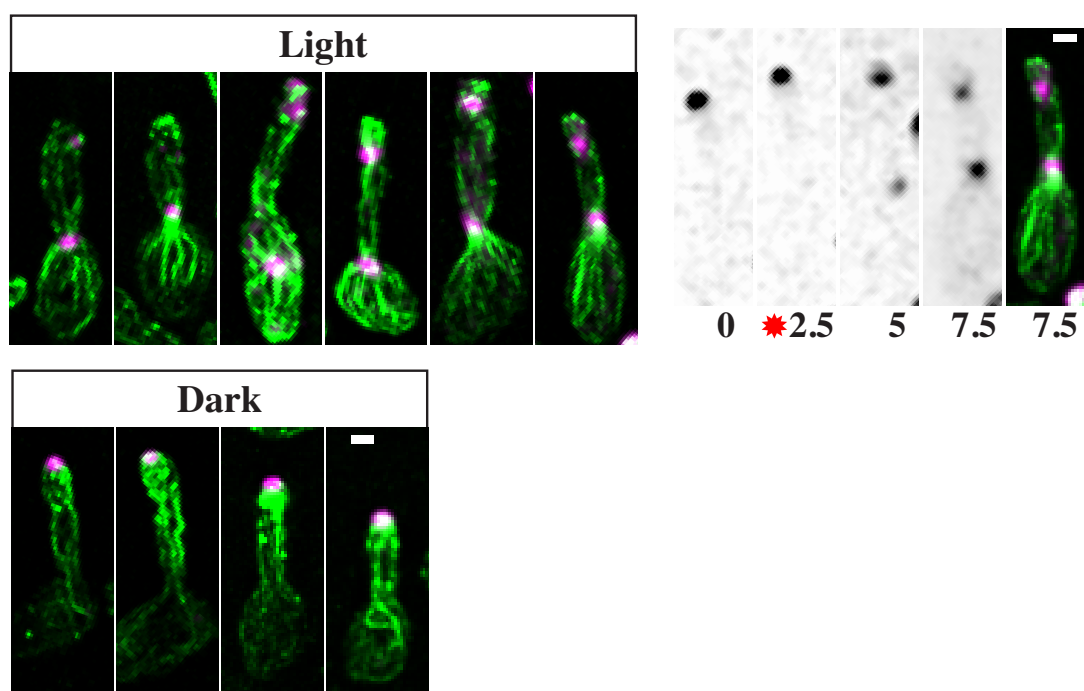
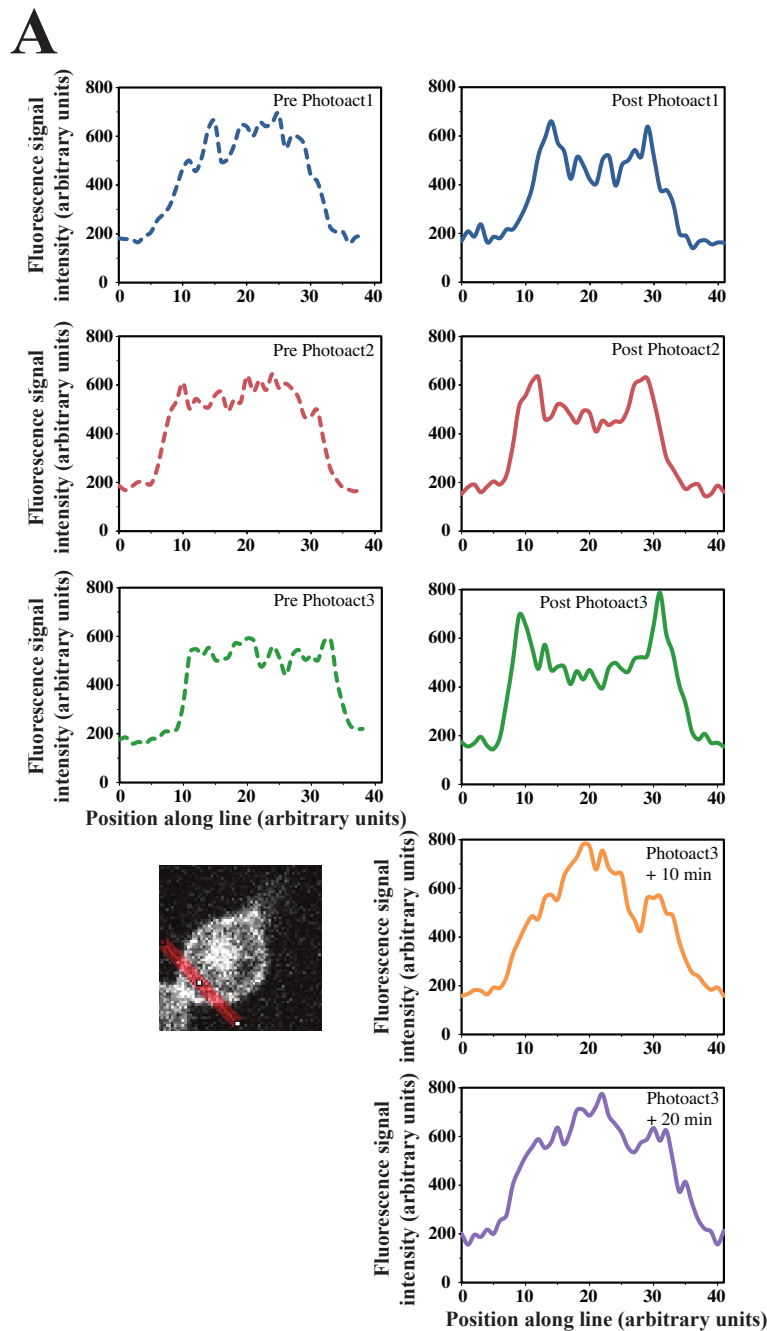


Figure S1



Supplementary Figure S1. New growth and location of recruited Cdc42•GTP do not correlate. A) Cdc42•GTP is rapidly recruited to the plasma membrane. Strain as in Fig. 1B was incubated as in Fig. 2C and subjected to 3 pulses of 488 nm light with 10 min between them. Line scan shows mCherry signal through the cell as indicated in bottom left hand image. B) New germ tube emergence occurs subsequent to Cdc42•GTP photorecruitment. Images showing mCherry signal (top) immediately after the 3 photo-activation pulses. Line scan of mCherry signal along the plasma membrane with location of new growth indicated, which occurred 30 min after last photo-activation pulse.

Figure S1

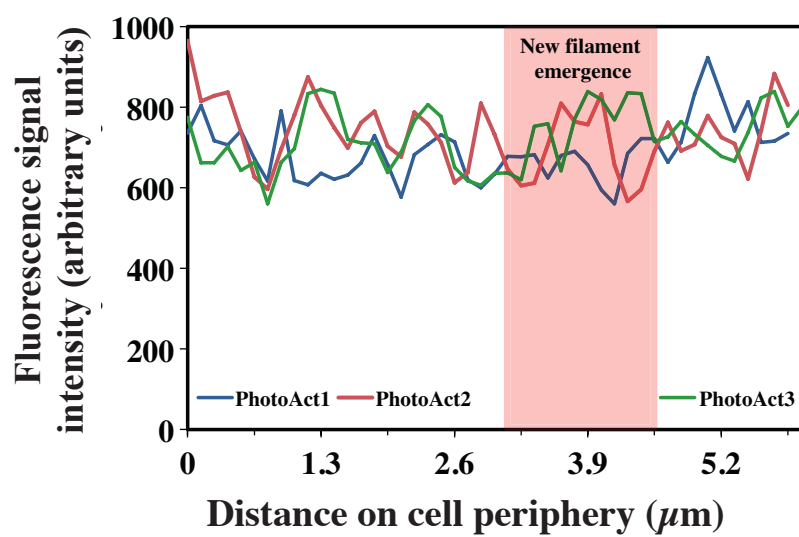
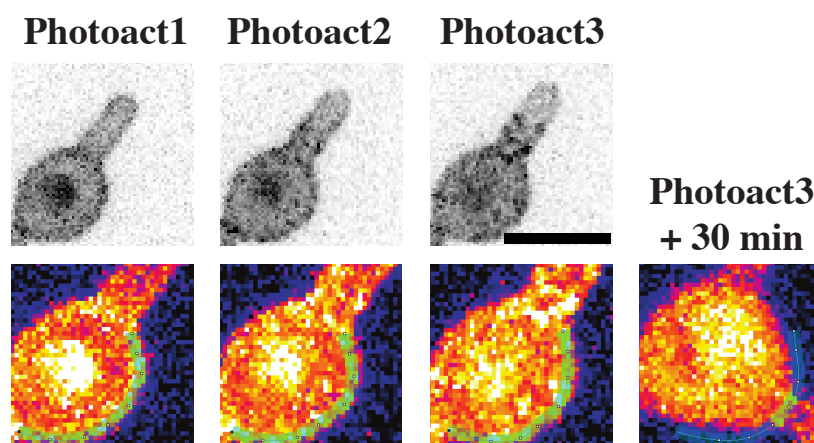
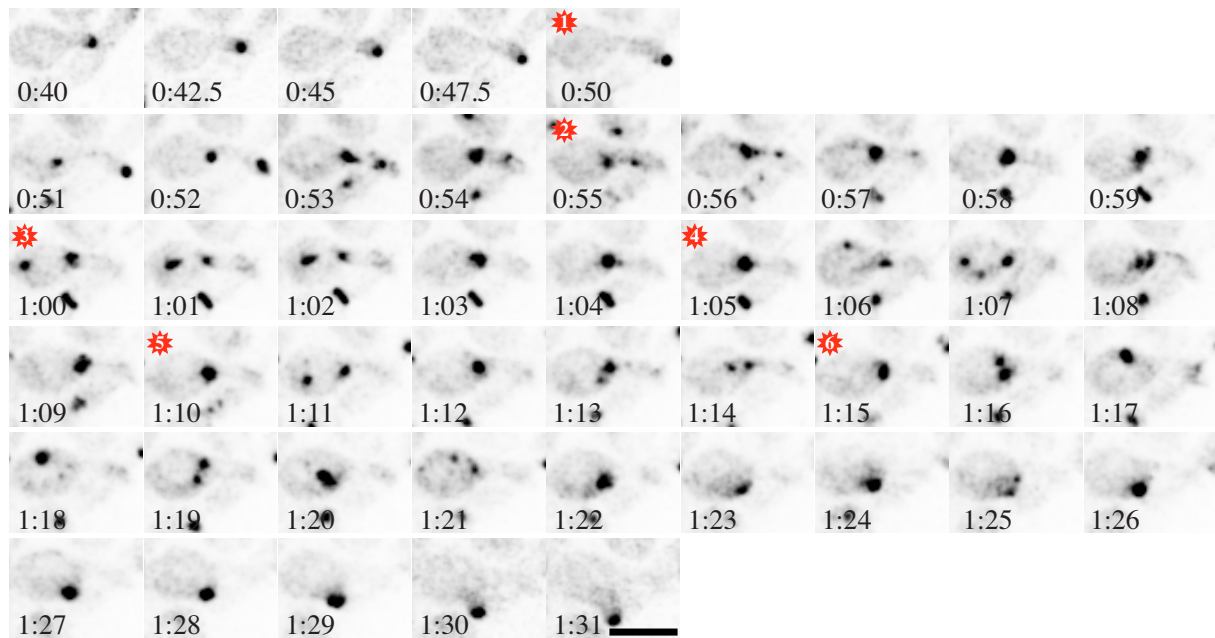
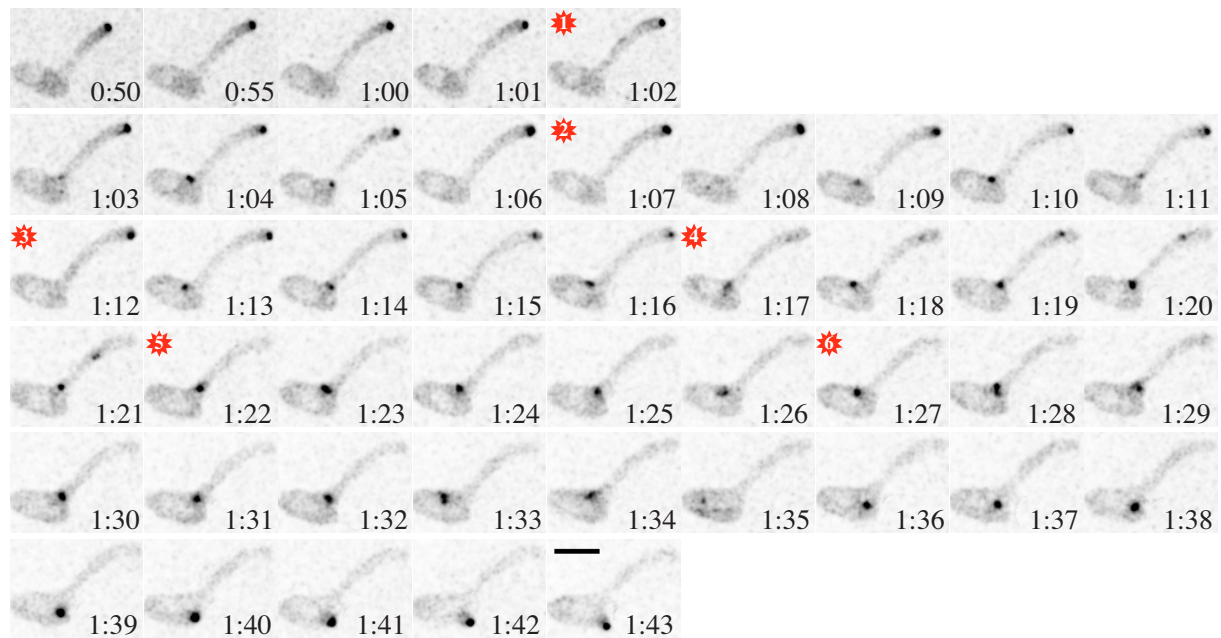
B

Figure S2

A



B



Supplementary Figure S2. Mlc1 cluster dynamics following recruitment of Cdc42•GTP.

Location of Mlc1 cluster following photo-activation from 3 different time lapses (A-C). Strain as in Fig. 3E with red star indicating photo-activation. At each time (every 2.5 min prior to photoactivation and every 1 min thereafter) DIC and mCherry images were acquired and sum projections are shown from a representative time lapse.

Figure S2

C

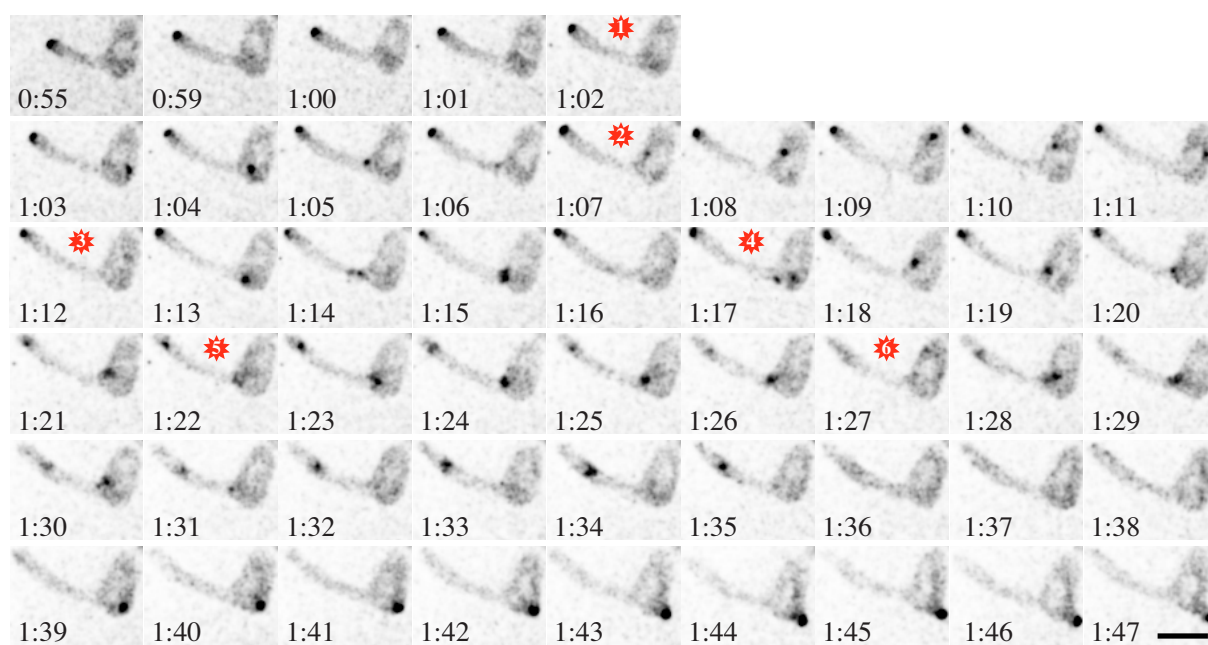
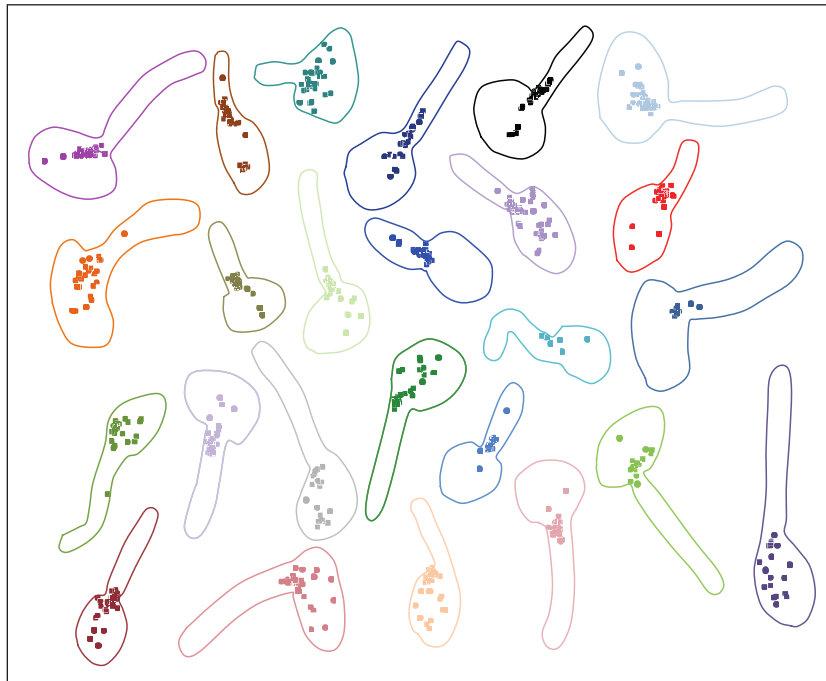
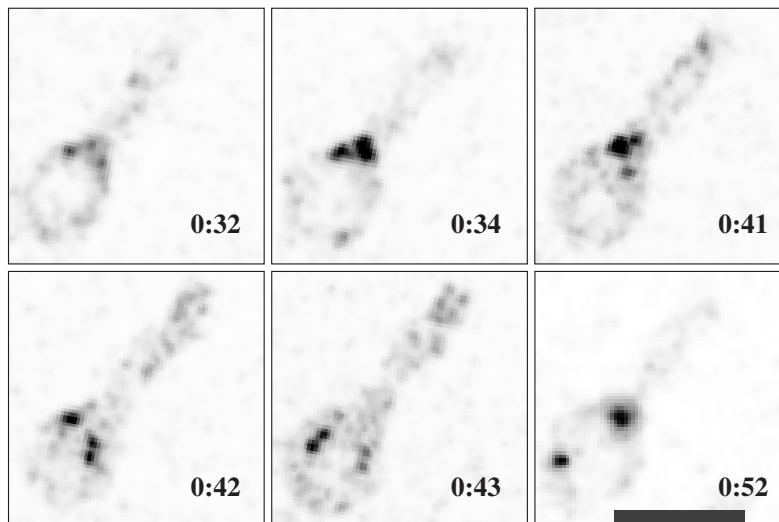


Figure S3

A



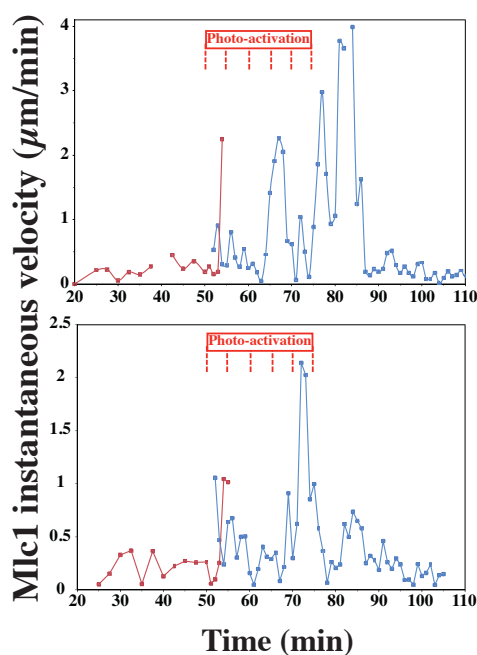
B



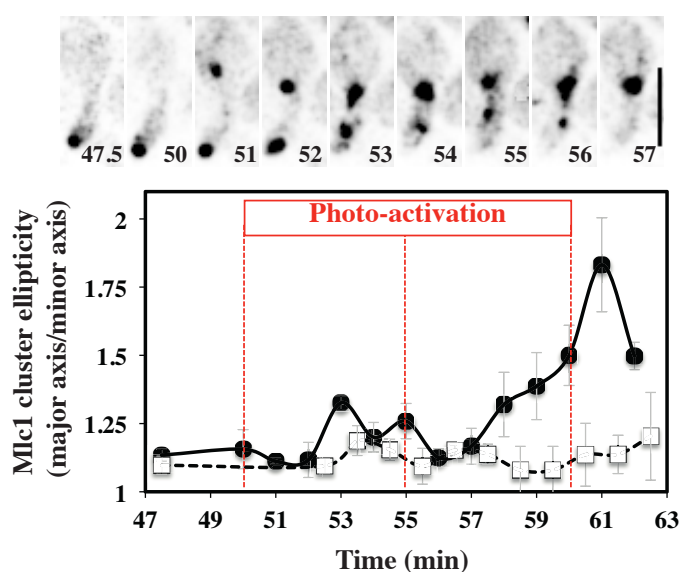
Supplementary Figure S3. Cluster of Mlc1 is highly dynamic in mother cell following recruitment of Cdc42•GTP. A) Location of Mlc1 cluster following photo-activation. Outline of cells at time of photo-activation, from 9 experiments with a total of 25 cells followed by time-lapse microscopy. Position of dynamic cluster of Mlc1-mCh, after the two clusters have coalesced, is shown (25-55 min in different time lapses), with images every min. B) Occasionally multiple Mlc1 clusters are observed following photo-activation. Individual z-sections at indicated times showing multiple clusters of Mlc1-mCh.

Figure S4

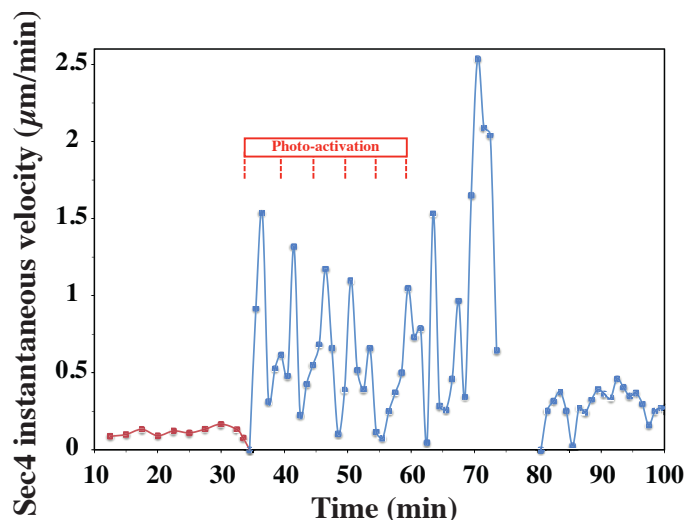
A



B

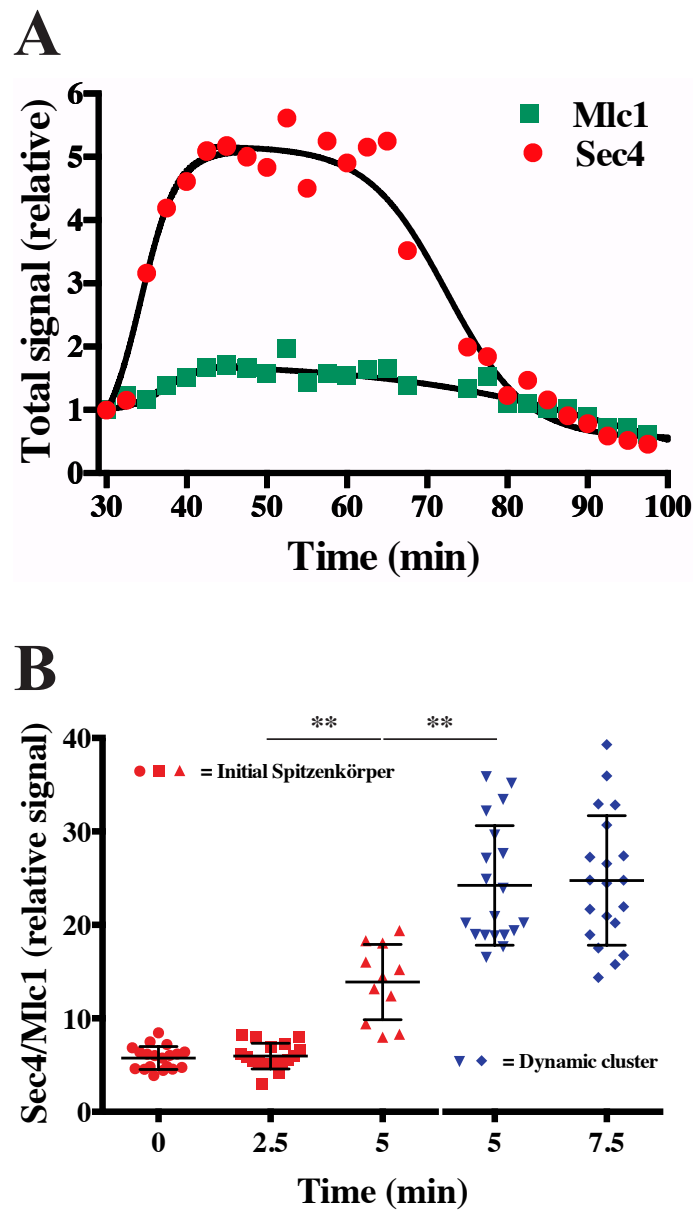


C



Supplementary Figure S4. The cluster of secretory vesicles is highly dynamic subsequent to the recruitment of Cdc42•GTP. A) Dramatic increase in the instantaneous velocity of Mlc1 cluster. The instantaneous velocity of the Mlc1 cluster from 2 time-lapses is shown with initial Spitzenkörper (red) and new dynamic cluster (blue) indicated. B) The Mlc1 cluster elongates along the axis of movement. The ratio of major over minor axis of the Mlc1 cluster at the initial Spitzenkörper was determined from 4 cells (solid lines and symbol) exposed to 488 nm light and 3 cells kept in the dark (dashed lines and open symbols), with mean and standard deviation indicated. C) The Sec4 cluster is highly dynamic. The instantaneous velocity of the Sec4 cluster from one time-lapse is shown with initial Spitzenkörper (red) and new dynamic cluster (blue) indicated.

Figure S5



Supplementary Figure S5. A dramatic increase in Sec4 cluster occurs upon photo-activation.

A) Total levels of Sec4 and Mlc1 at the Spitzenkörper following photo-activation. A strain expressing CibN-CtRac1, Cry2-GFP-Cdc42[G12V]cyto, mScarlet-Sec4 and Mlc1-miRFP incubated as in Fig. 2C, was subjected to 6 pulses of 488 nm light every 5 minutes at times indicated, RFP (red) and miRFP (green) images were acquired and quantified. Values are the averages from 6 cells followed by time-lapse microscopy in which the signal at time 0 was set to 1. B) Sec4 is recruited to both the initial Spitzenkörper and a new dynamic cluster subsequent to Cdc42•GTP recruitment. The ratio of mScarlet-Sec4 signal to Mlc1-miRFP signal at the initial Spitzenkörper (red) and new dynamic cluster (blue) from a total of 20 cells followed by time-lapse microscopy is shown. Cells were exposed to 488 nm light at 2.5 min. The differences between indicated conditions were statistically significant, $p < 0.0001$.

Methods

Strain and plasmid construction

Standard methods were used for *C. albicans* cell culture, molecular, and genetic manipulations as described³². Strains used in this study are listed in Table S1. To generate optogenetic strains, the sequences encoding Cry2Phr and CibN¹⁸ were codon optimized, synthesized and cloned into pUC57 (Genscript). CibN was cloned into pEXPARG-ACT1p-CRIB-GFP-ADH1t replacing CRIB using unique RsrII and SacI sites. GFP γ ³³ was then amplified with a unique 5' SacI site and 3' primer encoding the Rac1 Ct membrane targeting domain (KKRKIKRAKKCTIL)³⁴ followed by a stop codon and MluI site. This GFP γ -CtRAC1 was subsequently cloned into pEXPARG-ACT1p-CibN-GFP-ADH1t to replace GFP resulting in pEXPARG-ACT1p-CibN-GFP γ -CtRac1-ADH1t. An *ADH1* promoter and *ACT1* terminator were cloned into pDUP5³⁵ using unique XmaI and NotI sites resulting in pDUP5-ADH1p-(AscI-PacI-SpeI-SbfI)-ACT1t. CibN was amplified with a unique 5' PacI site and a 3' 15 aa linker encoding EFDSAGSAGSAGGSS followed by Rac1 Ct membrane targeting domain and a PacI site and this was cloned into pDUP5-ADH1p-(AscI-PacI-SpeI-SbfI)-ACT1t resulting in pDUP5-ADH1p-CibN-CtRac1-ACT1t. The *TEF1* promoter and terminator were cloned into pDUP3³⁵ using unique XmaI and NotI sites resulting in pDUP3-TEF1-(AscI-PacI-SpeI-SbfI)-TEF1t. Cry2 was cloned using unique AscI and PacI sites into pDUP3-TEF1-(AscI-PacI-SpeI-SbfI)-TEF1t resulting in pDUP3-TEF1-Cry2-(PacI-SpeI-SbfI)-TEF1t. The gene encoding yemCherry³⁶ was then amplified with unique PacI and SpeI sites and cloned into pDUP3-TEF1-Cry2-(PacI-SpeI-SbfI)-TEF1t resulting in pDUP3-TEF1-Cry2-mCh-(SpeI-SbfI)-TEF1t. Cdc42 or Cdc42[C188S] was then cloned into the SpeI and SbfI sites resulting in pDUP3-TEF1-Cry2-mCh-Cdc42-TEF1t. A mutation encoding the G12V alteration was generated by site directed mutagenesis resulting in pDUP3-TEF1p-Cry2-GFP γ -Cdc42[G12V,C188S]-Tef1t. Cry2 was amplified with 5' AscI site and a linker encoding EFDSAGSAGSAGGSS followed

by a PacI site. GFP γ was subsequently cloned into unique PacI and SpeI and finally Cdc42[G12V,C188S] was cloned into unique SpeI and SbfI sites resulting in pDUP3-TEF1p-Cry2-GFP γ -Cdc42[G12V,C188S]-Tef1t. The CibN and Cry plasmids were linearized and transformed into strains and grown in absence of light. The Abp1-mCh, Mlc1-mCh, and Mlc1-yemiRFP670 strains were generated by homologous recombination, using pFA-yemCherry-HIS1³⁷ and pFA-yemiRFP670-HIS1 (to be described elsewhere) as described previously³⁷. pEXPARG-Sec4p-mSc-Sec4 was constructed using 1311 bp Sec4 promoter with unique NotI and RsrII sites, followed by codon optimized mScarlet (to be described elsewhere) with RsrII and AscI sites and Sec4 ORF flanked by AscI and MluI sites. The pEXPARG-Act1p-CRIB-mCh was constructed by replacing GFP in pEXPARG-Act1p-CRIB-GFP¹⁵ with yemCherry³⁶. CRIB and Sec4 plasmids were linearized with StuI and transformed into optogenetic strains.

Microscopy

Cells were imaged as described using a spinning-disk confocal microscopy^{38,20}. A long pass LP540 filter was used in the transmission light path to prevent premature photoactivation. Exponentially growing cells (grown in the dark) were spotted on YEPD agar pads at 30 °C or mixed with an equal volume of fetal calf serum (FCS) and spotted on 25% (vol/vol) YEPD agar–75% (vol/vol) FCS pads at 37 °C³⁸. Typically cells on FCS/agar pads were incubated with for 30 – 40 min at 37 °C prior to microscopy and, in some experiments, in order to have cells with short filaments, incubation was for 10-30 min. For photoactivation, a 300 msec 488 nm image (10 % of a 25 mW diode-pumped solid-state laser) image was acquired, either 3 images 10 minutes apart or 6 images 5 minutes apart. Images were acquired at indicated times with 9 – 15 0.5 μ m z-sections to capture the entire cell. For live cell imaging followed by actin visualization, cells were grown in a Concanavalin A treated (0.1 mg/mL) glass bottom microwell dish (MatTek Corporation). Following photoactivation cells were fixed with 4% paraformaldehyde for 10 min, subsequently washed with PBS and actin was labeled with

Alexa Fluor-568 as described³⁹. Fixed cells with imaged with 18-26 0.2 μm z-sections. All images were deconvolved with Huygens Professional software and sum or maximum projections are shown. Image analysis was carried out with ImageJ and Volocity Software Version 5 (PerkinElmer). Objects were identified as previously described using the SD mode in Volocity²⁰, where the selection is based on SDs above the mean intensity. Scale bar is 5 μm in all images except for actin images where it is 1 μm .

Table S1. Strains used in this study

Strain	Genotype	Source
BWP17	<i>ura3Δ::imm434/ura3Δ::imm434 his1Δ::hisG/his1Δ::hisG arg4Δ::hisG/arg4Δ::hisG</i>	40
PY2935	Same as BWP17 but with <i>RP10::ARG4-ACT1p-CibN-GFPγ- CtRac1-ADH1t</i>	This study
PY3451	Same as PY2935 but with <i>NEUT5L::NAT1-TEF1p-Cry- mCh-Cdc42[G12V,C188S]-TEF1t</i>	This study
PY3643	Same as BWP17 but with <i>NEUT5L::NAT1-TEF1p-Cry- GFPγ-Cdc42[G12V,C188S]-TEF1t</i>	This study
PY4059	Same as PY3643 but with <i>NEUT5L::URA3-ADH1p-CibN- CtRac1-ACT1t</i>	This study
PY4172	Same as PY4059 but with <i>RP10::ARG4-ACT1p-CRIB-mCh- ADH1t</i>	This study
PY4175	Same as PY4059 but with <i>ABP1/ABP1::HIS1-ABP1mCh</i>	This study
PY4268	Same as PY4059 but with <i>MLC1/MLC1::HIS1-MLC1mCh</i>	This study
PY4510	Same as PY3643 but with <i>NEUT5L::URA3-ADH1p-CibN- CtRac1-ACT1t</i>	This study
PY4534	Same as PY4510 but with <i>RP10::ARG4-SEC4p-mSc-Sec4-ADH1t</i>	This study
PY4623	Same as PY4534 but with <i>MLC1/MLC1::HIS1-MLC1yemiRFP67</i>	This study
PY4642	Same as PY4510 but with <i>MLC1/MLC1::HIS1-MLC1yemiRFP670</i>	This study

References

- 1 Chiou, J. G., Balasubramanian, M. K. & Lew, D. J. Cell Polarity in Yeast. *Annu Rev Cell Dev Biol* **33**, 77-101, doi:10.1146/annurev-cellbio-100616-060856 (2017).
- 2 Goryachev, A. B. & Leda, M. Many roads to symmetry breaking: molecular mechanisms and theoretical models of yeast cell polarity. *Mol Biol Cell* **28**, 370-380, doi:10.1091/mbc.E16-10-0739 (2017).
- 3 Martin, S. G. Spontaneous cell polarization: Feedback control of Cdc42 GTPase breaks cellular symmetry. *Bioessays* **37**, 1193-1201, doi:10.1002/bies.201500077 (2015).
- 4 Wu, C. F. & Lew, D. J. Beyond symmetry-breaking: competition and negative feedback in GTPase regulation. *Trends Cell Biol* **23**, 476-483, doi:10.1016/j.tcb.2013.05.003 (2013).
- 5 Freisinger, T. *et al.* Establishment of a robust single axis of cell polarity by coupling multiple positive feedback loops. *Nat Commun* **4**, 1807, doi:10.1038/ncomms2795 (2013).
- 6 Kuo, C. C. *et al.* Inhibitory GEF phosphorylation provides negative feedback in the yeast polarity circuit. *Curr Biol* **24**, 753-759, doi:10.1016/j.cub.2014.02.024 (2014).
- 7 Witte, K., Strickland, D. & Glotzer, M. Cell cycle entry triggers a switch between two modes of Cdc42 activation during yeast polarization. *Elife* **6**, doi:10.7554/eLife.26722 (2017).
- 8 Woods, B. & Lew, D. J. Polarity establishment by Cdc42: Key roles for positive feedback and differential mobility. *Small GTPases*, 1-8, doi:10.1080/21541248.2016.1275370 (2017).
- 9 Wu, C. F. *et al.* Role of competition between polarity sites in establishing a unique front. *Elife* **4**, doi:10.7554/eLife.11611 (2015).
- 10 Martin, S. G. & Arkowitz, R. A. Cell polarization in budding and fission yeasts. *FEMS Microbiol Rev* **38**, 228-253, doi:10.1111/1574-6976.12055 (2014).
- 11 Park, H. O. & Bi, E. Central roles of small GTPases in the development of cell polarity in yeast and beyond. *Microbiol Mol Biol Rev* **71**, 48-96, doi:10.1128/MMBR.00028-06 (2007).
- 12 Sudbery, P. E. Growth of *Candida albicans* hyphae. *Nat Rev Microbiol* **9**, 737-748, doi:10.1038/nrmicro2636 (2011).
- 13 Bassilana, M., Blyth, J. & Arkowitz, R. A. Cdc24, the GDP-GTP exchange factor for Cdc42, is required for invasive hyphal growth of *Candida albicans*. *Eukaryot Cell* **2**, 9-18 (2003).
- 14 Brand, A. C. *et al.* Cdc42 GTPase dynamics control directional growth responses. *Proc Natl Acad Sci U S A* **111**, 811-816, doi:10.1073/pnas.1307264111 (2014).
- 15 Corvest, V., Bogliolo, S., Follette, P., Arkowitz, R. A. & Bassilana, M. Spatiotemporal regulation of Rho1 and Cdc42 activity during *Candida albicans* filamentous growth. *Mol Microbiol* **89**, 626-648, doi:10.1111/mmi.12302 (2013).
- 16 Ushinsky, S. C. *et al.* CDC42 is required for polarized growth in human pathogen *Candida albicans*. *Eukaryot Cell* **1**, 95-104 (2002).

- 17 VandenBerg, A. L., Ibrahim, A. S., Edwards, J. E., Jr., Toenjes, K. A. & Johnson, D. I. Cdc42p GTPase regulates the budded-to-hyphal-form transition and expression of hypha-specific transcripts in *Candida albicans*. *Eukaryot Cell* **3**, 724-734, doi:10.1128/EC.3.3.724-734.2004 (2004).
- 18 Kennedy, M. J. *et al.* Rapid blue-light-mediated induction of protein interactions in living cells. *Nat Methods* **7**, 973-975, doi:10.1038/nmeth.1524 (2010).
- 19 Caballero-Lima, D., Kaneva, I. N., Watton, S. P., Sudbery, P. E. & Craven, C. J. The spatial distribution of the exocyst and actin cortical patches is sufficient to organize hyphal tip growth. *Eukaryot Cell* **12**, 998-1008, doi:10.1128/EC.00085-13 (2013).
- 20 Ghugtyal, V. *et al.* Phosphatidylinositol-4-phosphate-dependent membrane traffic is critical for fungal filamentous growth. *Proc Natl Acad Sci U S A* **112**, 8644-8649, doi:10.1073/pnas.1504259112 (2015).
- 21 Zeng, G., Wang, Y. M. & Wang, Y. Cdc28-Cln3 phosphorylation of Sla1 regulates actin patch dynamics in different modes of fungal growth. *Mol Biol Cell* **23**, 3485-3497, doi:10.1091/mbc.E12-03-0231 (2012).
- 22 Riquelme, M. Tip growth in filamentous fungi: a road trip to the apex. *Annu Rev Microbiol* **67**, 587-609, doi:10.1146/annurev-micro-092412-155652 (2013).
- 23 Riquelme, M. & Sanchez-Leon, E. The Spitzenkörper: a choreographer of fungal growth and morphogenesis. *Curr Opin Microbiol* **20**, 27-33, doi:10.1016/j.mib.2014.04.003 (2014).
- 24 Wagner, W., Bielli, P., Wacha, S. & Ragnini-Wilson, A. Mlc1p promotes septum closure during cytokinesis via the IQ motifs of the vesicle motor Myo2p. *EMBO J* **21**, 6397-6408 (2002).
- 25 Crampin, H. *et al.* *Candida albicans* hyphae have a Spitzenkörper that is distinct from the polarisome found in yeast and pseudohyphae. *J Cell Sci* **118**, 2935-2947, doi:10.1242/jcs.02414 (2005).
- 26 Jones, L. A. & Sudbery, P. E. Spitzenkörper, exocyst, and polarisome components in *Candida albicans* hyphae show different patterns of localization and have distinct dynamic properties. *Eukaryot Cell* **9**, 1455-1465, doi:10.1128/EC.00109-10 (2010).
- 27 Li, C. R., Lee, R. T., Wang, Y. M., Zheng, X. D. & Wang, Y. *Candida albicans* hyphal morphogenesis occurs in Sec3p-independent and Sec3p-dependent phases separated by septin ring formation. *J Cell Sci* **120**, 1898-1907, doi:10.1242/jcs.002931 (2007).
- 28 Wakade, R., Labbaoui, H., Stalder, D., Arkowitz, R. A. & Bassilana, M. Overexpression of YPT6 restores invasive filamentous growth and secretory vesicle clustering in a *Candida albicans* arl1 mutant. *Small GTPases*, 1-7, doi:10.1080/21541248.2017.1378157 (2017).
- 29 Merrifield, C. J. *et al.* Endocytic vesicles move at the tips of actin tails in cultured mast cells. *Nat Cell Biol* **1**, 72-74, doi:10.1038/9048 (1999).
- 30 Southwick, F. S., Li, W., Zhang, F., Zeile, W. L. & Purich, D. L. Actin-based endosome and phagosome rocketing in macrophages: activation by the secretagogue antagonists lanthanum and zinc. *Cell Motil Cytoskeleton* **54**, 41-55, doi:10.1002/cm.10083 (2003).
- 31 Taunton, J. *et al.* Actin-dependent propulsion of endosomes and lysosomes by recruitment of N-WASP. *J Cell Biol* **148**, 519-530 (2000).

- 32 Hope, H., Bogliolo, S., Arkowitz, R. A. & Bassilana, M. Activation of Rac1 by the guanine nucleotide exchange factor Dck1 is required for invasive filamentous growth in the pathogen *Candida albicans*. *Mol Biol Cell* **19**, 3638-3651, doi:10.1091/mbc.E07-12-1272 (2008).
- 33 Zhang, C. & Konopka, J. B. A photostable green fluorescent protein variant for analysis of protein localization in *Candida albicans*. *Eukaryot Cell* **9**, 224-226, doi:10.1128/EC.00327-09 (2010).
- 34 Vauchelles, R., Stalder, D., Botton, T., Arkowitz, R. A. & Bassilana, M. Rac1 dynamics in the human opportunistic fungal pathogen *Candida albicans*. *PLoS One* **5**, e15400, doi:10.1371/journal.pone.0015400 (2010).
- 35 Gerami-Nejad, M., Zacchi, L. F., McClellan, M., Matter, K. & Berman, J. Shuttle vectors for facile gap repair cloning and integration into a neutral locus in *Candida albicans*. *Microbiology* **159**, 565-579, doi:10.1099/mic.0.064097-0 (2013).
- 36 Keppler-Ross, S., Noffz, C. & Dean, N. A new purple fluorescent color marker for genetic studies in *Saccharomyces cerevisiae* and *Candida albicans*. *Genetics* **179**, 705-710, doi:10.1534/genetics.108.087080 (2008).
- 37 Reijntjens, P., Walther, A. & Wendland, J. Dual-colour fluorescence microscopy using yEmCherry-/GFP-tagging of eisosome components Pil1 and Lsp1 in *Candida albicans*. *Yeast* **28**, 331-338, doi:10.1002/yea.1841 (2011).
- 38 Bassilana, M., Hopkins, J. & Arkowitz, R. A. Regulation of the Cdc42/Cdc24 GTPase module during *Candida albicans* hyphal growth. *Eukaryot Cell* **4**, 588-603, doi:10.1128/EC.4.3.588-603.2005 (2005).
- 39 Vernay, A., Schaub, S., Guillas, I., Bassilana, M. & Arkowitz, R. A. A steep phosphoinositide bis-phosphate gradient forms during fungal filamentous growth. *J Cell Biol* **198**, 711-730, doi:10.1083/jcb.201203099 (2012).
- 40 Wilson, R. B., Davis, D. & Mitchell, A. P. Rapid hypothesis testing with *Candida albicans* through gene disruption with short homology regions. *J Bacteriol* **181**, 1868-1874 (1999).

Additional Results

Data in the previous chapter shows the repetitive recruitment of constitutively active Cdc42 in budding cells (Figure 1C in the paper). Constitutively active Cdc42 can be repetitively recruited multiple times to the plasma membrane of filamentous cells as well (Figure S6). Since most of the experiments were performed in filamentous cells, it is relevant to show that recruitment and dissociation are not affected by the type of growth. It is important to note that the time between photoactivations is of 20 minutes, and that growth occurs in between pulses of 488 nm light. The two reporters used to visualize the Spitzenkörper, Mlc1 and Sec4, which are also present at the new cluster of secretory vesicles that forms after photorecruitment, are localized at the tip of growing hyphae that do not go through photorecruitment of constitutively active Cdc42, in cells that express the Cry-CibN system (Figure S7A and S7B). This result shows that the Cry-CibN system is not activated when red and far-red images are taken, and that recruitment only occurs when a 488 nm pulse is used. The filaments extend during the whole experiment without any perturbation in growth.

Figure S6

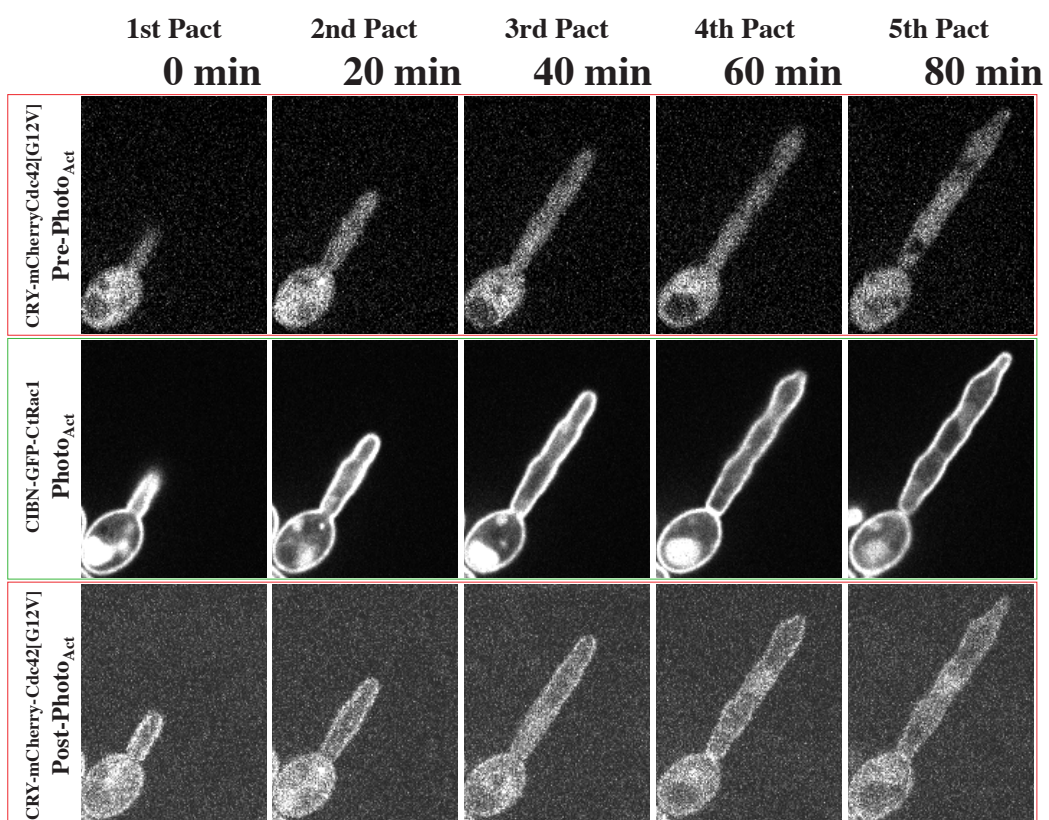
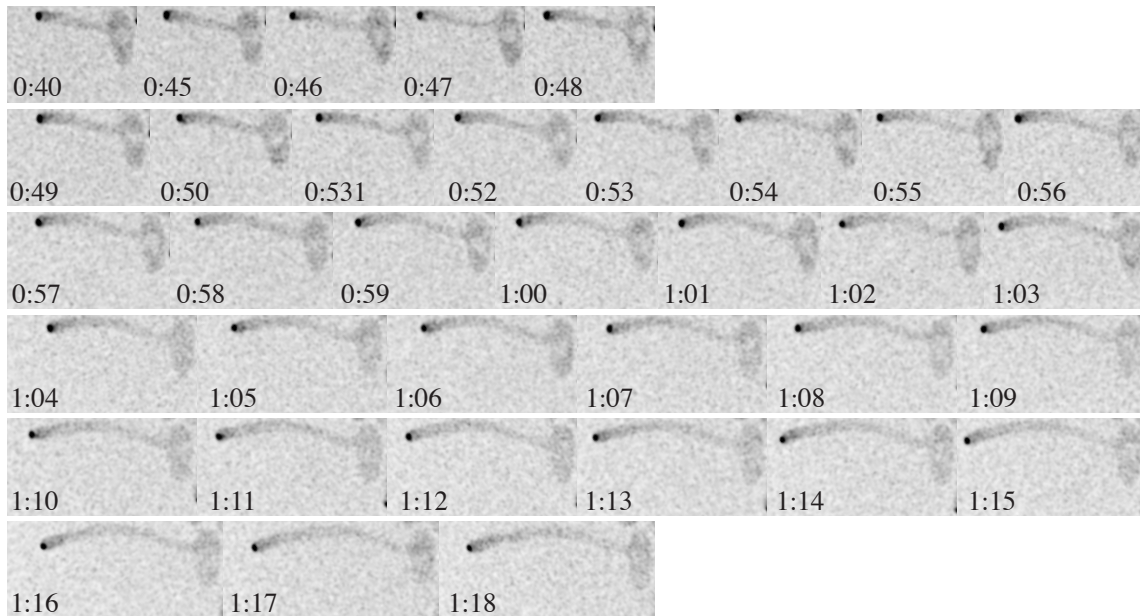


Figure S6. Cdc42•GTP can be recruited to the plasma membrane multiple times. A strain expressing CibN-GFP-CtRac1 and Cry2-mCh-Cdc42[G12V]cyto was incubated on agar pads containing FCS at 37 °C and exposed to six 300 msec 488 nm pulses (10 % of a 5 mWatt laser) after filamentous response had initiated. Cells were exposed to a 488 nm light pulse every 20 min.

Figure S7

A



B

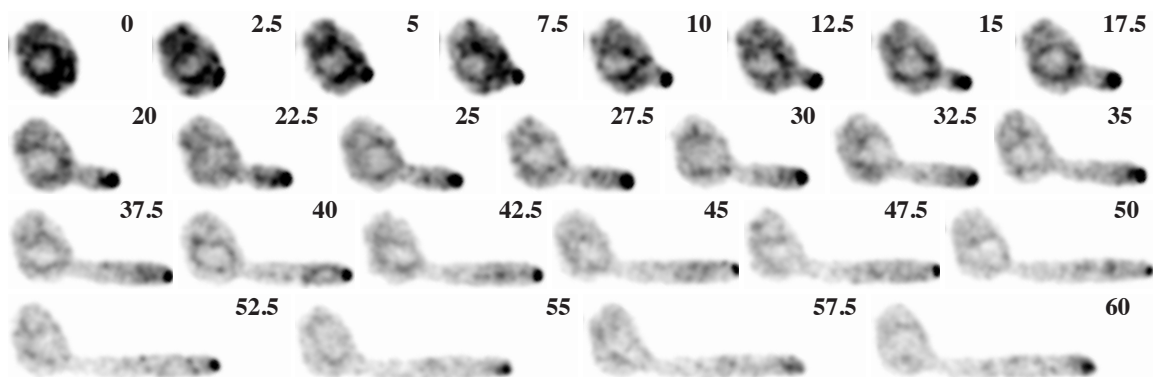


Figure S7. The Spitzenkörper remains undisturbed without recruitment of Cdc42•GTP. Strains expressing CibN-CtRac1, Cry2-GFP-Cdc42[G12V]cyto and Mlc1-Cherry (Fig. S7A) or CibN-CtRac1, Cry2-GFP-Cdc42[G12V]cyto and mScarlet-Sec4 (Fig. S7B) were incubated on agar pads containing FCS at 37 °C and mCherry/mScarlet were visualized every 2.5 min.

Discussion

The generation of cell polarity in symmetrical cells has been extensively studied. Yet, little is known about how a new site of polarized growth is established in an already asymmetric cell, and what its relationship with the initial growth site is. This study focused on polarized growth in the human fungal pathogen *C. albicans*, specifically on the role of the small Rho-GTPase Cdc42. In this work, optogenetic methods have been used to transiently disrupt polarity by recruiting constitutively active Cdc42 uniformly to the plasma membrane, in filamentous *C. albicans* cells, *i.e.*, cells that are highly asymmetric. Upon recruitment of constitutively active Cdc42 to the plasma membrane I observed:

- Polarized growth is perturbed and the filament stops extending;
- New growth can subsequently occur along the filament or in the mother cell;
- A cluster of endogenous active Cdc42 is disrupted and endocytic sites are dispersed;
- A dramatic increase in *de novo* secretory vesicle clustering occurs, resulting in a new cluster of Sec4 labelled vesicles.

This light dependent recruitment approach has made it possible to control polarized growth temporally, and demonstrated that a cluster of secretory vesicles, which is also found in plants, fungi and neurons, does not require directed cell growth to form (Toyooka *et al.*, 2009; Bykhovskaia, 2011; Riquelme, 2013; Riquelme and Sánchez-León, 2014). A number of questions have been raised in this study including *i)* How is the initial polarized growth site disrupted? *ii)* How is new growth initiated? *iii)* What dictates the location of new growth? *iv)* What is the relationship between the Spitzenkörper and the new cluster of

secretory vesicles? *v)* What is the Spitzenkörper? And *iv)* How does the new cluster of secretory vesicles form, move, and ultimately localize to the incipient growth site?

***i)* How is the initial polarized growth site disrupted?**

Previous studies have used optogenetic approach to perturb the activation of Cdc42 in different organisms (Levsikaya *et al.*, 2009; Zhou *et al.*, 2012; Valon *et al.*, 2015, 2017; O'Neill *et al.*, 2016; Furuya *et al.*, 2017; Witte *et al.*, 2017; Zimmerman *et al.*, 2017). These studies have done so by using light-dependent protein recruitment to activate of Cdc42 and have all shown that polarized growth can be regulated or controlled by this approach. Here, I have manipulated the location of active Cdc42 in already asymmetric *C. albicans* cells, which appears to reset polarized growth. When constitutively active Cdc42 is uniformly recruited to the plasma membrane, polarized growth is disrupted and growth at the tip of the filament abolished. The cluster of active Cdc42 at the tip of the filament, visualized with the CRIB reporter, is dramatically reduced following recruitment of constitutively active Cdc42. A plausible explanation for this observation could be that the uniformly recruited constitutively active Cdc42 is competing for effectors with the native cluster of active Cdc42 present at the tip of the growing hyphae, *i.e.* sequestering these effectors, leading to the inactivation of endogenous Cdc42 *via* its GTPase activity and/or GAP facilitated GTPase activity. In *S. cerevisiae*, the singularity of a cluster of active Cdc42 has been proposed to be the result of a competitive mechanism built into the Cdc42 amplification feedback system (Gulli *et al.*, 2000; Bose *et al.*, 2001; Goryachev and Pokhilko, 2008; Kozubowski *et al.*, 2008; Howell *et al.*, 2009, 2012; Johnson *et al.*, 2011; Kuo *et al.*, 2014; Woods *et al.*, 2015; Rapali *et al.*, 2017). This system is maintained in equilibrium by positive and negative feedback loops: positive feedback by the scaffold protein Bem1, promoting proximity between Cdc42 and its GEF Cdc24, and negative feedback maintained by the PAK-kinase Cla4, which phosphorylates Cdc24 causing its release from the Cdc42-Cdc24 module (Howell *et al.*, 2012; Kuo *et al.*, 2014; Rapali *et al.*, 2017). A similar mechanism could be in place in *C. albicans* and the recruited constitutively active Cdc42 could be titrating effectors – such as Bem1, Cla4 or Cst20 (*C. albicans* homolog of the *S. cerevisiae* PAK kinase Ste20) – away from the cluster of active Cdc42 at the tip, ultimately resulting in the disruption of this cluster.

In the majority of the cases, growth restarts again from the tip of the filament, but when the initial growth site is disrupted, new growth can subsequently initiate elsewhere in the cell, *i.e.* along the filament or in the mother cell. While optimizing the Cry-CibN system to recruit constitutively active Cdc42 to the plasma membrane of filamentous *C. albicans* cells, it appears that there is a trade-off between the number of photoactivation pulses and the outcome: too many photoactivation pulses, *i.e.*, constitutively active Cdc42 remains at the plasma membrane for a longer period of time, resulting in cells that do not restart filamentous growth; too few photoactivation pulses, and filamentous growth is not disrupted. These observations indicate that disruption is likely to be time dependent – given enough time, plasma membrane photo-recruitment of constitutively active Cdc42 promotes the dissipation of the endogenous cluster of active Cdc42.

***ii)* How is new growth initiated?**

I have observed that after disruption of the endogenous cluster of active Cdc42 and following the dissociation of the constitutively active Cdc42 from the plasma membrane, a new cluster of active Cdc42 forms elsewhere in the cell, where new growth will emerge. The location of new growth, which occurs approximately 30 minutes after photo-recruitment, does not correlate with location of the recruited constitutively active Cdc42, which appears to be uniform. We assume that the recruitment of the GTP-locked Cdc42[G12V,C188S], is initially responsible for the disruption of the endogenous Cdc42•GTP cluster, however, the timing of appearance of the new cluster of Cdc42•GTP, as visualized by the CRIB reporter, suggests that it is unlikely to be comprised of Cdc42[G12V,C188S]. In *S. cerevisiae* the ability of Cdc42 to cycle between the active and inactive states, coupled with a GDI-dependent recycling of Cdc42 (Freisinger *et al.*, 2013), play an important role in the maintenance of Cdc42 proper function (Ziman *et al.*, 1991; Wedlich-Söldner *et al.*, 2004; Vanni *et al.*, 2005), specifically ensuring the formation of a single polarization site. Therefore, a GTP-locked form of Cdc42 appears to be sufficient to compete for effectors with the endogenous cluster of active Cdc42 but it is unlikely to be sufficient to form a functional cluster of active Cdc42, as it lacks the ability to cycle between activation states. Hence, following disruption of the initial growth site, and given that Cdc42[G12V,C188S] was not detected to be recruited preferentially to the site of new growth, it is likely that the new site of growth is part of the filamentous growth response

that has already been initiated in these cells and it is the consequence of the clustering of endogenous active Cdc42.

iii) What influences the location of new growth?

The ability to disrupt polarized filamentous growth depends on the length of the filament at the time of recruitment of constitutively active Cdc42, with shorter filaments being more easily perturbed than longer filaments. This could be due to how established sites of growth are as a function of filaments length, with growth sites in shorter filaments less robust compared to that of longer filaments. Membrane traffic and cytoskeleton-dependent feedback loops are likely to reinforce the growth site at the filament tip, which could be dependent of how long the filament has extended, hence filament length. Following photo-recruitment of constitutively active Cdc42, there appears to be a switch from apical to isotropic growth, as swelling of the hyphal tips was observed in many cases. It would be important to quantitate the volume of these cells to determine if growth (increase in volume) is constant following photo-recruitment of constitutively active Cdc42 and simply changes from apical to isotropic, or whether growth is temporally reduced. Given the relatively slow extension rates of *C. albicans* hyphae ($\sim 0.3 \mu\text{m}/\text{min}$), switch to isotropic growth, following photo-recruitment of constitutively active Cdc42, would result in changes in hyphal diameter near the resolution limit. The swelling of the hyphal tips, following photo-recruitment of constitutively active Cdc42, suggests that secretory vesicles fuse in the apex area, but are no longer restricted to the tip (alternatively, this result could be due to the dispersion of the endocytic collar). Subsequent to photo-recruitment, new growth is more likely to occur in the mother cell than along the filament. In all the cases when a new site of growth occurred, subsequent to photo-recruitment, $\sim 20\%$ occurred along the filament. An explanation for some of this disparity could be the smaller surface area of the filament compared to the mother cell, a $5 \mu\text{m}$ long filament is roughly $1/3 - 1/2$ the surface area of a $2.5 \mu\text{m}$ radius mother cell. Another possibility is that there is an increased level of cellular components, such as actin cytoskeleton or ER membrane in the mother cell compared to the filament, that are critical in providing feedback loops to stabilize transient increases in active Cdc42. Analyses of the distribution of the actin cytoskeleton and membrane compartment in the mother cell and filament would be necessary to confirm this possibility. When new growth emerges in the mother cell, it is preferentially towards the opposite pole of the cell, similar to the bipolar bud site selection

pattern of *C. albicans* cells. Bud site selection patterns depend on the Rsr1/Bud1 GTPase module, however, the site of germ tube appears to be random in *C. albicans*. To determine if this preference for location of new growth subsequent to photo-recruitment of constitutively active Cdc42 depends on the bud site selection machinery, it would be necessary to carry out similar experiments in an *rsr1/bud1* mutant.

iv) What is the relationship between the Spitzenkörper and the new cluster of secretory vesicles?

Upon photo recruitment of constitutively active Cdc42, the endocytic collar is dispersed whereas the Spitzenkörper is still observed, even in the absence of directed cell growth. Strikingly, a new cluster of secretory vesicles is formed, typically originating in the mother cell. This highly dynamic cluster was visualized with both the Rab GTPase Sec4 and the myosin light chain Mlc1, and actin cables were also associated with it. After the appearance of this new cluster of secretory vesicles, the filament would stop extending and for a period of time the Spitzenkörper and the new, highly dynamic, cluster would co-exist in the cell. Subsequently two possible outcomes were observed: *i)* either the Spitzenkörper would coalesce with the new cluster of vesicles, which was highly dynamic and ultimately would settle at a new location, where a second germ tube would emerge, or *ii)* the Spitzenkörper would remain intact, the new cluster would disappear and growth would restart from the tip of the filament. I hypothesize that the new cluster of secretory vesicles and the Spitzenkörper compete for a limiting component, which is perhaps secretory vesicles themselves. As these clusters of secretory vesicles are dynamic, a small increase in stability or size of one cluster is likely to be reinforced by positive feedback loops resulting in its stabilization and concomitant destabilization of the other cluster, *i.e.* two clusters do not co-exist for long time periods. Disruption of the initial Spitzenkörper was not the same in all cells: in cells with shorter filaments, less than three photo-activations were necessary to disrupt the Spitzenkörper, while three or more photoactivations were necessary in cells with longer filaments. This corroborates the suggestion that the growth site is more robust or stable in longer filaments.

v) What is the Spitzenkörper?

Sec4 and Mlc1 colocalized to the new cluster of secretory vesicles that forms following photorecruitment of constitutively active Cdc42 in filamentous cells; our data

also show that these two proteins also colocalize at the Spitzenkörper. Based on phalloidin staining, actin cables associate with the new cluster, as they do with the Spitzenkörper. The cluster of secretory vesicles is dynamic, with movement being observed until a new cluster of endogenous active Cdc42 forms. The dynamic behaviour of this new cluster is in contrast to the Spitzenkörper, which remains associated with the hyphal tip as it extends. The fungal Spitzenkörper – from German Spitze (“point”) + Körper (“body”) – is defined as a cluster of vesicles at the tip of growing hyphae, first visualized by Brunswick in 1924 (Brunswick, 1924). It remains to be clearly established whether this cluster of vesicles is functionally important or rather represents a transient build-up of vesicles prior to plasma membrane fusion. It should be noted that the Spitzenkörper can also be labelled with the lipophilic dye FM4-64, indicating that it also is accessible *via* endocytosis.

The similarities observed between the Spitzenkörper and the newly formed cluster of secretory vesicles upon photorecruitment of constitutively active Cdc42 raise the question whether they are the same entities. Upon photorecruitment of constitutively active Cdc42, directional growth ceases. A Spitzenkörper can be defined by three criteria: *i*) location – at the tip of growing filaments – as the name indicates; *ii*) cytology – it is composed of vesicles, which was first confirmed in 1969 using electron microscopy (Girbardt, 1969; Grove and Bracker, 1970); and *iii*) protein composition – Mlc1, Sec4, Sec2 and Bni1 have been localized to a sphere-like structure at the tip of the hyphae, presumably at the Spitzenkörper, in *C. albicans* (Crampin *et al.*, 2005; Bishop *et al.*, 2010; Jones and Sudbery, 2010).

Both Mlc1 and Sec4 localize to the cluster that forms upon photorecruitment of constitutively active Cdc42, although it is not localized to the filament tip. In preliminary experiments, I have also observed the formin Bni1 at this structure that is labelled with Mlc1, yet low signal intensities precluded imaging over time. To determine the organization of this new cluster (vesicle number, size and proximity) serial section electron microscopy or super-resolution microscopy will be necessary. If the cytology and organization of this new cluster that forms upon photorecruitment of constitutively active Cdc42 is confirmed to be consistent with a Spitzenkörper, it would suggest that sustained directional growth is not necessary to form a Spitzenkörper and that this structure can move within the cell.

vi) How does the new cluster of secretory vesicles form, move, and settle?

The formation of a new cluster of secretory vesicles, substantially larger and with more Sec4 signal than the initial Spitzenkörper, occurs concomitant with a substantial decrease in the cytoplasmic Sec4 signal, suggesting that secretory vesicles in the cytoplasm are recruited to this new cluster. In addition to inducing *de novo* formation of a cluster of secretory vesicles, recruitment of constitutively active Cdc42 also increases the Sec4 signal at the initial Spitzenkörper. An attractive explanation for the increase in Sec4 signal, and hence likely number of secretory vesicles, at the initial Spitzenkörper could be that the disruption of the endogenous active Cdc42 cluster at the tip of the filament largely blocks membrane traffic to this location. Hence the number of vesicles fusing with the plasma membrane at the hyphal tip would decrease, but vesicles would still be targeted to the Spitzenkörper, from the secretory pathway, contributing to the apparent increase Sec4 at the Spitzenkörper. This view is consistent with the reduction in polarized growth together with the dispersion of endocytic sites. The reason for the dramatic clustering of secretory vesicles immediately after recruitment of constitutively active Cdc42, or why the cell would maintain such a cluster in the absence of polarized growth is not clear. It appears that as long as a new cluster of endogenous active Cdc42 does not form, the cluster of secretory vesicles is highly dynamic moving on the cell cortex - a movement that could be driven by actin cables.

Conclusions and Future Perspectives

The formation of a *de novo* cluster of secretory vesicles and the fact that cells are able to maintain such a cluster in the absence of directed growth was unexpected. Why do secretory vesicles cluster upon photo-recruitment of constitutively active Cdc42? Following this recruitment, actin cables are associated with the new cluster of secretory vesicles. Is the clustering of vesicles a consequence of actin cable reorganization elsewhere in the cell, or *vice versa*? Further characterization of this secretory vesicle cluster would be important to understand the mechanism behind its formation. Specifically, to assess whether other polarity markers colocalize with it, such as the exocyst component Sec3 or components of the Cdc24-Cdc42 module.

The results of this study point to the maintenance of a cluster of constitutively active Cdc42 at the tip of growing *C. albicans* hyphae *via* feedback loops, which have been

extensively studied in the budding yeast *S. cerevisiae*. It is unclear if such mechanisms are present in *C. albicans*, and if so, how recruitment of a GTP-locked form of Cdc42 would interfere with such feedback loops. Is constitutively active Cdc42 able to sequester some or all of the proteins involved in such feedback loops, which directly bind active Cdc42? These proteins, including Bem1, Cst20 and Cla4, have been studied in budding yeast. It would be interesting to assess whether the overexpression of any of these proteins would eliminate effect of growth after recruitment of constitutively active Cdc42 to the plasma membrane, although overexpression could by itself interfere with polarized growth, even prior to constitutively active Cdc42 recruitment. In this study I have only recruited constitutively active Cdc42 to the whole plasma membrane, it would be interesting to test whether recruiting the same form of Cdc42 to a restricted area of the plasma membrane, or to the whole cell except the tip of the filament, would have similar consequences.

The tendency of new growth to emerge on the distal half of the mother cell, relative to initial filament, could be linked to bud site selection machinery. To test this hypothesis, similar experiments (recruitment of constitutively active Cdc42 in an already asymmetric cell) should be performed in an *rsr1* mutant, which exhibits random bud site selection. If Rsr1/Bud1 is indeed important, bipolar distribution of new filamentous growth would not be observed in this mutant.

Based on the results of this study, I propose that photo-recruitment of constitutively active Cdc42 to the plasma membrane resets growth by disrupting a link to a cluster of secretory vesicles. Increasing the levels of constitutively active Cdc42 favors the spontaneous clustering of secretory vesicles elsewhere in the cell, which is highly dynamic and could be driven by actin-dependent propulsion. Re-establishment of active Cdc42 at a new location anchors the cluster of secretory vesicles allowing subsequent fusion with the plasma membrane. Optogenetic manipulation of cell polarity reveals that such a cluster of secretory vesicles does not require directed cell growth to form.

Materials & Methods

Standard methods were used for *C. albicans* cell culture, cell staining and molecular and genetic manipulations. Plasmids, oligonucleotides, synthesized genes and strains used in this study are listed in Tables 3, 4, 5 and 6, respectively.

Genetic Nomenclature: The nomenclature used in *Candida albicans* is employed as follows: *CDC42*, a gene; Cdc42, the protein encoded by the *CDC42* gene; CRIB-yemCherry, a C-terminal fusion between CRIB and yemCherry; mScarlet-Sec4, an N-terminal fusion between Sec4 and mScarlet; *arg4*, an allele deletion; *RP10::ARG4 ACT1p CRIB-yemCherry ADH1t*, an insertion of *ACT1p CRIB-yemCherry ADH1t* in the *RP10* locus, with *ARG4* selection. Plasmids and oligos names, although being DNA sequences, are not italicized. With the presence of two HIS1 homologues from either *C. albicans* or *C. dubliniensis*, a species prefix is added to the module, *i.e.*, CaHIS1 or CdHis1. Autofluorescent proteins (AFPs) that are *C. albicans* codon optimized have a prefix – ye, yeast enhanced - indicating so, *e.g.*, yemCherry, or a suffix in the case of GFP γ (γ gamma, *i.e.*, yeast enhanced). Point mutations are in square brackets. This indicates the position at which an aminoacid (aa) has been changed by mutagenesis, *e.g.*, Cdc42[C188S], in which the sequence encoding Cdc42 has been mutated to change of the cysteine in the position 188 to a serine.

I – Molecular biology

Enzymes and Kits – Restriction enzymes and respective buffers were purchased from New England Biolabs, Invitrogen and Takara; PCR oligonucleotides were purchased from Eurofins Genomics and Biologio; PfuI DNA polymerase was purchased from Promega; Phusion DNA polymerase was purchased from Ozyme; Calf Intestinal Alkaline

Phosphatase (CIAP) was purchased from Fermentas; RNase was purchased from Sigma. Extraction of DNA from plasmids was carried out with Macherey-Nagel Plasmid DNA purification kit NucleoSpin Plasmid; extraction of DNA from agarose gel and cleaning of PCR and digestion products was carried out using Macherey-Nagel PCR clean-up Gel Extraction kit NucleoSpin Extract II. Precipitation of DNA was carried out using isopropanol and ammonium acetate.

Polymerase Chain Reaction – Reactions were with Phusion DNA polymerase and a standard PCR mixture (Phusion buffer 1X, 200 μ M dNTP, 0.5 μ M oligonucleotides, Phusion 0.02 U/ μ L) and performed on a Biometra T3 Thermocycler or Analytik Jena Biometra Trio, using the following program:

1. 98 °C 30 s
2. 98 °C 15 s
3. 56 °C 20 s
4. 72 °C 20 s/1 kB (go back to step 2, x cycle repetitions)
5. 72 °C 10 min
6. 10 °C Pause

Number of x cycle repetitions = 25 for amplification of products to be used in cloning, 39 for amplification from bacteria to check for positive clones after cloning steps.

Site-Directed Mutagenesis – performed by mixing DNA plasmid template (1 μ g) with oligonucleotides (0.1 μ M), PfuI buffer (10X), dNTPs (0.2 mM) and PfuI DNA polymerase (3 U), completed with DH₂O to the final volume of 50 μ L. Reactions were performed on a Biometra T3 Thermocycler or Analytik Jena Biometra Trio, followed by digestion with DpnI at 37 °C for 1 h and an inactivation step at 68 °C for 20 min. Reactions were transformed into competent XL1-Blue *E. coli* cells (Weiner *et al.*, 1994).

Plasmid Amplification – performed with competent XL1-Blue *E. coli* cells prepared by the calcium chloride method (Inoue *et al.*, 1990). DNA plasmids were mixed with competent cells and incubated on ice for 15 min, heat shocked at 42 °C for 2 min and then incubated at 37 °C for 1 h, prior to being spread on TYE plates containing ampicillin (100 μ g/mL, Euromedex). Plates were incubated at 37 °C and colonies were visible after

overnight incubation. Selection of positive clones was done by plasmid digestion or PCR amplification.

II – Plasmids

All plasmids, oligonucleotides and synthesized genes² used in this study are listed in the end of the Materials & Methods Section. Unless stated otherwise, plasmids were constructed by me for the purpose of this study. All plasmids generated in this study were confirmed by sequencing (Eurofins Genomics).

Plasmids with pDUP3 backbone: the pDUP3 plasmids contain the sequences for integration into the intergenic region NEUT5L and NAT1 selection. Starting with the pDUP3 plasmid (Gerami-Nejad *et al.*, 2013), the *TEF1* promoter (500 bp upstream from the start codon of *C. albicans TEF1*) and terminator (400 bp downstream from the stop codon of *C. albicans TEF1*), amplified from genomic DNA, were added. Primers with a unique XmaI site at the 5' end and unique AscI, PacI and SpeI sites at the 3' end (TEF1.P1 and P2) were used to amplify the *TEF1* promoter sequence and this product was then digested with XmaI and SpeI. Primers with unique SpeI and SbfI sites at the 5' end and a unique NotI site at the 3' end (TEF1.P3 and P4) were used to amplify *TEF1* terminator sequence and this product was then digested with SpeI and NotI. Both of these inserts were simultaneously cloned into pDUP3 plasmid digested with XmaI and NotI, yielding

pDUP3 (XmaI) TEF1p (AscI-PacI-SpeI-SbfI) TEF1t (NotI).

The resulting plasmid was then used to clone in *C. albicans* codon-optimized DNA sequences that gave rise to the pDUP3 plasmids used in this study.

Plasmids with pDUP5 backbone: the pDUP5 plasmids contain the sequences for integration into the intergenic region NEUT5L and URA3-dpl200 selection. Starting with pDUP5 plasmid (Gerami-Nejad *et al.*, 2013), the *ADH1* promoter sequence (1 kbp upstream from the start codon of *ADH1*) and the *ACT1* terminator sequence (1 kbp

² Sequences encoding Cry2PHR, CibN, yemiRFP670 and mScarlet were codon optimized for *C. albicans* and cloned into pUC57 plasmids (GenScript).

downstream from the stop codon of *ACT1*), were amplified from genomic DNA and inserted into this plasmid. Primers with a unique XmaI site at the 5' end and unique AscI, PacI and SpeI sites at the 3' end (ADH1.P3 and P5) were used to amplify the *ADH1* promoter and this product was then digested with XmaI and SpeI. Primers with unique SpeI and SbfI sites at the 5' end

and a unique NotI site at the 3' end (ACT1.P2 and P3) were used to amplify *ACT1* terminator and this product was then digested with SpeI and NotI. Both these inserts were simultaneously cloned into pDUP5 plasmid digested with XmaI and NotI, yielding

pDUP5 (XmaI) ADH1p (AscI PacI SpeI SbfI) ACT1t (NotI).

The resulting plasmid was then used to clone in *C. albicans* codon-optimized DNA sequences that gave rise to the pDUP5 plasmid used in this study.

Plasmids with pEXPARG backbone: the pEXPARG plasmids contain the sequences for integration into the *RP10* locus and ARG4 selection. The pEXPARG (NotI) ACT1p (RsrII) CRIB (SacI) GFP (MluI) ADH1t (XhoI) plasmid was used to clone in *C. albicans* codon-optimized DNA sequences that gave rise to the pEXPARG plasmids used in this study.

a) CRY2PHR-CDC42 plasmids – constructed from the pDUP3 TEF1p TEF1t plasmid in sequential steps, yielding

i. pDUP3 (XmaI) TEF1p (AscI) CRY2PHR (PacI) yemCherry (SpeI)
CDC42[C188S] (SbfI) TEF1t (NotI),

ii. pDUP3 (XmaI) TEF1p (AscI) CRY2PHR (PacI) yemCherry (SpeI)
CDC42[G12V,C188S] (SbfI) TEF1t (NotI)

iii. pDUP3 (XmaI) TEF1p (AscI) CRY2PHR-linker (PacI) GFP γ (SpeI)
CDC42[G12V,C188S] (SbfI) TEF1t (NotI).

The inserts used to construct these plasmids were obtained as follows: the sequence encoding Cry2PHR was released from a pUC57 CRY2PHR plasmid using AscI and PacI (for plasmids i and ii); the sequence encoding Cry2PHR linker was amplified from the pUC57 CRY2PHR plasmid using a primer with a unique AscI site at the 5' end and a

primer with a linker and a unique PacI site at the 3' end (CRY2PHR.P5 and P6; 15 aa linker – EFDSAGSAGSAGGSS; for plasmid iii); the sequence encoding yemCherry was amplified using primers with a unique PacI site at the 5' end and with a unique SpeI site at the 3' end (yemCherry.P3 and P4; for plasmids i and ii); the sequence encoding GFP γ was amplified using primers with a unique PacI site at the 5' end and a unique SpeI site at the 3' end (GFP.P6 and P7; for plasmid iii); the sequence encoding *C. albicans* Cdc42 was amplified from genomic DNA using a primer with a unique SpeI site at the 5' end and a primer with the sequence to add the mutation C188S and a unique SbfI site at the 3' end (CDC42.P1 and P2; for plasmid i); site directed mutagenesis was then performed on the plasmid i. pDUP3 TEF1p CRY2PHR-yemCherry-CDC42[C188S] TEF1t to add the G12V mutation, yielding plasmid ii (CDC42.P3 and P4); the sequence encoding Cdc42[G12V,C188S] was then released from plasmid ii using SpeI and SbfI and used in the final cloning step that yielded plasmid iii.

b) Plasma Membrane CIBN plasmids – constructed from the pDUP5 ADH1p ADH1t and the pEXPARG ACT1p CRIB-GFP ADH1t plasmids in sequential steps, yielding

- i. pDUP5 (XmaI) ADH1p (AscI) CIBN-linker-CtRAC1 (PacI SpeI SbfI) ACT1t (NotI)
- ii. pEXPARG (NotI) ACT1p (RsrII) CIBN (SacI) GFP γ -CtRAC1 (MluI) ADH1t (XhoI).

Inserts used to construct these plasmids were obtained as follows: the sequence encoding CibN was amplified from the pUC57 CIBN plasmid using a primer with a unique AscI site at the 5' end and a primer with a linker, C-terminal part of *RAC1* and a unique PacI site at the 3' end (CIBN.P1 and P4; 15 aa linker – EFDSAGSAGSAGGSS; 14 last aa of CtRAC1– KKRKIKRAKKCTIL, Vauchelles *et al.*, 2010; for plasmid i); the sequence encoding CibN was released from a pUC57-CIBN plasmid using RsrII and SacI (for plasmid ii); a primer with a unique SacI site at the 5' end and a primer with the sequence encoding the C-terminal part of Rac1 and unique MluI site at the 3' end were used to amplify the sequence encoding GFP γ (GFP.P8 and P1).

c) CRIB plasmids – the CRIB domain from *S. cerevisiae* Gic2, a Cdc42 effector (Cdc24/Rac1-Interactive Binding domain; encoding the first 208 aa of Gic2), constructed from the pEXPARG ACT1p CRIB-GFP ADH1t plasmid, replacing *GFP* by both *mCherry* and *mScarlet* in one cloning step, yielding

pEXPARG (NotI) ACT1p (RsrII) CRIB (SacI) yemCherry (MluI) ADH1t (XhoI) and

pEXPARG (NotI) ACT1p (RsrII) CRIB (SacI) yemScarlet (MluI) ADH1t (XhoI).

Inserts used were obtained by PCR. Primers with a unique SacI 5' site and a unique MluI 3' site were used to amplify *yemCherry* and *yemScarlet* (*yemCherry*.P5 and P6, *yemScarlet*.P2 and P3).

d) Reporters plasmids – pExpARG SEC4p yemScarlet-SEC4 ADH1t plasmid was generated by C. Puerner. Plasmids used to amplify AFP cassettes for knock-in into the 3' end of *MLC1*, *SEC3*, *SEC61*, *ABP1*, *SEC7* were:

- i. pFA mCherry CaHIS1, from Reijnt *et al.*, 2011;
- ii. pFA mScarlet CdHIS1 and pFA yemiRFP670 CdHIS1, generated by C. Puerner;
- iii. pFA yemEos2 CaHIS1 was generated from pFA yemEos2 URA3 (V. Ghugtyal), replacing *URA3* by *CaHIS1* in a single cloning step.

III – Strains

Strain used to analyze the light-activated recruitment of Cdc42 – To generate these strains, the StuI linearized pEXPARG CIBN-GFP γ -CtRAC1 plasmid was first integrated by homology recombination into the RP10 gene of *C. albicans* BWP17 genome, resulting in PY2935. The NgoMIV digested pDUP3 CRY2PHR-yemCherry-CDC42[G12V,C188S] plasmid was then integrated in the NEUT5L intergenic region of the PY2935 genome, resulting in PY3451.

Reporter tagged strains – To generate these strains, CRY2PHRlinker-GFP γ -CDC42[G12V,C188S] was first integrated in *C. albicans* BWP17 genome, using the pDUP3 plasmid as described previously (Gerami-Nejad *et al.*, 2013). The NgoMIV digested pDUP3 CRY2PHRlinker-GFP γ -CDC42[G12V,C188S] was transformed into BWP17, resulting in PY3643. The NgoMIV digested pDUP5 CIBNlinker-CtRAC1 was then

integrated in PY3643 genome, using the NEUT5L intergenic sequence and URA3 selection, resulting in PY4510.

This strain was then used to integrate the sequences encoding mScarlet-Sec4, CRIB-yemCherry or CRIB-yemScarlet into the *RP10* locus, using the pEXPARG plasmids described previously and/or to knock-in the different AFPs into the genes of interest. The cassettes were amplified from the appropriate pFA plasmids for knock-in into the genes *MLC1*, *SEC3*, *SEC61*, *ABP1* and *SEC7* (MLC1.P1 and P2, SEC3.P1 and P2, SEC61.P1 and P2, ABP1.P1 and P2, SEC7.P1 and P2).

IV – Growth conditions

Yeast extract peptone dextrose or synthetic complete medium, supplemented with 80 mg/L of uridine (Uri), were used and are referred to as YEPD or SC media, respectively. In general, strains were grown at 30 °C, with 250 rpm orbital shaking overnight and stationary phase cultures were back-diluted the next day into fresh media to an optical density OD_{600nm} of 0.1, unless otherwise stated (Sherman 1991). Cells were used for experiments after exponential phase growth at ~ OD₆₀₀ of 0.6.

V – Yeast transformation

Polyethylene Glycol-Lithium Acetate (PEG/LiAc) Transformations – Cells were grown overnight in YEPDUri media at 30 °C and stationary phase cultures were back-diluted the next day into fresh media at an OD₆₀₀ of 0.1 (10 mL culture for one DNA transformation). Cell were grown to an OD₆₀₀ of 0.6-0.8, centrifuged (2,000 rpm, RT 5 min) and the pellets were resuspended in 1/10 of the initial culture's volume in LATE buffer (100 mM LiAc, 1 mM EDTA, 10 mM Tris-HCl pH 7.5). After centrifugation (2,000 rpm, RT 5 min), the pellets were resuspended in 1/100 of the initial volume culture in LATE buffer. A mixture of purified DNA cassette (7 to 10 µL) and single stranded salmon sperm DNA (5 µg, freshly heat denaturated) was added to cells in LATE (100 µL). After incubation of the transformation mixture at 30 °C for 30 min, PLATE buffer was added (700 µL; LATE buffer with 50% of polyethylene glycol), vortexed briefly and incubated at 30 °C overnight. The following day, cells were heat shocked at 42 °C for 1 h and briefly centrifuged (2,000 rpm, RT 30 sec). Pellets were then resuspended in LATE buffer (400 µL) and spread onto selective plates. Colonies were visible after 3 to 5 days at 30 °C (Gietz

et al., 1995; Walther and Wendland, 2003). For nourseothricin (NAT; Werner Bioagents) selection, following the heat shock, cells were resuspended in YEPDURi media and grown for at least 4 h at 30 °C prior to being spread on YEPDNAT plates (200 µg/mL). Colonies were visible after 2 to 4 days at 30 °C (Reuß *et al.*, 2004; Shen *et al.*, 2005).

Electroporation Transformations – Cells were grown overnight on YEPDURi media at 30 °C and stationary phase cultures were centrifuged (4,000 rpm, RT 5 min) and pellet was resuspended in DH₂O (8 mL). TE buffer (1 mL; 100 mM Tris-HCl, 10 mM EDTA pH 7.5) and lithium acetate (1 mL; 1 M pH 7.5) were added and the mixture was incubated at 30 °C for 45 min. DTT (250 µL; 1 M) was added and the mixture was incubated for an additional 15 min at 30 °C. Chilled DH₂O (40 mL) was added and the cells were centrifuged (4,000 rpm, 4 °C 5 min). Cells were subsequently washed with chilled DH₂O (25 mL), chilled sorbitol (5 mL; 1 M) and finally resuspended in chilled sorbitol (40 µL/electroporation). Purified DNA cassette (5 µL of isopropanol precipitated and resuspended in DH₂O) was mixed with 40 µL of electrocompetent cells kept on ice and transferred into a chilled electroporation cuvette (0.2 cm electrode gap, Cell Projects) and stored on ice. Each mixture was pulsed in an electroporation chamber (electric pulse of 1.8 kV, time constant between 5 to 6 ms; Eppendorf Electroporator 2510) and then resuspended in 1 mL of chilled sorbitol. Cells were centrifuged (2,000 rpm, RT 30 sec), resuspended in YEPD and plated on selective media (Thompson *et al.*, 1998). For nourseothricin selection, , cells were resuspended in YEPDURi media and grown for at least 4 h at 30 °C prior to being spread on YEPDNAT plates (200 µg/mL). Colonies were visible after 2 to 4 days at 30 °C (Reuß *et al.*, 2004; Shen *et al.*, 2005).

VI – Actin cytoskeleton staining and actin cables quantification

Visualization of F-Actin was carried out with phalloidin Alexa Fluor-568 (1 U/µL stock solution in MeOH, stored at -20 °C; Thermo Fisher Scientific). Exponential phase cells (typically OD₆₀₀ of 0.1) were induced to filament with 50% FCS at 37 °C in liquid for 20 minutes, in a shaking incubator. After this step, the cells were incubated in a Concanavalin A treated (0.1 mg/mL, 1 min) glass bottom microwell dish (MatTek Corporation) for 10 minutes at 37 °C, in the microscope heated chamber, to adhere to the dish glass. The photoactivation protocol was performed in the cells in the microwell dish. Following

photoactivation protocol (details of protocol in the Materials & Methods Section, Photoactivation Protocols Sub-section), cells were fixed in 4% paraformaldehyde for 10 min, subsequently washed with PBS (Phosphate Buffered Saline; 1X pH 7.4), incubated with Buffer B (100 mM sodium phosphate, 1.2 M sorbitol, 2 μ L/mL β -mercaptoethanol, pH 7.4) for 20 min, followed by washing with PBS. Phalloidin Alexa Fluor-568 was added to the cells (0.01 U/ μ L in PBS, 200 μ L) and incubated for 1 h in the dark, subsequently washed with PBS prior to microscopy (Hazan and Liu, 2002).

VII – Microscopy

Cells in exponential growth phase were mixed with 50% FCS, placed on agar pads (SC medium, 75% FCS and 2% agar on a glass slide – Thermo Scientific) and covered with glass coverslips (0.13 - 0.17mm thickness, Menzel-Gläser) for most microscopy experiments or, as explained in previous section, placed on glass bottom microwell dish for actin visualization experiments. Microscopy images for all experiments were acquired on an Olympus IX81 inverted microscope (Olympus Corporation of the Americas), equipped with a motorized XY stage (Prior Scientific), a confocal head Yokogawa CSU-X1 (Yokogawa Electric Corporation) and a sensitive iXON DU-897-BV EMCCD camera (Andor Technology). The LASER lines were at 488 nm (DPSS), 561 nm (DPSS) and 640 nm (Diode) (Andor Technology). The objectives used were a UPLANFLN 10X dry 0.3 numerical aperture (NA) and a UPLSAPO 100X oil 1.4 or 1.45 NA (Olympus Corporation of the Americas). Z stacks were acquired using a piezo stage NanoScan Z100 (Prior Scientific). The 37 °C controlled atmosphere was created in an incubator box, an air heating system and an air pump system (Okolab). The system was controlled using MetaMorph Software (Molecular Devices). Images were acquired in DIC (LED, 40 ms), 561 nm (10-15%, 300 ms), 470 nm (10%, 300 ms) and 640 nm channels (10-15%, 300 ms). For all the experiments a long-pass red filter was used to filter out wavelengths that photoactivate the Cry2PHR-CibN system while acquiring DIC images (LP 540 nm, Leica). The microscopy was done in the Prism facility, “Plateforme PRISM - IBV- CNRS UMR 7277 - INSERM U1091 - UNS”.

Photoactivation Protocols – In the incubator box with a 37 °C controlled atmosphere, cells were induced until short germ tubes were grown (3-5 μ m, approximately 30 min). To

photoactivate the cells a green fluorescent image is taken (470 nm, 300 ms pulse) and the photoactivation protocol (PAct) performed on the filamentous cells consisted of a sequence of photoactivation pulses: 3 pulses-10 minutes apart or 6 pulses-5 minutes apart. To visualize the effects of the photoactivation protocol, DIC and 561 nm images were acquired up to 2 hours after the PAct protocol. For actin cytoskeleton visualization, the PAct protocol was shorter, with 1 to 3 pulses-5 minutes apart - when a second Mlc1 cluster was visible in the cells. Afterwards, the cells were fixed and the actin staining protocol was carried out.

Image Processing – To improve the quality of microscopy images and reduce the background, an algorithm-based processing, *i.e.* deconvolution, was performed. The deconvolution settings used were adjusted to each image set according to the wavelength and filters used, objective NA, background and signal to noise ratio (SNR; from 5 to 20). All deconvolution processing was done using 40 iterations. For some images, a bleaching correction with exponential fit was done using ImageJ.

Analysis – Image analysis was done using ImageJ v1.6.0_20 (Sun Microsystems Inc.) and Volocity v6.3 (Perkin Elmer Inc.). The data obtained – cell counts, germ tube length, signal intensity and area, actin cables counts, clusters center of mass and ellipticity, was compiled and processed in Excel.

Table 3. Plasmids

Plasmid	Source
pDUP3	Gerami-Nejad
pDUP5	<i>et al.</i> , 2013
pDUP3 TEF1p TEF1t	This study
pDUP5 ADH1p ACT1t	
pDUP3 TEF1p CaCRY2PHR-yemCherry-CDC42[C188S] TEF1t	
pDUP3 TEF1p CaCRY2PHR-yemCherry-CDC42[G12V,C188S] TEF1t	
pDUP3 TEF1p CaCRY2PHR-linker-GFP γ -CDC42[G12V,C188S] TEF1t	
pDUP5 ADH1p CaCIBN-linker-CtRAC1 ACT1t	
pEXPARG ACT1p CaCIBN-GFP γ -CtRAC1 ADH1t	
pEXPARG ACT1p CRIB-yemCherry ADH1t	
pEXPARG ACT1p CRIB-yemScarlet ADH1t	
pEXPARG ACT1p CRIB-GFP ADH1t	
pEXPARG SEC4p yemScarlet-SEC4 ADH1t	Charles
pFA yemScarlet CdHIS1	Puerner,
pFA yemiRFP670 CdHIS1	unpublished
pFA yemCherry CaHIS1	(Reijnt <i>et al.</i> , 2011)
pFA yemEOS2 CaHIS1	This study
pFA yemEOS2 URA3	Vikram Ghugtyal, unpubl.

Table 4. Oligonucleotides

Primer	Sequence
ABP1.P1	TGTTGAAATCGAATTTGTTGACGATGATTGGTGGCAAGGAAAACATTC CAAGACAGGAGAAGTCGGATTGTTCCCTGCTAACTATGTTGTCTTGAA TGAGGGTGCTGGCGCAGGTGCTTC
ABP1.P2	CAATTTATCTTTTCTTTGTATTTATATTATAGATTCATATAAAAAAAAA AACGAATATTGTTTATACTAAATTCTGATATCATCGATGAATTCGAG
ACT1.P1	CTCACCAGGATTTATTGCC
ACT1.P2	TTACTAGTGGCCTGCAGGGAGTGAAATTCTGGAAATCTGG
ACT1.P3	CGCCGCGGCCGCGTCGACATTTTATGATGG
ADH1.P1	TTATCTCGAGCCATGAGATTGATGCTAGATATTTTC
ADH1.P2	TTTGCTTATTTACTGGTG
ADH1.P3	ATTCCTGCAGCCCGGGGCACGGACAAGCTTATTGAG
ADH1.P4	TTAATTAAGGGCGCGCCAATTGTTTTTGTATTTGTTGTTGTTGTTG
ADH1.P5	TTACTAGTTTAATTAAGGGCGCGCCAATTGTTTTTGTATTTGTTGTTG TTGTTG
CDC42.P1	GGAAAAC TAGTGATGCAAAC TATAAAATGTG
CDC42.P2	ATCCTGCAGGCTATAAAATAGTACTCTTTTTTCGATTTTTTAATTAC
CDC42.P3	GTGTTGTTGTCGGTGACGTCGCCGTTGGTAAAAC TTGCTTATTAATCT CG
CDC42.P4	CGAGATTAATAAGCAAGTTTTACCAACGGCGACGTCACCGACAACAAC AC
CDC42.P5	CCTTGGGATTATTTGATACTGCTGGTCTAGAAGATTACGACAGATTAA GGCC
CDC42.P6	GGCCTTAATCTGTCGTAATCTTCTAGACCAGCAGTATCAAATAATCCC AAGG
CDC42.P7	GCCTTAATTA AAAATGCAAAC TATAAAATGTGTTG
CDC42.P8	TGTACAAAAA ACTAGTGATGCAAAC TATAAAATGTGTTG
CDC42.P9	ATATTCAACTAGCCCTGCAGGCTATAAAATAGTACTCTTTTTTCG
CIBN1.P1	CGGCGCGCCCATGAATGGTGCTATTGGTGG

CIBN1.P2	TTTAATTAAAATATAATCAGTTTTTTCC
CIBN1.P3	CGGACCGCCCGGGATGAATGGTGCTATTGGTGG
CIBN1.P4	CTTAATTAATTATAATATAGTACATTTTTTTAGCTCTCTTAATTTTTCT TTTCTTTGATGAACCACCAGCTGAACCAGCTGAACCAGCTGAATCAAA TTCAATATAATCAGTTTTTTCC
CIBN1.P5	CACCACCAGTAATCATTGATGAATCAGC
CIBN1.P6	CGACGCGTATTATAATATAGTACATTTTTTTAGCTCTCTTAATTTTTCT TTTCTTTGATGAACCACCAGCTGAACCAGCTGAACCAGCTGAATCAAA TTCAATATAATCAGTTTTTTCC
yemCherry. P1	TCATCAGAAAGAATGTATCCAGAAG
yemCherry. P2	ACAATTTTAAATAATCTG
yemCherry. P3	GCCTTAATTAAAATGGTTTCAAAGGTGAAG
yemCherry. P4	GATCACTAGTTTTTTTATATAATTCATCCATACC
yemCherry. P5	GGGAGCTCGATGGTTTCAAAGGTGAAGAAG
yemCherry. P6	CGACGCGTACCCTGCAGGTTTATATAATTCATCCATACCACCAG
yemCherry. P7	CTTCTAGTATACGCGTCTTATAATATAGTACATTTTTTTAGCTCTCTTA ATTTTTCTTTTCTTTTTTATATAATTCATCCATACCACC
yemCherry. P8	GCTGGATCCATGGTTTCAAAGGTGAAGAAG
yemCherry. P9	TACGGTCCGTATTTATATAATTCATCCATACC
CRIB.P1	CCACACCATTTGATTTTCAAC
CRIB.P2	CCTCCTCCTCAAGCAAGCGGG
CRY2PHR. P1	TACGGACCGATGAAAATGGATAAAAAAACTATTGTTTGG
CRY2PHR.	GGAGCTCCCAGCAGCACCAATCATAATTTGAGC

P2	
CRY2PHR. P3	CTTCTAGTATACGCGTCTTATAATATAGTACATTTTTTTAGCTCTCTTA ATTTTTCTTTTCTTAGCAGCACCAATCATAATTTGAGC
CRY2PHR. P4	GGAGCTCCCTGATGAACCACCAGCTGAACCAGCTGAACCAGCTGAATC AAATTCAGCAGCACCAATCATAATTTGAGC
CRY2PHR. P5	CGGCGCGCCCATGAAAATGGATAAAAAAACTATTGTTTGG
CRY2PHR. P6	TTTAATTAATGATGAACCACCAGCTGAACCAGCTGAACCAGCTGAATC AAATTCAGCAGCACCAATCATAATTTGAGC
CRY2PHR. P7	ATCCCGGGGGCGCGCCAGGTGGATCTGGAGGTTTCAGGTGGAAGTCCTA GGATGAAAATGGATAAAAAAACTATTGTTTGG
CRY2PHR. P8	TACAGCGTTTAAGCAGCACCAATCATAATTTGAGC
CRY2PHR. P9	CATCATCCATGGGATGCTC
CRY2PHR. P10	CCTTCTTCTTCTGGACACC
CRY2PHR. P11	GATCACTAGTTTAGCAGCACCAATCATAATTTGAGC
GFP.P1	CTTCTAGTATACGCGTCTTATAATATAGTACATTTTTTTAGCTCTCTTA ATTTTTCTTTTCTTGTACAATTCATCCATACCATGGGTAATACC
GFP.P2	CCGGAGACAGAAAATTTG
GFP.P3	TATACGCGTTTATTTGTACAATTCATCCATACC
GFP.P4	GTTTACATCATGGCTGAC
GFP.P5	CGAGCTCCCTTTGTACAATTCATCCATACC
GFP.P6	GCCTTAATTAAAATGTCTAAAGGTGAAGAA
GFP.P7	GATCACTAGTTTTTTTGTACAATTCATCCATACC
GFP.P8	GGGAGCTCGATGTCTAAAGGTGAAGAA
GFP.P9	CGACGCGTACCCTGCAGGTTTGTACAATTCATCCATACCATGGG
GFP.P10	TACGGACCGGGGAGCTCGATGTCTAAAGGTGAAGAA
GFP.P11	CGACGCGTACGGCGGCCTTTGTACAATTCATCCATACCATGGG

GFP.P12	ATCCCGGGATGTCTAAAGGTGAAGAA
GFP.P13	CGAGCTCGGCGCGCCTTTGTACAATTCATCCATACC
MLC1.P1	GATGAGTTATTAAAAGGGGTCAATGTAACCTTCTGATGGAAATGTGGAT TATGTTGAATTTGTCAAATCAATTTTAGACCAAGGTGCTGGCGCAGGT GCTTC
MLC1.P2	CGAACAAGACTATAACAATAACTATAATTTGTAAAACCTTGTAGTATATA TATTTCAATGGTTAATTGTAAATTTTCTTTTATTCTGATATCATCGAT GAATTCGAG
yemScarlet. P1	CGGCGCGCCTTTATATAATTCATCCATACCACC
yemScarlet. P2	GGGAGCTCGATGGTTTCAAAGGTGAAGCTG
yemScarlet. P3	CTTCTAGTATACGCGTCTTATTTATATAATTCATCCATACCACC
SEC3.P1	GGAAATGATATAGGGTCTGCTTTGAATGAAGTGGATAATATGACTCAG ATTTTCCAGAAGATGGAGGTGAGATTGAACTTGTACGAAATGAGCTA CAAAGTTCTGCTACTGCTGGTCTGGCGCAGGTGCTTC
SEC3.P2	GTTGTATATGTAGTAGAGAAAGCAGTACTAAAACAGTATTAATTAAT TAAAGCTATACTATACAAACCTTAATAATTACTATACTCTTGATAAAAA GACTTGCTCCATTTCTGATATCATCGATGAATTCGAG
SEC61.P1	CCACTATCTATGGATACTACGAGTTGGCTGTAAAAGAAGGTGGATTCA ACAAATCAATTGTCAGTGGATTCTCCGATGGCATTGGTCTGGCGCAG GTGCT
SEC61.P2	GTCATTTTGGTGATGAGGAAAAGAATATTTTTTTTTTTGATTTTTTTTT TTCTACACGTTTATAAACGAGAAAAGTTTTTATTCTGATATCATCGAT GAATTCGAG
SEC7.P1	GGCAATGAAAGCTTTTTTAACTAGAGTGGGTGAAGAGTTTGTTAGTAT TTCTGACAACAATAAGGAAAGAAGGGGTGCTGGCGCAGGTGCTTC
SEC7.P2	GTAAATGATACACTTACAGTTGTTTTAACATAATTGATAAATTATTAT TATACATTATTCCTACTTTCATCTGATATCATCGATGAATTCGAG
TEF1.P1	TACCCGGGACGCTGATACGGCATGCC
TEF1.P2	TTACTAGTTTAATTAAGGGCGCGCCGATTGATTATGACTATAATG
TEF1.P3	TTACTAGTGGCCTGCAGGGCTAGTTGAATATTATGTAAGATCTG

TEF1.P4	CGCCGCGGCCGCATATACTTCCATTTATCACATCC
TEF1.P5	CCCATGAGGAACAGCGAGAAAG
TEF1.P6	CCGGACTACCAAAAATTC

Table 5. Synthesized Genes

GENE
SEQUENCE
<p><i>CRY2PHR</i></p> <p>ATGAAAATGGATAAAAAAACTATTGTTTGGTTTAGAAGAGATTTAAGAATTGAAGATA ATCCAGCTTTGGCTGCTGCTGCTCATGAAGGTTTCAGTTTTTCCAGTTTTTATTTGGTG TCCAGAAGAAGAAGGTCAATTTTATCCAGGTAGAGCTTCAAGATGGTGGATGAAACAA TCATTAGCTCATTTGTCACAATCATTAAAAGCTTTGGGTTTCAGATTTAACTTTGATTA AAACTCATAATACTATTTTCAGCTATTTTAGATTGTATTAGAGTTACTGGTGCTACTAA AGTTGTTTTTAATCATTTGTATGATCCAGTTTCATTAGTTAGAGATCATACTGTTAAA GAAAAATTGGTTGAAAGAGGTATTTTCAGTTCAATCATATAATGGTGATTTATTGTATG AACCATGGGAAATTTATTGTGAAAAAGGTAAACCATTTACTTCATTTAATTCATATTG GAAAAATGTTTAGATATGTCAATTGAATCAGTTATGTTGCCACCACCATGGAGATTA ATGCCAATTACTGCTGCTGCTGAAGCTATTTGGGCTTGTTCAATTGAAGAATTGGGTT TAGAAAATGAAGCTGAAAAACCATCAAATGCTTTGTTAAGTAGAGCTTGGTCAACCAGG TTGGTCAAATGCTGATAAATTGTTAAATGAATTTATTGAAAAACAATTGATTGATTAT GCTAAAAATTCAAAAAAGTTGTTGGTAATTCAACTTCATTATTGTCACCATATTTAC ATTTTGGTGAAATTTTCAGTTAGACATGTTTTTCAATGTGCTAGAATGAAACAAATTAT TTGGGCTAGAGATAAAAATTCAGAAGGTGAAGAATCAGCTGATTTGTTTTTAAGAGGT ATTGGTTTGAGAGAATATTCAAGATATATTTGTTTTAATTTTCCATTTACTCATGAAC AATCATTATTGTCACATTTAAGATTTTTTCCATGGGATGCTGATGTTGATAAATTTAA AGCTTGAGACAAGGTAGAAGTGGTTATCCATTGGTTGATGCTGGTATGAGAGAATTA TGGGCTACTGGTTGGATGCATAATAGAATTAGAGTTATTGTTTCATCATTTGCTGTTA AATTTTTATTGTTACCATGGAAATGGGGTATGAAATATTTTTGGGATACTTTGTTAGA TGCTGATTTGGAATGTGATATTTTAGGTTGGCAATATATTTTCAGGTTCAATTCAGAT GGTCATGAATTGGATAGATTAGATAATCCAGCTTTGCAAGGTGCTAAATATGATCCAG AAGGTGAATATATTAGACAATGGTTACCAGAATTGGCTAGATTACCAACTGAATGGAT TCATCATCCATGGGATGCTCCATTGACTGTTTTAAAAGCTTCAGGTGTTGAATTGGGT ACTAATTATGCTAAACCAATTGTTGATATTGATACTGCTAGAGAATTATTGGCTAAAG CTATTTCAAGAACTAGAGAAGCTCAAATTATGATTGGTGCTGCT</p>
<p><i>CIBN</i></p> <p>ATGAATGGTGCTATTGGTGGTGATTTATTGTTAAATTTTCCAGATATGTCAGTTTTAG</p>

AAAGACAAAGAGCACATTTGAAATATTTAAATCCAACCTTTTGATTCCACCATTGGCTGG
TTTTTTTGGCTGATTCATCAATGATTACTGGTGGTCAAATGGATTCATATTTGTCAACT
GCTGGTTTAAATTTGCCAATGATGTATGGTCAAACACTGTTGAAGGTGATTCAAGAT
TATCAATTTCCACCAGAACTACTTTGGGTACTGGTAATTTTAAAGCTGCTAAATTTGA
TACTGAACTAAAGATTGTAATGAAGCTGCTAAAAAATGACTATGAATAGAGATGAT
TTAGTTGAAGAAGGTGAAGAAGAAAAATCAAAAATTACTGAACAAAATAATGGTTCAA
CTAAATCAATTAAAAAAATGAAACATAAAGCTAAAAAAGAAGAAAATAATTTTTCAA
TGATTCATCAAAAGTTACTAAAGAATTGGAAAAAAGCTGATTATATT

yemiRFP670

ATGGCTAGAAAAGTTGATTTAACTTCATGTGATAGAGAACCAATTCATATTCAGGTT
CAATTCACCATGTGGTTGTTTATTAGCTTGTGATGCTCAAGCTGTTAGAATTACTAG
AATTACTGAAAATGCTGGTGCTTTTTTTGGTAGAGAACTCCAAGAGTTGGTGAATTA
TTAGCTGATTATTTTGGTCAAACACTGAAGCTCATGCTTTAAGAAATGCTTTAGCTCAAT
CATCAGATCCAAAAGACCAGCTTTAATTTTTGGTTGGAGAGATGGTTTAACTGGTAG
AACTTTTGATATTTTCATTACATAGACATGATGGTACTTCAATTATTGAATTTGAACCA
GCTGCTGCTGAACAAGCTGATAATCCATTAAGATTAAGTAACTAGACAAATTATTGCTAGAA
CTAAAGAATTAAAATCATTAGAAGAAATGGCTGCTAGAGTTCCAAGATATTTACAAGC
TATGTTAGGTTATCATAGAGTTATGTTATATAGATTTGCTGATGATGGTTCAGGTATG
GTTATTGGTGAAGCTAAAAGATCAGATTTAGAATCATTTTTAGGTCAACATTTTCCAG
CTTCATTAGTTCCACAACAAGCTAGATTATTATATTTAAAAAATGCTATTAGAGTTGT
TTCAGATTCAGAGGTTATTTTCATCAAGAATTGTTCCAGAACATGATGCTTCAGGTGCT
GCTTTAGATTTATCATTGCTCATTAAAGATCAATTTCCACCATGTCATTTAGAATTTT
TAAGAAATATGGGTGTTTTCAGCTTCAATGTCATTATCAATTATTATTGATGGTACTTT
ATGGGGTTTAAATTATTTGTCATCATTATGAACCAAGAGCTGTTCCAATGGCTCAAAGA
GTTGCTGCTGAAATGTTTGGCTGATTTTTTATCATTACATTTTACTGCTGCTCATCATC
AAAGATAA

yemScarlet

ATGGTTTCAAAGGTGAAGCTGTTATTAAAGAATTTATGAGATTTAAAGTTCATATGG
AAGTTCAATGAATGGTCATGAATTTGAAATTGAAGGTGAAGGTGAAGGTAGACCATA
TGAAGGTACTCAAACACTGCTAAATTAAGGTTACTAAAGGTGGTCCATTACCATTTTCA
TGGGATATTTTATCACCACAATTTATGTATGGTTCAAGAGCTTTTACTAAACATCCAG
CTGATATTCAGATTATTATAAACAATCATTTCAGAAAGGTTTAAATGGGAAAGAGT
TATGAATTTTGAAGATGGTGGTGCTGTTACTGTTACTCAAGATACTTCATTAGAAGAT
GGTACTTTAATTTATAAAGTTAAATTAAGAGGTTACTAATTTTCCACCAGATGGTCCAG
TTATGCAAAAAAAGCTATGGGTGGGAAGCTTCAACTGAAAGATTATATCCAGAAGA
TGGTGTTTTAAAGGTGATATTAAATGGCTTTAAGATTAAAGATGGTGGTAGATAT
TTAGCTGATTTTAAACTACTTATAAAGCTAAAAAACCAGTTCAAATGCCAGGTGCTT
ATAATGTTGATAGAAAATTAGATATTACTTCACATAATGAAGATTATACTGTTGTTGA
ACAATATGAAAGATCAGAAGGTAGACATTCAACTGGTGGTATGGATGAATTATATAAA
TAA

Table 6. Strains

Strain	Genotype	Source
BWP17	<i>ura3Δ::λimm434/ura3Δ::λimm434 his1Δ::hisG/his1Δ::hisG arg4Δ::hisG/arg4Δ::hisG</i>	(Wilson <i>et al.</i> , 1999)
PY2935	Same as BWP17 but with <i>RP10::ARG4 ACT1p CaCIBN-GFPγ- CtRAC1 ADH1t</i>	This study
PY3451	Same as PY2935 but with <i>NEUT5L::NAT1 TEF1p CaCRY2PHR- yemCherry-CDC42[G12V,C188S] TEF1t</i>	
PY3643	Same as BWP17 but with <i>NEUT5L::NAT1 TEF1p CaCRY2PHR- linker-GFPγ-CDC42[G12V,C188S] TEF1t</i>	
PY4059	Same as PY3643 but with <i>NEUT5L::URA3 ADH1p CaCIBN-linker- CtRAC1 ACT1t</i>	
PY4172	Same as PY4059 but with <i>RP10::ARG4 ACT1p CRIB-yemCherry ADH1t</i>	
PY4175	Same as PY4059 but with <i>ABP1/ABP1::HIS1 ABP1-yemCherry</i>	
PY4268	Same as PY4059 but with <i>MLC1/MLC1::HIS1 MLC1-yemCherry</i>	
PY4510	Same as PY3643 but with <i>NEUT5L::URA3 ADH1p CIBN-linker- CtRAC1 ACT1t</i>	
PY4534	Same as PY4510 but with <i>RP10::ARG4 SEC4p yemScarlet-SEC4 ADH1t</i>	
PY4623	Same as PY4534 but with <i>MLC1/MLC1::HIS1 MLC1-yemiRFP670</i>	
PY4642	Same as PY4510 but with <i>MLC1/MLC1::HIS1 MLC1-yemiRFP670</i>	

Annex

Additional plasmids and strains generated, but not used for results of this study, are listed in the following tables.

Table 7. Additional Plasmids

Plasmid
pDUP5 ADH1p CaCIBN-linker-CtRAC1 ACT1t
pEXPARG ACT1p CaCIBN-GFP γ -CtRAC1 ADH1t
pEXPARG ACT1p CRIB-yemCherry-CtRAC1 ADH1t
pEXPARG ACT1p GPA2MLS-GFP γ -CaLOV _{pep} ADH1t
pDUP3 TEF1p yemCherry TEF1t
pDUP3 TEF1p GFP γ TEF1t
pDUP3 TEF1p CaCRY2PHR-yemCherry TEF1t
pDUP3 TEF1p CaPDZ-GFP γ TEF1t
pDUP3 TEF1p CaPIF-GFP γ TEF1t
pDUP3 TEF1p CaPDZ-yemCherry TEF1t
pDUP3 TEF1p CaCRY2PHR-yemCherry-CDC24FL TEF1t
pEXPARG ACT1p GPA2MLS-GFP γ -CaLOV _{pep} ^{CA} (MluI) ADH1t
pEXPARG ACT1p CaCRY2PHR-GFP γ -CtRAC1 (MluI) ADH1t
pDUP3 TEF1p CaCIBN-yemCherry TEF1t
pEXPARG ACT1p CaCIBN-GFP γ ADH1t
pEXPARG ACT1p CaCRY2PHR-GFP γ ADH1t
pEXPARG ACT1p CRIB-yemTurquoise2 ADH1t
pEXPARG ACT1p CRIB-yemiRFP670 ADH1t
pEXPARG ACT1p CRIB-yemYPet ADH1t
pDUP3 TEF1p CaCRY2PHR-yemCherry-CDC24CAT TEF1t
pDUP3 TEF1p CaCRY2PHR-yemCherry-MSS4CAT TEF1t
pDUP3 TEF1p CaCRY2PHR-yemCherry-STT4 TEF1t

pDUP3 TEF1p CaCRY2PHR-yemCherry-STT4CAT TEF1t
pDUP3 TEF1p CaCIBN-yemCherry-CDC24 TEF1t
pDUP3 TEF1p CaCIBN-yemCherry-CDC24CAT TEF1t
pEXPARG ACT1p GFP γ ADH1t
pEXPARG ACT1p GFP γ -CaSSO2 ADH1t
pEXPARG ACT1p CaCIBN-GFP γ -CaSSO2 ADH1t
pEXPARG ACT1p CaCIBN-GFP γ ADH1t
pEXPARG ACT1p CaCIBN-GFP γ -CaSSO2TMD ADH1t
pEXPARG ACT1p CaCIBN-GFP γ -GRIP ADH1t
pEXPARG ACT1p CaCRY2PHR-GFP γ -CaSSO2 ADH1t
pEXPARG ACT1p CaCRY2PHR-linker-GFP γ -CtRAC1 ADH1t
pEXPARG ACT1p CaCRY2PHR-linker-GFP γ -CaSSO2 ADH1t
pDUP3 TEF1p CaCRY2PHR-linker-yemCherry-CDC24 TEF1t
pDUP3 TEF1p CaCRY2PHR-yemCherry-CDC24C-DH TEF1t
pDUP3 TEF1p CaCRY2PHR-yemCherry-CDC24C-DHPH TEF1t
pDUP3 TEF1p CaCRY2PHR-yemCherry-CDC42[Q61L,C188S] TEF1t
pDUP3 TEF1p PHR2 TEF1t
pDUP3 PHR2p PHR2 TEF1t
pDUP3 TEF1p CaCIBN-yemCherry-CDC24-DHPH TEF1t
pDUP3 TEF1p CaCIBN-yemCherry-CDC24-DH TEF1t
pDUP3 TEF1p CaCIBN-yemCherry-CDC42[C188S] TEF1t
pDUP3 TEF1p PHR2SS-(PacI bp70)-PHR2 TEF1t
pDUP3 TEF1p PHR2-(PacI bp1420)-PHR2GPI TEF1t
pDUP3 PHR2p PHR2SS-(PacI bp70)-PHR2 TEF1t
pDUP3 PHR2p PHR2-(PacI bp1420)-PHR2GPI TEF1t
pDUP3 TEF1p CaCIBN-yemCherry-CDC42[G12V,C188S] TEF1t
pDUP3 TEF1p CaCIBN-yemCherry-CDC42[Q61L,C188S] TEF1t

pExpARG ADH1p CaCRY2PHR-linker-GFP γ -CtRAC1 ADH1t
pDUP3 TEF1p PHR2SS-yemCherry-yemCherry-PHR2 TEF1t
pDUP3 TEF1p PHR2SS-yemCherry-PHR2 TEF1t
pEXPARG ACT1p CaWSC1-GFP γ -GFP γ ADH1t
pEXPARG ACT1p CaDFI1-GFP γ -GFP γ ADH1t
pDUP3 TEF1p PHR2SS-FAP α 2-PHR2 TEF1t
pDUP3 TEF1p CaCRY2PHR-yemCherry-RHO1[C195S] TEF1t
pDUP3 TEF1p CaCRY2PHR-yemCherry-RHO1[Q67H,C195S] TEF1t
pDUP5 ADH1p CaCIBN-GFP γ -CtRAC1 ACT1t
pDUP3 TEF1p CaCRY2PHR-linker-CDC42[G12V,C188S] TEF1t
pDUP3 TEF1p PHR2SS-yemCherry-PHR2 TEF1t
pDUP3 TEF1p PHR2SS- β Lactamase-yemCherry-PHR2 TEF1t
pDUP5 TEF1p CaCRY2PHR-yemCherry-CDC42[G12V,C188S] TEF1t
pJET1.2 TEF1 Δ LifeAct-yemScarlet HIS1 TEF1 Δ
pDUP3 PHR2p PHR2-yemCherry-PHR2GPI TEF1t
pEXPARG ACT1p ActinChromobody-yemScarlet-yemScarlet-yemScarlet ADH1t

Table 8. Additional Strains

Strain	Genotype
PY2927-28	Same as BWP17 but with <i>RP10::ARG4 ACT1p CRIB-GFPγ-CtRAC1 ADH1t</i>
PY2929-30	Same as BWP17 but with <i>RP10::ARG4 ACT1p CRIB-yemCherry-CtRAC1 ADH1t</i>
PY2931-34	Same as BWP17 but with <i>RP10::ARG4 ACT1p GPA2MLS-GFPγ-CaLOV_{pep} ADH1t</i>
PY2937-38, 2951-52	Same as BWP17 but with <i>NEUT5L::NAT1 TEF1p GFPγ TEF1t</i>
PY2949-50	Same as BWP17 but with <i>NEUT5L::NAT1 TEF1p yemCherry TEF1t</i>
PY2953-54	Same as BWP17 but with <i>NEUT5L::NAT1 TEF1p CaPDZ-GFPγ TEF1t</i>

PY2955-56	Same as PY2931 but with <i>NEUT5L::NAT1 TEF1p yemCherry TEF1t</i>
PY2957-58	Same as PY2931 but with <i>NEUT5L::NAT1 TEF1p CaPDZ-GFPγ TEF1t</i>
PY2959-60	Same as PY2935 but with <i>NEUT5L::NAT1 TEF1p yemCherry TEF1t</i>
PY2961-62	Same as BWP17 but with <i>NEUT5L::NAT1 TEF1p CaPIF-GFPγ TEF1t</i>
PY2963-64	Same as PY2931 but with <i>NEUT5L::NAT1 TEF1p CaPDZ-yemCherry TEF1t</i>
PY2965-66	Same as BWP17 but with <i>NEUT5L::NAT1 TEF1p CaCRY2PHR-yemCherry TEF1t</i>
PY2974-75. 3018	Same as BWP17 but with <i>NEUT5L::NAT1 TEF1p CaPDZ-yemCherry TEF1t</i>
PY3009-11	Same as BWP17 but with <i>NEUT5L::NAT1 TEF1p CaCRY2PHR-yemCherry-CDC24 TEF1t</i>
PY3012-13	Same as BWP17 but with <i>RP10::ARG4 ACT1p GPA2MLS-GFPγ-CaLOV_{pep}^{CA} ADH1t</i>
PY3014-15, 3017	Same as PY223 but with <i>NEUT5L::NAT1 TEF1p CaCRY2PHR-yemCherry-CDC24 TEF1t</i>
PY3016	Same as PY425 but with <i>NEUT5L::NAT1 TEF1p CaCRY2PHR-yemCherry-MSS4 TEF1t</i>
PY3019-20	Same as PY3010 but with <i>RP10::ARG4 ACT1p CaCIBN-GFPγ-CtRAC1 ADH1t</i>
PY3021-22	Same as BWP17 but with <i>NEUT5L::NAT1 TEF1p CaCRY2PHR-yemCherry-MSS4 TEF1t</i>
PY3037-38	Same as PY3013 but with <i>NEUT5L::NAT1 TEF1p CaPDZ-yemCherry TEF1t</i>
PY3039-40	Same as PY3017 but with <i>RP10::ARG4 ACT1p CaCIBN-GFPγ-CtRAC1 ADH1t</i>
PY3041-42	Same as PY3022 but with <i>RP10::ARG4 ACT1p CaCIBN-GFPγ-CtRAC1 ADH1t</i>
PY3043-44	Same as BWP17 but with <i>RP10::ARG4 ACT1p CaCRY2PHR-GFPγ-CtRAC1 ADH1t</i>
PY3045-46	Same as PY223 but with <i>RP10::ARG4 ACT1p CaCRY2PHR-GFPγ-CtRAC1 ADH1t</i>
PY3047-48	Same as PY425 but with <i>RP10::ARG4 ACT1p CaCRY2PHR-GFPγ-CtRAC1 ADH1t</i>
PY3054-55	Same as PY223 but with <i>NEUT5L::NAT1 TEF1p CaCRY2PHR-yemCherry-CDC24 TEF1t</i>
PY3056-57	Same as BWP17 but with <i>RP10::ARG4 ACT1p CaCRY2PHR-GFPγ ADH1t</i>
PY3058-59	Same as PY425 but with <i>RP10::ARG4 ACT1p CaCIBN-GFPγ-CtRAC1 ADH1t</i>

PY3060-61	Same as BWP17 but with <i>NEUT5L::NAT1</i>
PY3062-65	Same as PY3047 but with <i>NEUT5L::NAT1 TEF1p CaCIBN-yemCherry-MSS4 TEF1t</i>
PY3066-68	Same as BWP17 but with <i>NEUT5L::NAT1 TEF1p CaCRY2PHR-yemCherry-MSS4 TEF1t</i>
PY3069-72	Same as PY425 but with <i>NEUT5L::NAT1 TEF1p CaCRY2PHR-yemCherry-MSS4 TEF1t</i>
PY3077-79	Same as PY3046 but with <i>NEUT5L::NAT1 TEF1p CaCIBN-yemCherry-CDC24 TEF1t</i>
PY3080-82, 3186-88	Same as PY3047 but with <i>NEUT5L::NAT1 TEF1p CaCIBN-yemCherry-MSS4 TEF1t</i>
PY3094-97	Same as BWP17 but with <i>RP10::ARG4 ACT1p CRIB-yemTurquoise2 ADH1t</i>
PY3101,3156, 3181	Same as BWP17 but with <i>RP10::ARG4 ACT1p CRIB-yemYPET ADH1t</i>
PY3157-58	Same as BWP17 but with <i>RP10::ARG4 ACT1p GPA2MLS-GFPγ-GFPγ ADH1t</i>
PY3159-61	Same as BWP17 but with <i>RP10::ARG4 ACT1p GFPγ-CaSSO2 ADH1t</i>
PY3162-64	Same as BWP17 but with <i>NEUT5L::NAT1 TEF1p CaCRY2PHR-yemCherry-CDC24CAT TEF1t</i>
PY3165, 3185	Same as PY223 but with <i>NEUT5L::NAT1 TEF1p CaCIBN-yemCherry-CDC24CAT TEF1t</i>
PY3166-68	Same as BWP17 but with <i>NEUT5L::NAT1 TEF1p CaCRY2PHR-yemCherry-MSS4CAT TEF1t</i>
PY3169-71	Same as PY425 but with <i>NEUT5L::NAT1 TEF1p CaCRY2PHR-yemCherry-MSS4CAT TEF1t</i>
PY3172-73	Same as BWP17 but with <i>RP10::ARG4 ACT1p CRIB-yemiRFP670 ADH1t</i>
PY3182	Same as PY223 but with <i>NEUT5L::NAT1 TEF1p CaCIBN-yemCherry-CDC24 TEF1t</i>
PY3183-84	Same as BWP17 but with <i>NEUT5L::NAT1 TEF1p CaCIBN-yemCherry-CDC24 TEF1t</i>
PY3189-90	Same as PY3044 but with <i>NEUT5L::NAT1 TEF1p CaCIBN-yemCherry-CDC24CAT TEF1t</i>
PY3200-01	Same as BWP17 but with <i>RP10::ARG4 ACT1p CaCIBN-GFPγ ADH1t</i>
PY3252-53	Same as BWP17 but with <i>RP10::ARG4 ACT1p CaCRY2PHR-GFPγ-CaSSO2 ADH1t</i>
PY3254-55	Same as BWP17 but with <i>NEUT5L::NAT1 TEF1p CaCIBN-yemCherry-CDC24 TEF1t</i>
PY3256-58	Same as BWP17 but with <i>RP10::ARG4 ACT1p CRIB-yemCherry ADH1t</i>

PY3259-60	Same as PY223 but with <i>NEUT5L::NAT1 TEF1p CaCRY2PHR-yemCherry-CDC24 TEF1t</i>
PY3261-62	Same as PY223 but with <i>RP10::ARG4 ACT1p CaCRY2PHR-GFPγ-CaSSO2 ADH1t</i>
PY3263-65, 3276-78	Same as PY223 but with <i>NEUT5L::NAT1 TEF1p CaCIBN-yemCherry-CDC24 TEF1t</i>
PY3266-67	Same as PY3010 but with <i>RP10::ARG4 ACT1p CaCIBN-GFPγ-CaSSO2 ADH1t</i>
PY3268-69	Same as PY3055 but with <i>RP10::ARG4 ACT1p CaCIBN-GFPγ-CaSSO2 ADH1t</i>
PY3270	Same as PY3162 but with <i>RP10::ARG4 ACT1p CaCIBN-GFPγ-CaSSO2 ADH1t</i>
PY3271-73, 3322-23	Same as PY3165 but with <i>RP10::ARG4 ACT1p CaCRY2PHR-GFPγ-CaSSO2 ADH1t</i>
PY3324-26	Same as PY3165 but with <i>RP10::ARG4 ACT1p CaCRY2PHR-GFPγ-CtRAC1 ADH1t</i>
PY3327	Same as PY3259 but with <i>RP10::ARG4 ACT1p CaCIBN-GFPγ-CtRAC1 ADH1t</i>
PY3328	Same as PY3165 but with <i>RP10::ARG4 ACT1p CaCRY2PHR-GFPγ-CtRAC1 ADH1t</i>
PY3329-31, 3402	Same as BWP17 but with <i>RP10::ARG4 ACT1p CaCRY2PHR-linker-GFPγ-CtRAC1 ADH1t</i>
PY3333-36	Same as PY223 but with <i>NEUT5L::NAT1 TEF1p CaCRY2PHR-yemCherry-CDC24DHPH TEF1t</i>
PY3337-40	Same as PY223 but with <i>NEUT5L::NAT1 TEF1p CaCRY2PHR-yemCherry-CDC24DH TEF1t</i>
PY3332, 3341-42	Same as PY47 but with <i>NEUT5L::NAT1 TEF1p CaCRY2PHR-yemCherry-CDC42[C188S] TEF1t</i>
PY3352-54	Same as PY3333 but with <i>RP10::ARG4 ACT1p CaCIBN-GFPγ-CtRAC1 ADH1t</i>
PY3355-57, 3359	Same as PY47 but with <i>NEUT5L::NAT1 TEF1p CaCRY2PHR-yemCherry-CDC42[G12V,C188S] TEF1t</i>
PY3358	Same as PY47 but with <i>NEUT5L::NAT1 TEF1p CaCRY2PHR-yemCherry-CDC42[Q61L,C188S] TEF1t</i>
PY3383-86	Same as PY3341 but with <i>RP10::ARG4 ACT1p CaCIBN-GFPγ-CtRAC1 ADH1t</i>
PY3387-88	Same as PY3355 but with <i>RP10::ARG4 ACT1p CaCIBN-GFPγ-CtRAC1 ADH1t</i>
PY3389-91	Same as PY3358 but with <i>RP10::ARG4 ACT1p CaCIBN-GFPγ-CtRAC1 ADH1t</i>
PY3392-93	Same as BWP17 but with <i>NEUT5L::NAT1 TEF1p CaCIBN-yemCherry-CDC24DHPH TEF1t</i>
PY3394	Same as BWP17 but with <i>NEUT5L::NAT1 TEF1p CaCIBN-yemCherry-CDC24DH TEF1t</i>

PY3395-96	Same as BWP17 but with <i>NEUT5L::NAT1 TEF1p CaCIBN-yemCherry-CDC42[C188S] TEF1t</i>
PY3397	Same as PY223 but with <i>NEUT5L::NAT1 TEF1p CaCIBN-yemCherry-CDC24DHPH TEF1t</i>
PY3398-99	Same as PY47 but with <i>NEUT5L::NAT1 TEF1p CaCIBN-yemCherry-CDC42[C188S] TEF1t</i>
PY3400	Same as BWP17 but with <i>NEUT5L::NAT1 TEF1p CaCIBN-yemCherry-CDC42[Q61L,C188S] TEF1t</i>
PY3401	Same as PY47 but with <i>NEUT5L::NAT1 TEF1p CaCIBN-yemCherry-CDC42[Q61L,C188S] TEF1t</i>
PY3403	Same as PY223 but with <i>RP10::ARG4 ACT1p CaCRY2PHR-linker-GFPγ-CtRAC1 ADH1t</i>
PY3404	Same as PY47 but with <i>RP10::ARG4 ACT1p CaCRY2PHR-linker-GFPγ-CtRAC1 ADH1t</i>
PY3448-50	Same as PY2935 but with <i>NEUT5L::NAT1 TEF1p CaCRY2PHR-yemCherry-CDC42[C188S] TEF1t</i>
PY3458-59	Same as PY220 but with <i>NEUT5L::NAT1 TEF1p CaCRY2PHR-yemCherry-CDC42[C188S] TEF1t</i>
PY3460-61	Same as PY220 but with <i>NEUT5L::NAT1 TEF1p CaCRY2PHR-yemCherry-CDC42[G12V,C188S] TEF1t</i>
PY3462-63	Same as PY223 but with <i>NEUT5L::NAT1 TEF1p CaCRY2PHR-yemCherry-CDC42[C188S] TEF1t</i>
PY3464-65	Same as PY223 but with <i>NEUT5L::NAT1 TEF1p CaCRY2PHR-yemCherry-CDC42[G12V,C188S] TEF1t</i>
PY3521-22	Same as PY3355 but with <i>RP10::ARG4 ACT1p CaCIBN-GFPγ ADH1t</i>
PY3523	Same as PY3458 but with <i>RP10::ARG4 ACT1p CaCIBN-GFPγ ADH1t</i>
PY3524-26	Same as PY220 but with <i>RP10::ARG4 ACT1p CaCIBN-GFPγ ADH1t</i>
PY3527	Same as PY3458 but with <i>RP10::ARG4 ACT1p CaCIBN-GFPγ ADH1t</i>
PY3518-20	Same as BWP17 but with <i>NEUT5L::URA3</i>
PY3528-30	Same as BWP17 but with <i>RP10::ARG4 ACT1p CaCIBN-GFPγ-GRIP ADH1t</i>
PY3531-32	Same as PY3313 but with <i>RP10::ARG4 ACT1p CaCIBN-GFPγ-GRIP ADH1t</i>
PY3533-35	Same as PY2937 but with <i>NEUT5L::URA3</i>
PY3353-54, 3619	Same as BWP17 but with <i>NEUT5L::NAT1 TEF1p PHR2-yemCherry-PHR2GPI TEF1t</i>
PY3555-58	Same as PY3111 but with <i>NEUT5L::NAT1 TEF1p PHR2-yemCherry-PHR2GPI TEF1t</i>

PY3566-67	Same as BWP17 but with <i>NEUT5L::NAT1 TEF1p PHR2SS-yemCherry-PHR2 TEF1t</i>
PY3568-69	Same as BWP17 but with <i>NEUT5L::NAT1 TEF1p PHR2SS-yemCherry-yemCherry-PHR2 TEF1t</i>
PY3613-14	Same as BWP17 but with <i>RP10::ARG4 ACT1p DFI1-GFPγ-GFPγ ADH1t</i>
PY3646-48	Same as PY47 but with <i>NEUT5L::NAT1 TEF1p CaCRY2PHR-linker-GFPγ-CDC42[G12V,C188S] TEF1t</i>
PY3723-25	Same as BWP17 but with <i>NEUT5L::NAT1 TEF1p CaCRY2PHR-yemCherry-RHO1[C195S] TEF1t</i>
PY3726-29, 3848-49	Same as BWP17 but with <i>NEUT5L::NAT1 TEF1p CaCRY2PHR-yemCherry-RHO1[Q67H,C195S] TEF1t</i>
PY3730-31	Same as PY733 but with <i>NEUT5L::NAT1 TEF1p CaCRY2PHR-yemCherry-RHO1[C195S] TEF1t</i>
PY3732-34, 3850-51	Same as PY733 but with <i>NEUT5L::NAT1 TEF1p CaCRY2PHR-yemCherry-RHO1[Q67H,C195S] TEF1t</i>
PY3822-24	Same as PY47 but with <i>RP10::ARG4 ACT1p CRIB-yemCherry ADH1t</i>
PY3825-26	Same as PY3643 but with <i>RP10::ARG4 ACT1p CRIB-yemCherry ADH1t</i>
PY3827-29	Same as PY3566 but with <i>RP10::ARG4 ADH1p GFPγ-CtRAC1 ADH1t</i>
PY3830-31	Same as PY3568 but with <i>RP10::ARG4 ADH1p GFPγ-CtRAC1 ADH1t</i>
PY3832-34	Same as PY3724 but with <i>RP10::ARG4 ACT1p CaCIBN-GFPγ-CtRAC1 ADH1t</i>
PY3835-37	Same as PY3458 but with <i>RP10::ARG4 ACT1p CaCIBN-GFPγ-CtRAC1 ADH1t</i>
PY3838-40	Same as PY3462 but with <i>RP10::ARG4 ACT1p CaCIBN-GFPγ-CtRAC1 ADH1t</i>
PY3841	Same as PY3464 but with <i>RP10::ARG4 ACT1p CaCIBN-GFPγ-CtRAC1 ADH1t</i>
PY3861-64	Same as PY3848 but with <i>RP10::ARG4 ACT1p CaCIBN-GFPγ-CtRAC1 ADH1t</i>
PY3865-68	Same as PY3734 but with <i>RP10::ARG4 ACT1p CaCIBN-GFPγ-CtRAC1 ADH1t</i>
PY3961	Same as BWP17 but with <i>ABP1/ABP1::HIS1 ABP1-yemCherry</i>
PY3962	Same as BWP17 but with <i>CDC10/CDC10::HIS1 CDC10-yemCherry</i>
PY3963	Same as BWP17 but with <i>ABP1/ABP1::URA3 ABP1-yemCherry</i>
PY3964	Same as BWP17 but with <i>CDC10/CDC10::URA3 CDC10-yemCherry</i>

PY3965	Same as BWP17 but with <i>MLC1/MLC1::URA3 MLC1-yemCherry</i>
PY3966-67	Same as PY3451 but with <i>ABP1/ABP1::HIS1 ABP1-yemCherry</i>
PY3968-69	Same as PY3451 but with <i>CDC10/CDC10::HIS1 CDC10-yemCherry</i>
PY3970-71	Same as PY3451 but with <i>MLC1/MLC1::HIS1 MLC1-yemCherry</i>
PY3972	Same as PY3451 but with <i>CDC10/CDC10::URA3 CDC10-yemCherry</i>
PY3973	Same as PY3451 but with <i>MLC1/MLC1::URA3 MLC1-yemCherry</i>
PY4006-11, 4058	Same as PY3826 but with <i>NEUT5L::URA3 ADH1p CaCIBN-GFPγ-CtRAC1 ACT1t</i>
PY4012-15	Same as BWP17 but with <i>NEUT5L::URA3 ADH1p CaCIBN-GFPγ-CtRAC1 ACT1t</i>
PY4030-33	Same as PY3256 but with <i>NEUT5L::URA3 ADH1p CaCIBN-GFPγ-CtRAC1 ACT1t</i>
PY4060-62	Same as BWP17 but with <i>NEUT5L::NAT1 TEF1p CaCRY2PHR-yemCherry-CDC42[G12V,C188S] TEF1t</i>
PY4063-68	Same as PY2935 but with <i>NEUT5L::NAT1 TEF1p CaCRY2PHR-linker-GFPγ-CDC42[G12V,C188S] TEF1t</i>
PY4078-79	Same as PY3643 but with <i>NEUT5L::URA3 ADH1p CaCIBN-GFPγ-CtRAC1 ACT1t</i>
PY4080	Same as PY3826 but with <i>NEUT5L::URA3 ADH1p CaCIBN-GFPγ-CtRAC1 ACT1t</i>
PY4114-15	Same as PY2936 but with <i>NEUT5L::NAT1 TEF1p CaCRY2PHR-linker-CDC42[G12V,C188S] TEF1t</i>
PY4116-17	Same as PY4012 but with <i>NEUT5L::NAT1 TEF1p CaCRY2PHR-linker-CDC42[G12V,C188S] TEF1t</i>
PY4118-19	Same as PY4030 but with <i>NEUT5L::NAT1 TEF1p CaCRY2PHR-linker-CDC42[G12V,C188S] TEF1t</i>
PY4173-74	Same as PY3826 but with <i>NEUT5L::URA3 ADH1p CaCIBN-GFPγ-CtRAC1 ACT1t</i>
PY4177-78	Same as PY4059 but with <i>CDC10/CDC10::HIS1 CDC10-yemCherry</i>
PY4229-31	Same as PY2935 but with <i>NEUT5L::NAT1 TEF1p CaCRY2PHR-yemCherry-CDC42[G12V,C188S] TEF1t</i>
PY4360-63	Same as PY4059 but with <i>BEM1/BEM1::HIS1 BEM1-yemCherry</i>
PY4507-09	Same as BWP17 but with <i>NEUT5L::NAT1 TEF1p CaCRY2PHR-linker-CDC42[G12V,C188S] TEF1t</i>
PY4513-15	Same as PY4510 but with <i>MLC1/MLC1::HIS1 MLC1-yemCherry</i>

PY4516-17	Same as PY4510 but with <i>BNI1/BNI1::HIS1 BNI1-yemCherry</i>
PY4548-49	Same as PY4510 but with <i>MLC1/MLC1::HIS1 MLC1-mEOS2</i>
PY4559-61	Same as PY4510 but with <i>ADH1Δ yemRFP670 HIS1 ADH1Δ</i>
PY4562-64	Same as PY4510 but with <i>TEF1Δ LifeAct-yemScarlet HIS1 TEF1Δ</i>
PY4592-93	Same as PY4534 but with <i>ADH1Δ yemRFP670 HIS1 ADH1Δ</i>
PY4610	Same as PY4510 but with <i>SEC61/SEC61::HIS1 SEC61-yemCherry</i>
PY4621	Same as PY4510 but with <i>SEC3/SEC3::HIS1 SEC3-yemCherry</i>
PY4643	Same as PY4510 but with <i>SEC7/SEC7::HIS1 SEC7-yemScarlet</i>
PY4646	Same as PY4642 but with <i>SEC61/SEC61::HIS1 SEC61-yemScarlet</i>
PY4663	Same as PY4510 but with <i>SEC3/SEC3::HIS1 SEC3-yemScarlet</i>
PY4724	Same as PY4642 but with <i>NUP49/NUP49::HIS1 NUP49-yemScarlet</i>
PY4725-28	Same as PY4642 but with <i>RP10::ARG4 ACT1p CRIB-yemScarlet ADH1t</i>
PY4756, 4760-61	Same as PY4642 but with <i>RP10::ARG4 ACT1p ActinChromobody-yemScarlet-yemScarlet-yemScarlet ADH1t</i>
PY4762	Same as PY4642 but with <i>BNI1/BNI1::HIS1 BNI1-yemScarlet</i>
PY4763-64	Same as PY4642 but with <i>BEM1/BEM1::HIS1 BEM1-yemScarlet</i>
PY4772-75	Same as PY4548 but with <i>MLC1/MLC1::ARG4 MLC1-miRFP670</i>

References

- Abdul-Manan, N., Aghazadeh, B., Liu, G.A., Majumdar, A., Ouerfelli, O., Simlnovitch, K.A. and Rosen, M.K. (1999) 'Structure of Cdc42 in complex with the GTPase-binding domain of the "Wiskott-Aldrich syndrome" protein', *Nature*, 399(6734), pp. 379–383.
- Adams, A.E.M., Johnson, D.I., Longnecker, R.M., Sloat, B.F. and Pringle, J.R. (1990) 'CDC42 and CDC43, two additional genes involved in budding and the establishment of cell polarity in the yeast *Saccharomyces cerevisiae*', *Journal of Cell Biology*, 111(1), pp. 131–142.
- Adikes, R.C., Hallett, R.A., Saway, B.F., Kuhlman, B. and Slep, K.C. (2018) 'Control of microtubule dynamics using an optogenetic microtubule plus end-F-actin cross-linker', *Journal of Cell Biology*, 217(2), pp. 779–793.
- Adrian, M., Nijenhuis, W., Hoogstraaten, R.I., Willems, J. and Kapitein, L.C. (2017) 'A Phytochrome-Derived Photoswitch for Intracellular Transport', *ACS Synthetic Biology*, 6(7), pp. 1248–1256.
- Akashi, T., Kanbe, T. and Tanaka, K. (1994) 'The role of the cytoskeleton in the polarized growth of the germ tube in *Candida albicans*', *Microbiology*, 140(2), pp. 271–280.
- Alonso-Monge, R., Navarro-Garcia, F., Molero, G., Diez-Orejas, R., Gustin, M., Pla, J., Sanchez, M. and Nombela, C. (1999) 'Role of the Mitogen-Activated Protein Kinase Hog1p in Morphogenesis and Virulence of *Candida albicans* Role of the Mitogen-Activated Protein Kinase Hog1p in Morphogenesis and Virulence of *Candida albicans*', *Journal of Bacteriology*, 181(10), pp. 3058–3068.
- Ando, R., Mizuno, H. and Miyawaki, A. (2004) 'Regulated Fast Nucleocytoplasmic Shuttling Observed by Reversible Protein Highlighting', *Science*, 306(5700), pp. 1370–1373.
- Andresen, M., Stiel, A.C., Trowitzsch, S., Weber, G., Eggeling, C., Wahl, M.C., Hell, S.W. and Jakobs, S. (2007) 'Structural basis for reversible photoswitching in Dronpa', *Proceedings of the National Academy of Sciences*, 104(32), pp. 13005–13009.
- Araujo-Bazán, L., Peñalva, M.A. and Espeso, E.A. (2008) 'Preferential localization of the endocytic internalization machinery to hyphal tips underlies polarization of the actin cytoskeleton in *Aspergillus nidulans*', *Molecular Microbiology*, 67(4), pp. 891–905.
- Araujo-Palomares, C.L., Richthammer, C., Seiler, S. and Castro-Longoria, E. (2011) 'Functional characterization and cellular dynamics of the CDC-42 - RAC - CDC-24 module in *Neurospora crassa*', *PLoS ONE*. Edited by A. Herrera-Estrella, 6(11), p. e27148.
- Arkowitz, R.A. (2009) 'Chemical gradients and chemotropism in yeast', *Cold Spring Harbor Perspectives in Biology*, p. a001958.
- Arkowitz, R.A. (2013) 'Cell polarity: Wanderful exploration in yeast sex', *Current Biology*, 23(1).
- Arkowitz, R.A. and Bassilana, M. (2015) 'Regulation of hyphal morphogenesis by Ras and Rho small GTPases', *Fungal Biology Reviews*. Elsevier, pp. 7–19.
- Ayscough, K.R., Stryker, J., Pokala, N., Sanders, M., Crews, P. and Drubin, D.G. (1997) 'High rates of actin filament turnover in budding yeast and roles for actin in establishment and maintenance of cell polarity revealed using the actin inhibitor latrunculin-A', *Journal of Cell Biology*, 137(2), pp. 399–416.
- Bar-Yosef, H., Gildor, T., Ramírez-Zavala, B., Schmauch, C., Weissman, Z., Pinsky, M., Naddaf, R., Morschhäuser, J., Arkowitz, R.A. and Kornitzer, D. (2018) 'A Global Analysis of Kinase Function in *Candida albicans* Hyphal Morphogenesis Reveals a Role for the Endocytosis Regulator Akl1', *Frontiers in Cellular and Infection Microbiology*. Frontiers Media SA, 8, p. 17.
- Bar-Yosef, H., Vivanco Gonzalez, N., Ben-Aroya, S., Kron, S.J. and Kornitzer, D. (2017) 'Chemical inhibitors of *Candida albicans* hyphal morphogenesis target endocytosis', *Scientific Reports*. Nature Publishing Group, 7(1), p. 5692.
- El Barkani, A., Kurzai, O., Fonzi, W.A., Ramon, A., Porta, A., Frosch, M. and Mühlischlegel, F.A. (2000)

- 'Dominant active alleles of RIM101 (PRR2) bypass the pH restriction on filamentation of *Candida albicans*', *Molecular Microbiology*, 20(13), pp. 4635–47.
- Bartnicki-Garcia, S., Hergert, F. and Gierz, G. (1989) 'Computer simulation of fungal morphogenesis and the mathematical basis for hyphal (tip) growth', *Protoplasma*, 153, pp. 46–57.
- Bartnicki-Garcia, S. and Lippman, E. (1969) 'Fungal morphogenesis: cell wall construction in *Mucor rouxii*.', *Science*, 165(3890), pp. 302–304.
- Baschieri, F. and Farhan, H. (2015) 'Endomembrane control of cell polarity: Relevance to cancer', *Small GTPases*, 6(2), pp. 104–107.
- Basilana, M. and Arkowitz, R.A. (2006) 'Rac1 and Cdc42 have different roles in *Candida albicans* development', *Eukaryotic Cell*, 5(2), pp. 321–9.
- Basilana, M., Blyth, J. and Arkowitz, R.A. (2003) 'Cdc24, the GDP-GTP exchange factor for Cdc42, is required for invasive hyphal growth of *Candida albicans*', *Eukaryotic Cell*, 2(1), pp. 9–18.
- Basilana, M., Hopkins, J. and Arkowitz, R.A. (2005) 'Regulation of the Cdc42/Cdc24 GTPase Module during *Candida albicans* Hyphal Growth', *Eukaryotic Cell*, 4(3), pp. 588–603.
- Bender, A. and Pringle, J.R. (1989) 'Multicopy suppression of the *cdc24* budding defect in yeast by CDC42 and three newly identified genes including the ras-related gene RSR1', *Proceedings of the National Academy of Sciences USA*, 86(4), pp. 9976–80.
- Bendezú, F.O. and Martin, S.G. (2011) 'Actin cables and the exocyst form two independent morphogenesis pathways in the fission yeast', *Molecular Biology of the Cell*, 22(1), pp. 44–53.
- Bendezú, F.O., Vincenzetti, V., Vavylonis, D., Wyss, R., Vogel, H. and Martin, S.G. (2015) 'Spontaneous Cdc42 Polarization Independent of GDI-Mediated Extraction and Actin-Based Trafficking', *PLoS Biology*. Edited by D. Lew, 13(4), p. e1002097.
- Benedetti, L., Barentine, A.E.S., Messa, M., Wheeler, H., Bewersdorf, J. and De Camilli, P. (2018) 'Light-activated protein interaction with high spatial subcellular confinement', *Proceedings of the National Academy of Sciences USA*, p. 201713845.
- Bennett, R.J. (2015) 'The parasexual lifestyle of *Candida albicans*', *Current Opinion in Microbiology*, 28, pp. 10–17.
- Bennett, R.J. and Johnson, A.D. (2003) 'Completion of a parasexual cycle in *Candida albicans* by induced chromosome loss in tetraploid strains', *EMBO Journal*, 22(10), pp. 2505–15.
- Bensen, E.S., Clemente-Blanco, A., Finley, K.R., Correa-Bordes, J. and Berman, J. (2005) 'The mitotic cyclins Clb2p and Clb4p affect morphogenesis in *Candida albicans*', *Molecular Biology of the Cell*, 16(7), pp. 3387–400.
- Berepiki, A., Lichius, A., Shoji, J.Y., Tilsner, J. and Read, N.D. (2010) 'F-actin dynamics in *Neurospora crassa*', *Eukaryotic Cell*, 9, pp. 547–557.
- Van Bergeijk, P., Adrian, M., Hoogenraad, C.C. and Kapitein, L.C. (2015) 'Optogenetic control of organelle transport and positioning', *Nature*, 518(7537), pp. 111–114.
- Berman, J. and Hadany, L. (2012) 'Does stress induce (para)sex? Implications for *Candida albicans* evolution', *Trends in Genetics*, 28(5), pp. 197–203.
- Bernardo, S.M., Rane, H.S., Chavez-Dozal, A. and Lee, S.A. (2014) 'Secretion and filamentation are mediated by the *Candida albicans* t-SNAREs Sso2p and Sec9p', *FEMS Yeast Research*, 14(5), pp. 762–775.
- Bi, E. and Park, H.O. (2012) 'Cell polarization and cytokinesis in budding yeast', *Genetics*, 191(2), pp. 347–387.
- Bishop, A., Lane, R., Beniston, R., Chapa-Y-Lazo, B., Smythe, C. and Sudbery, P. (2010) 'Hyphal growth in *Candida albicans* requires the phosphorylation of Sec2 by the Cdc28-Ccn1/Hgc1 kinase', *EMBO Journal*, 29(17), pp. 2930–2942.

- Biswas, K. and Morschhäuser, J. (2005) 'The Mep2p ammonium permease controls nitrogen starvation-induced filamentous growth in *Candida albicans*', *Molecular Microbiology*, 56(3), pp. 649–69.
- Blankenship, J.R., Cheng, S., Woolford, C.A., Xu, W., Johnson, T.M., David Rogers, P., Fanning, S., Hong Nguyen, M., Clancy, C.J. and Mitchell, A.P. (2014) 'Mutational analysis of essential septins reveals a role for septin-mediated signaling in filamentation', *Eukaryotic Cell*, 13(11), pp. 1403–1410.
- Bonazzi, D., Haupt, A., Tanimoto, H., Delacour, D., Salort, D. and Minc, N. (2015) 'Actin-Based Transport Adapts Polarity Domain Size to Local Cellular Curvature', *Current Biology*, 25(20), pp. 2677–2683.
- Bos, J.L., Rehmann, H. and Wittinghofer, A. (2007) 'GEFs and GAPs: critical elements in the control of small G proteins', *Cell*, 129(5), pp. 865–77.
- Bose, I., Irazoqui, J.E., Moskow, J.J., Bardes, E.S.G., Zyla, T.R. and Lew, D.J. (2001) 'Assembly of Scaffold-mediated Complexes Containing Cdc42p, the Exchange Factor Cdc24p, and the Effector Cla4p Required for Cell Cycle-regulated Phosphorylation of Cdc24p', *Journal of Biological Chemistry*, 276(10), pp. 7176–7186.
- Böttcher, B., Pöllath, C., Staib, P., Hube, B. and Brunke, S. (2016) 'Candida species rewired hyphae developmental programs for chlamydospore formation', *Frontiers in Microbiology*, 7(OCT), pp. 1–17.
- Boulina, M., Samarajeewa, H., Baker, J.D., Kim, M.D. and Chiba, A. (2013) 'Live imaging of multicolor-labeled cells in *Drosophila*', *Development*, 140(7), pp. 1605–1613.
- Boyce, K.J., Hynes, M.J. and Adrianopoulos, A. (2003) 'Control of morphogenesis and actin localization by the *Penicillium marneffei* RAC homolog', *Journal of Cell Biology*, 116(Pt7), pp. 1249–60.
- Boyden, E.S., Zhang, F., Bamberg, E., Nagel, G. and Deisseroth, K. (2005) 'Millisecond-timescale, genetically targeted optical control of neural activity', *Nature Neuroscience*, 8(9), pp. 1263–1268.
- Brach, T., Godlee, C., Moeller-Hansen, I., Boeke, D. and Kaksonen, M. (2014) 'The initiation of clathrin-mediated endocytosis is mechanistically highly flexible', *Current Biology*, 24(5), pp. 548–554.
- Bramkamp, M. and van Baarle, S. (2009) 'Division site selection in rod-shaped bacteria', *Current Opinion in Microbiology*, 12, pp. 683–688.
- Brand, A., Vacharaksa, A., Bendel, C., Norton, J., Haynes, P., Henry-Stanley, M., Wells, C., Ross, K., Gow, N.A.R. and Gale, C.A. (2008) 'An internal polarity landmark is important for externally induced hyphal behaviors in *Candida albicans*', *Eukaryotic Cell*. American Society for Microbiology, 7(4), pp. 712–720.
- Brand, A.C., Morrison, E., Milne, S., Gonia, S., Gale, C.A. and Gow, N.A.R. (2014) 'Cdc42 GTPase dynamics control directional growth responses', *Proceedings of the National Academy of Sciences USA*, 111(2), pp. 811–816.
- Braun, B.R. and Johnson, A.D. (1997) 'Control of filament formation in *Candida albicans* by the transcriptional repressor TUP1', *Science*, 277(5322), pp. 105–9.
- Braun, B.R. and Johnson, A.D. (2000) 'TUP1, CPH1 and EFG1 make independent contributions to filamentation in *Candida albicans*', *Genetics*, 155(1), pp. 57–67.
- Braun, B.R., Kadosh, D. and Johnson, A.D. (2001) 'NRG1, a repressor of filamentous growth in *C. albicans*, is down-regulated during filament induction', *EMBO Journal*, 20(17), pp. 4753–61.
- Brown, A.J.P., Argimón, S. and Gow, N.A.R. (2007) 'Signal Transduction and Morphogenesis in *Candida albicans*', in Howard, R. J. and Gow, N. A. R. (eds) *Biology of the Fungal Cell*. 2nd edn. Berlin, Heidelberg: Springer (The Mycota (A Comprehensive Treatise on Fungi as Experimental Systems for Basic and Applied Research)), pp. 168–194.
- Brown, D.H., Giusani, A.D., Chen, X. and Kumamoto, C.A. (1999) 'Filamentous growth of *Candida albicans* in response to physical environmental cues and its regulation by the unique CZF1 gene', *Molecular Microbiology*, 34(4), pp. 651–62.
- Brunswick, H. (1924) 'Untersuchungen über geschlechts und kernverhältnisse bei der Hymenomyzete gattung *Coprinus*', *Botanische Abhandlungen*, 5.

- Buffo, J., Herman, N. and Soll, D.R. (1984) 'A characterization of pH regulated dimorphism in *Candida albicans*', *Mycopathologia*, 85(1–2), pp. 21–30.
- Bugaj, L.J., Choksi, A.T., Mesuda, C.K., Kane, R.S. and Schaffer, D. V (2013) 'Optogenetic protein clustering and signaling activation in mammalian cells', *Nature Methods*, 10(3), pp. 249–252.
- Burri, L. and Lithgow, T. (2004) 'A complete set of SNAREs in yeast', *Traffic*, pp. 45–52.
- Burridge, K. and Wennerberg, K. (2004) 'Rho and Rac take center stage', *Cell*, 116(2), pp. 167–79.
- Butty, A.C., Perrinjaquet, N., Petit, A., Jaquenoud, M., Segall, J.E., Hofmann, K., Zwahlen, C. and Peter, M. (2002) 'A positive feedback loop stabilizes the guanine-nucleotide exchange factor Cdc24 at sites of polarization', *EMBO Journal*, 21(7), pp. 1565–1576.
- Bykhovskaia, M. (2011) 'Synapsin regulation of vesicle organization and functional pools', *Seminars in Cell and Developmental Biology*. Academic Press, pp. 387–392.
- Caballero-Lima, D., Kaneva, I.N., Watton, S.P., Sudbery, P.E. and Craven, C.J. (2013) 'The spatial distribution of the exocyst and actin cortical patches is sufficient to organize hyphal tip growth', *Eukaryotic Cell*, 12(7), pp. 998–1008.
- Caballero-Lima, D. and Sudbery, P.E. (2014) 'In *Candida albicans*, phosphorylation of Exo84 by Cdk1-Hgc1 is necessary for efficient hyphal extension', *Molecular Biology of the Cell*, 25(7), pp. 1097–1110.
- Calderón-Noreña, D.M., González-Novo, A., Orellana-Muñoz, S., Gutiérrez-Escribano, P., Arnáiz-Pita, Y., Dueñas-Santero, E., Suárez, M.B., Bougnoux, M.E., del Rey, F., Sherlock, G., D'Enfert, C., Correa-Bordes, J. and de Aldana, C.R.V. (2015) 'A Single Nucleotide Polymorphism Uncovers a Novel Function for the Transcription Factor Ace2 during *Candida albicans* Hyphal Development', *PLoS Genetics*. Edited by G. Butler, 11(4), p. e1005152.
- Campanale, J.P., Sun, T.Y. and Montell, D.J. (2017) 'Development and dynamics of cell polarity at a glance', *Journal of Cell Science*, 130(7), pp. 1201–1207.
- Cao, F., Lane, S., Raniga, P.P., Lu, Y., Zhou, Z., Ramon, K., Chen, J. and Liu, H. (2006) 'The Flo8 transcription factor is essential for hyphal development and virulence in *Candida albicans*', *Molecular Biology of the Cell*, 17(1), pp. 295–307.
- Chaffin, W.L. (1984) 'Site selection for bud and germ tube emergence in *Candida albicans*', *Journal of General Microbiology*. Microbiology Society, 130(2), pp. 431–440.
- Chang, F. and Peter, M. (2003) 'Yeasts make their mark', *Nature Cell Biology*, pp. 294–299.
- Chant, J. and Herskowitz, I. (1991) 'Genetic control of bud site selection in yeast by a set of gene products that constitute a morphogenetic pathway', *Cell*, 65–7(1203–12).
- Chant, J. and Pringle, J.R. (1995) 'Patterns of Bud-Site Selection in the Yeast *Saccharomyces cerevisiae*', *Journal of Cell Biology*, 129(3), pp. 754–765.
- Chapa-y-Lazo, B., Lee, S., Regan, H. and Sudbery, P. (2011) 'The mating projections of *Saccharomyces cerevisiae* and *Candida albicans* show key characteristics of hyphal growth', *Fungal Biology*, 115(6), pp. 547–556.
- Che, D.L., Duan, L., Zhang, K. and Cui, B. (2015) 'The Dual Characteristics of Light-Induced Cryptochrome 2, Homo-oligomerization and Heterodimerization, for Optogenetic Manipulation in Mammalian Cells', *ACS Synthetic Biology*, 4(10), pp. 1124–1135.
- Chen, H., Fugita, M., Feng, Q.H., Clardy, J. and Fink, G.R. (2004) 'Tyrosol is a quorum-sensing molecule in *Candida albicans*', *Proceedings of the National Academy of Sciences USA*, 101(14), pp. 5048–52.
- Chen, T., Hiroko, T., Chaudhuri, A., Inose, F., Lord, M., Tanaka, S., Chant, J. and Fujita, A. (2000) 'Multigenerational cortical inheritance of the Rax2 protein in orienting polarity and division in yeast', *Science*, 290(5498), pp. 1975–1978.
- Chenevert, J., Corrado, K., Bender, A., Pringle, J. and Herskowitz, I. (1992) 'A yeast gene (BEM1) necessary for cell polarization whose product contains two SH3 domains', *Nature*, 356(6364), pp. 77–

79.

- Chesarone, M.A., DuPage, A.G. and Goode, B.L. (2010) 'Unleashing formins to remodel the actin and microtubule cytoskeletons', *Nature Reviews Molecular Cell Biology*, 11, pp. 62–74.
- Chibana, H., Beckerman, J.L. and Magee, P.T. (2000) 'Fine-resolution physical mapping of genomic diversity in *Candida albicans*', *Genome Research*, 10(12), pp. 1865–77.
- Clément, M., Fournier, H., De Repentigny, L. and Belhumeur, P. (1998) 'Isolation and characterization of the *Candida albicans* SEC4 gene', *Yeast*, 14(7), pp. 675–680.
- Coll, P.M., Trillo, Y., Ametzazurra, A. and Perez, P. (2003) 'Gef1p, a new guanine nucleotide exchange factor for Cdc42p, regulates polarity in *Schizosaccharomyces pombe*', *Molecular Biology of the Cell*, 14(1), pp. 313–23.
- Corvest, V., Bogliolo, S., Follette, P., Arkowitz, R.A. and Bassilana, M. (2013) 'Spatiotemporal regulation of Rho1 and Cdc42 activity during *Candida albicans* filamentous growth', *Molecular Microbiology*. Wiley-Blackwell, 89(4), pp. 626–648.
- Court, H. and Sudbery, P. (2007) 'Regulation of Cdc42 GTPase activity in the formation of hyphae in *Candida albicans*', *Molecular Biology of the Cell*, 18(1), pp. 265–81.
- Crampin, H., Finley, K., Gerami-Nejad, M., Court, H., Gale, C., Berman, J. and Sudbery, P. (2005) '*Candida albicans* hyphae have a Spitzenkörper that is distinct from the polarisome found in yeast and pseudohyphae', *Journal of Cell Science*, 118(13), pp. 2935–2947.
- Croft, C.A., Culibrk, L., Moore, M.M. and Tebbutt, S.J. (2016) 'Interactions of *Aspergillus fumigatus* conidia with airway epithelial cells: A critical review', *Frontiers in Microbiology*, 7, pp. 1–15.
- Csank, C., Schröppel, K., Leberer, E., Harcus, D., Mohamed, O., Meloche, S., Thomas, D.Y. and Whiteway, M. (1998) 'Roles of *Candida albicans* mitogen activated protein kinase homolog, Cek1p, in hyphal development and systemic candidiasis', *Infection and Immunity*, 66(6), pp. 2713–2721.
- Davis, D., Wilson, R.B. and Mitchell, A.P. (2000) 'RIM101 dependent and independent pathways govern pH responses in *Candida albicans*', *Molecular and Cellular Biology*, 20(3), pp. 971–8.
- DerMardirossian, C. and Bokoch, G.M. (2005) 'GDIs: central regulatory molecules in Rho GTPase activation', *Trends in Cell Biology*, 15(7), pp. 356–63.
- Derose, R., Miyamoto, T. and Inoue, T. (2013) 'Manipulating signaling at will: Chemically-inducible dimerization (CID) techniques resolve problems in cell biology', *Pflügers Archives European Journal of Physiology*. NIH Public Access, pp. 409–417.
- Diezmann, S., Cox, C.J., Schöniand, G., Vilgalys, R.J. and Mitchell, T.G. (2004) 'Phylogeny and evolution of medical species of *Candida* and related taxa: a multigenic analysis.', *Journal of Clinical Microbiology*. American Society for Microbiology, 42(12), pp. 5624–35.
- Dijksterhuis, J. and Molenaar, D. (2013) 'Vesicle trafficking via the Spitzenkörper during hyphal tip growth in *Rhizoctonia solani*', *Antonie van Leeuwenhoek, International Journal of General and Molecular Microbiology*, 103(4), pp. 921–931.
- Dominguez, R. and Holmes, K.C. (2011) 'Actin structure and function', *Annual Review of Biophysics*, 40, pp. 169–186.
- Donovan, K.W. and Bretscher, A. (2015) 'Tracking individual secretory vesicles during exocytosis reveals an ordered and regulated process', *Journal of Cell Biology*. Rockefeller University Press, 210(2), pp. 181–189.
- Du, L.L. and Novick, P. (2001) 'Yeast rab GTPase-activating protein Gyp1p localizes to the Golgi apparatus and is a negative regulator of Ypt1p.', *Molecular biology of the cell*, 12(5), pp. 1215–26.
- Eitzen, G., Thorngren, N. and Wickner, W. (2001) 'Rho1p and Cdc42p act after Ypt7p to regulate vacuole docking', *EMBO Journal*, 20(20), pp. 5650–6.
- Enserink, J.M. and Kolodner, R.D. (2010) 'An overview of Cdk1-controlled targets and processes.', *Cell*

Division, 5(1), p. 11.

- Epp, E., Nazarova, E., Regan, H., Douglas, L.M., Konopka, J.B., Vogel, J. and Whiteway, M. (2013) 'Clathrin- and arp2/3-independent endocytosis in the fungal pathogen *Candida albicans*', *mBio*. American Society for Microbiology (ASM), 4(5), pp. e00476-13.
- Epp, E., Walther, A., Lépine, G., Leon, Z., Mullick, A., Raymond, M., Wendland, J. and Whiteway, M. (2010) 'Forward genetics in *Candida albicans* that reveals the Arp2/3 complex is required for hyphal formation, but not endocytosis', *Molecular Microbiology*, 75(5), pp. 1182–1198.
- Erickson, J.W. and Cerione, R.A. (2004) 'Structural Elements, Mechanism, and Evolutionary Convergence of Rho Protein–Guanine Nucleotide Exchange Factor Complexes', *Biochemistry*, 43(4), pp. 837–842.
- Estravís, M., Rincón, S.A., Santos, B. and Pérez, P. (2011) 'Cdc42 Regulates Multiple Membrane Traffic Events in Fission Yeast', *Traffic*, 12(12), pp. 1744–1758.
- Etienne-Manneville, S. (2004) 'Cdc42 - the centre of polarity', *Journal of Cell Science*, 117(Pt 8), pp. 1291–1300.
- Etienne-Manneville, S. and Hall, A. (2002) 'Rho GTPases in cell biology', *Nature*, 420(6916), pp. 629–635.
- Ettema, T.J.G., Lindås, A.C. and Bernander, R. (2011) 'An actin-based cytoskeleton in archaea', *Molecular Microbiology*, 80(4), pp. 1052–1061.
- Evangelista, M., Blundell, K., Longtine, M.S., Chow, C.J., Adames, N., Pringle, J.R., Peter, M. and Boone, C. (1997) 'Bni1p, a yeast formin linking Cdc42p and the actin cytoskeleton during polarized morphogenesis', *Science*, 276(5309), pp. 118–122.
- Evangelista, M., Pruyne, D., Amberg, D.C., Boone, C. and Bretscher, A. (2002) 'Formins direct Arp2/3-independent actin filament assembly to polarize cell growth in yeast', *Nature Cell Biology*, 4, pp. 260–269.
- Fabry, Q., Schmid, E.N., Schrap, M. and Ansorg, R. (2003) 'Isolation and purification of chlamydospores of *Candida albicans*', *Medical Mycology*, 41(1), pp. 53–8.
- Fan, Y., He, H., Dong, Y. and Pan, H. (2013) 'Hyphae-Specific Genes HGC1, ALS3, HWP1, and ECE1 and Relevant Signaling Pathways in *Candida albicans*', *Mycopathologia*, pp. 329–335.
- Fang, H.M. and Wang, Y. (2006) 'RA domain-mediated interaction of Cdc35 with Ras1 is essential for increasing cellular cAMP level for *Candida albicans* hyphal development', *Molecular Microbiology*, 61(2), pp. 484–96.
- Fehrenbacher, K.L., Boldogh, I.R. and Pon, L.A. (2003) 'Taking the A-train: actin-based force generators and organelle targeting', *Trends in Cell Biology*, 13(9), pp. 472–477.
- Feijó, J.A. (2010) 'The mathematics of sexual attraction', *Journal of Biology*, 9(18), pp. 1–5.
- Feng, Q.H., Summers, E., Guo, B. and Fink, G. (1999) 'Ras signaling is required for serum-induced hyphal differentiation in *Candida albicans*', *Journal of Bacteriology*, 181(20), pp. 6339–46.
- Ferro-Novick, S. and Jahn, R. (1994) 'Vesicle fusion from yeast to man', *Nature*, 370(6486), pp. 191–193.
- Finger, F.P. and Novick, P. (1998) 'Spatial regulation of exocytosis: Lessons from yeast', *Journal of Cell Biology*, pp. 609–612.
- Finley, K.R. and Berman, J. (2005) 'Microtubules in *Candida albicans* hyphae drive nuclear dynamics and connect cell cycle progression to morphogenesis', *Eukaryotic Cell*. American Society for Microbiology (ASM), 4(10), pp. 1697–711.
- Fischer-Parton, S., Parton, R.M., Hickey, P.C., Dijksterhuis, J., Atkinson, H.A. and Read, N.D. (2000) 'Confocal microscopy of FM4-64 as a tool for analysing endocytosis and vesicle trafficking in living fungal hyphae', in *Journal of Microscopy*, pp. 246–259.
- Fitzpatrick, D.A., Logue, M.E., Stajich, J.E. and Butler, G. (2006) 'A fungal phylogeny based on 42 complete genomes derived from supertree and combined gene analysis', *BMC Evolutionary Biology*.

- BioMed Central, 6(1), p. 99.
- Freisinger, T., Klünder, B., Johnson, J., Müller, N., Pichler, G., Beck, G., Costanzo, M., Boone, C., Cerione, R.A., Frey, E. and Wedlich-Söldner, R. (2013) 'Establishment of a robust single axis of cell polarity by coupling multiple positive feedback loops', *Nature Communications*, 4, pp. 1–11.
- Furuya, A., Kawano, F., Nakajima, T., Ueda, Y. and Sato, M. (2017) 'Assembly Domain-Based Optogenetic System for the Efficient Control of Cellular Signaling', *ACS Synthetic Biology*, 6(6), pp. 1086–1095.
- Gambetta, G.A. and Lagarias, J.C. (2001) 'Genetic engineering of phytochrome biosynthesis in bacteria', *Proceedings of the National Academy of Sciences USA*, National Academy of Sciences, 98(19), pp. 10566–10571.
- Gao, X.D., Sperber, L.M., Kane, S.A., Tong, Z., Tong, A.H., Boone, C. and Bi, E. (2007) 'Sequential and distinct roles of the cadherin domain-containing protein Axl2p in cell polarization in yeast cell cycle', *Molecular Biology of the Cell*, 18(7), pp. 2542–2560.
- García, P., Tajadura, V., García, I. and Sánchez, Y. (2006) 'Role of Rho GTPases and Rho-GEFs in the regulation of cell shape and integrity in fission yeast', *Yeast*, 23(13), pp. 1031–1043.
- Gauthier, G.M. (2015) 'Dimorphism in Fungal Pathogens of Mammals, Plants, and Insects', *PLoS Pathogens*, 11(2), p. e1004608.
- Gauwerky, K., Borelli, C. and Korting, H.C. (2009) 'Targeting virulence: A new paradigm for antifungals', *Drug Discovery Today*, pp. 214–222.
- Gerami-Nejad, M., Zacchi, L.F., McClellan, M., Matter, K. and Berman, J. (2013) 'Shuttle vectors for facile gap repair cloning and integration into a neutral locus in *Candida albicans*', *Microbiology*, 159(Pt3), pp. 565–579.
- Ghugtyal, V., Garcia-Rodas, R., Seminara, A., Schaub, S., Bassilana, M. and Arkowitz, R.A. (2015) 'Phosphatidylinositol-4-phosphate-dependent membrane traffic is critical for fungal filamentous growth', *Proceedings of the National Academy of Sciences*, 112(28), pp. 8644–8649.
- Gierz, G. and Bartnicki-Garcia, S. (2001) 'A three-dimensional model of fungal morphogenesis based on the vesicle supply center concept', *Journal of Theoretical Biology*, 208(2), pp. 151–164.
- Gietz, R.D., Schiestl, R.H., Willems, A.R. and Woods, R.A. (1995) 'Studies on the transformation of intact yeast cells by the LiAc/SS-DNA/PEG procedure', *Yeast*, 11(4), pp. 355–360.
- Gimona, M., Djinovic-Carugo, K., Kranewitter, W.J. and Winder, S.J. (2002) 'Functional plasticity of CH domains', *FEBS Letters*, 513(1), pp. 98–106.
- Girbardt, M. (1969) 'Die Ultrastruktur der Apikalregion von Pilzhyphen', *Protoplasma*, 67(4), pp. 413–441.
- Gladfelter, A.S., Moskow, J.J., Zyla, T.R. and Lew, D.J. (2001) 'Isolation and characterization of effector-loop mutants of CDC42 in yeast', *Molecular Biology of the Cell*, 12(5), pp. 1239–1255.
- Gomes, A.C., Moura, G.R. and Santos, M.A.S. (2012) 'The Genetic Code of the *Candida* CTG Clade', in Calderone, A. and Clancy, C. (eds) *Candida and Candidiasis*. 2nd Ed. Washington DC: ASM Press, pp. 45–56.
- González-Novo, A., Labrador, L., Pablo-Hernando, M.E., Correa-Bordes, J., Sánchez, M., Jiménez, J. and De Aldana, C.R.V. (2009) 'Dbf2 is essential for cytokinesis and correct mitotic spindle formation in *Candida albicans*', *Molecular Microbiology*, 72(6), pp. 1364–1378.
- Goryachev, A.B. and Pokhilko, A. V (2006) 'Computational model explains high activity and rapid cycling of Rho GTPases within protein complexes', *PLoS Computational Biology*, 2(12), p. e172.
- Goryachev, A.B. and Pokhilko, A. V (2008) 'Dynamics of Cdc42 network embodies a Turing-type mechanism of yeast cell polarity', *FEBS Letters*, 582(10), pp. 1437–43.
- Grosshans, B.L., Ortiz, D. and Novick, P. (2006) 'Rabs and their effectors: achieving specificity in membrane traffic', *Proceedings of the National Academy of Sciences USA*, 103(32), pp. 11821–11827.

- Grove, S.N. and Bracker, C.E. (1970) 'Protoplasmic organization of hyphal tips among fungi: vesicles and Spitzenkörper', *Journal of Bacteriology*, 104(2), pp. 989–1009.
- Guglielmi, G., Barry, J.D., Huber, W. and De Renzis, S. (2015) 'An Optogenetic Method to Modulate Cell Contractility during Tissue Morphogenesis', *Developmental Cell*. Elsevier, 35(5), pp. 646–660.
- Guglielmi, G., Falk, H.J. and De Renzis, S. (2016) 'Optogenetic Control of Protein Function: From Intracellular Processes to Tissue Morphogenesis', *Trends in Cell Biology*, pp. 864–874.
- Gulli, M.P., Jaquenoud, M., Shimada, Y., Niederhäuser, G., Wiget, P. and Peter, M. (2000) 'Phosphorylation of the Cdc42 exchange factor Cdc24 by the PAK-like kinase Cla4 may regulate polarized growth in yeast', *Molecular Cell*, 6(5), pp. 1155–1167.
- Guntas, G., Hallett, R.A., Zimmerman, S.P., Williams, T., Yumerefendi, H., Bear, J.E. and Kuhlman, B. (2015) 'Engineering an improved light-induced dimer (iLID) for controlling the localization and activity of signaling proteins', *Proceedings of the National Academy of Sciences USA*. National Academy of Sciences, 112(1), pp. 112–117.
- Guo, M., Kilaru, S., Schuster, M., Latz, M. and Steinberg, G. (2015) 'Fluorescent markers for the Spitzenkörper and exocytosis in *Zygomycota tritici*', *Fungal Genetics and Biology*, 79, pp. 158–165.
- Guo, P.P., Yong, J.Y.A., Wang, Y.M. and Li, C.R. (2016) 'Sec15 links bud site selection to polarised cell growth and exocytosis in *Candida albicans*', *Scientific Reports*. Nature Publishing Group, 6(1), p. 26464.
- Guo, W., Roth, D., Walch-Solimena, C. and Novick, P. (1999) 'The exocyst is an effector for Sec4P, targeting secretory vesicles to sites of exocytosis', *EMBO Journal*, 18(4), pp. 1071–1080.
- Gupta, G.D. and Brent Heath, I. (2002) 'Predicting the distribution, conservation, and functions of SNAREs and related proteins in fungi', *Fungal Genetics and Biology*, pp. 1–21.
- Gurkan, C., Koulov, A. V and Balch, W.E. (2007) 'An Evolutionary Perspective on Eukaryotic Membrane Trafficking', in Jékely, G. (ed.) *Eukaryotic Membranes and Cytoskeleton*. Landes Bioscience and Springer Science+Business Media, LLC, pp. 73–83.
- Gurunathan, S., Chapman-Shimshoni, D., Trajkovic, S. and Gerst, J.E. (2000) 'Yeast exocytic v-SNAREs confer endocytosis.', *Molecular Biology of the Cell*, 11(10), pp. 3629–3643.
- Haarer, B.K., Corbett, A., Kweon, Y., Petzold, A.S., Silver, P. and Brown, S.S. (1996) 'SEC3 mutations are synthetically lethal with profilin mutations and cause defects in diploid-specific bud-site selection', *Genetics*, 144(2), pp. 495–510.
- Halaoui, R. and McCaffrey, L. (2015) 'Rewiring cell polarity signaling in cancer', *Oncogene*. Nature Publishing Group, 34(8), pp. 939–950.
- Hallett, R.A., Zimmerman, S.P., Yumerefendi, H., Bear, J.E. and Kuhlman, B. (2016) 'Correlating in Vitro and in Vivo Activities of Light-Inducible Dimers: A Cellular Optogenetics Guide', *ACS Synthetic Biology*, 5(1), pp. 53–64.
- Hammond, G.R. and Hong, Y. (2017) 'Phosphoinositides and Membrane Targeting in Cell Polarity', *Cold Spring Harbor Perspectives in Biology*, 10(a027938).
- Harkins, H.A., Pagé, N., Schenkman, L.R., De Virgilio, C., Shaw, S., Bussey, H. and Pringle, J.R. (2001) 'Bud8p and Bud9p, proteins that may mark the sites for bipolar budding in yeast', *Molecular Biology of the Cell*, 12(8), pp. 2497–2518.
- Harper, S.M., Neil, L.C. and Gardner, K.H. (2003) 'Structural basis of a phototropin light switch', *Science*, 301(5639), pp. 1541–1544.
- Harris, S.D., Read, N.D., Roberson, R.W., Shaw, B., Seiler, S., Plamann, M. and Momany, M. (2005) 'Polarisome meets Spitzenkörper: Microscopy, genetics, and genomics converge', *Eukaryotic Cell*, pp. 225–229.
- Harterink, M., Van Bergeijk, P., Allier, C., De Haan, B., Van Den Heuvel, S., Hoogenraad, C.C. and Kapitein, L.C. (2016) *Light-controlled intracellular transport in *Caenorhabditis elegans**, *Current Biology*. Elsevier.

- Hausauer, D.L., Gerami-Nejad, M., Kistler-Anderson, C. and Gale, C.A. (2005) 'Hyphal guidance and invasive growth in *Candida albicans* require the ras-like GTPase Rsr1p and its GTPase-activating protein Bud2p', *Eukaryotic Cell*, American Society for Microbiology, 4(7), pp. 1273–1286.
- Hazan, I. and Liu, H. (2002) 'Hyphal tip-associated localization of Cdc42 is F-actin dependent in *Candida albicans*', *Eukaryotic Cell*, 11(6), pp. 856–864.
- He, B. and Guo, W. (2009) 'The exocyst complex in polarized exocytosis', *Current Opinion in Cell Biology*, pp. 537–542.
- Herskowitz, I. (1988) 'Life cycle of the budding yeast *Saccharomyces cerevisiae*', *Microbiological Reviews*, 52(4), pp. 536–53.
- Hervás-Aguilar, A. and Peñalva, M.A. (2010) 'Endocytic machinery protein SlaB is dispensable for polarity establishment but necessary for polarity maintenance in hyphal tip cells of *Aspergillus nidulans*', *Eukaryotic Cell*, 9(10), pp. 1504–1518.
- Hervé, J.C. and Bourmeyster, N. (2015) 'Rho GTPases at the crossroad of signaling networks in mammals', *Small GTPases*. Taylor & Francis, 6(2), pp. 43–48.
- Hickman, M.A., Paulson, C., Dudley, A. and Berman, J. (2015) 'Parasexual ploidy reduction drives population heterogeneity through random and transient aneuploidy in *Candida albicans*', *Genetics*, 200(3), pp. 781–794.
- Hirota, K., Tanaka, K., Ohta, K. and Yamamoto, M. (2003) 'Gef1p and Scd1p, the Two GDP-GTP exchange factors for Cdc42p, form a ring structure that shrinks during cytokinesis in *Schizosaccharomyces pombe*', *Molecular Biology of the Cell*, 14(9), pp. 3617–27.
- Hogan, D.A. (2006) 'Talking to themselves: autoregulation and quorum sensing in fungi', *Eukaryotic Cell*, 5(4), pp. 613–9.
- Hogan, D.A. and Kolter, R. (2002) 'Pseudomonas-Candida interactions: an ecological role for virulence factors', *Science*, 296(5576), pp. 2229–32.
- Hogan, D.A., Vik, Å. and Kolter, R. (2004) 'A *Pseudomonas aeruginosa* quorum-sensing molecule influences *Candida albicans* morphology', *Molecular Microbiology*, 54(4), pp. 1212–23.
- Holly, S.P. and Blumer, K.J. (1999) 'PAK-family kinases regulate cell and actin polarization throughout the cell cycle of *Saccharomyces cerevisiae*', *Journal of Cell Biology*, 147(4), pp. 845–856.
- Hope, H., Bogliolo, S., Arkowitz, R.A. and Bassilana, M. (2008) 'Activation of Rac1 by the guanine nucleotide exchange factor Dck1 is required for invasive filamentous growth in the pathogen *Candida albicans*', *Molecular Biology of the Cell*, 19(9), pp. 3638–51.
- Hornby, J.M., Dumitru, R. and Nickerson, K.W. (2004) 'High phosphate (up to 600 mM) induces pseudohyphal development in five wild type *Candida albicans*', *Journal of Microbiological Methods*, 56(1), pp. 119–24.
- Hornby, J.M., Jensen, E.C., Lisec, A.D., Tasto, J.J., Jahnke, B., Shoemaker, R., Dussault, P. and Nickerson, K.W. (2001) 'Quorum sensing in the dimorphic fungus *Candida albicans* is mediated by farnesol', *Applied and Environmental Microbiology*, 67(7), pp. 2982–92.
- Howard, R.J. (1981) 'Ultrastructural analysis of hyphal tip cell growth in fungi: Spitzenkörper, cytoskeleton and endomembranes after freeze-substitution', *Journal of Cell Science*, 48, pp. 89–103.
- Howell, A.S., Jin, M., Wu, C.F., Zyla, T.R., Elston, T.C. and Lew, D.J. (2012) 'Negative feedback enhances robustness in the yeast polarity establishment circuit', *Cell*, 149(2), pp. 322–333.
- Howell, A.S., Savage, N.S., Johnson, S.A., Bose, I., Wagner, A.W., Zyla, T.R., Nijhout, H.F., Reed, M.C., Goryachev, A.B. and Lew, D.J. (2009) 'Singularity in Polarization: Rewiring Yeast Cells to Make Two Buds', *Cell*, 139(4), pp. 731–43.
- Hoyer, L.L., Oh, S.H., Jones, R. and Cota, E. (2014) 'A proposed mechanism for the interaction between the *Candida albicans* Als3 adhesin and streptococcal cell wall proteins', *Frontiers in Microbiology*, 5(OCT).

- Huang, Z.X., Wang, H., Wang, Y.M. and Wang, Y. (2014) 'Novel mechanism coupling cyclic amp-protein kinase a signaling and golgi trafficking via Gyp1 phosphorylation in polarized growth', *Eukaryotic Cell*. American Society for Microbiology, 13(12), pp. 1548–1556.
- Huckaba, T.M., Gay, A.C., Pantalena, L.F., Yang, H.C. and Pon, L.A. (2004) 'Live cell imaging of the assembly, disassembly, and actin cable-dependent movement of endosomes and actin patches in the budding yeast, *Saccharomyces cerevisiae*', *Journal of Cell Biology*, 167(3), pp. 519–530.
- Hughes, R.M., Bolger, S., Tapadia, H. and Tucker, C.L. (2012) 'Light-mediated control of DNA transcription in yeast', *Methods*, 58(4), pp. 385–391.
- Idevall-Hagren, O., Dickson, E.J., Hille, B., Toomre, D.K. and De Camilli, P. (2012) 'Optogenetic control of phosphoinositide metabolism', *Proceedings of the National Academy of Sciences USA*, 109(35), pp. E2316–E2323.
- Ihara, K., Muraguchi, S., Kato, M., Shimizu, T., Shirakawa, M., Kuroda, S., Kaibuchi, K. and Hakoshima, T. (1998) 'Crystal structure of human RhoA in a dominantly active form complexed with a GTP analogue', *Journal of Biological Chemistry*, 273(16), pp. 9656–9666.
- Inoue, H., H, N. and Okayama, H. (1990) 'High efficiency transformation of *Escherichia coli* with plasmids', *Gene*, 96(1), pp. 23–28.
- Iranzo, M., Canizares, J. V, Sainz-Pardo, I., Aguado, C., Ponton, J. and Mormeneo, S. (2003) 'Isolation and characterization of an avirulent *Candida albicans* yeast monomorphic mutant', *Medical Mycology*, 41(1), pp. 43–52.
- Irazoqui, J.E., Gladfelter, A.S. and Lew, D.J. (2003) 'Scaffold-mediated symmetry breaking by Cdc42p', *Nature Cell Biology*, 5(12), pp. 1062–1070.
- Ito, T., Matsui, Y., Ago, T., Ota, K. and Sumimoto, H. (2001) 'Novel modular domain PB1 recognizes pc motif to mediate functional protein-protein interactions', *EMBO Journal*, 20(15), pp. 3938–3946.
- Jacobsen, I.D., Wilson, D., Wächtler, B., Brunke, S., Naglik, J.R. and Hube, B. (2012) 'Candida albicans dimorphism as a therapeutic target', *Expert Review of Anti-Infective Therapy*, 10(1), pp. 85–93.
- Jahn, R. and Südhof, T.C. (1999) 'Membrane Fusion and Exocytosis', *Annual Review of Biochemistry*, 68(1), pp. 863–911.
- Jakubovics, N.S. (2017) 'The sixth sensor: A *Candida albicans* biofilm master regulator that responds to inter-kingdom interactions', *Virulence*, pp. 1465–1467.
- Ji, C., Fan, F. and Lou, X. (2017) 'Vesicle Docking Is a Key Target of Local PI(4,5)P2 Metabolism in the Secretory Pathway of INS-1 Cells', *Cell Reports*, 20(6), pp. 1409–1421.
- Johnson, D.I. and Pringle, J.R. (1990) 'Molecular characterization of Cdc42, a *Saccharomyces cerevisiae* gene involved in the development of cell polarity', *Journal of Cell Biology*, 111(1), pp. 143–52.
- Johnson, J.M., Jin, M. and Lew, D.J. (2011) 'Symmetry breaking and the establishment of cell polarity in budding yeast', *Current Opinion in Genetics & Development*, 21(6), pp. 740–6.
- Johnston, G.C., Prendergast, J.A. and Singer, R.A. (1991) 'The *Saccharomyces cerevisiae* MYO2 gene encodes an essential myosin for vectorial transport of vesicles', *Journal of Cell Biology*, 113(3), pp. 539–551.
- Jones, L.A. and Sudbery, P.E. (2010) 'Spitzenkörper, Exocyst, and Polarisome Components in *Candida albicans* Hyphae Show Different Patterns of Localization and Have Distinct Dynamic Properties', *Eukaryotic Cell*, 9(10), pp. 1455–1465.
- Jose, M., Tollis, S., Nair, D., Sibarita, J.B. and McCusker, D. (2013) 'Robust polarity establishment occurs via an endocytosis-based cortical corralling mechanism', *Journal of Cell Biology*. Rockefeller University Press, 200(4), pp. 407–418.
- Kadosh, D. and Johnson, A.D. (2005) 'Induction of the *Candida albicans* filamentous growth program by relief of transcriptional repression: a genome-wide analysis', *Molecular Biology of the Cell*, 16(6), pp. 2903–12.

- Kaksonen, M. and Roux, A. (2018) 'Mechanisms of clathrin-mediated endocytosis', *Nature Reviews Molecular Cell Biology*. Nature Publishing Group.
- Kang, P.J., Angerman, E., Nakashima, K., Pringle, J.R. and Park, H.O. (2004) 'Interactions among Rax1p, Rax2p, Bud8p, and Bud9p in marking cortical sites for bipolar bud-site selection in yeast', *Molecular Biology of the Cell*, 15(11), pp. 5145–5157.
- Kang, P.J., Béven, L., Hariharan, S. and Park, H.-O. (2010) 'The Rsr1/Bud1 GTPase Interacts with Itself and the Cdc42 GTPase during Bud-Site Selection and Polarity Establishment', *Molecular Biology of the Cell*, 21, pp. 3007–3016.
- Kang, P.J., Sanson, A., Lee, B. and Park, H.O. (2001) 'A GDP/GTP exchange factor involved in linking a spatial landmark to cell polarity', *Science*, 292(5520), pp. 1376–1378.
- Karpova, T.S., Reck-Peterson, S.L., Elkind, N.B., Mooseker, M.S., Novick, P.J. and Cooper, J.A. (2000) 'Role of actin and Myo2p in polarized secretion and growth of *Saccharomyces cerevisiae*.' *Molecular Biology of the Cell*, 11(5), pp. 1727–37.
- Kavanaugh, N.L., Zhang, A.Q., Nobile, C.J., Johnson, A.D. and Ribbeck, K. (2014) 'Mucins suppress virulence traits of *Candida albicans*', *mBio*. American Society for Microbiology (ASM), 5(6), p. e01911.
- Kawano, F., Suzuki, H., Furuya, A. and Sato, M. (2015) 'Engineered pairs of distinct photoswitches for optogenetic control of cellular proteins', *Nature Communications*, 6.
- Kelly, F.D. and Nurse, P. (2011) 'Spatial control of Cdc42 activation determines cell width in fission yeast', *Molecular Biology of the Cell*. American Society for Cell Biology, 22(20), pp. 3801–3811.
- Kelly, M.T., MacCallum, D.M., Clancy, S.D., Odds, F.C., Brown, A.J. and Butler, G. (2004) 'The *Candida albicans* CaACE2 gene affects morphogenesis, adherence and virulence', *Molecular Microbiology*, 53(3), pp. 969–83.
- Kennedy, M.J., Hughes, R.M., Peteya, L.A., Schwartz, J.W., Ehlers, M.D. and Tucker, C.L. (2010) 'Rapid blue-light-mediated induction of protein interactions in living cells', *Nature Methods*, 7(12), pp. 973–975.
- Kim, J. and Rose, M.D. (2015) 'Stable Pseudohyphal Growth in Budding Yeast Induced by Synergism between Septin Defects and Altered MAP-kinase Signaling', *PLoS Genetics*, 11(12).
- Kim, J.Y. (2016) 'Human fungal pathogens: Why should we learn?', *Journal of Microbiology*, 54(3), pp. 145–148.
- Klumperman, J. (2011) 'Architecture of the mammalian Golgi', *Cold Spring Harbor Perspectives in Biology*, 3(7), pp. 1–19.
- Knechtle, P., Wendland, J. and Philippsen, P. (2006) 'The SH3/PH domain protein AgBoi1/2 collaborates with the Rho-type GTPase AgRho3 to prevent nonpolar growth at hyphal tips of *Ashbya gossypii*', *Eukaryotic Cell*, 5(10), pp. 1635–1647.
- Kohler, J.R. and Fink, G.R. (1996) 'Candida albicans strains heterozygous and homozygous for mutations in mitogen-activated protein kinase signaling components have defects in hyphal development', *Proceedings of the National Academy of Sciences USA*, 93(23), pp. 13223–13228.
- Köhli, M., Galati, V., Boudier, K., Robertson, R.W. and Philippsen, P. (2008) 'Growth-speed-correlated localization of exocyst and polarisome components in growth zones of *Ashbya gossypii* hyphal tips', *Journal of Cell Science*, 121(Pt23), pp. 3878–3889.
- Komatsu, T., Kukelyansky, I., McCaffery, J.M., Ueno, T., Varela, L.C. and Inoue, T. (2010) 'Organelle-specific, rapid induction of molecular activities and membrane tethering', *Nature Methods*, 7(3), pp. 206–208.
- Konermann, S., Brigham, M.D., Trevino, A.E., Hsu, P.D., Heidenreich, M., Cong, L., Platt, R.J., Scott, D.A., Church, G.M. and Zhang, F. (2013) 'Optical control of mammalian endogenous transcription and epigenetic states', *Nature*, 500(7463), pp. 472–476.

- Kotýnková, K., Su, K.C., West, S.C. and Petronczki, M. (2016) 'Plasma Membrane Association but Not Midzone Recruitment of RhoGEF ECT2 Is Essential for Cytokinesis', *Cell Reports*, 17(10), pp. 2672–2686.
- Kovar, D.R., Kuhn, J.R., Tichy, A.L. and Pollard, T.D. (2003) 'The fission yeast cytokinesis formin Cdc12p is a barbed end actin filament capping protein gated by profilin', *Journal of Cell Biology*, 161(5), pp. 875–887.
- Kozubowski, L., Saito, K., Johnson, J.M., Howell, A.S., Zyla, T.R. and Lew, D.J. (2008) 'Symmetry-breaking polarization driven by a Cdc42p GEF–PAK complex', *Current Biology*, 18(22), pp. 1719–26.
- Kullas, A.L., Li, M. and Davis, D.A. (2004) 'Snf7p, a component of the ESCRT-III protein complex, is an upstream member of the RIM101 pathway in *Candida albicans*', *Eukaryotic Cell*, 3(6), pp. 1609–18.
- Kumamoto, C.A. (2005) 'A contact-activated kinase signals *Candida albicans* invasive growth and biofilm development', *Proceedings of the National Academy of Sciences USA*, 102(15), pp. 5576–81.
- Kumamoto, C.A. (2011) 'Inflammation and gastrointestinal *Candida* colonization', *Current Opinion in Microbiology*, 14(4), pp. 386–91.
- Kuo, C.C., Savage, N.S., Chen, H., Wu, C.F., Zyla, T.R. and Lew, D.J. (2014) 'Inhibitory GEF phosphorylation provides negative feedback in the yeast polarity circuit', *Current Biology*. NIH Public Access, 24(7), pp. 753–759.
- Kwon, M.J., Arentshorst, M., Fiedler, M., de Groen, F.L.M., Punt, P.J., Meyer, V. and Ram, A.F.J. (2014) 'Molecular genetic analysis of vesicular transport in *Aspergillus niger* reveals partial conservation of the molecular mechanism of exocytosis in fungi', *Microbiology*, 160(PART 2), pp. 316–329.
- Köhler, J.R., Casadevall, A. and Perfect, J. (2015) 'The Spectrum of Fungi That Infects Humans', *Cold Spring Harbor Perspectives in Medicine*, 5(a019273), pp. 1–22.
- Labbaoui, H., Bogliolo, S., Ghugtyal, V., Solis, N. V., Filler, S.G., Arkowitz, R.A. and Bassilana, M. (2017) 'Role of Arf GTPases in fungal morphogenesis and virulence', *PLoS Pathogens*, 13(2), p. e1006205.
- Lane, S., Birse, C., Zhou, S., Matson, R. and Liu, H.P. (2001) 'DNA array studies demonstrate convergent regulation of virulence factors by Cph1, Cph2, and Efg1 in *Candida albicans*', *Journal of Biological Chemistry*, 276(52), pp. 48988–96.
- Lane, S., Zhou, S., Pan, T., Dai, Q. and Liu, H. (2001) 'The basic helix–loop–helix transcription factor Cph2 regulates hyphal development in *Candida albicans* partly via Tec1', *Molecular and Cellular Biology*, 21(19), pp. 6418–28.
- Leberer, E., Hargus, D., Broadbent, I.D., Clark, K.L., Dignard, D., Ziegelbauer, K., Schmidt, A., Gow, N.A., Brown, A.J. and Thomas, D.Y. (1996) 'Signal transduction through homologs of the Ste20p and Ste7p protein kinases can trigger hyphal formation in the pathogenic fungus *Candida albicans*', *Proceedings of the National Academy of Sciences USA*, 93(23), pp. 13217–22.
- Leberer, E., Hargus, D., Dignard, D., Johnson, L., Ushinsky, S., Thomas, D.Y. and Schröppel, K. (2001) 'Ras links cellular morphogenesis to virulence by regulation of the MAP kinase and cAMP signalling pathways in the pathogenic fungus *Candida albicans*', *Molecular Microbiology*, 42(3), pp. 673–87.
- Leberer, E., Ziegelbauer, K., Schmidt, A., Hargus, D., Dignard, D., Ash, J., Johnson, L. and Thomas, D.Y. (1997) 'Virulence and hyphal formation of *Candida albicans* require the Ste20p-like protein kinase CaCla4p.', *Current Biology*, 7(8), pp. 539–46.
- Lee, M. and Vasioukhin, V. (2008) 'Cell polarity and cancer - cell and tissue polarity as a non-canonical tumor suppressor', *Journal of Cell Science*, 121(Pt8), pp. 1141–1150.
- Lemmon, M.A. (2008) 'Membrane recognition by phospholipid-binding domains', *Nature Reviews Molecular Cell Biology*, 9(2), pp. 99–111.
- Lenardon, M.D., Milne, S.A., Mora-Montes, H.M., Kaffarnik, F.A., Peck, S.C., Brown, A.J., Munro, C.A. and Gow, N.A. (2010) 'Phosphorylation regulates polarisation of chitin synthesis in *Candida albicans*', *Journal of Cell Science*, 123(Pt 13), pp. 2199–206.

- Leng, P., Lee, P.R., Wu, H. and Brown, A.J. (2001) 'Efg1, a morphogenetic regulator in *Candida albicans*, is a sequence-specific DNA binding protein', *Journal of Bacteriology*, 183(13), pp. 4090–3.
- Levsikaya, A., Weiner, O.D., Lim, W.A. and Voigt, C.A. (2009) 'Spatiotemporal control of cell signalling using a light-switchable protein interaction', *Nature*. NIH Public Access, 461(7266), pp. 997–1001.
- Lew, D.J. and Reed, S.I. (1993) 'Morphogenesis in the yeast cell cycle: Regulation by Cdc28 and cyclins', *Journal of Cell Biology*. The Rockefeller University Press, 120(6), pp. 1305–1320.
- Li, C.-R., Lee, R.T.-H., Wang, Y.-M., Zheng, X.-D. and Wang, Y. (2007) 'Candida albicans hyphal morphogenesis occurs in Sec3p-independent and Sec3p-dependent phases separated by septin ring formation', *Journal of Cell Science*, 120(11), pp. 1898–1907.
- Li, H.M., Shimizu-Imanishi, Y., Tanaka, R., Li, R.Y. and Yaguchi, T. (2016) 'White-opaque switching in different mating type-like locus gene types of clinical *Candida albicans* isolates', *Chinese Medical Journal*, 129(22), pp. 2725–2732.
- Li, M., Martin, S.J., Bruno, V.M., Mitchell, A.P. and Davis, D.A. (2004) 'Candida albicans Rim13p, a protease required for Rim101p processing at acidic and alkaline pHs', *Eukaryotic Cell*, 3(3), pp. 741–51.
- Li, W.J., Wang, Y.M., Zheng, X.D., Shi, W.M., Zhang, T.T., Bai, C., Li, D., Sang, J.L. and Wang, Y. (2006) 'The F-box protein Grr1 regulates the stability of Ccn1, Cln3 and Hof1 and cell morphogenesis in *Candida albicans*', *Molecular Microbiology*, 62(1), pp. 212–26.
- Lichius, A., Berepiki, A. and Read, N.D. (2011) 'Form follows function - The versatile fungal cytoskeleton', *Fungal Biology*, 115(6), pp. 518–540.
- Lichius, A., Yáñez-Gutiérrez, M.E., Read, N.D. and Castro-Longoria, E. (2012) 'Comparative live-cell imaging analyses of SPA-2, BUD-6 and BNI-1 in *Neurospora crassa* reveal novel features of the filamentous fungal polarisome', *PLoS ONE*, 7(1), p. e30372.
- Lin, C., Schuster, M., Guimaraes, S.C., Ashwin, P., Schrader, M., Metz, J., Hacker, C., Gurr, S.J. and Steinberg, G. (2016) 'Active diffusion and microtubule-based transport oppose myosin forces to position organelles in cells', *Nature Communications*. Nature Publishing Group, 7, p. 11814.
- Lindsay, A.K., Deveau, A., Piispanen, A.E. and Hogan, D.A. (2012) 'Farnesol and cyclic AMP signaling effects on the hypha-to-yeast transition in *Candida albicans*', *Eukaryotic Cell*. American Society for Microbiology (ASM), 11(10), pp. 1219–1225.
- Liu, H., Yu, X., Li, K., Klejnot, J., Yang, H., Lisiero, D. and Lin, C. (2008) 'Photoexcited CRY2 interacts with CIB1 to regulate transcription and floral initiation in *Arabidopsis*', *Science*, 322(5907), pp. 1535–1539.
- Liu, H.P., Kohler, J., Fink, G.R., Köhler, J.R. and Fink, G.R. (1994) 'Suppression of hyphal formation in *Candida albicans* by mutation of a STE12 homolog', *Science*. American Association for the Advancement of Science, 266(5191), pp. 1723–6.
- Liu, Q. and Tucker, C.L. (2017) 'Engineering genetically-encoded tools for optogenetic control of protein activity', *Current Opinion in Chemical Biology*, pp. 17–23.
- Lo, H.J., Köhler, J.R., DiDomenico, B., Loebenberg, D., Cacciapuoti, A. and Fink, G.R. (1997) 'Nonfilamentous *C. albicans* mutants are avirulent', *Cell*, 90(5).
- Lorenz, M.C., Bender, J.A. and Fink, G.R. (2004) 'Transcriptional response of *Candida albicans* upon internalization by macrophages', *Eukaryotic Cell*, 3(5), pp. 1076–87.
- Lu, R., Drubin, D.G. and Sun, Y. (2016) 'Clathrin-mediated endocytosis in budding yeast at a glance', *Journal of Cell Science*, 129(8), pp. 1531–1536.
- Lu, Y., Su, C., Unoje, O. and Liu, H. (2014) 'Quorum sensing controls hyphal initiation in *Candida albicans* through Ubr1-mediated protein degradation.', *Proceedings of the National Academy of Sciences USA*, 111(5), pp. 1975–80.
- Maiuri, P., Rupprecht, J.F., Wieser, S., Rupprecht, V., Bénichou, O., Carpi, N., Coppey, M., De Beco, S.,

- Gov, N., Heisenberg, C.P., Lage Crespo, C., Lautenschlaeger, F., Le Berre, M., Lennon-Dumenil, A.M., Raab, M., Thiam, H.R., Piel, M., Sixt, M. and Voituriez, R. (2015) 'Actin flows mediate a universal coupling between cell speed and cell persistence', *Cell*, 161(2), pp. 374–386.
- Malathi, K., Ganesan, K. and Dattas, A. (1994) 'Identification of a Putative Transcription Factor in *Candida albicans* That Can Complement the Mating Defect *stel2* Mutants', *Biochemistry*. American Society for Biochemistry and Molecular Biology, 269(37), pp. 22945–51.
- Marco, E., Wedlich-Söldner, R., Li, R., Altschuler, S.J. and Wu, L.F. (2007) 'Endocytosis Optimizes the Dynamic Localization of Membrane Proteins that Regulate Cortical Polarity', *Cell*, 129(2), pp. 411–422.
- Mardon, D., Balish, E. and Phillips, A.W. (1969) 'Control of dimorphism in a biochemical variant of *Candida albicans*', *Journal of Bacteriology*, 100(2), pp. 701–7.
- Marston, A.L., Chen, T., Yang, M.C., Belhumeur, P. and Chant, J. (2001) 'A localized GTPase exchange factor, Bud5, determines the orientation of division axes in yeast', *Current Biology*, 11(10), pp. 803–807.
- Martin, R., Hellwig, D., Schaub, Y., Bauer, J., Walther, A. and Wendland, J. (2007) 'Functional analysis of *Candida albicans* genes whose *Saccharomyces cerevisiae* homologues are involved in endocytosis', *Yeast*, 24(6), pp. 511–522.
- Martin, S.G. and Arkowitz, R.A. (2014) 'Cell polarization in budding and fission yeasts', *FEMS Microbiology Reviews*, 38(2), pp. 228–253.
- Más, P., Devlin, P.F., Panda, S. and Kay, S.A. (2000) 'Functional interaction of phytochrome B and cryptochrome 2', *Nature*, 408(6809), pp. 207–211.
- Massey, S.E., Moura, G., Beltrão, P., Almeida, R., Garey, J.R., Tuite, M.F. and Santos, M.A.S. (2003) 'Comparative evolutionary genomics unveils the molecular mechanism of reassignment of the CTG codon in *Candida* spp', *Genome Research*. Cold Spring Harbor Laboratory Press, 13(4), pp. 544–557.
- Masuda, T., Tanaka, K., Nonaka, H., Yamochi, W., Maeda, A. and Takai, Y. (1994) 'Molecular cloning and characterization of yeast rho GDP dissociation inhibitor', *Journal of Biological Chemistry*, 269(31), pp. 19713–8.
- Mayer, F.L., Wilson, D. and Hube, B. (2013) '*Candida albicans* pathogenicity mechanisms', *Virulence*, 4(2), pp. 119–128.
- McManus, B.A. and Coleman, D.C. (2014) 'Molecular epidemiology, phylogeny and evolution of *Candida albicans*', *Infection, Genetics and Evolution*, 21, pp. 166–178.
- McTaggart, S.J. (2006) 'Isoprenylated proteins', *Cellular and Molecular Life Sciences*, 63(3), pp. 255–267.
- Mei, K., Li, Y., Wang, S., Shao, G., Wang, J., Ding, Y., Luo, G., Yue, P., Liu, J.-J., Wang, X., Dong, M.-Q., Wang, H.-W. and Guo, W. (2018) 'Cryo-EM structure of the exocyst complex', *Nature Structural & Molecular Biology*, 25(2), pp. 139–146.
- Meller, N. (2005) 'CZH proteins: a new family of Rho-GEFs', *Journal of Cell Science*. The Company of Biologists Ltd, 118(21), pp. 4937–4946.
- Mellman, I. and Nelson, W.J. (2008) 'Coordinated protein sorting, targeting and distribution in polarized cells', *Nature Reviews Molecular Cell Biology*, 9(11), pp. 833–845.
- Merlini, L., Dudin, O. and Martin, S.G. (2013) 'Mate and fuse: how yeast cells do it', *Open Biology*, 3(3), p. 130008.
- Merlini, L., Khalili, B., Bendezú, F.O., Hurwitz, D., Vincenzetti, V., Vavylonis, D. and Martin, S.G. (2017) 'Local pheromone release from dynamic polarity sites underlies cell-cell pairing during yeast mating', *Current Biology*, 26(8), pp. 1117–1125.
- Miller, P.J. and Johnson, D.I. (1994) 'Cdc42P GTPase is involved in controlling polarized cell growth in *Schizosaccharomyces pombe*', *Molecular and Cellular Biology*, 14(2), pp. 1075–83.

- Miranda, T.T., Vianna, C.R., Rodrigues, L., Monteiro, A.S., Rosa, C.A. and Côrrea, A.J. (2009) 'Diversity and frequency of yeasts from the dorsum of the tongue and necrotic root canals associated with primary apical periodontitis', *International Endodontic Journal*, 42(9), pp. 839–44.
- Miyazaki, K., Komatsu, S. and Ikebe, M. (2006) 'Dynamics of RhoA and ROK α translocation in single living cells', *Cell Biochemistry and Biophysics*, 45(3), pp. 243–254.
- Modrezewka, B. and Kurnatowski, P. (2015) 'Adherence of *Candida* sp. to host tissues and cells as one of its pathogenicity features', *Annals of Parasitology*, 61(1), pp. 3–9.
- Moffat, J. and Andrews, B. (2004) 'Late-G1 cyclin-CDK activity is essential for control of cell morphogenesis in budding yeast', *Nature Cell Biology*. Nature Publishing Group, 6(1), pp. 59–66.
- Moran, G., Stokes, C., Thewes, S., Hube, B., Coleman, D.C. and Sullivan, D. (2004) 'Comparative genomics using *Candida albicans* DNA microarrays reveals absence and divergence of virulence-associated genes in *Candida dubliniensis*', *Microbiology*, 150(Pt 10), pp. 3363–82.
- Morin, A., Moores, A.W. and Sacher, M. (2009) 'Dissection of *Saccharomyces Cerevisiae* Asci', *Journal of Visualized Experiments*, (27), pp. 6–8.
- Morreale, A., Venkatesan, M., Mott, H.R., Owen, D., Nietlispach, D., Lowe, P.N. and Laue, E.D. (2000) 'Structure of Cdc42 bound to the GTPase binding domain of PAK', *Nature Structural Biology*, 7(5), pp. 384–388.
- Morschhäuser, J. (2010) 'Regulation of white-opaque switching in *Candida albicans*', *Medical Microbiology and Immunology*, 199(3), pp. 165–172.
- Moseley, J.B. (2003) 'A Conserved Mechanism for Bni1- and mDia1-induced Actin Assembly and Dual Regulation of Bni1 by Bud6 and Profilin', *Molecular Biology of the Cell*, 15(2), pp. 896–907.
- Moseley, J.B. and Goode, B.L. (2006) 'The Yeast Actin Cytoskeleton: from Cellular Function to Biochemical Mechanism', *Microbiology and Molecular Biology Reviews*, 70(3), pp. 605–645.
- Motegi, F., Arai, R. and Mabuchi, I. (2001) 'Identification of two type V myosins in fission yeast, one of which functions in polarized cell growth and moves rapidly in the cell', *Molecular Biology of the Cell*, 12, pp. 1367–1380.
- Motta-Mena, L.B., Reade, A., Mallory, M.J., Glantz, S., Weiner, O.D., Lynch, K.W. and Gardner, K.H. (2014) 'An optogenetic gene expression system with rapid activation and deactivation kinetics', *Nature Chemical Biology*, 10(3), pp. 196–202.
- Moyes, D.L., Wilson, D., Richardson, J.P., Mogavero, S., Tang, S.X., Wernecke, J., Höfs, S., Gratacap, R.L., Robbins, J., Runglall, M., Murciano, C., Blagojevic, M., Thavaraj, S., Förster, T.M., Hebecker, B., Kasper, L., Vizcay, G., Iancu, S.I., Kichik, N., Häder, A., Kurzai, O., Luo, T., Krüger, T., Kniemeyer, O., Cota, E., Bader, O., Wheeler, R.T., Gutschmann, T., Hube, B. and Naglik, J.R. (2016) 'Candidalysin is a fungal peptide toxin critical for mucosal infection', *Nature*, 532(7597), pp. 64–68.
- Mukaremera, L., Lee, K.K., Mora-Montes, H.M. and Gow, N.A.R. (2017) '*Candida albicans* yeast, pseudohyphal, and hyphal morphogenesis differentially affects immune recognition', *Frontiers in Immunology*, 8(JUN), pp. 1–12.
- Müller, K., Engesser, R., Timmer, J., Nagy, F., Zurbriggen, M.D. and Weber, W. (2013) 'Synthesis of phycocyanobilin in mammalian cells', *Chemical Communications*, 49(79), p. 8970.
- Mullins, R.D. (2010) 'Cytoskeletal Mechanisms for Breaking Cellular Symmetry', *Cold Spring Harbor Perspectives in Biology*, 2(a003392), pp. 1–16.
- Munemitsu, S., Innis, M.A., Clark, R., McCormick, F., Ullrich, A. and Polakis, P. (1990) 'Molecular cloning and expression of a G25K cDNA, the human homolog of the yeast cell cycle gene CDC42.', *Molecular and Cellular Biology*, 10(11), pp. 5977–82.
- Murad, A.M., Leng, P., Straffon, M., Wishart, J., Macaskill, S., MacCallum, D., Schnell, N., Talibi, D., Marechal, D., Tekaiia, F., D'Enfert, C., Gaillardin, C., Odds, F.C. and Brown, A.J. (2001) 'Nrg1 represses yeast–hypha morphogenesis and hypha–specific gene expression in *Candida albicans*',

EMBO Journal, 20(17), pp. 4742–52.

- Murray, J.M. and Johnson, D.I. (2001) ‘The Cdc42p GTPase and Its Regulators Nrf1p and Scd1p Are Involved in Endocytic Trafficking in the Fission Yeast *Schizosaccharomyces pombe*’, *Journal of Biological Chemistry*, 276(5), pp. 3004–3009.
- Nagel, G., Ollig, D., Fuhrmann, M., Kateriya, S., Musti, A.M., Bamberg, E. and Hegemann, P. (2002) ‘Channelrhodopsin-1: A light-gated proton channel in green algae’, *Science*, 296(5577), pp. 2395–2398.
- Nagel, G., Szellas, T., Huhn, W., Kateriya, S., Adeishvili, N., Berthold, P., Ollig, D., Hegemann, P. and Bamberg, E. (2003) ‘Channelrhodopsin-2, a directly light-gated cation-selective membrane channel’, *Proceedings of the National Academy of Sciences USA*, 100(24), pp. 13940–13945.
- Navarro, N.G. and Miller, E. (2016) ‘Protein sorting at the ER – Golgi interface’, *Journal of Cell Biology*, 215(6), pp. 769–778.
- Ni, M., Tepperman, J.M. and Quail, P.H. (1999) ‘Binding of phytochrome B to its nuclear signalling partner PIF3 is reversibly induced by light’, *Nature*, 400(6746), pp. 781–784.
- Nicholls, S., MacCallum, D.M., Kaffarnik, F.A., Selway, L., Peck, S.C. and Brown, A.J. (2011) ‘Activation of the heat shock transcription factor Hsf1 is essential for the full virulence of the fungal pathogen *Candida albicans*’, *Fungal Genetics and Biology*, 48(3), pp. 297–305.
- Nobile, C.J., Fox, E.P., Nett, J.E., Sorrells, T.R., Mitrovich, Q.M., Hernday, A.D., Tuch, B.B., Andes, D.R. and Johnson, A.D. (2012) ‘A recently evolved transcriptional network controls biofilm development in *Candida albicans*’, *Cell*, 148(1–2), pp. 126–138.
- Noble, S.M., Gianetti, B.A. and Witchley, J.N. (2017) ‘*Candida albicans* cell-type switching and functional plasticity in the mammalian host’, *Nature Reviews Microbiology*. Nature Publishing Group, 15(2), pp. 96–108.
- Novick, P. and Botstein, D. (1985) ‘Phenotypic analysis of temperature-sensitive yeast actin mutants’, *Cell*, 40(2), pp. 405–416.
- O’Brien, H.E., Parrent, J.L., Jackson, J.A., Moncalvo, J.M. and Vilgalys, R. (2005) ‘Fungal community analysis by large-scale sequencing of environmental samples’, *Applied and Environmental Microbiology*, 71(9), pp. 5544–5550.
- O’Neill, P.R., Kalyanaraman, V. and Gautam, N. (2016) ‘Subcellular optogenetic activation of Cdc42 controls local and distal signaling to drive immune cell migration’, *Molecular Biology of the Cell*, 27(9), pp. 1442–1450.
- Okada, S., Lee, M.E., Bi, E. and Park, H.O. (2017) ‘Probing Cdc42 Polarization Dynamics in Budding Yeast Using a Biosensor’, in *Methods in Enzymology*, pp. 171–190.
- Olofsson, B. (1999) ‘Rho guanine dissociation inhibitors: Pivotal molecules in cellular signalling’, *Cellular Signalling*, 11(8), pp. 545–554.
- Orsi, C.F., Borghi, E., Colombari, B., Neglia, R.G., Quaglino, D., Ardizzoni, A., Morace, G. and Blasi, E. (2014) ‘Impact of *Candida albicans* hyphal wall protein 1 (HWP1) genotype on biofilm production and fungal susceptibility to microglial cells’, *Microbial Pathogenesis*, 69–70(1), pp. 20–27.
- Ozbudak, E.M., Becskei, A. and van Oudenaarden, A. (2005) ‘A system of counteracting feedback loops regulates Cdc42p activity during spontaneous cell polarization’, *Developmental Cell*, 9(4), pp. 565–571.
- Palade, G. (1975) ‘Intracellular aspects of the process of protein synthesis’, *Science*, 189(4206), p. 867.
- Palige, K., Linde, J., Martin, R., Böttcher, B., Citiulo, F., Sullivan, D.J., Weber, J., Staib, C., Rupp, S., Hube, B., Morschhäuser, J. and Staib, P. (2013) ‘Global Transcriptome Sequencing Identifies Chlamydospore Specific Markers in *Candida albicans* and *Candida dubliniensis*’, *PLoS ONE*, 8(4).
- Pan, X., Eathiraj, S., Munson, M. and Lambright, D.G. (2006) ‘TBC-domain GAPs for Rab GTPases accelerate GTP hydrolysis by a dual-finger mechanism’, *Nature*. Nature Publishing Group, 442(7100), pp. 303–306.

- Pantazopoulou, A. (2016) 'The Golgi apparatus: insights from filamentous fungi', *Mycologia*, 108(3), pp. 603–622.
- Pantazopoulou, A. and Penalva, M.A. (2009) 'Organization and dynamics of the *Aspergillus nidulans* Golgi during apical extension and mitosis', *Molecular Biology of the Cell*, 20, pp. 4335–4347.
- Pantazopoulou, A. and Peñalva, M.A. (2011) 'Characterization of *Aspergillus nidulans* RabC/Rab6', *Traffic*, 12(4), pp. 386–406.
- Pantazopoulou, A., Pinar, M., Xiang, X. and Penalva, M.A. (2014) 'Maturation of late Golgi cisternae into RabE(RAB11) exocytic post-Golgi carriers visualized in vivo', *Molecular Biology of the Cell*, 25(16), pp. 2428–2443.
- Papadopoulos, A. (2017) 'Membrane shaping by actin and myosin during regulated exocytosis', *Molecular and Cellular Neuroscience*. Elsevier Inc., 84, pp. 93–99.
- Park, H., Kim, N.N.Y., Lee, S., Kim, N.N.Y., Kim, J. and Heo, W. Do (2017) 'Optogenetic protein clustering through fluorescent protein tagging and extension of CRY2', *Nature Communications*. Nature Publishing Group, 8(1), p. 30.
- Park, H.O. and Bi, E. (2007) 'Central Roles of Small GTPases in the Development of Cell Polarity in Yeast and Beyond', *Microbiology and Molecular Biology Reviews*, 71(1), pp. 48–96.
- Park, H.O., Kang, P.J. and Rachfal, A.W. (2002) 'Localization of the Rsr1/Bud1 GTPase involved in selection of a proper growth site in yeast', *Journal of Biological Chemistry*, 277(30), pp. 26721–26724.
- Park, H.O., Sanson, A. and Herskowitz, I. (1999) 'Localization of Bud2p, a GTPase-activating protein necessary for programming cell polarity in yeast to the presumptive bud site', *Genes & Development*, 13(15), pp. 1912–1917.
- Parri, M. and Chiarugi, P. (2010) 'Rac and Rho GTPases in cancer cell motility control', *Cell Communication and Signaling*, p. 23.
- Pelham Jr, R.J. and Chang, F. (2001) 'Role of actin polymerization and actin cables in actin-patch movement in *Schizosaccharomyces pombe*', *Nature Cell Biology*, 3, pp. 235–244.
- Peñalva, M.Á. (2010) 'Endocytosis in filamentous fungi: Cinderella gets her reward', *Current Opinion in Microbiology*, pp. 684–692.
- Perez, P. and Rincón, S.A. (2010) 'Rho GTPases: regulation of cell polarity and growth in yeasts', *The Biochemical Journal*, 426(3), pp. 243–253.
- Pfaller, M.A., Castanheira, M., Masser, S.A., Moet, G.J. and Jones, R.N. (2010) 'Variation in *Candida* spp. distribution and antifungal resistance rates among bloodstream infection isolates by patient age: report from the SENTRY Antimicrobial Surveillance Program (2008-2009)', *Diagnostic Microbiology and Infectious Disease*, 68(3), pp. 278–83.
- Piispanen, A.E., Bonnefoi, O., Carden, S., Deveau, A., Bassilana, M. and Hogan, D.A. (2011) 'Roles of ras1 membrane localization during *Candida albicans* hyphal growth and farnesol response', *Eukaryotic Cell*, 10(11), pp. 1473–1484.
- Piispanen, A.E., Grahl, N., Hollomon, J.M. and Hogan, D.A. (2013) 'Regulated proteolysis of *Candida albicans* Ras1 is involved in morphogenesis and quorum sensing regulation', *Molecular Microbiology*. NIH Public Access, 89(1), pp. 166–178.
- Pinar, M., Pantazopoulou, A., Arst, H.N. and Peñalva, M.A. (2013) 'Acute inactivation of the *Aspergillus nidulans* Golgi membrane fusion machinery: Correlation of apical extension arrest and tip swelling with cisternal disorganization', *Molecular Microbiology*, 89(2), pp. 228–248.
- Pogorzala, L.A., Mishra, S.K. and Hoon, M.A. (2013) 'The Cellular Code for Mammalian Thermosensation', *Journal of Neuroscience*, 33(13), pp. 5533–5541.
- Pointer, B.R., Boyer, M.P. and Schmidt, M. (2015) 'Boric acid destabilizes the hyphal cytoskeleton and inhibits invasive growth of *Candida albicans*', *Yeast*, 32(4), pp. 389–398.

- Pollard, T.D. (2010) 'Mechanics of cytokinesis in eukaryotes', *Current Opinion in Cell Biology*, pp. 50–56.
- Pollard, T.D. (2017) 'Nine unanswered questions about cytokinesis', *Journal of Cell Biology*. Rockefeller University Press, pp. 3007–3016.
- Pringle, J.R., Bi, E., Harkins, H.A., Zahner, J.E., De Virgilio, C., Chant, J., Corrado, K. and Fares, H. (1995) 'Establishment of cell polarity in yeast', *Cold Spring Harbor Symposia on Quantitative Biology*, 60, pp. 729–744.
- Pruyne, D., Evangelista, M., Yang, C., Bi, E., Zigmond, S., Bretscher, A. and Boone, C. (2002) 'Role of formins in actin assembly: Nucleation and barbed-end association', *Science*, 297(5581), pp. 612–615.
- Quindós, G. (2014) 'Epidemiology of candidaemia and invasive candidiasis. A changing face', *Revista Iberoamericana de Micología*, 31(1), pp. 42–48.
- Rapali, P., Mitteau, R., Braun, C., Massoni-Laporte, A., Ünlü, C., Bataille, L., Arramon, F. Saint, Gygi, S.P. and McCusker, D. (2017) 'Scaffold-mediated gating of cdc42 signalling flux', *eLife*, 6.
- Reijnt, P., Walther, A. and Wendland, J. (2011) 'Dual-colour fluorescence microscopy using yEmCherry-/GFP-tagging of eisosome components Pil1 and Lsp1 in *Candida albicans*', *Yeast*, 28(4), pp. 331–338.
- Repina, N.A., Rosenbloom, A., Mukherjee, A., Schaffer, D. V and Kane, R.S. (2017) 'At Light Speed: Advances in Optogenetic Systems for Regulating Cell Signaling and Behavior', *Annual Review of Chemical and Biomolecular Engineering*, 8(1), pp. 13–39.
- Reuß, O., Vik, Å., Kolter, R. and Morschhäuser, J. (2004) 'The SAT1 flipper, an optimized tool for gene disruption in *Candida albicans*', *Gene*, 341, pp. 119–127.
- Revilla-Guarinos, M.T., Martin-Garcia, R., Villar-Tajadura, M.A., Estravis, M., Coll, P.M. and Perez, P. (2016) 'Rga6 is a fission yeast Rho GAP involved in Cdc42 regulation of polarized growth', *Molecular Biology of the Cell*, 27(9), pp. 1524–1535.
- Richardson, J.P., Moyes, D.L., Ho, J. and Naglik, J.R. (2018) 'Candida innate immunity at the mucosa', *Seminars in Cell & Developmental Biology*, 17.
- Richman, T.J., Sawyer, M.M. and Johnson, D.I. (2002) '*Saccharomyces cerevisiae* Cdc42p localizes to cellular membranes and clusters at sites of polarized growth', *Eukaryotic Cell*, 1(3), pp. 458–468.
- Richman, T.J., Toenjes, K.A., Morales, S.E., Cole, K.C., Wasserman, B.T., Taylor, C.M., Koster, J.A., Whelihan, M.F. and Johnson, D.I. (2004) 'Analysis of cell-cycle specific localization of the Rdi1p RhoGDI and the structural determinants required for Cdc42p membrane localization and clustering at sites of polarized growth', *Current Genetics*, 45(6), pp. 339–349.
- Rida, P.C.G., Nishikawa, A., Won, G.Y. and Dean, N. (2006) 'Yeast-to-hyphal transition triggers formin-dependent Golgi localization to the growing tip in *Candida albicans*', *Molecular Biology of the Cell*, 17, pp. 4364–4378.
- Rincon, S., Coll, P.M. and Perez, P. (2007) 'Spatial regulation of Cdc42 during cytokinesis', *Cell Cycle*, 6(14), pp. 1687–1691.
- Riquelme, M. (2013) 'Tip Growth in Filamentous Fungi: A Road Trip to the Apex', *Annual Review of Microbiology*, 67(1), pp. 587–609.
- Riquelme, M., Bredeweg, E.L., Callejas-Negrete, O., Roberson, R.W., Ludwig, S., Beltran-Aguilar, A., Seiler, S., Novick, P. and Freitag, M. (2014) 'The *Neurospora crassa* exocyst complex tethers Spitzenkörper vesicles to the apical plasma membrane during polarized growth', *Molecular Biology of the Cell*, 25(8), pp. 1312–1326.
- Riquelme, M. and Sánchez-León, E. (2014) 'The Spitzenkörper: A choreographer of fungal growth and morphogenesis', *Current Opinion in Microbiology*, 20, pp. 27–33.
- Rivera-Molina, F.E. and Novick, P.J. (2009) 'A Rab GAP cascade defines the boundary between two Rab GTPases on the secretory pathway', *Proceedings of the National Academy of Sciences of the United States of America*. National Academy of Sciences, 106(34), pp. 14408–13.

- Rocha, C.R.C., Schroppel, K., Harcus, D., Marcil, A., Dignard, D., Taylor, B.N., Thomas, D.Y., Whiteway, M. and Leberer, E. (2001) 'Signaling through Adenylyl Cyclase Is Essential for Hyphal Growth and Virulence in the Pathogenic Fungus *Candida albicans*', *Molecular Biology of the Cell*, 12(11), pp. 3631–3643.
- Roncero, C. and Sanchez, Y. (2010) 'Cell separation and the maintenance of cell integrity during cytokinesis in yeast: the assembly of a septum', *Yeast*, 27(8), pp. 521–30.
- Rossanese, O.W., Reinke, C.A., Bevis, B.J., Hammond, A.T., Sears, I.B., O'Connor, J. and Glick, B.S. (2001) 'A role for actin, Cdc1p, and Myo2p in the inheritance of late Golgi elements in *Saccharomyces cerevisiae*', *Journal of Cell Biology*, 153(1), pp. 47–61.
- Rossmann, K.L., Der, C.J. and Sondek, J. (2005) 'GEF means go: Turning on Rho GTPases with guanine nucleotide-exchange factors', *Nature Reviews Molecular Cell Biology*, pp. 167–180.
- Rothman, J.E. (1994) 'Mechanisms of intracellular protein transport', *Nature*, 372(6501), pp. 55–63.
- Rottner, K., Faix, J., Bogdan, S., Linder, S. and Kerkhoff, E. (2017) 'Actin assembly mechanisms at a glance', *Journal of Cell Science*, 130, pp. 3427–3435.
- Sagot, I., Klee, S.K. and Pellman, D. (2002) 'Yeast formins regulate cell polarity by controlling the assembly of actin cables', *Nature Cell Biology*, 4, pp. 42–50.
- Sánchez-León, E., Bowman, B., Seidel, C., Fischer, R., Novick, P. and Riquelme, M. (2015) 'The Rab GTPase YPT-1 associates with Golgi cisternae and Spitzenkörper microvesicles in *Neurospora crassa*', *Molecular Microbiology*, 95(3), pp. 472–490.
- Saputo, S., Chabrier-Rosello, Y., Luca, F.C., Kumar, A. and Krysan, D.J. (2012) 'The RAM network in pathogenic fungi', *Eukaryotic Cell*. American Society for Microbiology (ASM), 11(6), pp. 708–717.
- Saville, S.P., Lazzell, A.L., Monteagudo, C. and Lopez-Ribot, J.L. (2003) 'Engineered control of cell morphology in vivo reveals distinct roles for yeast and filamentous forms of *Candida albicans* during infection', *Eukaryotic Cell*, 2(5), pp. 1053–60.
- Schott, D., Ho, J., Pruyne, D. and Bretscher, A. (1999) 'The COOH-terminal domain of Myo2p, a yeast myosin V, has a direct role in secretory vesicle targeting', *Journal of Cell Biology*, 147(4), pp. 791–807.
- Schultzhaus, Z., Yan, H. and Shaw, B.D. (2015) 'Aspergillus nidulans flippase DnfA is cargo of the endocytic collar and plays complementary roles in growth and phosphatidylserine asymmetry with another flippase, DnfB', *Molecular Microbiology*, 97(1), pp. 18–32.
- Schultzhaus, Z.S. and Shaw, B.D. (2015) 'Endocytosis and exocytosis in hyphal growth', *Fungal Biology Reviews*, 29(2), pp. 43–53.
- Selmecki, A., Forche, A. and Berman, J. (2006) 'Aneuploidy and isochromosome formation in drug-resistant *Candida albicans*', *Science*, 313(5785), pp. 367–370.
- Selmecki, A., Forche, A. and Berman, J. (2010) 'Genomic plasticity of the human fungal pathogen *Candida albicans*', *Eukaryotic Cell*, 9(7), pp. 991–1008.
- Selmecki, A.M., Dulmage, K., Cowen, L.E., Anderson, J.B. and Berman, J. (2009) 'Acquisition of aneuploidy provides increased fitness during the evolution of antifungal drug resistance', *PLoS Genetics*, 5(10), pp. 1–16.
- Shapiro, R.S., Robbins, N. and Cowen, L.E. (2011) 'Regulatory circuitry governing fungal development, drug resistance, and disease', *Microbiology and Molecular Biology Reviews*, 75(2), pp. 213–67.
- Shapiro, R.S., Uppuluri, P., Zaas, A.K., Collins, C., Senn, H., Perfect, J.R., Heitman, J. and Cowen, L.E. (2009) 'Hsp90 orchestrates temperature-dependent *Candida albicans* morphogenesis via Ras1–PKA signaling', *Current Biology*, 19(8), pp. 621–9.
- Shareck, J. and Belhumeur, P. (2011) 'Modulation of morphogenesis in *Candida albicans* by various small molecules', *Eukaryotic Cell*, 10(8), pp. 1004–12.
- Shaw, B.D., Chung, D.W., Wang, C.L., Quintanilla, L.A. and Upadhyay, S. (2011) 'A role for endocytic

- recycling in hyphal growth', *Fungal Biology*. Elsevier Ltd, 115(6), pp. 541–546.
- Shen, J., Guo, W. and Köhler, J.R. (2005) 'CaNAT1, a Heterologous Dominant Selectable Marker for Transformation of *Candida albicans* and Other Pathogenic *Candida* Species', *Infection and Immunity*, 73(2), pp. 1239–1242.
- Sheppard, D.C. and Filler, S.G. (2014) 'Host Cell Invasion by Medically Important Fungi.', *Cold Spring Harbor Perspectives in Medicine*, 5(1), pp. 1–16.
- Sheu, Y.J., Santos, B., Fortin, N., Costigan, C. and Snyder, M. (1998) 'Spa2p interacts with cell polarity proteins and signaling components involved in yeast cell morphogenesis.', *Molecular and Cellular Biology*, 18(7), pp. 4053–69.
- Shimada, Y., Wiget, P., Gulli, M.P., Bi, E. and Peter, M. (2004) 'The nucleotide exchange factor Cdc24p may be regulated by auto-inhibition', *EMBO Journal*, 23(5), pp. 1051–1062.
- Shimizu-Sato, S., Huq, E., Tepperman, J.M. and Quail, P.H. (2002) 'A light-switchable gene promoter system', *Nature Biotechnology*. Nature Publishing Group, 20(10), pp. 1041–1044.
- Shinjo, K., Koland, J.G., Hart, M.J., Narasimhan, V., Johnson, D.I., Evans, T. and Cerione, R.A. (1990) 'Molecular cloning of the gene for the human placental GTP-binding protein Gp (G25K): identification of this GTP-binding protein as the human homolog of the yeast cell-division-cycle protein CDC42.', *Proceedings of the National Academy of Sciences USA*, 87(24), pp. 9853–7.
- Simonneti, N., Stripolli, V. and Cassone, E.A. (1974) 'Yeast-mycelial conversion induced by N-acetyl-d-glucosamine in *Candida albicans*', *Nature*, 250(464), pp. 344–6.
- Singh, P., Das, A. and Li, R. (2017) 'Investigating symmetry breaking in yeast: From seeing to understanding', *Methods in Cell Biology*, 139, pp. 23–50.
- Slaughter, B.D., Das, A., Schwartz, J.W., Rubinstein, B. and Li, R. (2009) 'Dual Modes of Cdc42 Recycling Fine-Tune Polarized Morphogenesis', *Developmental Cell*, 17(6), pp. 823–835.
- Slaughter, B.D., Unruh, J.R., Das, A., Smith, S.E., Rubinstein, B. and Li, R. (2013) 'Non-uniform membrane diffusion enables steady-state cell polarization via vesicular trafficking', *Nature Communications*, 4, p. 1380.
- Sloat, B.F., Adams, A. and Pringle, J.R. (1981) 'Roles of the CDC24 Gene Product in Cellular Morphogenesis during the *Saccharomyces cerevisiae* Cell Cycle', *Journal of Cell Biology*, 89(3), pp. 395–405.
- Sohn, K., Urban, C., Brunner, H. and Rupp, S. (2003) 'EFG1 is a major regulator of cell wall dynamics in *Candida albicans* as revealed by DNA microarrays', *Molecular and Cellular Microbiology*, 47(1), pp. 89–102.
- Song, Y., Cheon, S.A., Lee, K.E., Lee, S.Y., Lee, B.K., Oh, D.B., Kang, H.A. and Kim, J.Y. (2008) 'Role of the RAM network in cell polarity and hyphal morphogenesis in *Candida albicans*', *Molecular Biology of the Cell*, 19(12), pp. 5456–77.
- De Sordi, L. and Muhlschlegel, F.A. (2009) 'Quorum sensing and fungal-bacterial interactions in *Candida albicans*: a communicative network regulating microbial coexistence and virulence', *FEMS Yeast Research*, 9(7), pp. 990–9.
- Sorkhoh, N.A., Ghannoum, M.A., Ibrahim, A.S., Stretton, R.J. and Radwan, S.S. (1990) 'Growth of *Candida albicans* on hydrocarbons: influence on lipids and sterols', *Microbios*, 64(260–261), pp. 159–71.
- Spencer, D.M., Wandless, T.J., Schreiber, S.L. and Crabtree, G.R. (1993) 'Controlling signal transduction with synthetic ligands.', *Science*, pp. 1019–1024.
- Stachowiak, M.R., Laplante, C., Chin, H.F., Guirao, B., Karatekin, E., Pollard, T.D. and O'Shaughnessy, B. (2014) 'Mechanism of cytokinetic contractile ring constriction in fission yeast', *Developmental Cell*. NIH Public Access, 29(5), pp. 547–561.
- Steinberg, G. (2007) 'Hyphal growth: A tale of motors, lipids, and the Spitzenkörper', *Eukaryotic Cell*, pp. 351–360.

- Steinberg, G., Peñalva, M.A., Riquelme, M., Wösten, H.A. and Harris, S.D. (2017) 'Cell Biology of Hyphal Growth.', *Microbiology Spectrum*, 5(2), pp. 1–34.
- Stoldt, V.R., Sonneborn, A., Leuker, C.E. and Ernst, J.F. (1997) 'Efg1p, an essential regulator of morphogenesis of the human pathogen *Candida albicans*, is a member of a conserved class of bHLH proteins regulating morphogenetic processes in fungi', *EMBO Journal*, 16(8), pp. 1982–91.
- Strickland, D., Lin, Y., Wagner, E., Hope, C.M., Zayner, J., Antoniou, C., Sosnick, T.R., Weiss, E.L. and Glotzer, M. (2012) 'TULIPs: Tunable, light-controlled interacting protein tags for cell biology', *Nature Methods*, 9(4), pp. 379–384.
- Sudbery, P., Gow, N. and Berman, J. (2004) 'The distinct morphogenic states of *Candida albicans*', *Trends in Microbiology*, 12(7), pp. 317–24.
- Sudbery, P.E. (2001) 'The germ tubes of *Candida albicans* hyphae and pseudohyphae show different patterns of septin ring localisation', *Molecular Microbiology*, 41(1), pp. 19–31.
- Sudbery, P.E. (2011) 'Growth of *Candida albicans* hyphae', *Nature Reviews Microbiology*, pp. 737–748.
- Suelmann, R. and Fischer, R. (2000) 'Mitochondrial movement and morphology depend on an intact actin cytoskeleton in *Aspergillus nidulans*', *Cell Motility and the Cytoskeleton*, 45(1), pp. 42–50.
- Suh, S.-O., Blackwell, M., Kurtzman, C.P. and Lachance, M.-A. (2006) 'Phylogenetics of Saccharomycetales, the ascomycete yeasts', *Mycologia*, 98(6), pp. 1006–1017.
- Taheri-Talesh, N., Horio, T., Araujo-Bazan, L., Dou, X., Espeso, E.A., Penalva, M.A., Osmani, S.A. and Oakley, B.R. (2008) 'The tip growth apparatus of *Aspergillus nidulans*', *Molecular Biology of the Cell*, 19(4), pp. 1439–1449.
- Takeshita, N. (2016) 'Coordinated process of polarized growth in filamentous fungi', *Bioscience, Biotechnology and Biochemistry*. Taylor & Francis, 80(9), pp. 1693–1699.
- Taschdjian, C.L., Burchall, J.J. and Kozinn, P.J. (1960) 'Rapid identification of *Candida albicans* by filamentation on serum and serum substitutes', *AMA Journal of Diseases of Children*, 99, pp. 212–5.
- Taslimi, A., Zoltowski, B., Miranda, J.G., Pathak, G.P., Hughes, R.M. and Tucker, C.L. (2016) 'Optimized second-generation CRY2-CIB dimerizers and photoactivatable Cre recombinase', *Nature Chemical Biology*, 12(6), pp. 425–430.
- Tatebe, H., Nakano, K., Maximo, R. and Shiozaki, K. (2008) 'Pom1 DYRK Regulates Localization of the Rga4 GAP to Ensure Bipolar Activation of Cdc42 in Fission Yeast', *Current Biology*, 18(5), pp. 322–330.
- Tebarth, B., Doedt, T., Krishnamurthy, S., Weide, M., Monterola, F., Dominguez, A. and Ernst, J.F. (2003) 'Adaptation of the Efg1p morphogenetic pathway in *Candida albicans* by negative autoregulation and PKA-dependent repression of the EFG1 gene', *Journal of Molecular Biology*, 329(5), pp. 949–962.
- TerBush, D.R., Maurice, T., Roth, D. and Novick, P. (1996) 'The Exocyst is a multiprotein complex required for exocytosis in *Saccharomyces cerevisiae*.' *EMBO Journal*, 15(23), pp. 6483–6494.
- Thompson, G.R. 3rd, Patel, P.K., Kirkpatrick, W.R., Westbrook, S.D., Berg, D., Erlandsen, J., Redding, S.W. and Patterson, T.F. (2010) 'Oropharyngeal candidiasis in the era of antiretroviral therapy', *Oral Surgery Oral Medicine Oral Pathology Oral Radiology*, 109(4), pp. 488–95.
- Thompson, J.R., Register, E., Curotto, J., Kurtz, N. and Kelly, R. (1998) 'An improved protocol for the preparation of yeast cells for transformation by electroporation', *Yeast*, 14(6), pp. 565–571.
- Tiedje, C., Sakwa, I., Just, U. and Hofken, T. (2008) 'The Rho GDI Rdi1 Regulates Rho GTPases by Distinct Mechanisms', *Molecular Biology of the Cell*. American Society for Cell Biology, 19(1), pp. 2885–2896.
- Tischer, D. and Weiner, O.D. (2014) 'Illuminating cell signalling with optogenetic tools', *Nature Reviews Molecular Cell Biology*, pp. 551–558.
- Tjandra, H., Compton, J. and Kellogg, D. (1998) 'Control of mitotic events by the Cdc42 GTPase, the Clb2

- cyclin and a member of the PAK kinase family.', *Current Biology*, 8(18), pp. 991–1000.
- Toenjes, K.A., Sawyer, M.M. and Johnson, D.I. (1999) 'The guanine-nucleotide-exchange factor Cdc24p is targeted to the nucleus and polarized growth sites', *Current Biology*, 9(20), pp. 1183–1186.
- Toettcher, J.E., Weiner, O.D. and Lim, W.A. (2013) 'Using optogenetics to interrogate the dynamic control of signal transmission by the Ras/Erk module', *Cell*, 155(6), pp. 1422–1434.
- Tong, Z., Gao, X.D., Howell, A.S., Bose, I., Lew, D.J. and Bi, E. (2007) 'Adjacent positioning of cellular structures enabled by a Cdc42 GTPase-activating protein-mediated zone of inhibition', *Journal of Cell Biology*, 179(7), pp. 1375–1384.
- Toyooka, K., Goto, Y., Asatsuma, S., Koizumi, M., Mitsui, T. and Matsuoka, K. (2009) 'A Mobile Secretory Vesicle Cluster Involved in Mass Transport from the Golgi to the Plant Cell Exterior', *Plant Cell*, 21(4), pp. 1212–1229.
- Trinci, A.P. (1974) 'A Study of the Kinetics of Hyphal Extension and Branch Initiation of Fungal Mycelia', *Journal of General Microbiology*, 81(1), pp. 225–236.
- Turrà, D., El Ghalid, M., Rossi, F. and Di Pietro, A. (2015) 'Fungal pathogen uses sex pheromone receptor for chemotropic sensing of host plant signals', *Nature*, 527(7579), pp. 521–524.
- Tyszkiewicz, A.B. and Muir, T.W. (2008) 'Activation of protein splicing with light in yeast', *Nature Methods*, 5(4), pp. 303–305.
- Upadhyay, S. and Shaw, B.D. (2008) 'The role of actin, fimbrin and endocytosis in growth of hyphae in *Aspergillus nidulans*', *Molecular Microbiology*, 68(3), pp. 690–705.
- Ushinsky, S.C., Marcus, D., Ash, J., Dignard, D., Marcil, A., Morchhauser, J., Thomas, D.Y., Whiteway, M. and Leberer, E. (2002) 'CDC42 is required for polarized growth in human pathogen *Candida albicans*', *Eukaryotic Cell*, 1(1), pp. 95–104.
- Valon, L., Etoc, F., Remorino, A., Di Pietro, F., Morin, X., Dahan, M. and Coppey, M. (2015) 'Predictive Spatiotemporal Manipulation of Signaling Perturbations Using Optogenetics', *Biophysical Journal*, 109(9), pp. 1785–1797.
- Valon, L., Marín-Llauradó, A., Wyatt, T., Charras, G. and Trepát, X. (2017) 'Optogenetic control of cellular forces and mechanotransduction', *Nature Communications*, 8.
- VandenBerg, A.L., Ibrahim, A.S., Edwards, J.E., Toenjes, K.A. and Johnson, D.I. (2004) 'Cdc42p GTPase regulates the budded-to-hyphal-form transition and expression of hypha-specific transcripts in *Candida albicans*', *Eukaryotic Cell*, 3(3), pp. 724–734.
- Vanni, C., Ottaviano, C., Guo, F., Puppo, M., Varesio, L., Zheng, Y. and Eva, A. (2005) 'Constitutively active Cdc42 mutant confers growth disadvantage in cell transformation', *Cell Cycle*, 4(11), pp. 1675–1682.
- Vauchelles, R., Stalder, D., Botton, T., Arkowitz, R.A. and Bassilana, M. (2010) 'Rac1 dynamics in the human opportunistic fungal pathogen *Candida albicans*', *PLoS ONE*, 5(10), p. e15400.
- Verdín, J., Bartnicki-Garcia, S. and Riquelme, M. (2009) 'Functional stratification of the Spitzenkörper of *Neurospora crassa*', *Molecular Microbiology*, 74(5), pp. 1044–1053.
- Vernay, A., Schaub, S., Guillas, I., Bassilana, M. and Arkowitz, R.A. (2012) 'A steep phosphoinositide bisphosphate gradient forms during fungal filamentous growth', *Journal of Cell Biology*, 198(4), pp. 711–730.
- Vetter, I.R. and Wittinghofer, A. (2001) 'The Guanine Nucleotide-Binding Switch in Three Dimensions', *Science*, 294(5545), pp. 1299–1304.
- Virag, A. and Griffiths, A.J. (2004) 'A mutation in the *Neurospora crassa* actin gene results in multiple defects in tip growth and branching', *Fungal Genetics and Biology*, 41, pp. 213–225.
- Virag, A. and Harris, S.D. (2006) 'The Spitzenkörper: a molecular perspective', *Mycological Research*, 110(1), pp. 4–13.

- Wai, S.C., Gerber, S.A. and Li, R. (2009) 'Multisite phosphorylation of the guanine nucleotide exchange factor Cdc24 during yeast cell polarization', *PLoS ONE*. Edited by N. Hotchin, 4(8), p. e6563.
- Wakade, R., Labbaoui, H., Stalder, D., Arkowitz, R.A. and Bassilana, M. (2017) 'Overexpression of YPT6 restores invasive filamentous growth and secretory vesicle clustering in a *Candida albicans* arl1 mutant', *Small GTPases*, pp. 1–7.
- Walther, A. and Wendland, J. (2003) 'An improved transformation protocol for the human fungal pathogen *Candida albicans*', *Current Genetics*, 42(6), pp. 339–343.
- Wang, X., Chen, X. and Yang, Y. (2012) 'Spatiotemporal control of gene expression by a light-switchable transgene system', *Nature Methods*, 9(3), pp. 266–269.
- Warena, A.J., Kauffman, S., Sherrill, T.P., Becker, J.M. and Konopka, J.B. (2003) 'Candida albicans Septin Mutants Are Defective for Invasive Growth and Virulence', *Society*, 71(7), pp. 4045–4051.
- Warena, A.J. and Konopka, J.B. (2002) 'Septin Function in *Candida albicans* Morphogenesis', *Molecular Biology of the Cell*, 13(8), pp. 2732–46.
- Wedlich-Söldner, R., Altschuter, S., Wu, L., Li, R., Altschuler, S., Wu, L. and Li, R. (2003) 'Spontaneous cell polarization through actomyosin-based delivery of the Cdc42 GTPase', *Science*, 299(5610), pp. 1231–1235.
- Wedlich-Söldner, R., Bolker, M., Kahmann, R. and Steinberg, G. (2000) 'A putative endosomal t-SNARE links exo- and endocytosis in the phytopathogenic fungus *Ustilago maydis*', *EMBO Journal*, 19, pp. 1974–1986.
- Wedlich-Söldner, R. and Li, R. (2003) 'Spontaneous cell polarization: Undermining determinism', *Nature Cell Biology*, 5(4), pp. 267–270.
- Wedlich-Söldner, R., Wai, S.C., Schmidt, T. and Li, R. (2004) 'Robust cell polarity is a dynamic state established by coupling transport and GTPase signaling', *Journal of Cell Biology*, 166(6), pp. 889–900.
- Weinberg, J. and Drubin, D.G. (2012) 'Clathrin-mediated endocytosis in budding yeast', *Trends in Cell Biology*, pp. 1–13.
- Weinberg, J.S. and Drubin, D.G. (2014) 'Regulation of Clathrin-mediated endocytosis by dynamic ubiquitination and deubiquitination', *Current Biology*, 24(9), pp. 951–959.
- Weiner, M.P., Costa, G.L., Schoettlin, W., Cline, J., Mathur, E. and Bauer, J.C. (1994) 'Site-directed mutagenesis of double-stranded DNA by the polymerase chain reaction', *Gene*, 151, pp. 119–123.
- Wendland, J. and Philippsen, P. (2001) 'Cell polarity and hyphal morphogenesis are controlled by multiple Rho-protein modules in the filamentous ascomycete *Ashbya gossypii*', *Genetics*, 157(2), pp. 601–10.
- Wennerberg, K., Kent, L. and Der, C.J. (2005) 'The Ras superfamily at a glance The Ras Superfamily at a Glance', *Journal of Cell Science*, 118(5), pp. 843–846.
- Wessels, J.G.H. (1988) 'A steady-state model for apical wall growth in fungi', *Acta Botanica Neerlandica*, 37(1), pp. 3–16.
- Wilson, R.B., Davis, D. and Mitchell, A.P. (1999) 'Rapid hypothesis testing with *Candida albicans* through gene disruption with short homology regions', *Journal of Bacteriology*, 181(6), pp. 1868–1874.
- Witte, K., Strickland, D. and Glotzer, M. (2017) 'Cell cycle entry triggers a switch between two modes of Cdc42 activation during yeast polarization', *eLife*, 6.
- Wodarz, A. and Näthke, I. (2007) 'Cell polarity in development and cancer', *Nature Cell Biology*, 9(9), pp. 1016–1024.
- Wolfe, K.H. and Shields, D.C. (1997) 'Molecular evidence for an ancient duplication of the entire yeast genome', *Nature*. Nature Publishing Group, 387(6634), pp. 708–713.
- Wood, L.A., Larocque, G., Clarke, N.I., Sarkar, S. and Royle, S.J. (2017) 'New tools for “hot-wiring” clathrin-mediated endocytosis with temporal and spatial precision', *Journal of Cell Biology*, 216(12), pp.

4351–4365.

- Woods, B., Kuo, C.C., Wu, C.F., Zyla, T.R. and Lew, D.J. (2015) 'Polarity establishment requires localized activation of Cdc42', *Journal of Cell Biology*, 211(1), pp. 19–26.
- Wu, C.F., Savage, N.S. and Lew, D.J. (2013) 'Interaction between bud-site selection and polarity-establishment machineries in budding yeast', *Philosophical Transactions of the Royal Society B: Biological Sciences*, 368(1629), pp. 20130006–20130006.
- Wu, Y.I., Frey, D., Lungu, O.I., Jaehrig, A., Schlichting, I., Kuhlman, B. and Hahn, K.M. (2009) 'A genetically encoded photoactivatable Rac controls the motility of living cells', *Nature*, 461(7260), pp. 104–108.
- Yaar, L., Mevarech, M. and Koltin, Y. (1997) 'A *Candida albicans* RAS-related gene (CaRSR1) is involved in budding, cell morphogenesis and hypha development', *Microbiology*, 143(9), pp. 3033–3044.
- Yamashita, A., Sakuno, T., Watanabe, Y. and Yamamoto, M. (2017) 'Analysis of *Schizosaccharomyces pombe* Meiosis', *Cold Spring Harbor Protocols*, 2017(9), p. pdb.top079855.
- Yang, H.-C. and Pon, L.A. (2002) 'Actin cable dynamics in budding yeast.', *Proceedings of the National Academy of Sciences USA*, 99(2), pp. 751–756.
- Yang, W., Yan, L., Wu, C., Zhao, X. and Tang, J. (2014) 'Fungal invasion of epithelial cells', *Microbiological Research*. Elsevier GmbH., 169(11), pp. 803–810.
- Yao, X., Rosen, M.K. and Gardner, K.H. (2008) 'Estimation of the available free energy in a LOV2-J α photoswitch', *Nature Chemical Biology*, 4(8), pp. 491–497.
- Yohe, M.E., Rossman, K. and Sondek, J. (2008) 'Role of the C-Terminal SH3 Domain and N-Terminal Tyrosine Phosphorylation in Regulation of Tim and Related Dbl-Family Proteins †', *Biochemistry*, 47(26), pp. 6827–6839.
- Yokoyama, K., Kaji, H., Nishimura, K. and Miyaji, M. (1990) 'The role of microfilaments and microtubules in apical growth and dimorphism of *Candida albicans*', *Journal of General Microbiology*, 136(6), pp. 1067–1075.
- Zeilinger, S., Tsui, C.K.M., Zeilinger, S., Gupta, V.K., Dahms, T.E.S., Silva, R.N., Singh, H.B., Upadhyay, R.S., Gomes, E.V., Tsui, C.K. and S, C.N. (2016) 'Friends or foes? Emerging insights from fungal interactions with plants', *FEMS Microbiology Reviews*, 40(November 2015), pp. 182–207.
- Zeng, G., Wang, Y.-M. and Wang, Y. (2012) 'Cdc28-Cln3 phosphorylation of Sla1 regulates actin patch dynamics in different modes of fungal growth', *Molecular Biology of the Cell*, 23(17), pp. 3485–3497.
- Zhang, K. and Cui, B. (2015) 'Optogenetic control of intracellular signaling pathways', *Trends in Biotechnology*, 33(2), pp. 92–100.
- Zhang, N., Magee, B.B., Magee, P.T., Holland, B.R., Rodrigues, E., Holmes, A.R., Cannon, R.D. and Schmid, J. (2015) 'Selective advantages of a parasexual cycle for the yeast *Candida albicans*', *Genetics*, 200(4), pp. 1117–1132.
- Zheng, X.D., Lee, R.T., Wang, Y.M., Ling, Q.S. and Wang, Y. (2007) 'Phosphorylation of Rga2, a Cdc42 GAP, by CDK/Hgc1 is crucial for *Candida albicans* hyphal growth', *EMBO Journal*, 26(16), pp. 3760–9.
- Zheng, Y., Cerione, R. and Bender, A. (1994) 'Control of the yeast bud-site assembly GTPase Cdc42-catalysis of guanine-nucleotide exchange by Cdc24 and stimulation of GTPase activity by Bem3', *Journal of Biological Chemistry*, 269(4), pp. 2369–72.
- Zhou, H., Zoltowski, B.D. and Tao, P. (2017) 'Revealing Hidden Conformational Space of LOV Protein VIVID Through Rigid Residue Scan Simulations', *Scientific Reports*, 7, p. 46626.
- Zhou, X.X., Chung, H.K., Lam, A.J. and Lin, M.Z. (2012) 'Optical Control of Protein Activity by Fluorescent Protein Domains', *Science*, 338(6108), pp. 810–814.
- Zigmond, S.H., Evangelists, M., Boone, C., Yang, C., Dar, A.C., Sicheri, F., Forkey, J. and Pring, M. (2003)

- 'Formin Leaky Cap Allows Elongation in the Presence of Tight Capping Proteins', *Current Biology*, 13(20), pp. 1820–1823.
- Ziman, M. and Johnson, D.I. (1994) 'Genetic evidence for a functional interaction between *Saccharomyces cerevisiae* CDC24 and CDC42', *Yeast*, 10(4), pp. 463–74.
- Ziman, M., O'Brien, J.M., Ouellette, L.A., Church, W.R. and Johnson, D.I. (1991) 'Mutational analysis of CDC42Sc, a *Saccharomyces cerevisiae* gene that encodes a putative GTP-binding protein involved in the control of cell polarity', *Molecular and Cellular Biology*, 11(7), pp. 3537–44.
- Zimmerman, S.P., Asokan, S.B., Kuhlman, B. and Bear, J.E. (2017) 'Cells lay their own tracks – optogenetic Cdc42 activation stimulates fibronectin deposition supporting directed migration', *Journal of Cell Science*, 130(18), pp. 2971–2983.
- Zoltowski, B.D., Schwerdtfeger, C., Widom, J., Loros, J.J., Bilwes, A.M., Dunlap, J.C. and Crane, B.R. (2007) 'Conformational switching in the fungal light sensor vivid', *Science*, 316(5827), pp. 1054–1057.
- Zoltowski, B.D., Vaccaro, B. and Crane, B.R. (2009) 'Mechanism-based tuning of a LOV domain photoreceptor', *Nature Chemical Biology*, 5(11), pp. 827–834.
- Zomorodian, K., Haghghi, N.N., Rajaei, N., Pakshir, K., Tarazooie, B., Vodjani, M., Sedaghat, F. and Vosoghi, M. (2011) 'Assessment of *Candida* species colonization and denture-related stomatitis in complete denture wearers', *Medical Mycology*, 49(2), pp. 208–11.
- Zou, H., Fang, H.M., Zhu, Y. and Wang, Y. (2010) '*Candida albicans* Cyr1, Cap1 and G-actin form a sensor/effector apparatus for activating cAMP synthesis in hyphal growth', *Molecular Microbiology*, 75(3), pp. 579–591.